

***Fundamental Studies of the Behaviour of
Biomass and Waste Materials in Gasification
Systems***

by

Barry Francis McGhee

A Thesis submitted to the Department of Pure and Applied Chemistry, University of Strathclyde, in part fulfilment of the regulations for the degree of Doctor of Philosophy.

Department of Pure and Applied Chemistry,
University of Strathclyde,
Thomas Graham Building,
295 Cathedral Street,
Glasgow G1 1XL

December 1999

Contents

Contents	ii
List of Tables	viii
List of Figures	xi
Acknowledgements	xviii
Abstract	xix
<u>Chapter 1</u> <i>Introduction</i>	
1.1 Background	1
References	10
<u>Chapter 2</u> <i>Literature</i>	
2.1 Introduction	13
2.2 Thermal Processing Reactions	14
2.2.1 Pyrolysis	14
2.2.2 Gasification	14
2.3 The Kinetics of Char Gasification Reactions	16
2.3.1 The Carbon-Molecular Oxygen Reaction	18
2.4 The Effect of Char Characteristics on the Kinetics of Gasification Reactions	21
2.5 Inhibition and Catalysis of the Carbon-Gas Reaction	23
2.5.1 Inhibition of the Carbon-Gas Reaction	24
2.5.2 Catalysis of the Carbon-Gas Reaction	25
2.5.3 Summary of Literature on the Gasification of Carbonaceous Char Materials	26
2.6 The Nature of Biomass and Wastes	27
2.6.1 Cellulose	28
2.6.2 Hemicellulose	28
2.6.3 Lignin	28
2.6.4 The Mineral Matter in Plant Materials	29
2.7 The Nature of RDF	29
2.7.1 Ash Material in RDF	31
2.8 Pyrolysis Mechanisms for Biomass and Biomass Components	31

2.8.1	Cellulose Pyrolysis	33
2.8.2	Hemicellulose Pyrolysis	34
2.8.3	Lignin Pyrolysis	34
2.9	Biomass Pyrolysis	35
2.9.1	Influence of Inorganic Constituents on Biomass and Biomass Components During Pyrolysis	36
2.10	Pyrolysis Reactions of Synthetic Polymers	40
2.10.1	Pyrolysis of Poly(vinylchloride)	40
2.10.2	Pyrolysis of Poly(ethene)	42
2.11	Influence of Inorganic Constituents on Biomass and Waste Gasification	43
	References	61
<u>Chapter 3</u>	<i>Objectives</i>	
3.1	Objectives	73
<u>Chapter 4</u>	<i>Experimental</i>	
4.1	Samples	75
4.1.1	Biomass Samples	75
4.1.2	Refuse Derived Fuels	76
4.1.3	Acid-Washed Samples	77
4.1.4	RDF Model Composites	78
4.2	Analysis Procedures	80
4.3	Thermal Decomposition of Samples in Air	80
4.4	Char Preparation	81
4.5	Char Reactivity Determination	82
4.6	BET Surface Area Analysis	84
<u>Chapter 5</u>	<i>Experimental Results - Biomass Materials</i>	
5.1	Analytical Data for the Biomass Samples	91
5.1.1	Proximate Analyses	91
5.1.2	Ultimate Analyses	92
5.1.3	Ash Analyses	92
5.2	Characteristics of the Chars Prepared from Biomass Samples	93
5.2.1	Char Yields	93

5.2.2	Ultimate Analyses of Chars Prepared from Biomass Samples	93
5.2.3	Relationships Between the Biomass Char Yields with the Raw Sample and Char Characteristics	94
5.3	Thermal Decomposition Analyses of the Biomass Samples	96
5.4	The Reactivities of the of Biomass Chars in Oxygen	97
5.4.1	Relationships of Biomass Char Reactivity with Raw Sample and Char Characteristics	97
5.5	BET Surface Area Determinations of the Biomass Chars	99
5.5.1	Relationships of Char Surface Area with Raw Sample and Char Characteristics	99
5.6	Relationships of Char Surface Area with the Reactivity of the Biomass Chars	100
5.7	Relationships of Ash Components with Biomass Char Characteristics and Reactivity	100
5.7.1	Relationships of Ash Components with Biomass Char Characteristics	101
5.7.2	Relationships of Ash Components with Biomass Char Reactivity	102
5.8	Summary of the Observed Behaviour of the Studied Biomass Materials During Gasification Processes	102
5.9	Analytical Data for the HNO ₃ and HCl Acid-Washed Biomass Samples	104
5.9.1	Proximate and Ultimate Analyses	104
5.10	Analytical Data of Chars Prepared from HNO ₃ and HCl Acid-Washed Biomass Samples	105
5.10.1	Char Yields and Ultimate Analyses of HNO ₃ and HCl Acid-Washed Biomass Sample Chars	105
5.10.2	Relationships Between the HNO ₃ and HCl Acid-Washed Biomass Sample Char Yields with the Precursor Sample and Char Characteristics	106
5.11	Thermal Decomposition Analyses of HNO ₃ and HCl Acid-Washed Biomass Samples	107
5.12	Reactivity Measurements of HNO ₃ and HCl Acid-Washed Biomass Sample Chars in Oxygen	107
5.12.1	Relationships Between the Reactivities of HNO ₃ and HCl Acid-Washed Biomass Sample Chars in Oxygen with the Precursor Material and Char Characteristics	108
5.13	77K N ₂ BET Surface Area Determination of HNO ₃ and HCl Acid-Washed Biomass Sample Chars	108
5.13.1	Relationships Between the Surface Areas of HNO ₃ and HCl Acid -Washed Biomass Sample Chars with the Precursor Material and Char Characteristics	108

5.14	Relationships Between the Char Surface Area with Reactivity of HNO₃ and HCl Acid-Washed Biomass Sample Chars	110
5.15	Relationships Between the Ash Contents of HNO₃ and HCl Acid-Washed Biomass Samples with the Precursor Characteristics and Char Characteristics	110
5.16	Relationships Between the Ash Concentrations of HNO₃ and HCl Acid-Washed Biomass Samples with Char Reactivity	111
5.17	Summary of the Effects of HNO₃ and HCl Acid-Washing on Biomass Sample Characteristics and Char Characteristics	111
Chapter 6	<i>Experimental Results - RDF Materials</i>	
6.1	Analytical Data for the Raw, HNO₃ and HCl Acid-Washed RDF Samples	148
6.1.1	Proximate and Ultimate Analyses of RDF Samples	148
6.1.2	Proximate and Ultimate Analyses of HNO ₃ and HCl Acid-Washed RDF Samples	149
6.1.3	Ash Analyses of Raw, HNO ₃ and HCl Acid-Washed RDF Samples	149
6.2	Analytical Data for Chars Prepared from of Raw, HNO₃ and HCl Acid-Washed RDF Samples	150
6.2.1	Char Yields and Ultimate Analyses Data of Raw, HNO ₃ and HCl Acid-Washed RDF Sample Chars	150
6.2.2	Relationships Between the Char Yields with the Raw Sample and Char Characteristics for the Untreated, HNO ₃ and HCl Acid-Washed RDF Materials	150
6.3	Reactivity Measurements of Raw, HNO₃ and HCl Acid-Washed RDF Samples	151
6.4	BET Surface Area Determination of Raw, HNO₃ and HCl Acid-Washed RDF Sample Chars	151
6.4.1	Relationships Between Char Surface Area with Precursor Characteristics and Char Reactivities for the Raw, HNO ₃ and HCl Acid-Washed RDF Samples	152
6.5	Relationships Between the Ash Compositions of Raw, HNO₃ and HCl Acid-Washed RDF Sample Chars and their Reactivity in Oxygen	152
6.6	Summary of the Effects of HNO₃ and HCl Acid-Washing on the RDF Samples	153
6.7	Analytical Data of the RDF Model Composites	154
6.7.1	Proximate and Ultimate Analyses of RDF Model Composites	154
6.8	Analytical Data of the Chars Prepared from RDF Model Composites	155

6.8.1	RDF Model Composites Char Yields and Char Proximate and Char Ultimate Analyses	156
6.9	Thermal Decomposition Analyses of RDF Model Composites	157
6.10	Reactivity Measurements of RDF Model Composites Chars in Oxygen	159
6.11	BET Surface Area Determination of RDF Model Composite Sample Chars	160
6.12	Summary of RDF Model Composites Experimental Results	161
<u>Chapter 7</u>	<i>Discussion</i>	
7.1	Discussion	182
7.2	The Influence of the Basic Characteristics of Biomass and Wastes on their Behaviour in Industrial Fuel Handling and Gasification Systems	183
7.3	The Behaviour of Biomass and Waste Materials During Pyrolysis Reactions	187
7.4	The Isothermal Reactivities of Chars Prepared from Biomass and Waste Materials in Oxygen and the Kinetics of these Reactions	188
7.5	The Influence of Mineral Matter on the Behaviour of Biomass and Waste Materials During Pyrolysis and the Reactivities of the Resultant Char Materials	192
7.6	The Effects of Component Interaction on Pyrolysis Behaviour and Resultant Char Characteristics for RDF Materials	194
7.7	The Relevance and Application of Results to Industrial-Scale Biomass and Waste Gasification Systems	198
	References	213
<u>Chapter 8</u>	<i>Conclusion</i>	
8.1	Biomass Materials	216
8.1.1	Basic Analyses of the Biomass Materials	216
8.1.2	Biomass Char Materials	217
8.1.3	Biomass Char Surface Area	218
8.1.4	Biomass Char Isothermal Reactivity in Oxygen	218
8.1.5	The Effects of Acid Washing on the Biomass Samples and Resultant Char Behaviour	220
8.2	Refuse Derived Fuels and Refuse Derived Fuel Model Compounds	221

8.2.1	Basic Analyses Data of Untreated and Acid-Washed Refused Derived Fuel Materials	221
8.2.2	Untreated and Acid-Washed Refuse Derived Fuel Material Char Analyses and Reactivity Results	222
8.2.3	Refuse Derived Fuel and Model Composites of RDF Components	222
8.2.4	Effectiveness of the Synthetic Blends at Modelling Refuse Derived Fuel Behaviour During Thermal Processing and Resultant Char Characteristics	224
	Future Work	226

List of Tables

Chapter 1 *Introduction*

- 1.1 Operating Conditions of Air-Blown Gasification Systems 8**

Chapter 2 *Literature*

- 2.1 Composition of Selected Plant Types 46**
- 2.2 Typical Ash Contents of Various Plants 46**
- 2.3 Ash Composition of Various Tree Types 47**
- 2.4 Ash Composition of Various Straw Types 48**
- 2.5 Average Category Assay of Typical British Refuse 49**
- 2.6 Category Assay and Gross Calorific Value of Pelletised RDF 50**
- 2.7 Average Distribution of Plastic Material in RDF 51**
- 2.8 Typical Components of RDF Ash 52**
- 2.9 Product Distribution from Slow Biomass Pyrolysis 52**

Chapter 5 *Experimental Results - Biomass Materials*

- 5.1 Basic Analytical Data for the Biomass Samples 113**
- 5.2 Ash Analysis Data for the Biomass Samples 114**
- 5.3 The Char Yields, Char Ash Contents and the Ultimate Analysis of Chars Prepared from the Biomass Samples at 10 K min⁻¹ to 1173 K in a Nitrogen Atmosphere 115**
- 5.4 The Temperatures for the Peak Rate of Weight Loss Associated with Moisture Loss, Devolatilisation, and Char Burn-out for the Biomass Materials 116**
- 5.5 The Reactivity Data for Chars Prepared from the Biomass Samples at 10 K min⁻¹ to 1173 K in a Nitrogen Atmosphere 116**

5.6	The BET Surface Area Data for Chars Prepared from the Biomass Samples at 10 K min ⁻¹ to 1173 K in a Nitrogen Atmosphere	117
5.7	The Proximate and Ultimate Analysis Data for the Untreated, and HNO ₃ and HCl Acid-Washed Biomass Samples	117
5.8	The Ash Analysis Data for the Untreated and HNO ₃ and HCl Acid-Washed Biomass Samples	118
5.9	The Char Yields, Char Ash Contents and Ultimate Analysis Data for Chars Prepared from the Untreated, and HNO ₃ and HCl Acid-Washed Biomass Samples at 10 K min ⁻¹ to 1173 K in a Nitrogen Atmosphere	119
5.10	The Temperatures for the Peak Rate of Weight Loss Associated with Moisture Loss, Devolatilisation, and Char Burn-out for the Untreated, and HNO ₃ and HCl Acid Washed Biomass Samples	120
5.11	The Reactivity Data for Chars Prepared from the Untreated, and HNO ₃ and HCl Acid-Washed Biomass Samples at 10 K min ⁻¹ to 1173 K in Nitrogen Atmosphere	120
5.12	The BET Surface Area Data for Chars Prepared from the Untreated, and HNO ₃ and HCl Acid-Washed Biomass Samples Prepared at 10 K min ⁻¹ to 1173 K in a Nitrogen Atmosphere	121

Chapter 6 *Experimental Results - RDF Materials*

6.1	Analytical Data for the Raw and Acid-Washed Byker and Isle of Wight RDF Samples	163
6.2	Ash Analyses Data for the Raw and Acid-Washed Byker and Isle of Wight RDF Samples	164
6.3	The Char Yields, Char Ash Contents and Ultimate Analysis of Chars Prepared from the Raw and Acid Washed Byker and Isle of Wight RDF Samples at 10 K min ⁻¹ to 1173 K in a Nitrogen Atmosphere	165
6.4	The Reactivity Data of Chars Prepared of Chars Prepared from the Raw and Acid Washed Byker and Isle of Wight RDF Samples at 10 K min ⁻¹ to 1173 K in a Nitrogen Atmosphere	166
6.5	BET Surface Area Data of Chars of Chars Prepared from the Raw and Acid Washed Byker and Isle of Wight RDF Samples at 10 K min ⁻¹ to 1173 K in a Nitrogen Atmosphere	166
6.6	The Proximate Analyses Data for Cellulose, Poly(ethene), PVC, Saran, Straw and the Composite Mixtures	167

6.7	The Ultimate Analyses Data for Cellulose, Poly(ethene), PVC, Saran, Straw and the Composite Mixtures	168
6.8	The Char Yields, Expected Char Yields and Ultimate Analyses Data for Chars Prepared from Cellulose, Poly(ethene), PVC, Saran, Straw and the Composite Mixtures at 10 K min⁻¹ to 1173 K in Nitrogen Atmosphere	169
6.9	The Temperatures for the Peak Rate of Weight Loss Associated with Moisture, Devolatilisation and Char Burn-out for Cellulose, Poly(ethene), PVC, Saran, Straw and the Composite Mixtures	170
6.10	The Reactivity Data for Chars Prepared from Cellulose, Poly(ethene), PVC, Saran, Straw and the Composite Mixtures at 10 K min⁻¹ to 1173 K in Nitrogen Atmosphere	171
6.11	The BET Surface Area Data for Chars Prepared from Cellulose, Poly(ethene), PVC, Saran, Straw and the Composite Mixtures at 10 K min⁻¹	172

Chapter 7 Discussion

7.1	Comparitive Physical Characteristics and Handling and Processing Requirements of Fossil Fuels and Biomass and Waste Materials	202
7.2	Proximate Analysis Data and 900 °C (1173 K) Char Yields for Biomass and Selected Coals	203
7.3	Calculated Rate Data and Reaction Order Values for Silsoe Sap Char Isothermal Reaction in Oxygen	204
7.4	Rate Constant Values and Linear Correlation Coefficients for Long Ashton and Silsoe Material Char Reaction in O₂ Over the Temperature Range 280-440 °C (553-713 K)	205
7.5	Arrhenius Data, Data Correlation Coefficients and Measured Isothermal Reactivity Values for Long Ashton and Silose Sample Chars	206
7.6	Experimental and Theoretical Fixed Carbon and Char Yields, and Measured Char Isothermal Reactivity Values for RDF Models and Components	207
7.7	The Char Yield Data and Char Reactivity Data for the Untreated and Acid-Washed Byker and Isle of Wight RDF and the RDF Model Blends	208

List of Figures

Chapter 1 Introduction

- 1.1 Diagrams of Gasification Reactor Systems 9**

Chapter 2 Literature

- 2.1 Linear Relationship Between the Reactive Surface Area and the Volatile Matter Content of Five Coals Ranging From Anthracite to Lignite 53**
- 2.2 Relationship Between the Reactivity and Reactive Surface Area for a Series of Demineralised Coal Chars, a PVDC Char and an Electrode Carbon Lignite 53**
- 2.3 Temperature Dependence of the Gasification Reaction Rates of a Range of Char Materials in Steam 54**
- 2.4 Intrinsic Reaction Rate as a Function of Reaction Temperature in an Arrhenius Form 54**
- 2.5 Illustration of Zig-Zag and Armchair Lammella Edge Structures 55**
- 2.6 Illustration of the Relationship Between the Wetting Tendency of a Catalyst and the Mode of Catalytic Attack 55**
- 2.7 Structure of Cellulose (Haworth Projection) 56**
- 2.8 Structure of Hemicellulose in Softwoods 56**
- 2.9 Structure of Hemicellulose in Hardwoods 57**
- 2.10 Precursors of Lignin Biosynthesis 57**
- 2.11 An Example of a Particular Lignin Structure, that of a Normal Conifer Wood 58**
- 2.12 Reaction Pathway for Cellulose Pyrolysis/Combustion 58**
- 2.13 Model for Cellulose Pyrolysis and Product Transformation 59**
- 2.14 Kilzer and Broido Proposed Model for Cellulose Pyrolysis 59**
- 2.15 Agrawal Proposed Model for Cellulose Pyrolysis 60**

Chapter 4 *Experimental*

- | | | |
|-----|--|----|
| 4.1 | Illustration of Stanton Redcroft TGA750 TGA and Data Recording Equipment | 88 |
| 4.2 | Normalised Weight Loss Profile of Cellulose, Heated at 10 K min⁻¹ from 293-1173 K | 88 |
| 4.3 | First Derivative Graph of Weight Loss Profile of Cellulose, Heated at 10 K min⁻¹ from 293-1173 K | 89 |
| 4.4 | Illustration of Stanton Redcroft Tube Furnace and Eurotherm Type 812 Controller Used for Char Preparation | 89 |
| 4.5 | Graph of Isothermal Weight Loss for a Sample Char | 90 |
| 4.6 | Illustration of Micromeritics Acusorb 2100E BET Surface Area Analysis Equipment Manifold | 90 |

Chapter 5 *Experimental Results - Biomass Materials*

- | | | |
|------|--|-----|
| 5.1a | The Biomass Sample Char Yields Plotted Against Fixed Carbon Contents of the Parent Materials | 122 |
| 5.1b | The Char Yields for the Fractionated Silsoe Samples Plotted Against their Fixed Carbon Contents | 122 |
| 5.2 | The Char Yields of the Biomass Materials Plotted Against the Carbon Content | 123 |
| 5.3a | The Biomass Char Carbon Content Plotted Against the Char Yields | 123 |
| 5.3b | The Silsoe Fractionated Sample Char Carbon Contents Plotted Against the Char Yields | 124 |
| 5.4a | The Biomass Sample Char Nitrogen Content Plotted Against Char Yields | 124 |
| 5.4b | The Fractionated Silsoe Samples Char Nitrogen Content Plotted Against their Char Yields | 125 |
| 5.5a | The Retained Nitrogen in Biomass Chars Plotted Against the Char Yields | 125 |
| 5.5b | The Fractionated Silsoe Samples Retained Nitrogen in Char Plotted Against the Char Yields | 126 |
| 5.6 | The Weight Loss Profile of Straw, Heated at 10 K min⁻¹ from 293-1173 K, Normalised for Ash Content | 126 |

5.7	The First Derivative Weight Loss Profile of Straw (-dWt/dT), Heated at 10 K min ⁻¹ from 293-1173 K, Normalised for Ash Content	127
5.8	The Biomass Sample Chars Isothermal Reactivity in O ₂ (3 l h ⁻¹) Data in the Temperature Range 553-713 K	127
5.9a	The Biomass Sample Chars Isothermal Reactivities in O ₂ (3 l h ⁻¹) at 613 and 633 K, Plotted Against the Fixed Carbon Contents of the Parent Materials	128
5.9b	The Fractionated Silsoe Sample Chars Isothermal Reactivities in O ₂ (3 l h ⁻¹) at 613 and 633 K, Plotted Against Sample Fixed Carbon Contents	128
5.10	The Biomass Chars Isothermal Reactivities in O ₂ (3 l h ⁻¹) at 613 and 633 K, Plotted Against the Carbon Contents of the Parent Materials	129
5.11a	The Biomass Chars Isothermal Reactivities in O ₂ (3 l h ⁻¹) at 613 and 633 K, Plotted Against Char Yield	129
5.11b	The Isothermal Reactivities in O ₂ (3 l h ⁻¹) at 613 and 633 K, of the Chars Prepared from the Fractionated Silsoe Samples, Plotted Against Char Yield	130
5.12a	The Isothermal Reactivities in O ₂ (3 l h ⁻¹) at 613 and 633 K, of all the Biomass Chars, Plotted Against the Char Carbon Content	130
5.12b	The Isothermal Reactivities in O ₂ (3 l h ⁻¹) at 613 and 633 K, of the Chars Prepared from the Fractionated Silsoe Samples, Plotted Against the Char Carbon Content	131
5.13a	The Surface Areas of the Biomass Chars Plotted Against the Fixed Carbon Content of the Parent Materials	131
5.13b	The Surface Areas of the Chars Prepared from the Fractionated Silsoe Samples Plotted Against the Fixed Carbon Content of the Parent Materials	132
5.14	The Carbon Content of the Biomass Chars Plotted Against Char Surface Area	132
5.15a	The Surface Areas of the Biomass Chars Plotted Against Char Yield	133
5.15b	The Surface Areas of the Chars Prepared from the Fractionated Silsoe Samples Plotted Against Char Yield	133
5.16a	The Surface Areas of the Biomass Chars Plotted Against Char Carbon Contents	134
5.16b	The Surface Areas of the Chars Prepared from the Fractionated Silsoe Samples Plotted Against Char Carbon Contents	134

5.17	The Isothermal Reactivities in O₂ (3 l h⁻¹) at 613 and 633 K of the Biomass Chars, Plotted Against Char Surface Areas	135
5.18a	The Biomass Fixed Carbon Contents Plotted Against Ash Content	135
5.18b	The Fixed Carbon Contents of the Fractionated Silsoe Samples Plotted Against Ash Content	136
5.19a	The Yields of Char Prepared from the Biomass Materials Plotted Against Ash Content	136
5.19b	The Yields of Char Prepared from the Silsoe Fractionated Materials Plotted Against Ash Content	137
5.20a	The Biomass Chars Carbon Content Plotted Against Ash Content	137
5.20b	The Carbon Content of the Chars Prepared from the Fractionated Silsoe Materials Plotted Against Ash Content	138
5.21	The Isothermal Reactivities in O₂ (3 l h⁻¹) at 613 and 633 K, of the Chars Prepared from the Biomass Samples, Plotted Against the Char Ash Content	138
5.22	The Isothermal Reactivities in O₂ (3 l h⁻¹) at 613 and 633 K, of the Chars Prepared from the Biomass Samples, Plotted Against the Char CaO Content	139
5.23	The Char Yields Plotted Against Fixed Carbon Content for the Untreated and Acid-Washed Straw and Danish Pine Samples	139
5.24	The Char Carbon Contents Plotted Against Char Yields for the Untreated and Acid-Washed Straw and Danish Pine Samples	140
5.25	The Char Nitrogen Contents Plotted Against Char Yield for the Untreated and Acid-Washed Straw and Danish Pine Samples	140
5.26	The Isothermal Reactivity in O₂ (3 l h⁻¹), in the Temperature Range 613 to 733 K, of the Chars Prepared from the Untreated and Acid-Washed Biomass Samples	141
5.27	The Isothermal Reactivity in O₂ (3 l h⁻¹) at 633 K, of the Chars Prepared from the Untreated and Acid-Washed Biomass Samples Plotted Against Fixed Carbon Content	141
5.28	The Isothermal Reactivity in O₂ (3 l h⁻¹) at 633 K, of the Chars Prepared from the Untreated and Acid-Washed Biomass Samples Plotted Against Char Yield	142
5.29	The Isothermal Reactivity in O₂ (3 l h⁻¹) at 633 K, of the Chars Prepared from the Untreated and Acid-Washed Biomass Samples Plotted Against Char Carbon Content	142

5.30	The Surface Areas of the Chars Prepared from the Untreated and Acid-Washed Biomass Samples Plotted Against Fixed Carbon Content	143
5.31	The Surface Areas of the Chars Prepared from the Untreated and Acid-Washed Biomass Samples Plotted Against Char Yield	143
5.32	The Surface Areas of the Chars Prepared from the Untreated and Acid-Washed Biomass Samples Plotted Against Char Carbon Content	144
5.33	The Isothermal Reactivity in O ₂ (3 l h ⁻¹) at 633 K of the Chars Prepared from the Untreated and Acid-Washed Biomass Samples Plotted Against Char Surface Area	144
5.34	The Fixed Carbon Contents of the Untreated and Acid-Washed Biomass Samples Plotted Against Ash Content	145
5.35	The Yields of Char Prepared from the Untreated and Acid-Washed Biomass Samples Plotted Against Ash Content	145
5.36	The the Untreated and Acid Washed Biomass Sample Char Carbon Contents Plotted Against Ash-Content	146
5.37	The Isothermal Reactivity in O ₂ (3 l h ⁻¹) at 633 K, of the Chars Prepared from the Untreated and Acid Washed Biomass Samples Plotted Against Ash Content	146
5.38	The Isothermal Reactivity, in O ₂ (3 l h ⁻¹) at 633 K, of the Chars Prepared from the Untreated and Acid-Washed Biomass Samples Plotted Against Char CaO Content	147

Chapter 6 *Experimental Results - RDF Materials*

6.1	The Raw and Acid-Washed Byker and Isle of Wight RDF Sample Char Yields Plotted Against Fixed Carbon Contents	173
6.2	The Raw and Acid-Washed Byker and Isle of Wight Sample Char Yields Plotted Against Sample Carbon Contents	173
6.3	The Raw and Acid-Washed Byker and Isle of Wight Sample Char Carbon Contents Plotted Against Char Yield	174
6.4	The Raw and Acid-Washed Byker and Isle of Wight RDF Sample Chars Isothermal Reactivity in O ₂ (3 l h ⁻¹) from 633 and 793 K	174
6.5	The Raw and Acid-Washed Byker and Isle of Wight Sample Surface Area Data Plotted Against Fixed Carbon Contents	175
6.6	The Raw and Acid-Washed Byker and Isle of Wight Sample Char Surface Area Data Plotted Against Char Yield	175

6.7	The Raw and Acid-Washed Byker and Isle of Wight Sample Char Reactivity in O ₂ (3 l h ⁻¹) Data at 683 K Plotted Against Char Surface Area	176
6.8	The Raw and Acid-Washed Byker and Isle of Wight Sample Char Reactivity in O ₂ (3 l h ⁻¹) Data at 683 K Plotted Against Char Ash Content	176
6.9	The Raw and Acid-Washed Byker and Isle of Wight Sample Char Reactivity in O ₂ (3 l h ⁻¹) Data at 683 K Plotted Against Char CaO Content	177
6.10	The Char Yield Data for Cellulose, Poly(ethene), PVC, Saran, Straw and Composite Blends Plotted Against Fixed Carbon Contents	177
6.11	The Isothermal Char Reactivity in O ₂ (3 l h ⁻¹) Data at 653 K Against Char Yields for Cellulose, Poly(ethene), PVC, Saran, Straw and Composite Blends	178
6.12	The Isothermal Char Reactivity in O ₂ (3 l h ⁻¹) from 653 to 713 K for PVC, Cellulose and Composite Blends	178
6.13	The Isothermal Char Reactivity in O ₂ (3 l h ⁻¹) from 633 to 663 K for Straw, PVC and Composite Blends	179
6.14	The Isothermal Char Reactivity in O ₂ (3 l h ⁻¹) from 653 to 713 K for Saran, Cellulose and Composite Blends	179
6.15	The Char Surface Area Data for PVC, Cellulose and Composite Blends	180
6.16	The Char Surface Area Data for Straw, PVC and Composite Blends	180
6.17	The Char Surface Area Data for Saran, Cellulose and Composite Blends	181

Chapter 7 Discussion

7.1	The Isothermal Weight Loss for Silsoe Sap 900 °C (1173 K) Char Reacting in Oxygen (3 l h ⁻¹) at 380 °C (653 K)	209
7.2	Plot of -ln(Wt/Wo) Plotted Against Time for Silsoe Sap 900 °C (1173 K) Char Isothermal Reaction in Oxygen at 440 °C (713 K)	209
7.3	Plot of ln(Rate Constant) Data Plotted Against (Temperature) ⁻¹ for the Silsoe Sap 900 °C (1173 K) Char Isothermal Reactions in the Temperature Range 340-440 °C (613-713 K)	210

- 7.4 **Plot of the 900 °C (1173 K) Char Isothermal Reactivities in Oxygen Data Determined at 340 and 360 °C (613 and 633 K) Plotted Against the Determined Char Activation Energy Data for the Long Ashton and Silsoe Materials** 210
- 7.5 **Plot of the 900 °C Char Isothermal Reactivity in Oxygen Determined at 360 °C (633 K) Versus Char SiO₂ Concentration for the Long Ashton and Silsoe Materials** 211
- 7.6 **Plot of the 900 °C (1173 K) Char Isothermal Reactivity in Oxygen Determined at 360 °C (633 K) Versus Char K₂O Concentrations for the Long Ashton and Silsoe Materials** 211
- 7.7 **Plot of the Activation Energies for Char Isothermal Reaction in Oxygen in the Temperature Range 340-440 °C (613-713 K) Versus Char CaO Concentration for Long Ashton and Silsoe Materials** 212
- 7.8 **Plot of the 900 °C (1173 K) Char Isothermal Reactivity in Oxygen at 360 °C (633 K) Versus Char CaO Concentrations for Untreated and Acid Washed Biomass Materials** 212

Acknowledgements

This work was completed under an SERC CASE award grant and was sponsored by Mitsui Babcock Energy Limited.

I would like to thank Professor Colin Snape and Dr Peter Hall of the Applied Chemistry Department at Strathclyde University for their assistance and guidance during this study, and also Sandy MacKinnon, Bernie Kelly, Stuart Mitchell, Carol McArthur, Frazer Norton, Brian McGhee, Gordon Love, Shona Martin, Khudzir Ismail, and Mirari Antxustegi for making my time in the laboratory an extremely enjoyable one. Michael Ross will always be remembered for his lunchtime companionship and frequent nights out. Technical assistance was gratefully received from Betty and Geoff in the Plant Laboratory, Margaret in the Micro-analytical Laboratory, and Pat Keating in the Fuel Laboratory.

I would also like to express my gratitude to Dr Bill Livingston, my industrial supervisor at Mitsui Babcock who devoted much time to guiding me through the writing of this thesis and ensuring that it was legible, and Margaret McFarlane for the typing of this thesis. The technical aid and expertise of Joe McLaughlan, Billy McSkimming and John Connell from the Fuels Laboratory was invaluable.

In addition, I would also like to acknowledge with thanks Mr N. Barker (ETSU), Mr T. Rampling (ex-Warren Springs) and Dr Samantha Cooke (former Ph.D. student at Imperial College, London) for the provision of samples, data and technical information.

Finally, I would like to thank my family, my parents Frank and Joan, my brother Paul, my sister Laura and my gran Maisie Harris for all their love support and kindness. This thesis is dedicated to them.

Abstract

The project described in this document is concerned with an experimental study, at laboratory scale, of the characteristics and behaviour of a range of biomass and waste materials, relevant to their utilisation as fuels in gasification systems. The range of fuels studied includes the biomass materials, cereal straw, short rotation coppice wood and pine round wood, and refuse derived fuels (RDF). These materials are increasingly being employed as renewable alternatives to fossil fuels in industrial energy conversion plants in Europe and elsewhere.

Chars were prepared from all of the materials at a temperature increase rate of 10 K min^{-1} to a final temperature of 1173 K ($900 \text{ }^\circ\text{C}$), in a N_2 atmosphere. The biomass materials gave yields of char in the range 22-29 % (dry, ash free) and relationships were found which indicated that the char yield values increased linearly both with increasing carbon content and also increasing ash content of the parent material. The isothermal reactivities of these chars were measured in a flowing O_2 atmosphere over the temperature range 553-713 K. A study of the influence of the ash on char reactivities indicated that the reactivity increased linearly with increasing ash content, the straw char being the sole exception to this. The reactivities of all the chars were found to increase linearly with increasing char CaO concentration.

The results of a standard kinetic analysis of the biomass char oxidation data indicated that the reaction is approximately first order with respect to the carbon concentration, and the activation energy values of the chars, derived using the Arrhenius equation, were in the range $91\text{-}137 \text{ kJ mole}^{-1}$. These values are typical of these types of highly disordered and impure carbonaceous materials. The influence of CaO content on char activation energy was also investigated and an excellent non-linear relationship was found which indicated that the char activation energy decreased with increasing CaO content.

The effects of mineral constituents on the behaviour of biomass materials was further studied by subjecting cereal straw and pine wood samples to acid washing in both 1 M HNO_3 and HCl solutions. The ash contents were reduced in all cases and the resultant char yields and char reactivity were significantly lower than those of the parent materials.

When plotted on the char reactivity-CaO content curve, the acid washed material values fitted the correlation for the untreated biomass materials.

An attempt was made to reproduce the behaviour of the RDF materials by preparing model composites containing mixtures of cellulosic materials and poly(ethene), PVC and Saran. The results indicated that char yields and char characteristics were influenced by component interactions during the pyrolysis process, with the presence of chlorine having a significant effect. The char yields of mixtures containing chlorinated polymers were found to be higher than expected from simple additive behaviour. There was evidence that the char yields and char reactivities were influenced by the behaviour of the polymers during pyrolysis and also by ash components of the mixture.

Chapter One

Introduction

1.1 Background

The potential benefits of the introduction of a higher level of renewable and sustainable energy production in reducing the dependence on fossil fuels are clear and obvious. The detrimental effects of fossil fuel use on the environment⁽¹⁻⁸⁾ and on human health^(9,10) have been well documented. The use of biomass and waste materials, in particular, is CO₂ neutral, and the conversion of these materials to usable energy forms, making use of modern technologies, is normally associated with lower levels of releases of environmentally-damaging species to air, land and water than are conventional energy supply systems and the current approaches to the disposal of wastes⁽¹¹⁾. This is beginning to be recognised at the highest political levels in most developed countries, and it is clear that, with some level of government financial assistance, at least in the short term, biomass and waste-to-energy projects will have an increasingly important role to play. Several estimates of the exploitable biomass and waste resources in Europe and elsewhere have been published in recent years^(4,11,12,15), and it is becoming clear that by the early years of the next century, up to around 5 % or so of the total electricity supply in Europe could be generated from biomass and waste, although the actual contribution will vary enormously from region to region, and there is clearly a great deal of

uncertainty about the level and the pace of the market development in specific technologies.

The size and type of individual projects for energy production are likely to vary widely, depending on local conditions and requirements, however a number of generalised scenarios can be identified, viz;

- (a) The development of small-scale farm-based projects providing local heat and/or electricity at up to 1 MWe ($1 \text{ MWe} \equiv 1 \times 10^6 \text{ J s}^{-1}$, effective energy value after all cycle losses) or so, based on waste materials or specific energy crops.
- (b) The development of medium-sized projects in the range 1-10 MWe operated by local farmer co-operatives or small local companies, providing electricity and/or heat.
- (c) Large projects up to 50 MWe based on purpose-built biomass or waste energy conversion plants, generating electricity as the main product but also, in some cases, with some heat production.
- (d) The co-conversion of biomass and waste materials with conventional fuels in large power plants.

The biomass and waste materials which are utilised in these projects will vary from region to region, however, in Northern European countries the principal materials will be;

- Wood wastes of various types, i.e. forestry, sawmill and demolition wastes,
- Dry agricultural wastes, principally cereal, oil seed rape and linseed straws,
- Domestic and industrial, non-hazardous dry wastes,
- Municipal, agricultural and industrial sludges, and

- Specific energy crops.

In this document, the concern is with some of the more important biomass and waste materials which are suitable as fuels for both combustion and gasification based energy production processes.

(a) Wood

There are several possible sources of wood material which can be identified, viz;

(i) Forestry Residues and Sawmill Wastes^(13,14).

Forestry wastes arise from harvesting and thinning operations where the residue materials can be collected and processed into a chipped form, suitable for transportation. The material usually has a high moisture content, typically around 50%, and this can cause a deterioration in the physical quality of material, when it is stored for extended periods of time, with an accompanied release of pathogens and loss of dry matter through respiration. The material has a low ash content if clean, however it can be contaminated with tramp materials which may affect processing.

Sawmill Waste. This is a relatively clean material, with variable moisture content and low ash content. It is usually available in the form of sawdust and chipped off-cuts.

(ii) Demolition Waste⁽¹⁵⁾

This material is generated from demolition activities and significant supplies are available from the major centres of population. The wood is generally dry, typically < 20 % moisture, however, it can contain significant quantities of tramp material such as nails, staples, wire, and masonry, which can give rise to problems in processing plant. The construction wood is normally treated with chemicals and this is regarded as a significant issue when these materials are burned or

gasified in energy generation plants. In a number of European countries demolition wood is regarded as being a hazardous waste material.

(iii) Short Rotation Coppice⁽¹⁴⁾

SRC is a specific form of energy crop, normally of willow and poplar tree species, harvested on a 3 year cycle. The harvesting operation, which yields 10-12 dry tonnes per hectare per year, is performed in winter to minimise nutrient losses. Normally 6-7 cycles are obtained from a single root stock. The material generated has high moisture content (40-60 %), and low ash content.

(b) Straw⁽¹⁶⁾

Straw is generated during the harvesting of cereals and other arable crops. In Britain around 14 million tonnes of straw are harvested each year of which, 6-7 million tonnes are currently used as components of animal feed, animal bedding, mulch or compost. Straw is a relatively dry material, containing 10-20 % moisture. It also has low sulphur and ash contents. There is potential for the use of surplus straw as a significant source of fuel in the short term, since there is an established infrastructure for its collection and supply. The material has however, a low bulk density and is difficult to handle and process.

(c) Municipal Solid Waste⁽¹⁷⁾

Municipal Solid Waste (MSW) is a heterogeneous material which is collected from residential areas, commerce and industry, and there are current annual arisings of around 30 million tonnes in the UK. The major components of MSW are paper and paperboard. It also has a relatively high moisture content of ~ 33 %, a high ash content of ~28 %, with a low GCV of 9-10 MJ kg⁻¹ (as received)⁽¹⁸⁾. In Britain, more than 90 % of this material is sent directly to landfill disposal, however this is becoming increasingly expensive and unpopular. An alternative disposal process, which is practised in the UK, and can handle untreated MSW, is mass burn incineration in purpose-built plant. These plants are large robust

installations incorporating specialised materials handling equipment and grate combustion systems. They are relatively expensive to built and operate, and are subject to increasingly stringent environmental control legislation.

One alternative to mass burn incineration is to pretreat the waste prior to combustion to produce a Refuse Derived Fuel (RDF)⁽¹⁹⁾ which can be handled and combusted using more conventional equipment. The pre-treatment process involves screening to remove fines (< 10 mm), putrescibles and miscellaneous non-combustibles, and magnetic ferrous metal removal to produce a material containing half the original mass, which can retain in excess of 80 % of the original heat content, depending on the extent of processing. The reject material from RDF processing is sent for landfill disposal.

Two basic types of RDF are produced⁽¹⁹⁾:

- (i) coarse (floc) RDF with a weight yield in excess of 50 %, produced by screening, ferrous metal extraction and coarse shredding, and
- (ii) pelletised (densified) and dried RDF with a weight yield of less than 50 %, which involves a high degree of sorting and pre-treatment.

The pelletised form of RDF has a relatively low moisture content (~ 8 %), a greatly reduced ash content of ~ 13 % and an enhanced calorific value of ~ 19 MJ kg⁻¹. This material can be combusted using relatively conventional equipment.

The principal energy conversion processes relevant to the utilisation of biomass and waste materials are⁽²⁰⁾:

- (a) processes involving combusting the material either as a pulverised fuel, in a fluidised bed or on a grate, depending on the physical characteristics of the fuel and the scale of operation.
- (b) gasification and pyrolysis processes.

In this study, the emphasis is on the gasification of biomass and wastes to produce a fuel gas for combustion in a furnace or kiln or in a modified gas turbine or engine.

Gasification is the conversion by partial oxidation at temperatures in excess of 600 °C of a carbonaceous material to produce a fuel gas consisting of carbon monoxide, some carbon dioxide, hydrogen, methane, trace amounts of higher hydrocarbons such as ethane and ethene, water, and various contaminants such as small char particles, ash, tars and oils. This process can be carried out using air, oxygen, steam, or a mixture of these, as gaseous reactants. For biomass and waste materials, the most conventional approach is air blown gasification at atmospheric pressure or at pressures up to 2.5 MPa (25 bar)⁽²¹⁻²³⁾.

The choice of gasification technology is generally dictated by the scale of operation. For small scale plants, below 1 tonne per hour throughput, fixed bed gasifiers are more commonly used. For larger applications, systems based on fluid bed gasification are employed. The fixed bed reactor systems tend to be more restricted on the physical characteristics of the fuel because of the requirement to maintain a stable bed structure. Fluid bed systems are much more flexible in terms of feedstock quality. The operating conditions of the various types of gasifiers, in air-blown applications, are presented in Table 1.1, and diagrams of the gasifier types are presented in Figure 1.1.

Most of the commercially available gasification technologies, which are relevant to the processing of biomass and waste materials, are based on fixed bed and fluidised bed processes, which were originally developed for the gasification of coal. The application of these technologies to the gasification of biomass and waste requires both equipment and process modifications, depending on the physical and chemical composition of the fuel. The work described in this document is concerned with the fundamental study, at laboratory scale, of the characteristics and behaviour of a range of biomass and waste materials, relevant to their utilisation as fuels in the gasification processes. The basic fuel characteristics of the materials have been

studied, and related to the char yields in pyrolysis processes and the characteristics of the resultant chars. The kinetics of the char oxidation reactions at low temperatures and the influence of the ash components of the biomass materials have been studied. The behaviour of the more complex waste and RDF materials have been studied using simple models containing chlorinated and non-chlorinated polymers.

FIXED BED SYSTEMS						
<i>Reactor</i>	<i>Reaction Temp °C</i>	<i>Exit Gas Temp °C</i>	<i>Tars</i>	<i>Particulates</i>	<i>Max-Size (t h⁻¹)</i>	<i>Min-Size (t h⁻¹)</i>
Downdraft	1000	800	v.low	mod	0.5	0.1
Updraft*	1000	250	v.high	mod	10	1
Cross Current	900	900	v.high	high	1	0.1

FLUIDISED BED SYSTEMS						
<i>Reactor</i>	<i>Reaction Temp °C</i>	<i>Exit Gas Temp °C</i>	<i>Tars</i>	<i>Particulates</i>	<i>Max-Size (t h⁻¹)</i>	<i>Min-Size (t h⁻¹)</i>
Single*	850	800	fair	high	10	1
Fast Fluid Bed*	850	850	low	v.high	20	2
Circulating Bed*	850	850	low	v.high	20	2
Entrained Bed*	1000	1000	low	v.high	20	5
Twin*	800	700	high	high	10	2

OTHER SYSTEMS						
<i>Reactor</i>	<i>Reaction Temp °C</i>	<i>Exit Gas Temp °C</i>	<i>Tars</i>	<i>Particulates</i>	<i>Max-Size (t h⁻¹)</i>	<i>Min-Size (t h⁻¹)</i>
Rotary Kiln	800	800	high	high	10	2
Cyclone*	900	900	low	v.high	5	1

(* denotes current maximum but capable of scaling to higher values)

Table 1.1 Operating Conditions of Air-Blown Gasification Reactor Systems

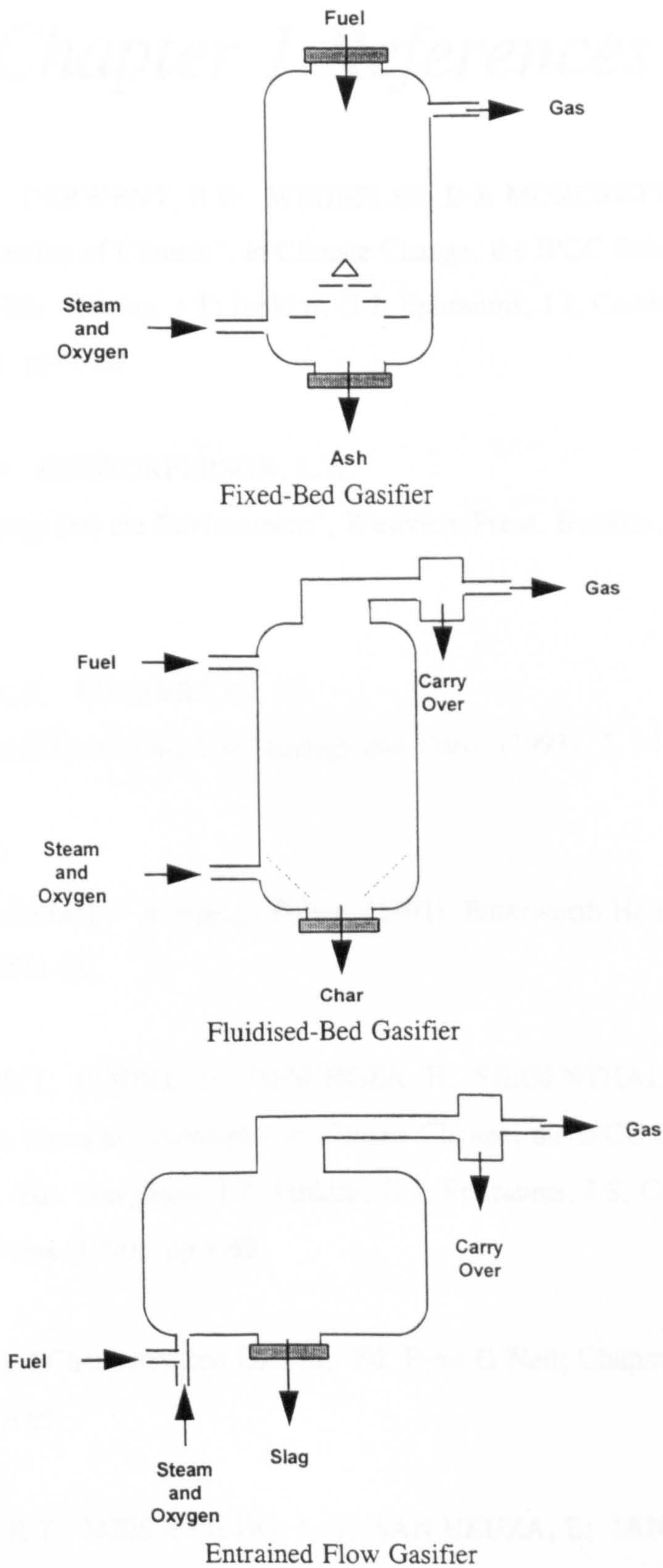


Figure 1.1 Diagrams of Gasification Reactor Systems

Chapter 1 References

1. SHIVE, K P; DERWENT, R G; WEUBBLES, D J; MORCLETTE, J J:
"Radiative Forcing of Climate", in Climate Change, the IPCC Scientific Assessment: Eds. Houton, J T; Jenkins, G J; Ephraums, J J; Cambridge University Press, (1990), pp41-68.
2. PASZTOR, J; KRISTORFERSON, L A:
Eds, "Bioenergy and the Environment", Westview Press, Boulder, CO, USA, (1990).
3. JUDKINS, R R; FULKERSON, W:
"The Dilema of Fossil Fuel Use" Energy and Fuels, (1993), 7, 14-22.
4. HALL, D O:
"Biomass and Energy" in Energy Policy, (1991), Buterworth Heinman Ltd., 0301-4215/91/080711-26.
5. WATSON, R T; RODHE, H; OESCHGER, H; SIEGENTHALER, V:
"Greenhouse Gases and Aerosols" in Climate Change, the IPCC Scientific Assessment: Eds. Haughton, J T; Jenkins, G J; Ephraums, J S; Cambridge University Press (1990), pp 1-40.
6. Environmental Chemistry 2nd Edition; Ed. Peter O'Neil; Chapman-Hall publishers, p 65.
7. WATSON, R T; MEIRA FILHO, L G; SAN HEUZA, E; JANETOS, A:
"Greenhouse Gases: Sources and Sinks", in Climate Change, the IPCC Scientific Assessment; Eds. Houghton, J T; Callander, B A; Varney, S K; Cambridge University Press, UK, (1992), pp 23-46.

8. KAUFMAN, Y J; FRASER, R S; MAHONEY, R L:
"Fossil Fuel and Biomass Burning Effect on Climate : Heating or Cooling?", *J Climate*, (1991), 4, pp 568-588.
9. SEARLE, C E:
Ed. "Chemical Carcinogens", ACS Monograph 173, American Chemical Society, Washington DC, (1976).
10. IRAC; IRAC "Monographs on the Evaluation of Carcinogenic Risks to Humans".
International Agency for Research on Cancer; Lyon, France, (1983-1989), vol 32-46.
11. JACKSON, T:
Renewable Energy - Summary of Papers for the Renewable Series; 0301-4215/92/090861-23, Butterworth Heineman Ltd, (1992).
12. HALL, D O:
Solar Energy; (1979), 22, 307.
13. MITCHELL, C P; MATHEWS, J D:
Forest Biomass as a Source of Energy in the UK : The Potential and the Practice; (1981), pp 239-43.
14. SPEDDING, C R W; BATHER, D M; WALSINGHAM, J M:
Fuel Crops - An Assessment of UK Potential; Rep No. 5. Watt Committee on Energy; (1979), London, pp 17-24.
15. BRIDGEWATER, A V:
"An Assessment of Thermochemical Conversion Systems for Processing Biomass and Refuse", ETS/B/T1/00207/REP, (Aston University), p 4.
16. *ibid* Ref 24, p 3.

17. **LANDY, M P:**
"Waste Derived Fuels - An Update; Combustion and Landfill Gas", Presented at 89th Annual Conference Institution of Waste Management, Torbay, UK, 16-19th June (1987).
18. **Emerging Technologies for Materials and Chemicals from Biomass; ACS Symposium Series, 476, Ch 23.**
19. **LIVINGSTON, W R: BIRCH, M C;**
"The Combustion of Pelletised Refuse-Derived Fuels", J of the Institute of Energy, (1990), 63, pp 151-159.
20. **BRIDGEWATER, A V:**
"Biomass Pyrolysis Technologies", Energy Research Group, Dept. Chem. Eng. Aston University, Birmingham B4 7ET, UK.
21. **HEDLEY, A:**
Gasification : Its Role in the Future Technological and Economic Development of the UK; Elsevier Applied Science Publishers, London (1989).
22. **MERRICK, D:**
"Coal Combustion and Conversion Technology", Coal Research Establishment. MacMillan, (1984).
23. "Clean Coal Technology - Options for the Future", A brochure published by ETSU on behalf of the IEA Committee on Energy Research and Technology.

Chapter Two

Literature

2.1 Introduction

The experimental work described in this document is concerned with the pyrolysis and gasification of biomass and waste materials. These reactions, i.e. the conversion of solid fuels into a gaseous product and a char residue, have been of significant importance for most of human history. The initial interest was in the production of char products from wood and coal i.e. cokes and charcoals principally for metallurgical and domestic uses. The earliest documented description of the production of a useful gaseous product was reported by *Felice Fontana* (1730-1805) who in 1780, noted that when a glowing coal was immersed in water it produced an ignitable gas⁽¹⁾.

Both the coke and gaseous products from the gasification of coal became of central importance during the 18th century. Charcoal was replaced by pit coal in blast furnaces, and the production of cokes and fuel gases for industrial and domestic utilisation became major industrial activities. For these reasons the pyrolysis and gasification of fuels, and in particular coal, have been very extensively studied and there is a substantial technical literature on these subjects. The commercial interest in the pyrolysis and gasification of biomass and waste materials is

relatively recent and is driven by environmental concerns about the over-dependency on the utilisation of fossil fuels and about the disposal of solid waste materials.

In this chapter the technical literature on the subject of pyrolysis and gasification is reviewed. In the first section the gasification of char materials will be discussed. These processes are common to all of the feed materials of interest, and there is extensive literature based principally on the work done on coal char gasification reactions. In the second section, the specific pyrolysis and thermal decomposition mechanisms of the biomass, wastes and synthetic polymer materials will be described in some detail.

The chapter will conclude with a review of the more important experimental studies of the gasification reactions undergone by the char residues produced by the thermal decomposition of a range of biomass and waste materials and synthetic polymers.

2.2 Thermal Processing Reactions

2.2.1 Pyrolysis

As a carbonaceous fuel is heated to temperatures in excess of around 200 °C in an inert atmosphere, it begins to decompose into gaseous and liquid species (principally H₂, CO, CO₂, H₂O and CH₄), tars, oils and a solid, carbonaceous char⁽²⁾. These pyrolysis reactions are important elements of all gasification processes but are also employed in the preparation of liquid fuels and cokes for industrial use.

2.2.2 Gasification

Gasification occurs when a carbonaceous material is heated to high temperatures in the presence of an oxidising agent such as air, steam or carbon dioxide, or a

mixture of these, to yield a low to medium calorific fuel gas⁽³⁾. The fuel gas consists principally of carbon monoxide, hydrogen and a range of volatile hydrocarbons.

The principal reactions involved in the gasification of carbonaceous char materials are as follows⁽³⁾:

(i) *Combustion Reactions*



The reactions of carbon with oxygen are exothermic and thermodynamically favoured up to 4000 K. Typically, the rates of these reactions are several orders of magnitude greater than the reactions involving H₂O or CO₂ with carbon, in the absence of a catalyst.

(ii) *Boudouard Reaction*



The rate of this endothermic reaction can be enhanced by the use of a catalyst.

(iii) *Steam Reaction*



The steam reaction is endothermic and is favoured by elevated temperatures and reduced pressure. This reaction is faster than the reaction of carbon with CO₂ under similar conditions.

(iv) *Hydrogasification Reaction*



These equations are concerned with the reaction of gaseous species with the char surface, however, a number of gas phase reactions also occur during a gasification process⁽³⁾, and principally:

(v) *Water-Gas Shift Reaction*



This reaction is exothermic and is an important secondary reaction process during steam gasification, however it is not thermodynamically favoured at high temperatures.

2.3 The Kinetics of Char Gasification Reactions

The rate of the gas-char reactions described above is a complex function of the following key parameters:

- (a) the properties of the char parent material,
- (b) the physical conditions under which the char was prepared, and
- (c) the gasification conditions.

For a given set of gasification conditions the conventional kinetic theory of gas-char reactions predicts that the rate of reaction is directly proportional to the total active site concentration. The concept of active surface sites, i.e. that the char-gas reaction proceeds by the formation of a C-O complex on active sites, was introduced in the 1960's⁽⁴⁾, and has proved to be useful in providing an insight into the kinetics of the gasification processes.

The gas-char reaction scheme involves:

- (i) adsorption of oxygen, or oxygen-containing species at the surface active sites,

- (ii) reaction at the surface sites involving the C-O complexes, and
- (iii) desorption of the products from the surface.

The desorption of carbon monoxide and carbon dioxide from active surface sites is an important step in most kinetic schemes for char gasification and, in many instances it is the rate controlling step.

For char materials, it is possible to attribute the location of the active surface sites to specific structural features on the surface of the char particle, i.e.

- defects in carbon planes and edge carbon atoms at dislocations,
- disordered carbon atoms and voids,
- heteroatoms, commonly O, N and S, and
- mineral matter occurrences.

The active surface areas of chars can be estimated experimentally by measurement of their oxygen chemisorption capacity. The key steps in this procedure are:

- (a) outgassing of the carbon surface to remove pre-adsorbed surface complexes,
- (b) formation of chemisorbed surface complexes by controlled exposure to oxygen, preferably at a temperature low enough to avoid gasification, and
- (c) removal of the chemisorbed oxygen as CO and CO₂ by heat treatment of the carbon.

The active surface area measurements can be estimated either by measurement of the chemisorbed oxygen by gravimetric means^(5, 6) or by quantitative analysis of the evolved gases, as in the original volumetric technique developed by Laine et al⁽⁴⁾.

It is important to note that adsorption experiments for the measurement of the total surface area are commonly conducted under conditions where gasification does not

occur. These are usually at low temperature and high partial pressures of the reacting gas. The gasification reactions that are of industrial interest, however, usually occur at relatively high temperatures and low partial pressures of the reacting gas. This has led to the definition of the concept of the reactive surface area, i.e. the concentration of active sites which participate in the gasification reaction as opposed to the total active surface area as measured by the adsorption experiments described above.

Reactive site concentrations can be measured using two basic experimental techniques.

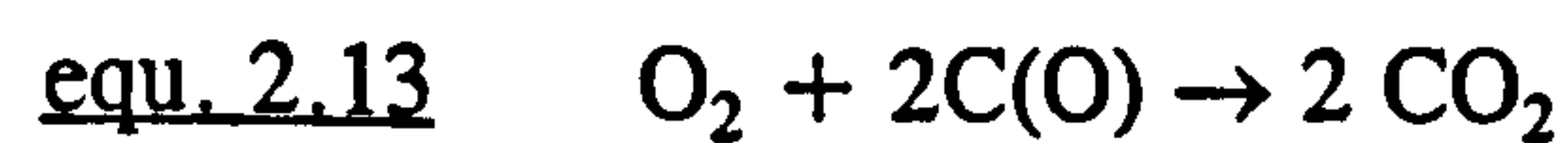
(a) *Gas Switching* experiments in which the progress of the gasification reaction is perturbed by rapid replacement of the reacting gas with an inert gas, and measurements of the decay in concentration of the product gases with time are made. This can provide an estimate of the concentration of surface species which are thermally stable in the inert gas flow. Simple kinetic analysis can be applied to derive the reactive surface area at the time of perturbation of the system⁽⁷⁻¹¹⁾.

(b) *Temperature Switching* experiments in which the gasification reaction is "frozen" by rapid quenching to a temperature at which gasification ceases. The reactive surface area is measured by conventional temperature programmed desorption either in an inert gas or in vacuum⁽¹⁰⁻¹²⁾.

2.3.1 The Carbon-Molecular Oxygen Reaction

The reaction between carbon and molecular oxygen relevant to industrial combustion and gasification reactions is not well understood in detail. Most experimental studies have been performed under conditions of very low oxygen partial pressures and low temperatures. Under these conditions, the reaction rates are thermally controlled, whereas in most industrial processes, the reaction is subject to heat and mass transfer limitations.

The following reaction scheme has been proposed:



The principal products of the reaction are CO and CO₂ with the ratio of CO/CO₂ increasing with increasing temperature and decreasing pressure⁽¹³⁾.

The kinetics of the carbon-molecular oxygen gasification reaction at low oxygen partial pressures and high temperatures were studied in a series of experiments by P L Walker and his co-workers, mainly during the 1960's^(4, 14-17). In these studies it was shown that the rate of reaction is given by the following equation:

equ. 2.14
$$\frac{-d[Po_2]}{dt} = k [Po_2] [(ASA).(1 - \theta)]$$

where, k = rate constant,

Po_2 = partial pressure of oxygen,

ASA = active surface area,

θ = fraction of ASA occupied by the C(O) complex.

In these experiments, the rate of reaction was measured using a gas switching technique, and at the end of the experiment, the occupied ASA was determined by Temperature Programmed Desorption (TPD) methods. Two major findings were made;

(a) the rate of reaction is proportional to the unoccupied ASA, and

- (b) the contribution of C(O) complexes to the production of gaseous CO and CO₂ is negligible.

These results imply that there are three products of the reaction of C with O₂, i.e. CO, CO₂ and a stable C(O) surface complex.

The gaseous CO and CO₂ are produced by two reaction pathways, i.e.;

- (i) via an unstable C(O) surface intermediate, and
 (ii) via the breakdown of a stable C(O) surface complex.

The first route is by far the most important i.e. the formation of the stable C(O) surface complex results in a decrease in the reaction rate. The unstable C(O) intermediate has a very short life and the surface concentrations of this species at any time are very small.

A more general equation has been proposed, viz⁽¹⁸⁾;

$$\text{equ. 2.15} \quad \frac{-d[\text{Cg}]}{dt} = \frac{kc [\text{Po}_2]^n [(ASA)(1 - \theta)]}{[1 - \kappa(\theta)]}$$

where $\frac{d[\text{Cg}]}{dt}$ = rate of total carbon gasified \equiv rate of oxygen depletion

kc = rate constant,

Po₂ = partial pressure of oxygen,

θ = fraction of ASA covered with complex,

$\kappa(\theta)$ = participating factor reflecting the contribution of complex in producing CO and CO₂;

n = order of reaction with respect to oxygen.

The studies by Walker and his co-workers reported reaction order values of 1, however, subsequent studies report values for the order of reaction in the range 0.5 to 0.6 at pressures of up to 0.1 MPa and temperatures of up to 1023 K^(18, 19). Since the measured order relates to the extent of coverage of the active surface,

and therefore is a sensitive function of surface structure and carbon origin, a close agreement between unrelated studies is not anticipated.

2.4 The Effect of Char Characteristics on the Kinetics of Gasification Reactions

In general terms, it has been found that the reactivity of char in gasification reactions depends upon:

- (a) the nature of the parent material,
- (b) the conditions of the pyrolysis process employed to produce the char,
- (c) the catalytic effects of the mineral material, and
- (d) the char gasification conditions.

The results of a number of comparative experimental studies have shown that biomass and low rank coal materials tend to produce chars with higher intrinsic reactivities than do higher rank coals and pitches. The reason for this is that the reactive surface areas of the chars produced from high volatile materials tend to be relatively high. There is considerable scatter in the data, which is generally attributed to the catalytic effects of the mineral matter constituents of the chars⁽²⁰⁻²²⁾.

For instance, the relationship between the reactive surface area and the volatile matter contents of coal char and other materials was studied by Wang and McEnaney⁽²⁰⁾. They found that there was positive a linear relationship between the reactive surface areas and the volatile matter contents of five coals ranging from an anthracite to a lignite. This correlation is illustrated in Figure 2.1.

The relationship between the reactivity and reactive surface area for a series of demineralised coal chars, a PVDC char and an electrode carbon, which were also

studied by Wang and McEnaney⁽²⁰⁾ is illustrated in Figure 2.2. This graph clearly indicates a positive linear relationship between the measured reactivity values of the materials and the measured RSA data. The experiments were performed using CO₂ as reactant gas and employed a TPD technique for the measurement of the reactive surface areas.

The temperature dependence of the gasification reaction rates of a range of char materials in steam is illustrated in Figure 2.3, which is reproduced from Van Heek and Mühlen (1991)⁽²¹⁾. In all cases, the reaction rate increased exponentially with increasing temperature, and the chars produced from the high volatile lignite materials were significantly more reactive than those of the coal and coke materials, at any given temperature. Coke and pitch char materials which had been treated at temperatures in excess of 1200 °C had very low reaction rates at temperatures up to 900 °C. It was considered that the principal factors which influence the intrinsic reaction rates of the different materials were:

- (a) the physical structure of the chars and hence the reactive surface areas, and
- (b) the catalytic influence of the ash materials.

The intrinsic reactivities of a wide range of carbon and char materials to oxygen were studied by Smith⁽²²⁾. Making use of published data from a number of sources, the measured kinetics were corrected for system effects, i.e. the extent to which external mass transfer effects influenced the reactivities, and then the effects of pore diffusion and chemical reaction on the surface were separated. Using data where there was sufficient information on mass transfer, pore structure and reaction temperature, the intrinsic reaction rates for 32 porous and 17 non-porous carbons and chars were derived, corrected to a common oxygen pressure of 101 kPa.

The data are summarised in Figure 2.4, which shows the intrinsic reaction rate as a function of reaction temperature in an Arrhenius form. The overall average activation energy of 179.4 kJ mol⁻¹ indicates a strong temperature dependence for

the reaction of carbon with oxygen. At any given temperature, the intrinsic reactivities of different carbons and chars varied by up to 4 orders of magnitude. This reflects the influence of atomic structure of the carbon and the presence of impurities.

Of particular interest in this regard are the results reported by Lang, Magnier and May⁽²³⁾. The intrinsic reactivities of a wide range of carbons and char materials were measured after pre-treatment by heating at temperatures in excess of 2700 °C (2973 K). Some of the carbons were also exposed to chlorine at these temperatures in an attempt to remove inorganic impurities. The intrinsic reactivities of these materials to oxygen were measured at 600 °C (873 K). They were found to be very low and varied only by a factor of 3, despite the wide range of parent materials. These results indicate that after extreme pre-treatment conditions, and the removal of inorganic impurities, the intrinsic reactivities of a wide range of materials were very similar. It was considered that the high temperature pre-treatment, in addition to the removal of catalytic impurities, also caused re-arrangement of the carbon atoms to a more uniform structure, with low active surface areas.

2.5 Inhibition and Catalysis of the Carbon-Gas Reaction

The reaction rates of carbonaceous material during gasification reactions are influenced by a number of factors, viz:

- a. the porosity of the material and hence the surface area available for reaction,
- b. the degree of crystalline order within the carbon structure, and hence the concentration of reactive surface sites,
- c. the presence of chemical species, which can act to inhibit or to catalyse the gasification reaction, and

- d. the formation of a glossy layer on the carbon surface, which can represent a barrier between the carbon and the reactant gas.

In highly ordered carbons, two principal types of active site have been identified, viz:

- i. zig-zag sites, and
- ii. armchair structures.

These are illustrated in Figure 2.5. The relative reactivities of these sites has proved difficult to measure, and are considered to vary depending on the reactant gas species, the reaction temperature and on steric effects⁽²⁶⁻³⁰⁾.

2.5.1 Inhibition of the Carbon-Gas Reaction

A range of chemical species have been found to inhibit the carbon-gas reaction. These are mainly compounds of phosphorus, boron, and the halogens. Specific chemical species which have been identified as inhibitors include⁽²⁴⁻²⁶⁾:

- organophosphorus compounds,
- phosphonyl and sulphonyl chloride,
- halogen gases and organohalogens,
- boron and boron oxide,
- organo-boron compounds, and
- some transition metal compounds.

It is thought that these species act as inhibitors of the carbon-gas reactions by competing for or masking active sites on the surface of the carbon. These compounds are commonly used in flame retardant materials.

2.5.2 Catalysis of the Carbon-Gas Reaction

It is known that the presence of alkali and alkaline earth metals and some of the transition metals can catalyse the gasification reaction of carbonaceous materials. This is a very important and generally desirable effect in that it enhances the reaction rates in gasification reactions. It can also be undesirable however, when these metals are present as impurities and lead to the reduction of the lifetimes of important industrial equipment such as carbon electrodes. For these reasons the subject of gasification catalysis has been studied extensively⁽³¹⁻³⁵⁾. These processes are very complex and difficult to study since most industrially important gasification reactions are rapid and are performed at high temperatures. The result is that although there has been a steady increase in the level of fundamental knowledge of the reaction mechanisms, there is still much to be resolved.

In the investigation of catalytic reactions of this type, the attractions of employing techniques which can study the process 'in-situ' are obvious. The most useful technique has been controlled atmosphere microscopy^(31, 36), especially electron microscopy, (CAEM), and most of the more important recent work has been done using this approach⁽³³⁾. It is possible to provide back-scattered or secondary electron images of the surface morphology, to perform Selected Area Diffraction (SAD) measurements, which provide information on the crystal structure of the material and to provide chemical analysis of selected areas using EDAX techniques⁽³³⁾.

The results of studies using the CAEM have been conducted with graphitic carbons and only a few studies of disordered carbons have been reported⁽³⁷⁾. A number of mechanism schemes have been suggested however in the majority of systems it is considered that the carbon-gas reaction occurs at the catalyst-carbon interface.

One of the key parameters which controls the nature of the morphological changes in the carbon surface during catalytic gasification reactions is the physical nature of

the catalyst and its distribution on the carbon surface. This is illustrated in Figure 2.6.

At one extreme, the catalyst can be in the form of a discrete particle, which does not wet the carbon material and the catalysed carbon loss tends to be in the form of channels and pits in the carbon's substrate. At the other extreme, where the catalyst is more evenly dispersed across the surface or in the form of a surface film, carbon loss is in the form of accelerated edge recession.

2.5.3 Summary of Literature on the Gasification of Carbonaceous Char Materials

It is clear from the material presented above that the kinetics of char gasification reactions are controlled by a number of factors, viz;

(a) The physical structure of the carbonaceous char which is dependant on the nature of the parent material and on the pyrolysis conditions. The char structure, i.e. the open porosity and char area, and the degree of order within the char, have a major influence on the concentration of reactive sites on the char surface which are available for reaction.

(b) The presence of other chemical species in the impure carbonaceous chars can act as both inhibitors of the gasification reaction, by competing for or masking reactive sites, or as catalysts. The mechanisms of the inhibition and catalysis processes are not well understood, however, the results of experimental studies have indicated that the progress of catalysed gasification is strongly influenced by the physical nature of the catalyst species and its distribution within the char. Discrete catalyst material occurrences can lead to channelling and pitting on the char surface, whereas catalyst species which are more uniformly dispersed within the char lead to reaction at the char surface by an edge recession mechanism.

(c) The results of analysis by the kinetics of the char gasification reactions, and principally the reactions of carbon with oxygen, indicate a strong temperature dependence, with the measured activation energies of the char-oxygen reaction in the range 100-200 kJ mol⁻¹. The carbon-oxygen reaction is generally considered to be first order or less, with respect to the carbon concentration.

These general observations refer to the results of experimental studies which have been concerned, in the main, with relatively pure carbonaceous chars and carbons. The more specific technical literature, concerned with the pyrolysis and gasification reactions of biomass and waste materials, will be discussed in more detail later in this chapter.

2.6 The Nature of Biomass and Wastes

The principal types of biomass and wastes materials which are used as fuels are:

- (i) Wood wastes of various types, i.e. forestry, sawmill and demolition wastes,
- (ii) Dry agricultural wastes, principally cereal, oil seed, rape and linseed straws,
- (iii) Domestic and industrial, non-hazardous dry wastes,
- (iv) Municipal, agricultural and industrial sludges, and
- (v) Specific energy crops.

The most important constituent of most biomass and waste materials is plant matter, which comprises three principal organic constituents, viz⁽³⁸⁾;

- cellulose (40-50 %),
- hemicellulose (25-40 %), and
- lignin (15-30 %).

Most plant materials also contain inorganic components, generally in small quantities, typically < 10% w/w. A general composition assay for a variety of biomass types is presented in Table 2.1⁽³⁹⁻⁴¹⁾.

2.6.1 Cellulose

Cellulose is the principal cell wall component in plant tissues. It is a linear condensation polymer consisting of D-anhydroglucopyranose units linked by β 1,4 glycosidic bonds⁽³⁸⁾. The anhydroglucose units form cellulosic strands which are interlinked by hydrogen bonding and Van der Waals forces. The structure of cellulose is illustrated in Figure 2.7⁽⁴²⁾.

2.6.2 Hemicellulose

Hemicellulose is a complex heteropolymer which has a branched molecular structure. It can show significant variation in composition among plant species and can contain two, four, five or six different sugar units such as D-xylose, D-mannose, D-galactose and L-arabose. In the case of hardwoods, xylon is the predominant hemicellulose and is a polymer of the pentosan sugar xylose. In softwoods, glucomannans (mannans) are the principal hemicellulose component⁽³⁹⁾. The structures of the hemicellulose materials in softwood and hardwood are presented in Figures 2.8 and 2.9, respectively⁽⁴³⁾.

2.6.3 Lignin

Lignin is a macromolecule which consist of an irregular array of hydroxy and methoxy phenylpropane units, bonded in a variety of ways. The precursors of lignin biosynthesis are presented in Figure 2.10.

'A' is a minor precursor of softwood and hardwood lignins. 'B' is the predominant precursor of softwood lignin and both 'B' and 'C' are precursors of hardwood lignin. These alcohols are linked in lignin by ether and carbon-carbon bonds⁽³⁸⁾. In woody materials, lignin acts as a binder for cellulose and

hemicellulose fibres, however there is no single chemical structure as it varies between different plant species⁽⁴⁴⁾. An example of a particular lignin structure, that of normal conifer wood, is presented in Figure 2.11.

2.6.4 The Mineral Matter in Plant Materials

All plant materials contain mineral matter in quantities which vary up to around 20%, but more commonly less than 5 %⁽⁴⁶⁾. The ash contents of various types of biomass are presented in Table 2.2⁽⁴⁵⁾. The major constituents of the mineral materials are SiO₂ either as quartz or in an amorphous form, and simple salts of Ca, Mg, Na or K, principally as oxides, hydroxides, phosphates, carbonates and oxalates⁽⁴⁶⁾.

The chemical compositions of a number of wood ash and straw ash materials are listed in Tables 2.3 and 2.4^(47, 48). These ash materials were prepared by combustion of the biomass materials in a muffle furnace at temperatures up to 600-800 °C, to a constant weight.

The major constituents of biomass ashes are generally very similar, although the concentrations of particular constituents, and particularly the SiO₂, K₂O, CaO and P₂O₅ can vary widely^(49, 50).

2.7 The Nature of RDF

Municipal solid waste (MSW) is a heterogeneous material which consists of residential, general industrial and institutional waste. The estimated annual arisings in Britain are of the order of 25 million tonnes of which about 90 % is currently landfilled and the remainder is disposed of at specially designed mass burn incinerators⁽⁵¹⁾.

The composition of MSW is highly variable, depending on factors such as season and location and therefore there is no exact composition. An average category

assay is presented in Table 2.5⁽⁵²⁾. The major constituents are, cellulose-based materials including paper, newsprint, packaging materials and food wastes which collectively account for over 50 % w/w of MSW. The remainder is a mixture of mineral fines, glass and plastics, the majority of which reduce the overall bulk calorific value and significantly increase the ash content.

An alternative to landfill and mass burn incineration is to pretreat the waste prior to combustion to produce a waste derived fuel which can be combusted in more conventional equipment. This pre-treatment involves the recovery of metals, glass, plastics and fines to produce a relatively homogenous fuel with an improved calorific value and reduced ash content. There are two basic types of refuse derived fuel which are commonly produced:

- (i) coarse ('floc') RDF with a yield weight in excess of 50 % produced by screening, ferrous metal extraction and coarse shredding and,
- (ii) densified or pelletised RDF with a yield weight of less than 50 % which involves a high degree of sorting and pre-treatment.

An average composition of densified and dried RDF is presented in Table 2.6⁽⁵³⁾.

The treated material has a high concentration of paper/board and sheet plastic which can account for ~ 85 % of the total weight composition. RDF also has a reduced ash and moisture content and a significantly improved Gross Calorific Value (GCV) of 16-19 MJ kg as received (20-25 MJ kg⁻¹, dry ash free).

The plastic fraction of RDF is important as it is present in significant quantity and has a calorific value of ~ 37 MJ kg⁻¹, almost double that of cellulose-based materials. The average distribution of plastic material is presented in Table 2.7⁽⁵⁴⁾. An important aspect of the plastic fraction is the significant quantity of poly(vinyl chloride) as this is one of the principal forms of chlorine in the fuel.

The combustible component of RDF can be treated as a composite of cellulosic (natural polymers) and plastic (synthetic polymer) fractions. Various components

of the cellulosic fraction, paper, food and garden waste etc. decompose over the temperature range 300-400 °C. The non-chlorinated plastic fraction decompose at higher temperatures, 400-500 °C while the chlorinated polymers decompose at lower temperatures of 250-400 °C⁽⁵⁵⁾.

2.7.1 Ash Material in RDF

The average composition of RDF ash is presented in Table 2.8⁽⁵³⁾. RDF ashes have levels of SiO₂ and Al₂O₃ similar to those of coal ashes, but they have relatively high CaO, MgO and Na₂O and relatively low K₂O and Fe₂O₃ contents. The RDF also have relatively low and short fusion temperature ranges, initial deformation to complete fusion occurs between about 1100-1250 °C. This is fairly typical of ashes with relatively high levels of alkali and alkaline earth metals⁽⁵³⁾.

The alkali metals can be present in the RDF in two forms

- as simple organic salts or in ion-exchangeable form associated with the organic material, or
- as a constituent of clay minerals, glass or other silicate based materials.

The alkali metals in simple inorganic salts or in ion-exchangeable form are likely to be more readily available for volatilisation during a combustion or gasification process than that present in the silicate systems⁽⁵³⁾.

2.8 Pyrolysis Mechanisms for Biomass and Biomass Components

Pyrolysis processes involve the thermal degradation of carbonaceous materials at temperatures in the range 400-1000 °C, in the absence of an oxidising agent or with such a limited supply that gasification does not readily occur to an appreciable extent. The products of the pyrolysis processes are a solid carbonaceous char, a combustible gas and a range of liquid and tar products. The relative proportions

of these products depend on the feed material and the pyrolysis conditions. Pyrolysis processes of industrial interest can be divided into the following three categories:

1. *Slow Pyrolysis* or carbonisation processes involve very low heating rates and low maximum temperatures, and are generally employed to provide solid carbonaceous char material as the primary product. The gaseous and liquid by-products are burned to provide energy for process heating or are recovered as feedstocks for the production of chemicals.

2. *Conventional Pyrolysis* processes employ moderate heating rates and maximum temperatures and generate solid, liquid and gaseous products in roughly equal proportions.

3. *Fast Pyrolysis* processes are employed to maximise the yields of gaseous and liquid products. Flash pyrolysis involves treatment at very high heating rates at moderate maximum temperatures, usually up to 600 °C or so, followed by rapid quenching to induce condensation of the liquid products. Fast pyrolysis at higher temperatures can be employed to maximise the yields of combustible gaseous products.

The results of numerous experimental studies of the pyrolysis of biomass materials have been published. In the main, these are of three types, viz;

- a. fundamental studies of the pyrolysis mechanisms of major components of biomass material, i.e. cellulose, hemicellulose and lignin,
- b. laboratory studies of the pyrolysis of biomass materials, principally of wood, and
- c. investigations of the influence of inorganic species on the pyrolysis of biomass materials and their constituents.

The pyrolysis reactions of biomass materials are complex and involve a wide range of solid, liquid and gaseous products, the yields and nature of which are dependent on the pyrolysis conditions, and principally on the heating rate and the maximum temperature.

2.8.1 Cellulose Pyrolysis

A number of reaction schemes which describe the pyrolysis of cellulose have been suggested. Shafizadeh proposed two general pathways of cellulose decomposition which are presented in Figure 2.12⁽⁵⁶⁾.

Heating at low temperatures, below 280 °C, results in pathway (a), with gradual decomposition and the charring of cellulose occurring. When higher temperatures are employed, (b) and (c) are the dominant reaction pathways, where rapid volatilisation of cellulose occurs leading to the formation of levoglucosan and combustible volatiles. It was suggested that these two reaction pathways are competitive with the pyrolysis conditions employed dictating which reaction path will dominate.

A more detailed model for cellulose pyrolysis was subsequently proposed by Shafizadeh and Fu⁽⁵⁷⁾. This was based on the previously described global reaction mechanism which incorporates a route for the formation of tar and volatile matter from the cellulose by a depolymerisation reaction. It was suggested that cleavage of the glycosidic groups proceeds through a transglycosylation mechanism with the participation of one of the free hydroxyl groups in the cellulose polymer. This model is presented in Figure 2.13⁽⁵⁷⁾.

An additional scheme for cellulose pyrolysis at low temperatures was proposed by Kilzer and Broido⁽⁵⁸⁾. This scheme which is based on three reaction processes is presented in Figure 2.14. Initially, dehydration reactions occur at approximately 220 °C, leading to pure cellulose losing water to yield dihydrocellulose i.e. "active cellulose". Following this, depolymerisation of the cellulose occurs at around 280°C with tar and volatile materials produced. This reaction competes with the

dehydration reaction. The third and final reaction is the decomposition of dihydrocellulose into gaseous products and char.

A modified reaction scheme based on the Kilzer and Broido model was proposed by Agrawal⁽⁵⁹⁾ who suggested that the formation of char and gas are not linked and that they are produced from two competitive first order reactions. This model is presented in Figure 2.15.

2.8.2 Hemicellulose Pyrolysis

The thermal decomposition of hemicellulose has been reported to start at temperatures as low as 120 °C and is completed by 325 °C⁽³⁸⁾. A reaction pathway comparable to that for cellulose is generally accepted with dehydration reactions predominant at the low temperatures. Dehydration is characterised by random cleavage of the C-O bonds which produces branched chain anhydride fragments, water soluble acids, char and light gases⁽³⁸⁾. During high temperature depolymerisation, a characteristic tarry intermediate (analogous to levoglucosan in cellulose pyrolysis) is considered to exist. It is thought to be a furan or furfural for hemicellulosic pentosans, but has not been clearly defined⁽³⁸⁾. These furan derivatives are difficult to isolate due to their extremely rapid formation and decomposition.

2.8.3 Lignin Pyrolysis

The study of lignin pyrolysis is extremely complex since it varies between different biomass materials and is affected by the nature of the extraction technique. Mass spectroscopy results have shown a series of methoxy phenols are the predominant pyrolysis products⁽³⁸⁾. In general, lignin is more thermally stable than the other plant components, and tends to give higher yields of carbonaceous residue and a higher fraction of aromatics in the liquid pyrolysis product compared with both cellulose and hemicellulose⁽³⁸⁾. Antal⁽⁶⁰⁾ proposed that primary pyrolysis occurs with the cleavage of the straight carbon chains which connect the aromatic units. In addition, it was suggested that rapid pyrolysis may initially result in the

formation of monomeric phenylpropane units, with increased pyrolysis producing a number of phenolic compounds including phenols, cresols, catechols, xylenols and char from the aromatic monomers.

2.9 Biomass Pyrolysis

There are a number of procedures employed for the study of biomass pyrolysis, many of which have been reviewed in publications by Bridgewater^(66, 67).

Maschio et al⁽⁶⁸⁾ carried out slow pyrolysis of wood with a final temperature of 500 °C. The yields of pyrolysis products are presented in Table 2.9. They found that the char was a carbonaceous residue with an elemental composition of carbon 72 %, hydrogen 3 % and oxygen 17.4 %. The tar fraction comprised insoluble organics, mainly high molecular weight aromatics. The gaseous products were mainly carbon oxides, hydrogen, methane and relatively small quantities of higher molecular weight hydrocarbon species.

The published details of the influence of carbonisation conditions on biomass char yields and their properties are limited, and there are relatively few detailed studies⁽⁶⁹⁾. Figueiredo et al⁽⁷⁰⁾, for instance published the results of studies of the effects of temperature and particle size on the pyrolysis of holm-oak wood. They found that the pyrolysis process was practically complete at 400 °C and that only a minimal quantity of further volatile matter and gas were produced when the temperature was increased to 700 °C. The carbon content of the residual char did not significantly change above 700 °C, however the nitrogen concentration, although small, did increase slightly with increasing temperature. When the product distributions were studied the optimum yield of liquid product was obtained with a final temperature of 500 °C, and an optimum yield of gas product was obtained with a final temperature of 600 °C. It was demonstrated that the particle size of the wood did not significantly affect the product yields.

Kumar and Gupta⁽⁷¹⁾ studied the influence of carbonisation conditions on the physical properties of wood chars. They found that for a range of chars prepared by slow pyrolysis over a range of temperatures up to 1000 °C, the porosity increased with increasing final temperature. However, if the chars were subjected to a prolonged soaking time between 800-1000 °C, their porosity was reduced. In agreement with Figueiredo⁽⁷⁰⁾ they also found that the char carbon content increased with increasing temperature, however, in addition they concluded that the specific density of the char also increased with carbon content and increasing final temperature.

These results and conclusions were similar to published data for pitch⁽⁷²⁾, coals⁽⁷³⁾, cokes⁽⁷⁴⁾, petroleum coke⁽⁷⁵⁾ and polymer carbons⁽⁷⁶⁾ which suggested that the specific density of chars prepared from these materials was a function of temperature and elemental composition.

2.9.1 Influence of Inorganic Constituents on Biomass and Biomass Components During Pyrolysis

It has been shown by many experimentalists, that the presence of inorganic additives or impurities has an effect on the behaviour of cellulosic materials during pyrolysis. These effects were summarised by Shafizadeh⁽⁵⁶⁾, who stated that their presence produces increases in the yields of CO, CO₂, H₂O and char and decreases in the yield of tars and oils. Kinetic studies by Shafizadeh have also indicated that the activation energy of the overall pyrolysis process is substantially lowered by the presence of inorganic materials.

The majority of the experimental work reported in the literature is concerned with the effects of individual metal ions, principally as carbonates and chlorides on the pyrolysis of cellulose and wood materials.

The effect of metal cations, calcium and potassium, on cellulose pyrolysis was studied by DeGroot and Shafizadeh⁽⁶⁵⁾. They found that the presence of calcium ions increased the decomposition temperature of cellulose but had only a slight

effect on the char yield, while potassium ions reduced the decomposition temperature and also significantly increased the char yield.

The effects of calcium and potassium which were added by an ion-exchange method, as well as the effect of other individual metal ions on the pyrolysis of wood were studied by Richards and Zheng⁽⁷⁷⁾ and their results were in general agreement with those of DeGroot and Shafizadeh⁽⁶⁵⁾. They found that potassium ions acted as a catalyst in wood pyrolysis reactions while calcium ions did not. The results of this study also showed that potassium ions in wood produce an increase in char yield accompanied with a corresponding decrease in tar formation. This was also found to occur for the calcium ions which is opposite to their effect in cellulose. This effect was found to occur for all alkali metal ions in wood.

Richards and Zheng⁽⁷⁷⁾ also impregnated wood samples with the transition metals Fe, Zn, Cu and Ni, all in the 2^+ oxidation state. During pyrolysis, all of the samples which were impregnated yielded similar products to those of the untreated wood. However, for ion exchanged samples, an increase in levoglucosan was observed which contradicted the decrease in levoglucosan which was found for cellulose with metal ions. It was suggested that the catalysis of levoglucosan formation in wood with metal ions may involve some interaction of lignin. They tentatively suggested that the presence of transition metal ions in particular, decrease interference by lignin on levoglucosan formation from cellulose. They state that transition metal ions are noted for their ability to form complexes with phenols, which are polymeric units of lignin.

The effects of carbonate addition on cellulose pyrolysis was studied by DeGroot and Shafizadeh⁽⁶⁵⁾ and also Mardorsky⁽⁶¹⁾. DeGroot and Shafizadeh⁽⁶⁵⁾ studied the effects of K_2CO_3 , and found it promoted an increase in the decomposition temperature and also produced a significant increase in char yield. The difference between the potassium ion catalysis and potassium carbonate salt was suggested to be attributable to counter ion effects occurring with the salt treated sample which are not present with the ion exchanged sample.

The conclusions of work by Mardorsky⁽⁶¹⁾ et al on Na_2CO_3 and NaCl addition in cellulose was that the activation energy and thermal decomposition temperature were lowered. These occurrences were attributed to the catalysis of the dehydration of cellulose by the cleavage of the C-O bonds, resulting in the destruction of the hexose units and an increase in the yield of water at the expense of tar.

Zaror⁽⁷⁸⁾ also investigated the effect of sodium and potassium carbonates on the pyrolysis of both wood and cellulose. He suggested that the impregnation of the sample with the salts has an influence on the pyrolysis products. He proposed that the impregnation of cellulose with Na_2CO_3 weakens the less resistant glycosidic bonds by hydrolytic action of the base, CO_3^{2-} . He observed that there was a size increase in the cellulose fibres due to adsorption of water during impregnation leading to inter-crystalline swelling. The higher the polarity of the liquid, the greater the extent of swelling, which leads to a weakening of the hydrogen bonds between the hydroxyl groups in the inter-crystalline region of cellulose. Zaror further suggested that the weakening of the cellulose structure through both chemical attack and swelling leads to char formation being impaired. On the other hand, he observed that in the presence of carbonate salts, char yields were increased. This was attributed to the possible catalytic effects of the alkali carbonates overcoming the changes induced by impregnation so that catalysis of the dehydration reaction dominated.

The effects of chloride addition to cellulose were studied by Oren et al⁽⁶²⁾. They added potassium chloride (KCl) to cellulose samples prior to pyrolysis in N_2 at atmospheric pressure between 300 and 325 °C. The addition of KCl produced an increase in the char yields, from 15-20 % for the untreated cellulose to 30-35 % for the pre-treated material. This was attributed to the salt catalysing the dehydration reaction and char formation reactions at the expense of the depolymerisation reaction.

Shafizadeh et al⁽⁶³⁾ studied the effect of zinc chloride (ZnCl_2) on the pyrolysis of cellulose. They found that as the concentration of ZnCl_2 was increased, the peak decomposition temperature was lowered, and the decomposition temperature range was broadened, from 280-330 °C to 200-358 °C. They also observed an increase in char and gas formation as the salt concentration was increased. The broadening of the decomposition temperature range and increase in char and gas yields was thought to be due to the presence of ZnCl_2 , which is a Lewis acid. The acidic material suppresses the production of the combustible volatiles, and catalyses the transglycosylation, dehydration and condensation reactions which lead to char formation. Levoglucosone was also found in the condensate which Shafizadeh had previously shown to be a product of the acid catalysed pyrolysis of cellulose⁽⁶⁴⁾. Shafizadeh⁽⁶³⁾ suggested that the increase in char and gas formation was due to the formation of hydrochloric acid (HCl). They proposed that HCl could initiate the acid catalysed dehydration reactions and could also catalyse the condensation reactions of the intermediate products. The condensation reactions would give rise to products which can no longer escape from the heated zone by evaporation and thus remain to be roasted and form char.

Zaror⁽⁷⁸⁾ compared the effects of carbonate addition and chloride addition in both cellulose and wood. He observed that an increase in concentration of carbonate salts in both cellulose and wood lead to a reduction in decomposition temperature. In the instances of sodium and potassium chloride salts, the decomposition temperature was only reduced by 10 °C, and was not affected by the salt concentration. The results also showed a decrease in dehydration efficiency with increasing amounts of alkali chloride salt added (> 2 %), which was attributed to the chloride anions. He proposed that the increasing chloride concentration may catalyse competing reactions to the dehydration reactions. It was concluded that for both carbonate and chloride salts, the sodium salt appeared to be the most effective catalyst which indicates that the cation must have an important role in the catalytic action of a salt.

Overall, it is clear that the presence of inorganic constituents, and particularly the salts of the alkali and alkaline earth metals can have a significant effect on the pyrolysis of cellulose and biomass materials. In general, the effect of the presence of the alkali metal salts was to increase the char yield and decrease the yield of tar materials. The precise mechanisms responsible for these effects are not well understood and the effects are dependent on the experimental details, i.e. whether the inorganic salts were introduced by ion exchange or by simple additive mixture. However, in a publication concerning the effects of ion exchange (Na^+ , K^+ , Ca^{2+} , or Ba^{2+}) on low rank coal, Britt et al have suggested some reaction mechanisms which may be applicable to biomass pyrolysis⁽⁷⁹⁾. They suggested that the presence of these ions, in the form of carboxylate salts, had an effect on the reaction pathways which lead to decarboxylation and subsequent cross-linking. The presence of chloride in biomass pyrolysis has also been found to have a significant effect on the yields of char and tars, and on the decomposition temperatures. Again, the precise mechanism is not well understood.

2.10 Pyrolysis Reactions of Synthetic Polymers

In addition to ligno-cellulose materials, most municipal waste and refuse derived fuel materials contain synthetic polymers in sheet and lump form. It is instructive therefore to consider the information in the technical literature about the pyrolysis of these materials.

2.10.1 Pyrolysis of Poly(vinylchloride)

The pyrolysis of PVC has been the subject of a number of experimental studies and is relevant to the current discussion since it is present in significant quantities in municipal waste and refuse derived fuel, and was one of the synthetic polymers selected for the experimental work.

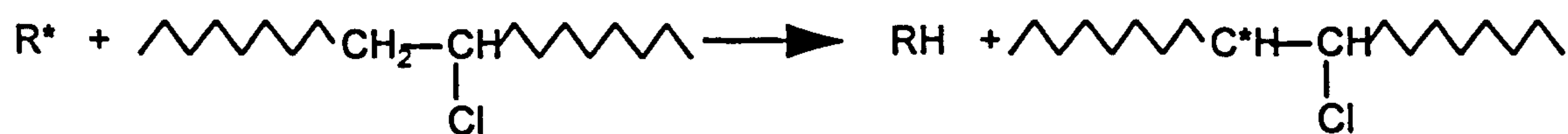
PVC is inherently stable at ambient temperatures, however an increase in temperature above 100 °C (373 K) leads to decomposition with the evolution of hydrogen chloride and the development of colouration. The intensity of this colour is a function of the degree of degradation, varying from yellow initially, to reddish brown and finally to black as the decomposition proceeds. The dehydrochlorination is practically complete after 30 minutes at 300 °C (573 K) when small amounts of aliphatic, unsaturated and aromatic hydrocarbons have been formed. Free chlorine and hydrogen have not been detected⁽⁸⁰⁾. The rates of decomposition and colour formation are temperature dependent, both increasing with increasing temperature. It is believed that the colouring of the polymer is the result of the formation of conjugated double bonds. Abbas and Sorvick⁽⁸¹⁾ have suggested that the most probable sequence length is below 10 units, and this is in agreement statements in earlier publications⁽⁸²⁾. The presence of such a sequence implies that the removal of HCl occurs systematically.

The exact mechanism for the dehydrochlorination of PVC remains uncertain, however, several mechanisms for the formation of polyene structures in non-oxygenated atmospheres have been proposed such as the radical chain, ionic and unimolecular elimination mechanisms. The only mechanism of relevance is in this study is the radical chain mechanism since it is the only one which can occur under pyrolysis conditions⁽⁸⁶⁾. This is described below;

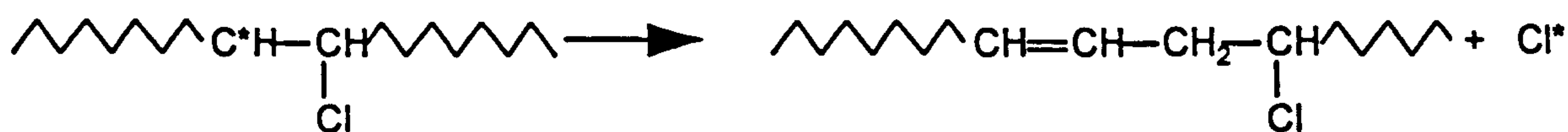
- *Radical Chain Mechanism*

Studies have indicated that polymer degradation proceeds by a free radical process, with the initial loss of hydrogen chloride initiated by the attack of radicals which are produced by the decomposition of residual catalyst or peroxide structures in the polymer chain. Winkler proposed a free radical chain reaction which consists of three basic steps⁽⁸³⁾, the generation of a halide atom, the abstraction of a hydrogen atom from PVC by the halide atom, and the rearrangement of the generated radical to give an alkene and another halide atom to continue the process. This reaction mechanism is outlined below in equations 2.16 to 2.18:

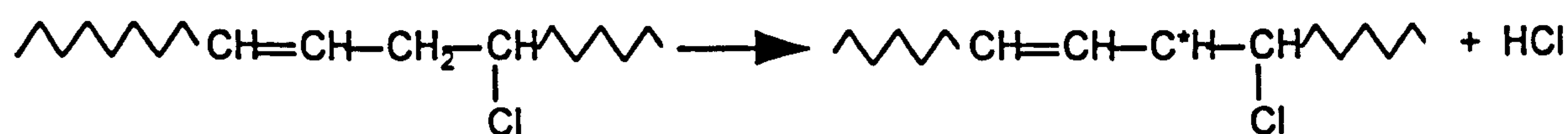
equ. 2.16



equ. 2.17



equ. 2.18



The main evidence supporting this mechanism was the detection of free radicals during polymer degradation by electron spin resonance techniques⁽⁸⁴⁾.

2.10.2 Pyrolysis of Poly(ethene)

Poly(ethene) is the most abundant synthetic polymer found in municipal waste and refuse derived fuel materials and can account for up to around 60 % of the total plastic fraction⁽⁵⁴⁾.

When it is heated, poly(ethene) begins to decompose at around 300 °C to give a range of products which mainly consist of lower molecular mass hydrocarbons. At temperatures above 350 °C, gaseous products are evolved with butene being the main component. Depolymerisation to ethene does not occur.

The main conclusion from kinetic studies is that poly(ethene) degradation is a random process of inter-carbon bond ruptures, however there is some evidence to support the theory that initial points of attack are the tertiary carbon atoms which occur in branched structures⁽⁸⁵⁾.

2.11 Influence of Inorganic Constituents on Biomass and Waste Gasification

The presence of certain alkali and alkaline earth metals are known to influence coal gasification reactions in a variety of atmospheres⁽⁸⁷⁾. This effect has been extensively studied for chars prepared from coals. Of most relevance in the current context is the work on low rank coals and on wood materials.

The effects of Ca, Mg, K and Na on the reactivity of Zap Indian Head Lignite were studied by Serio et al⁽⁸⁸⁾. Samples were prepared by HCl-HF demineralisation and then loaded with up to 2.0 wt % of metal by ion-exchange. The chars were prepared by heating at 30 °C min⁻¹ to 900 °C, and the reactivity was measured non-isothermally in air. Increasing the Ca and Mg loadings increased the reactivity of the demineralised Zap lignite char, until a saturation point was reached. The reactivity of the Na and K loaded chars increased sharply at low concentrations, up to around 0.5 wt % and then decreased sharply to a value less than that of the untreated demineralised char. The CO₂ BET surface areas of the Na-char were found to decrease from 274 m² g⁻¹ for the demineralised char to 0.5 m² g⁻¹ at 2.0 wt % loading. It was therefore concluded that at high loadings of Na and K, the inhibition of char reactivity was related to a reduction of the surface area during pyrolysis.

Fung et al⁽⁸⁹⁾ and Morales⁽⁹⁰⁾ studied the effect of a wider range of alkali and alkali earth metals on the reactivity of low rank coal gasification in oxygen. The authors concluded that char reactivity was influenced by the presence of Ca, Mg, Na, K, Cu and Cr.

It is clear from published studies, that calcium and calcium salts and oxides are important in the gasification of low rank coals in various atmospheres^(91, 92). This was shown by Hippo et al⁽⁹¹⁾ by an investigation of the reactivity in steam of 12 Texas lignite chars, which had been loaded with various concentrations of Ca. They found that there was a linear increase in the reactivity of the char as the Ca loading increased from 1.1 to 12.9 wt %.

This work was extended by Linares-Solano⁽⁹²⁾, who investigated the reactivity of the 12 Ca-loaded lignite chars in both air and CO₂. They reported that the reactivity of the chars increased with Ca-loading in both atmospheres.

The influence of the char preparation procedure and the nature of the catalyst material on the gasification of lignite chars was studied by Radovic et al⁽⁹³⁾. The chars were prepared from North Dakota lignite, and lignite samples which had been demineralised and loaded with 2.9 % w/w Ca. The char preparation involved heating to 1002 °C (1275 K), and holding for residence times up to an hour. The reactivity of the chars under gasification conditions was found to increase with decreasing residence time. For chars prepared with the same residence time, the reactivity increased with increasing Ca loading. Analysis of the chars using X-ray diffraction techniques indicated that the decrease in the char reactivity with the increase in residence time may have been due to the sintering of the CaO.

There have been a number of studies of the catalytic effects of alkali and alkaline earth metals on the gasification of biomass and wastes in various atmospheres. De Groot et al⁽⁹⁴⁾ gasified chars prepared from sphagnum peat, wheat straw, sugar beet, and potato pulp, in a CO₂ atmosphere and found that the reactivities increased with increasing concentrations of inherent K and Ca. The wheat straw did not conform to the char reactivity-Ca concentration curve. This was considered to be a consequence of the relatively high SiO₂ content of the straw.

De Groot et al⁽⁹⁵⁾ also studied the gasification of chars prepared from wood which had been ion-exchanged with Co, Ca, Na, K or Mg, or had been treated with acetate salt of Co, Ca or K to incorporate a higher concentration of alkali metal than is attainable via ion exchange. The results showed that the reaction rates of the chars prepared from all of the treated wood samples were increased. The Co and Ca ion-exchanged sample char gasified at a faster rate than the Na, K or Mg sample chars, while the chars prepared from the wood loaded with acetate salts of

K, Ca or Co gasified at a rate faster than their corresponding ion-exchanged samples.

It is evident from the available literature that those alkali and alkaline earth metals which are more catalytically active in the gasification of low rank coals are also the most effective catalysts for the gasification of biomass. A study completed by Kannan and Richards⁽⁹⁶⁾ indicated that the CO₂ gasification of biomass chars was affected by the concentrations of K and Ca, in the instances where the concentrations of all other metals were relatively low. The authors found that the molar catalytic activity of Ca and K was almost identical, and this was a similar finding to that by Walker⁽⁹⁷⁾ concerning the gasification of Texas lignite chars in CO₂. Kannan and Richards⁽⁹⁶⁾ also found that chars prepared from samples with high concentrations of Si, namely wheat straws and coir dust, deviated from the linear correlation. The authors concluded that the effect of K was reduced by Si. This finding was confirmed when the reactivity of chars prepared from potato pulp, the most reactive biomass char which also contained the highest concentration of K, was reduced when Si was added in increasing amounts.

A number of general conclusions can be made from the experimental studies of the influences of the presence of inorganic species on the gasification of chars prepared from low rank coals and biomass materials. In those studies where the parent materials and chars were artificially loaded with Ca and K compounds, an increase in the reactivity of the char under gasification conditions was measured. The reactivity of the chars was also influenced by the char preparation and inorganic material loading procedures. In a number of studies, it was found that the presence of significant quantities of SiO₂ in the char had the effect of suppressing the catalytic effect of the Ca and K compounds.

Species	Cellulose (%)	Hemicellulose (%)	Lignin (%)	Ash (%)
Softwood	41.0	24.0	27.8	0.4
Hardwood	39.0	35.0	19.5	0.3
Wheat Straw	39.9	28.2	16.7	6.6
Rice Straw	30.2	24.5	11.9	16.1

Table 2.1 Composition of selected plant types⁽³⁹⁻⁴¹⁾

Plant Type	Ash (%)	Plant Type	Ash (%)
Brazil Nut Husk	6.0	Palm Nut Shell	3.0
Clove Stalk	7.5	Peanut Shell	2.0
Coconut Shell	5.0	Straw Cereal	6.0
Cotton Seeds	3.0	Straw Rape	3.4
Cotton Pods	7.0	Wood	1.0

Table 2.2 Typical Ash Contents of Various Plants⁽⁴²⁾

	Average ⁽⁴⁸⁾	Softwood ⁽⁴⁷⁾	Oak ⁽⁴⁷⁾	Birch ⁽⁴⁷⁾
<i>Ash (wt, %)</i>				
SiO ₂	2-7	36.3	2-3	2.8
Al ₂ O ₃	0-2	4.7	0.9	1.4
Fe ₂ O ₃	1-2	1.5	0.5	0.7
CaO	30-60	32.0	65.0	45.0
MgO	5-10	4.4	8.3	10.8
K ₂ O	10-30	8.5	9.9	11.4
Na ₂ O	2-15	2.3	0.8	1.3
MnO	----	1.8	0.9	5.6
TiO ₂	----	0.3	0.1	0.1
SO ₃	1-5	1.7	2.2	2.2
P ₂ O ₅	5-15	4.8	7.5	17.0
<i>Soil Type</i>	---	Coastal Sand	Brown Earth	Peat

Table 2.3 Ash Composition of Various Tree Types^(47, 48)

	Wheat	Barley	Oats	Rye	Rape
<i>Ash (wt, %)</i>	3.3-3.5	2.9-6.1	4.0-7.4	2.0-5.4	1.7-2.7
SiO ₂	26.7-69.4	25.6-53.6	14.8-65.5	40.3-47.1	8.5-12.5
Al ₂ O ₃	0.1-1.1	0.1-5.6	0.3-5.3	1.4-5.9	0.1-2.8
Fe ₂ O ₃	0.4-0.9	0.4-2.8	0.2-2.5	1.4-2.5	0.6-4.4
CaO	8.4-15.1	5.9-11.8	3.8-8.9	8.1-15.8	40.0-46.6
MgO	1.8-5.4	1.9-4.3	2.1-6.6	4.1-5.5	4.5-5.4
K ₂ O	12.3-51.0	9.2-40.6	10.8-41.0	13.9-18.4	8.0-16.9
Na ₂ O	0.3-1.7	0.8-0.9	0.7-2.0	1.0-1.6	1.0-2.7
P ₂ O ₅	3.1-9.7	4.1-7.3	3.0-8.7	6.4-9.0	3.8-5.9
SO ₃	1.5-2.9	1.6-2.9	0.7-2.1	1.0-1.2	2.6-3.4

Table 2.4 Ash Composition of Various Straw Types⁽⁴⁹⁾

	As Received Weight. (%)	Moisture, (%, as rec)	Ash (%, as rec)	GCV (MJ kg ⁻¹)
Paper	33	30	8	12
Plastic film	3	25	9	27
Dense Plastic	3	15	6	30
Textile	4	25	8	15
Misc. combustible	5	25	1	12
Misc. non-combustible	5	15	85	---
Glass	9	10	90	---
Ferrous Metal	7	15	85	---
Non-Ferrous	1	10	90	---
Putrescible	20	65	8	6
< 10mm Fraction	10	40	40	4
Unseparated	100	33	29	8.4

Table 2.5 Average Category Assay of Typical British Refuse⁽⁵²⁾

	Range (%, wt dry)	Mean (%, wt dry)
Paper/board	79-90	84
Plastic sheet	9-16	11
Glass	1.5	
Wood	3.4	
Textile	1.0	
Tinfoil	0.5	
Others	1.0	
Ash (as analysed)	12-15 %	
Moisture (as analysed)	7-9 %	
GCV (as received)	16-19 MJ kg ⁻¹	

Table 2.6 Category Assay and Gross Calorific Value of Pelletised RDF⁽⁵³⁾

Plastic	Weight, (%)
Poly(ethene)	58
Poly(styrene)	20
Poly(vinylchloride)	8
Poly(propylene)	8
Others	6

Table 2.7 Average Distribution of Plastic Material in RDF⁽⁵⁴⁾

Ash Component (%)	Wt, (%)
SiO ₂	45.9-48.2
Al ₂ O ₃	15.0-18.9
Fe ₂ O ₃	4.7-6.3
CaO	14.3-16.2
MgO	2.5-3.1
Na ₂ O	4.4-6.1
K ₂ O	2.0-2.2
TiO ₂	2.0-3.6
P ₂ O ₅	0.5-1.1
SO ₃	1.0-1.8

Table 2.8 Typical Components of RDF Ash

Product	Yield (%)
Char	22.9
Tar	10.1
Aqueous	33.3
Gas	32.7

Table 2.9 Product Distribution from Slow Biomass Pyrolysis

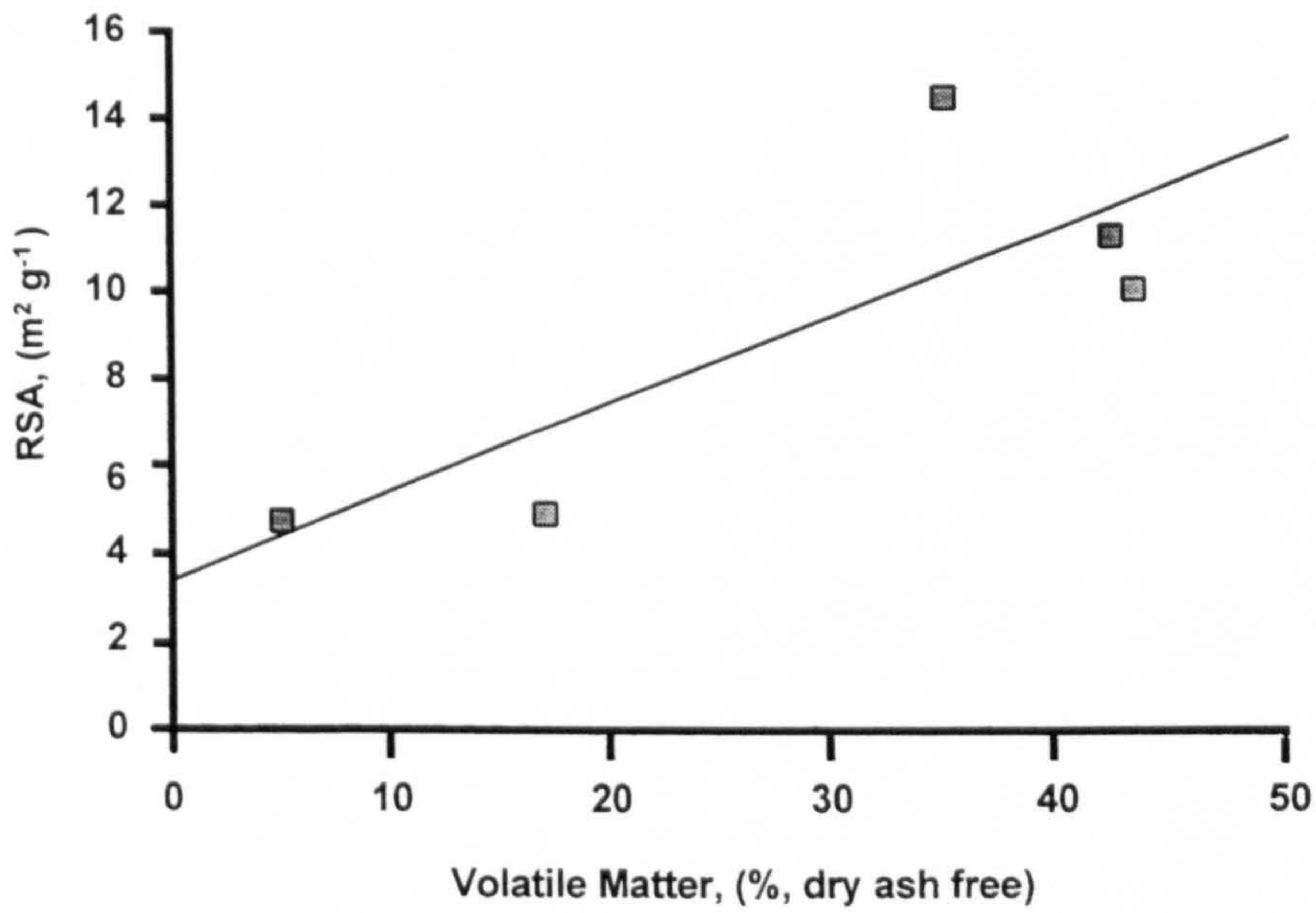


Figure 2.1 Linear Relationship Between the Reactive Surface Area and the Volatile Matter Contents of Five Coals Ranging from Anthracite to Lignite (after Wang and McEnaney)⁽²⁰⁾

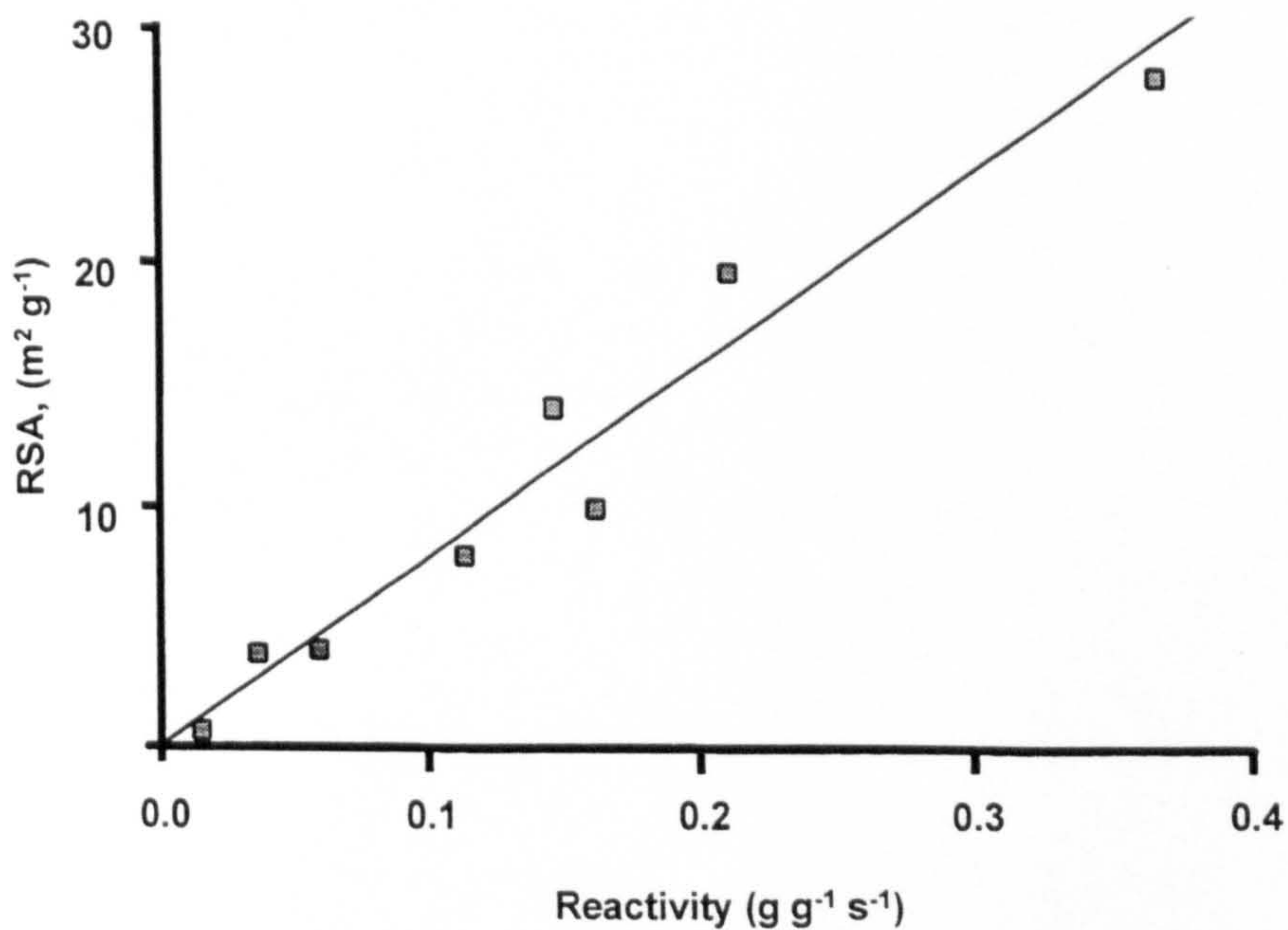


Figure 2.2 Relationship Between the Reactivity and Reactive Surface Area for a Series of Demineralised Coal Chars, a PVDC Char and an Electrode Carbon (after Wang and McEnaney)⁽²⁰⁾

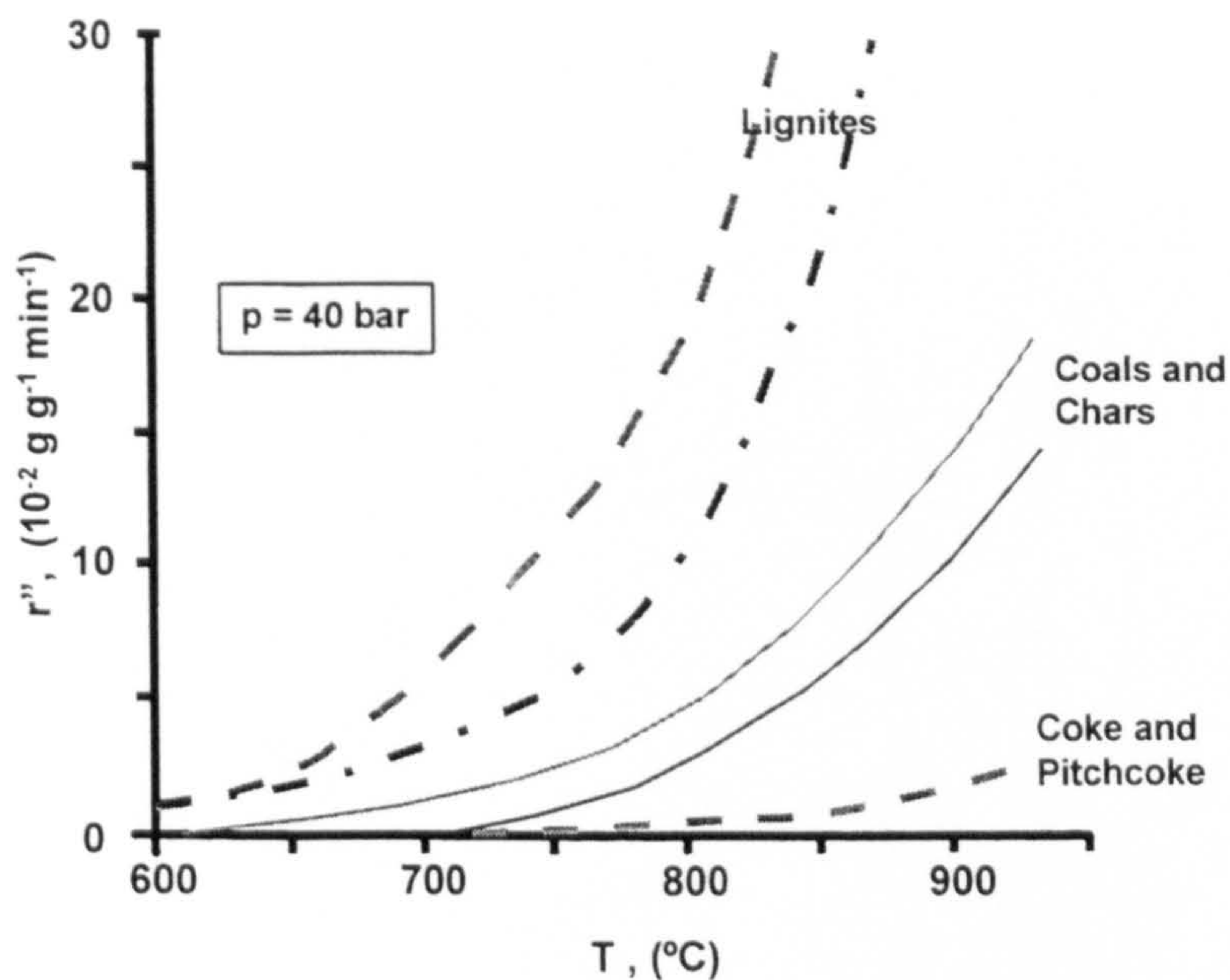


Figure 2.3 Temperature Dependence of the Gasification Reaction Rates of a Range of Char Materials in Steam (after Van Heek and Mühlen)⁽²¹⁾

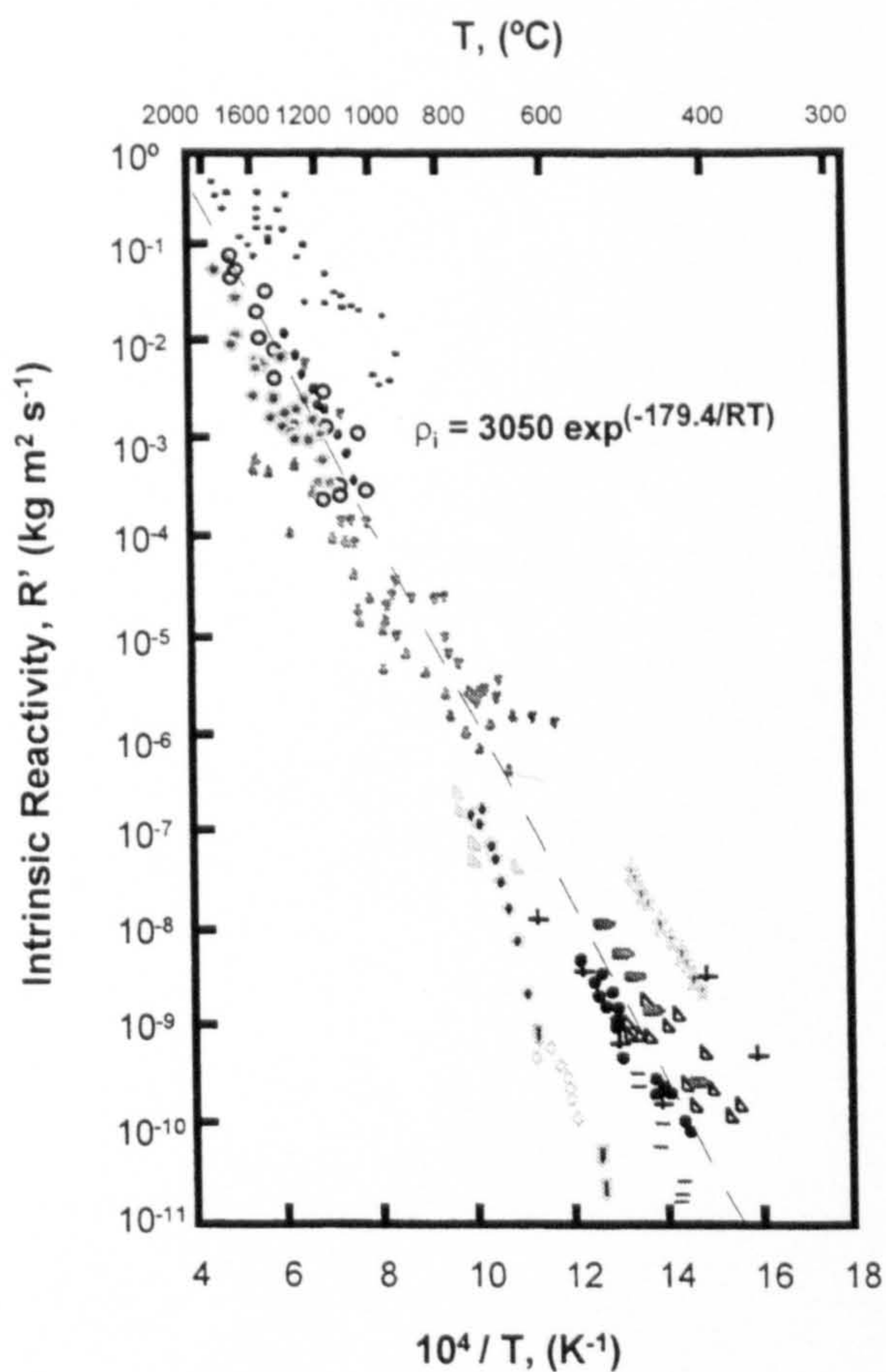


Figure 2.4 Intrinsic Reaction Rate as a Function of Reaction Temperature in an Arrhenius Form (after Smith)⁽²²⁾

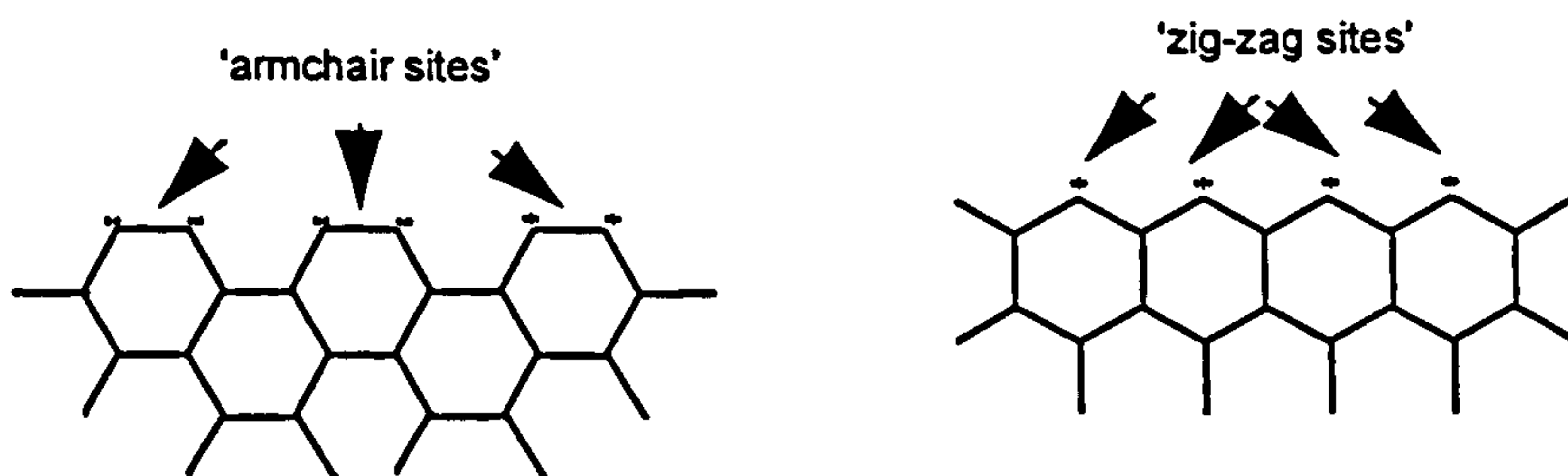


Figure 2.5 Illustration of Zig-Zag and Armchair Lamella Edge Structures

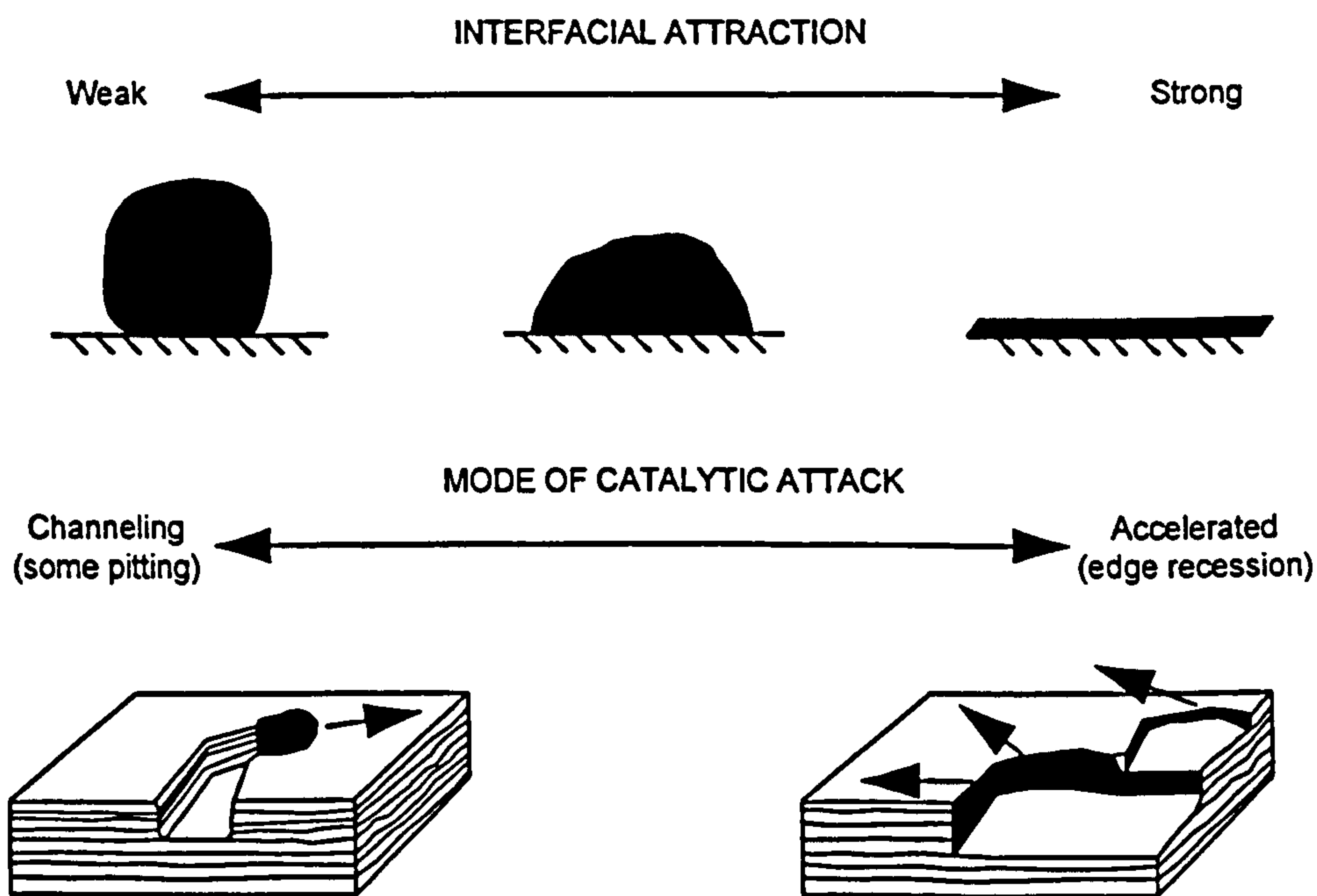


Figure 2.6 Illustration of the Relationship Between the Wetting Tendency of a Catalyst and the Mode of Catalytic Attack

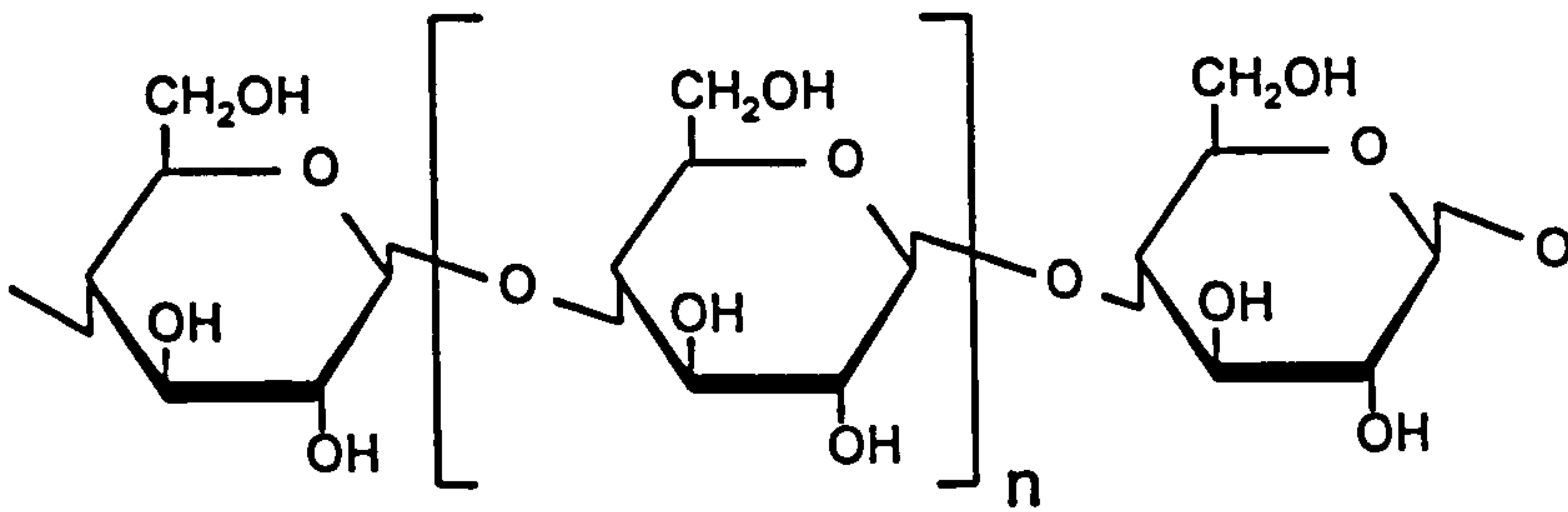


Figure 2.7 Structure of Cellulose (Haworth Projection)

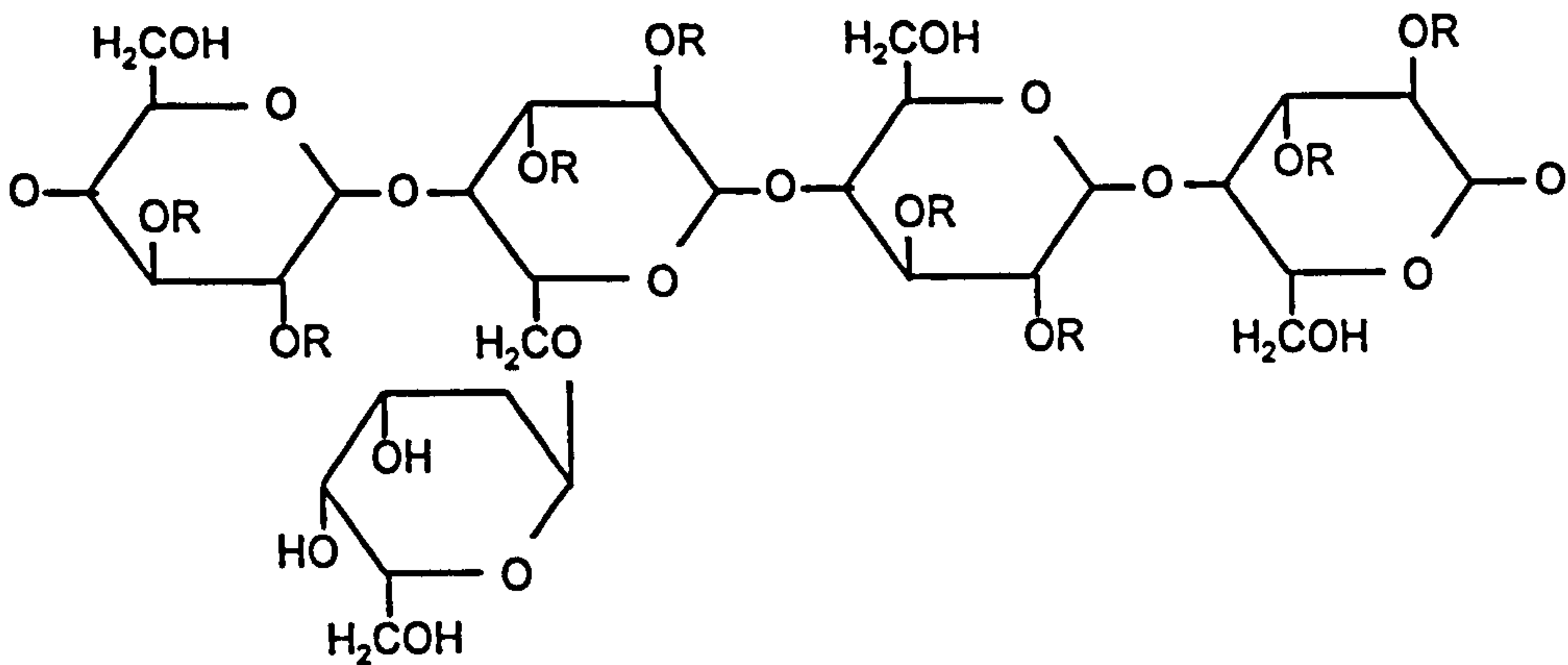


Figure 2.8 Structure of Hemicellulose in Softwoods

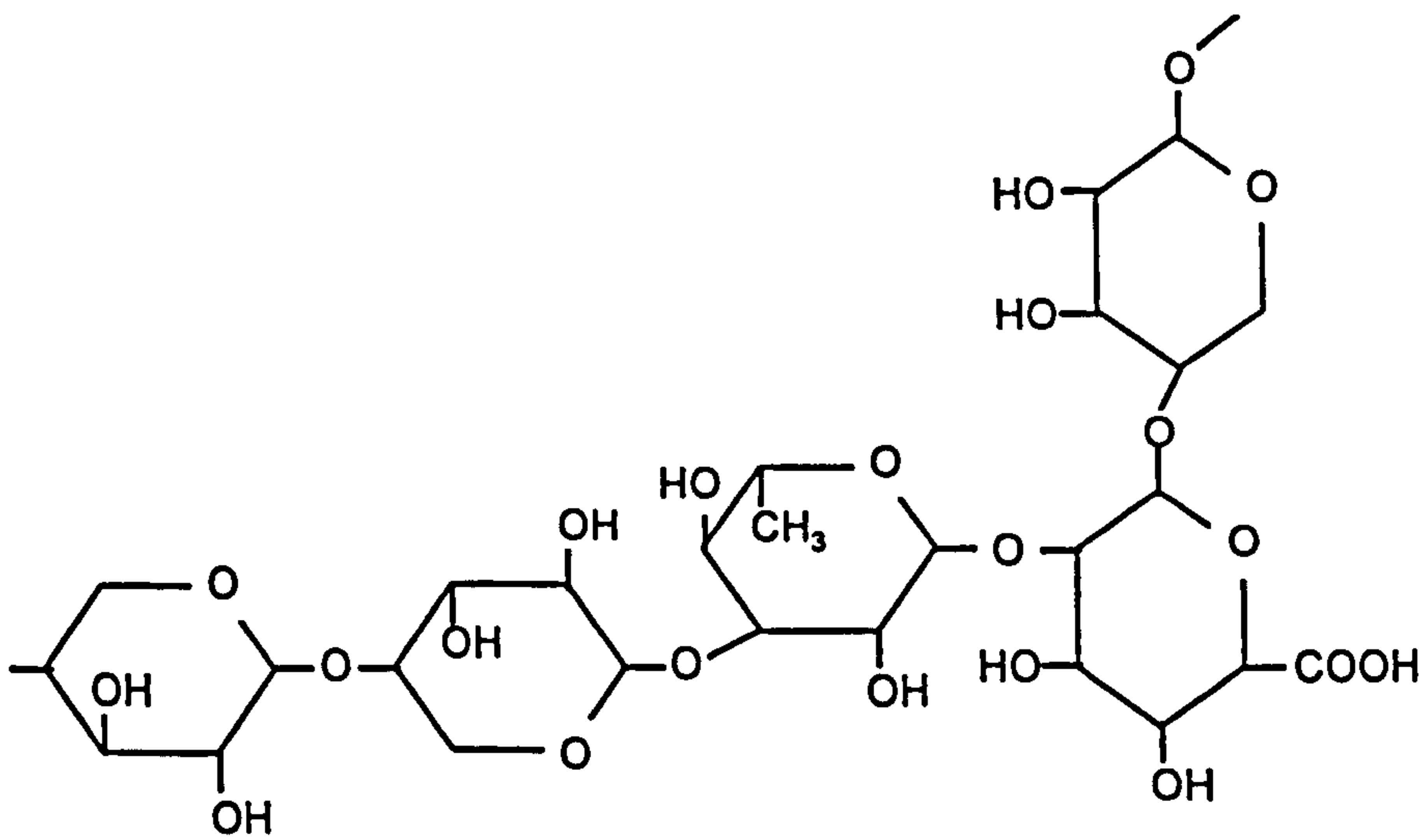
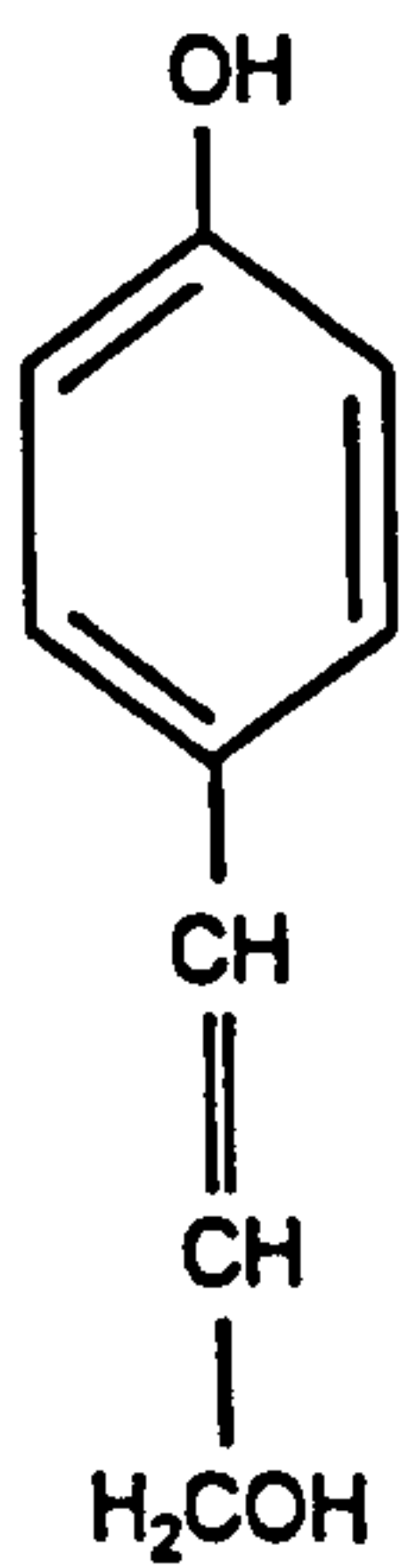
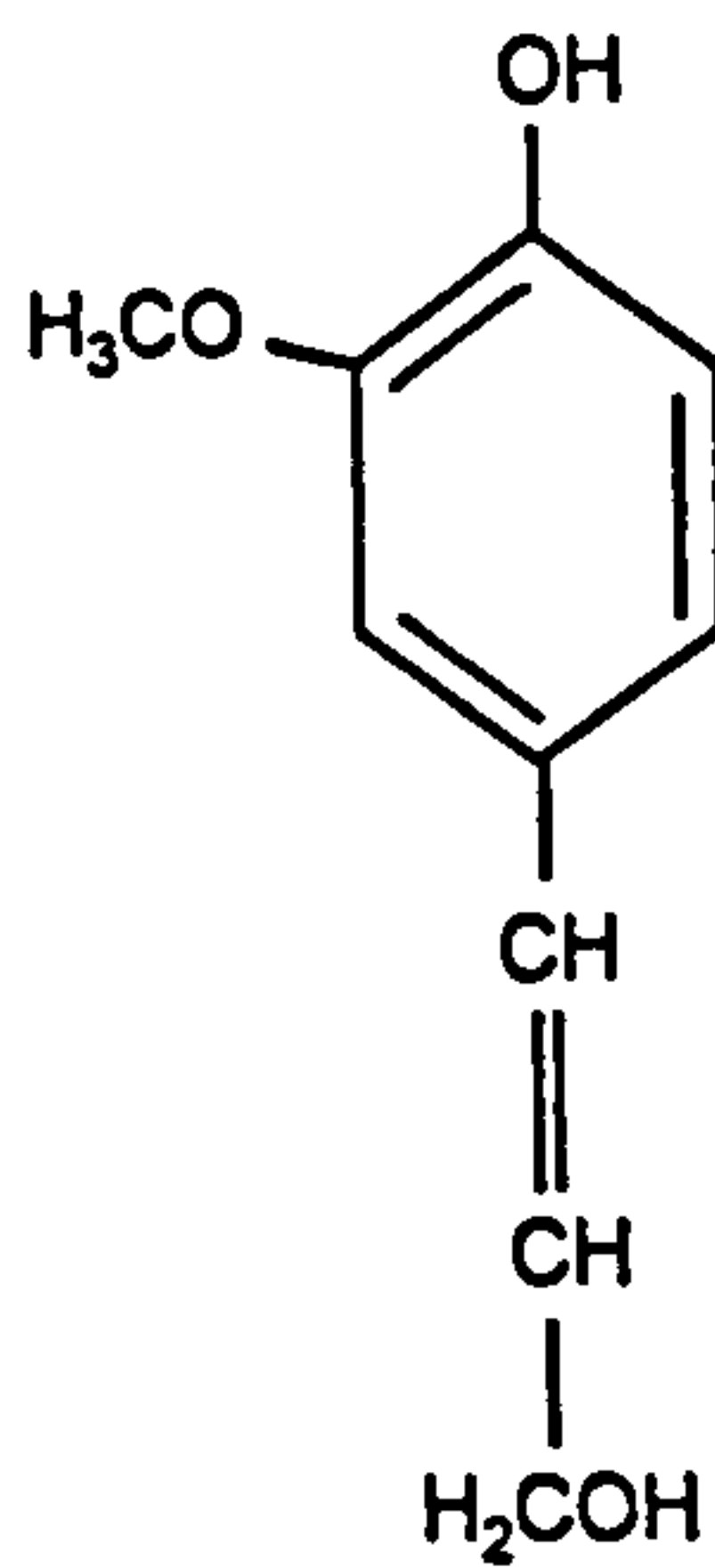


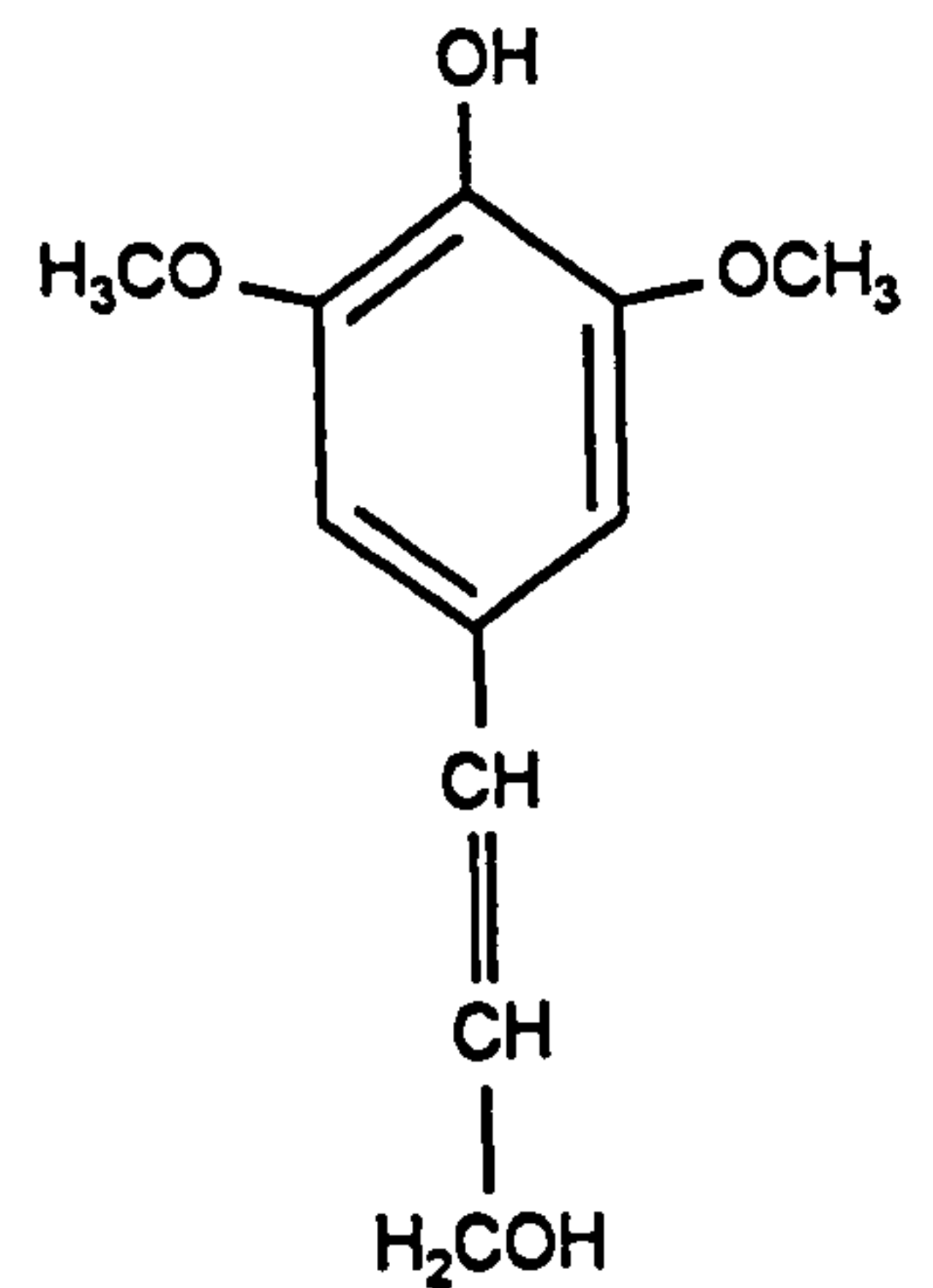
Figure 2.9 Structure of Hemicellulose in Hardwoods



p-Coumaryl Alcohol



Coniferyl Alcohol



Synapyl Alcohol

Figure 2.10 Precursors of Lignin Biosynthesis

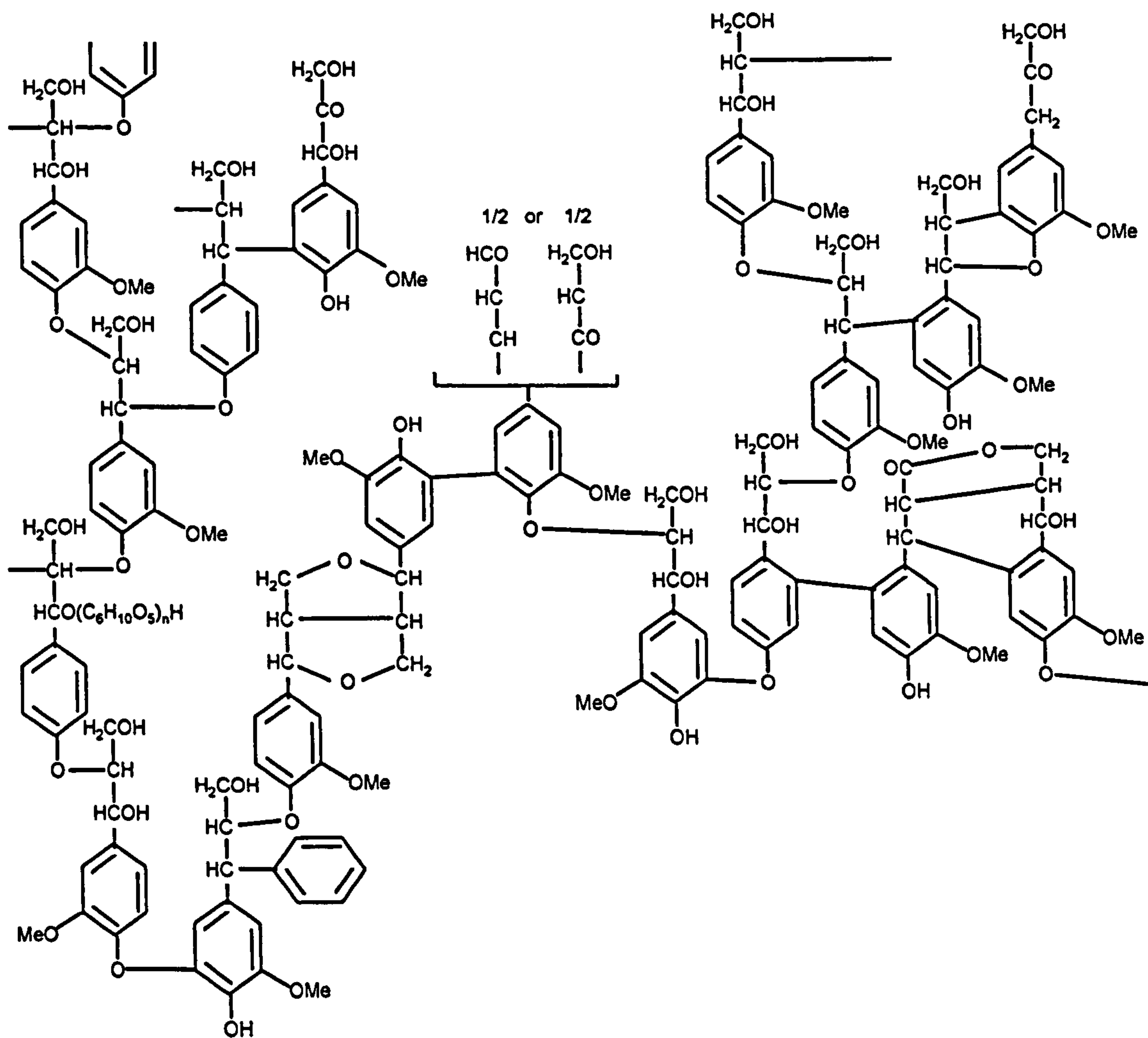


Figure 2.11 An Example of a Particular Lignin Structure, that of Normal Conifer Wood

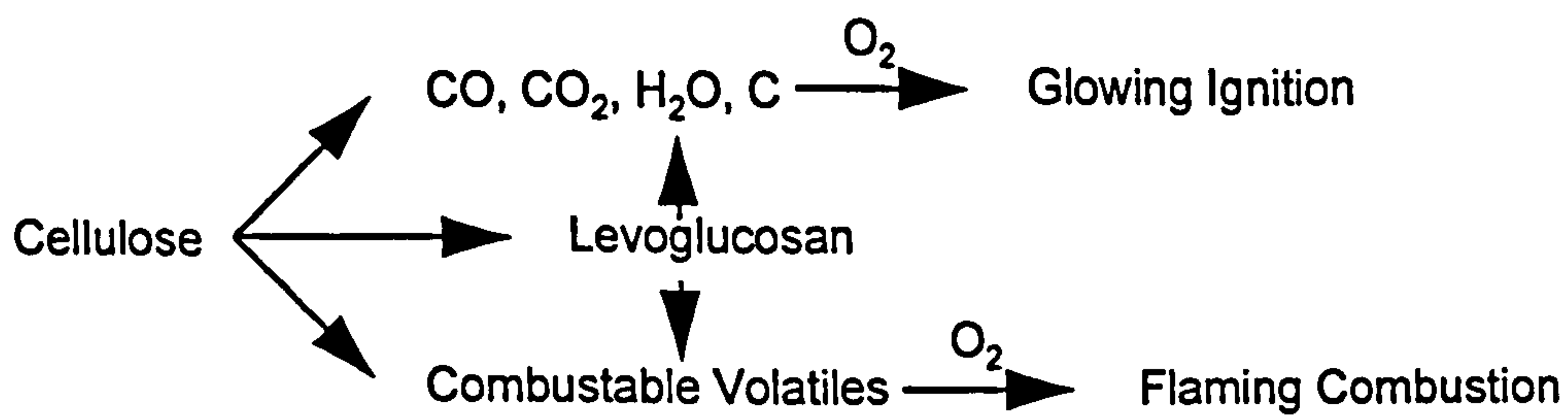


Figure 2.12 Reaction Pathway for Cellulose Pyrolysis/Combustion

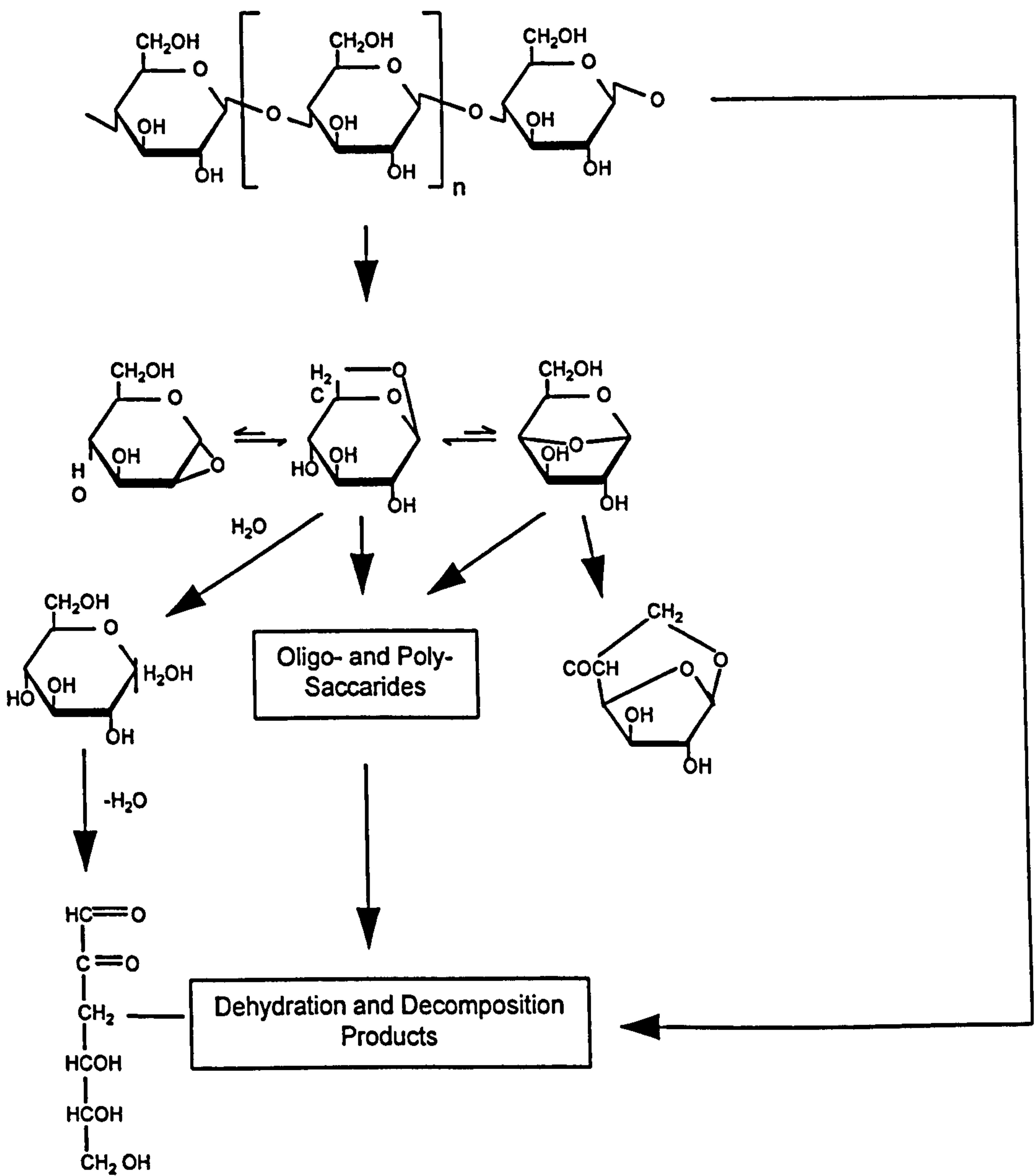


Figure 2.13 Model for Cellulose Pyrolysis and Product Transformation

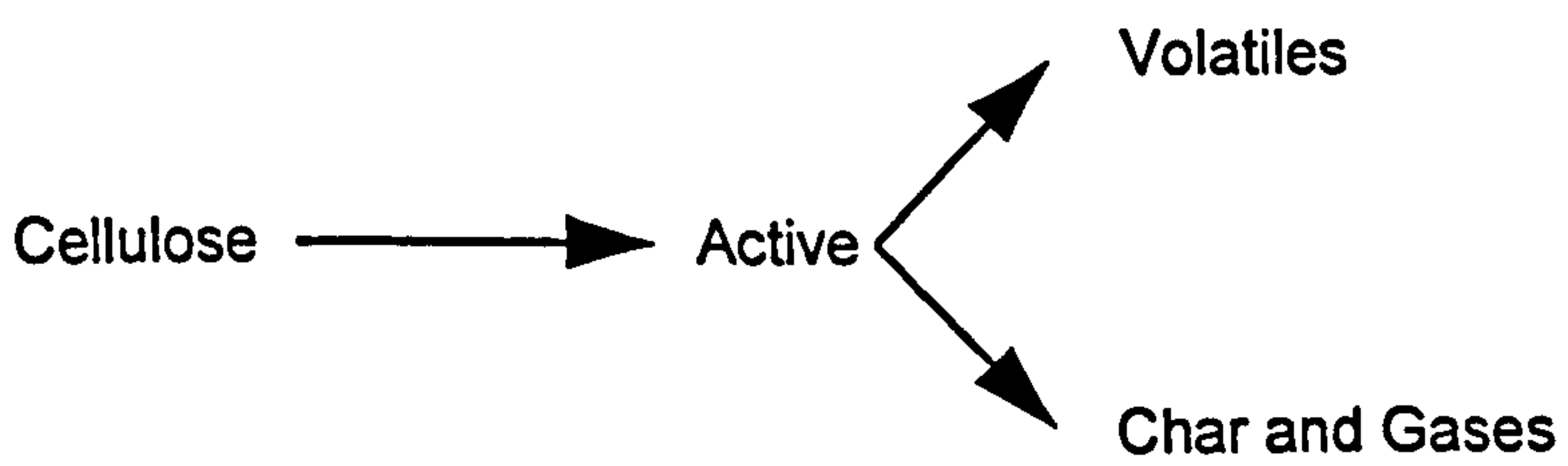


Figure 2.14 Kilzer and Broido Proposed Model for Cellulose Pyrolysis

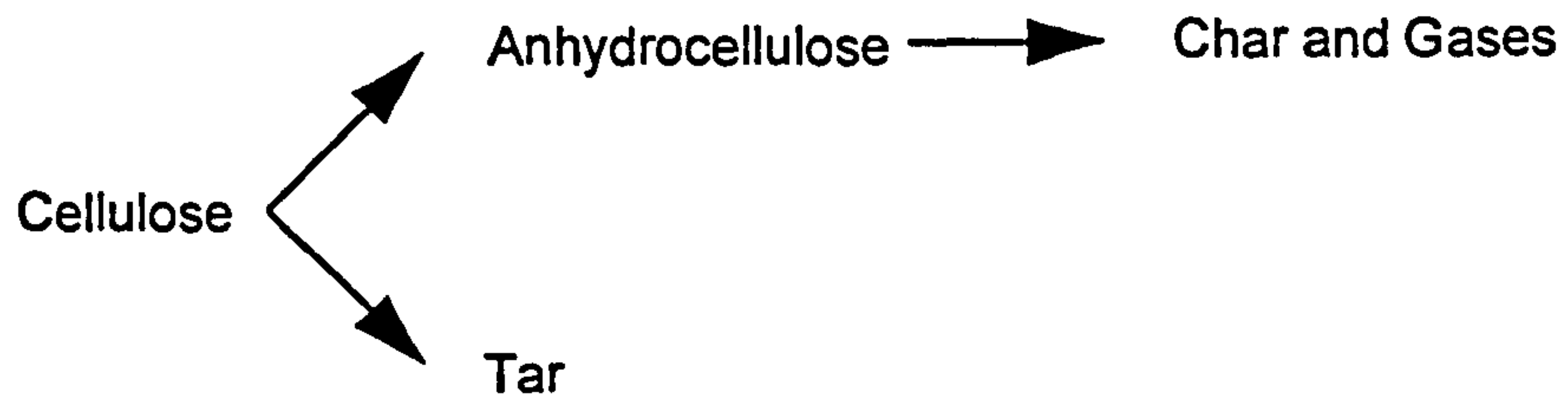


Figure 2.15 Agrawal Proposed Model for Cellulose Pyrolysis

Chapter 2 References

1. LAHAYE, J; EHRBURGER, P:
Eds; *Fundamental Issues on Control of Carbon Gasification Reactivity*; p 1-34,
(1991), Kluwer Academic Publishers.
2. MARSH, H:
Introduction to Carbon Science; Pub. by Butterworths; Ch 1, (1989).
3. SNAPE, C E:
2nd Year Fuel Chem Lecture Notes; Dept. of Pure and Applied Chemistry,
Strathclyde University, Cathedral St, Glasgow, G1 1XL.
4. LAINE, N R; VASTOLA, F J; WALKER, P L Jnr:
"The Importance of Active Surface Area in the Carbon-Oxygen Reaction", *J of
Physical Chemistry*, (1963), 67, 2030.
5. MUHLEN, H T; et al:
Abstracts of the Rolduc Symposium, The Netherlands, May (1989).
6. CHENG, A; HARRIOT, P:
"Kinetics of Oxidation and Chemisorption of Oxygen for Porous Carbons with High
Surface Area", *Carbon*, (1986), 24, 2, pp 143-150.
7. ZHU, Z B; FURUSAWA, T; ADSCHIN, T:
International Conference on Coal Science; Elsevier, Amsterdam, The Netherlands,
(1987), p 515.
8. ZHU, Z B; FURUSAWA, T; ADSCHIN, T; NOZAKI, T:
ACS Preprints (Fuel. Chem. Division), (1989), 34, 1, 87.

9. HUTTINGER, K J:
Carbon, (1990), 28, 453.
10. HUTTINGER, K J; NILL, J S:
ACS Preprints (Fuel Chem. Division), (1989), 34, 1, 79.
11. LIZZIO, A A; JIANG, H; RADOVIC, L R:
"On the Kinetics of Carbon (Char) Gasification: Reconciling Models with Experiments", Carbon, (1990), 28, 1, pp 7-19.
12. HERMAN, G; HUTTINGER, K J:
"Mechanisms of Water Vapour Gasification of Carbon - A New Model", Carbon, (1986), 24, 6, pp 705-713.
13. Von FREDERSDORFF, C G; ELLIOT, M A:
Coal Gasification, Chemistry of Coal Utilisation; Ed. H H Lowry; Supplementary Volume, Wiley, New York, 892, (1963).
14. VASTOLA, F J; HART, P J; WALKER Jnr, P L:
"A Study of Carbon-Oxygen Surface Complexes Using O¹⁸ as a Tracer", Carbon, (1964), 2, 65.
15. LAINE, N R; VASTOLA, F J; WALKER Jnr, P L:
"The Role of the Surface Complex in the Carbon-Oxygen Reaction", Proceedings of the 5th Conf. Carbon; vol 2, (1963), Pergamon Press, NY, pp 211-219.
16. WALKER, Jnr, P L; SHELEF, M; ANDERSON, R A:
Chemistry and Physics of Carbon; Eds. P L Walker Jnr, Marcel Dekker, NY, (1968), vol 4, 287.
17. PHILLIPS, R; VASTOLA, F J; WALKER Jnr, P L:
"The Thermal Decomposition of Surface Oxides Formed on Graphon", Carbon, (1970), 8, 197.

18. LEWIS, J B:
Modern Aspects of Graphite Technology; Ed Blackman, L C F; Ch 4, Academic Press, London, (1970), pp 129-199.
19. RODRIGUEZ-REINOSO, F; THROWER, P A; WALKER Jr, P L:
"Kinetic Studies of the Oxidation of Highly Orientated Pyrolytic Graphites", Carbon (1974), 12, 93.
20. WANG, J and McENANEY, B:
Abstracts of 19th American Conference on Carbon, Pennsylvania State University, 25-30 June, (1989), p 50.
21. Van HEEK, K H; MÜHLEN, H J:
"Chemical Kinetics of Carbon and Char Gasification", Fundamental Issues in Control of Carbon Gasification Reactivity; (1991), pp 1-34, Kluwer Academic Publishers.
22. SMITH, I W:
"The Intrinsic Reactivity of Carbons to Oxygen", Fuel, (1978), 57, p 409.
23. LANG, F M; MAGNIER, P; MAY, S:
Proceedings from 5th Conference on Carbon; Pergamon Press, NY, (1962), vol 1, p 171.
24. McKEE, D W; SPIRO, C L; LAMBY, E J:
"The Inhibition of Graphite Oxidation by Phosphones Additives", Carbon, (1984), 22, 285.
25. McKEE, D W; SPIRO, C L; LAMBY, E J:
"The Effects of Boron Additives on the Oxidation Behaviour of Carbons", Carbon, (1984), 22, 507.

26. McKEE, D W; SPIRO, C L; LAMBY, E J:
"The Effects of Chlorine Pretreatment on the Reactivity of Graphite in Air",
Carbon, (1985), 23, 427.
27. YANG, R T and DUAN, R Z:
"Kinetics and Mechanism of Gas-Carbon Reaction : Conformation of Etch-Pits,
Hydrogen Inhibition and Anisotropy in Reactivity", Carbon, (1985), 23, 325.
28. THOMAS, J M:
"Chemistry and Physics of Carbon", Microscopy Studies of Graphite Oxidation;
Ed. by P L Walker Jnr; Marcel Dekker, New York, (1965), vol 1, 121.
29. BROWN, E F:
"The Equilateral Nature of the Hexagonal Etch Pit Development During Carbon
Oxidation", Carbon, (1987), 25, 617.
30. STEIN, S E; BROWN, R L:
"Chemical Theory of Graphite-Like Molecules", Carbon, (1985), 23, 105.
31. McKEE, D W:
"Chemistry and Physics of Carbon", P L Walker Jnr and P A Thrower Eds, Marcel
Dekker, NY, (1981), 16, p 1.
32. QADER, S A:
"Natural Gas Substitutes from Coal and Oil", Coal Science and Technology 8; Ed.
by L Anderson; Elsevier (1985) Ch 4, p 150.
33. BAKER, R T K:
"Carbon and Coal Gasification", NATO ASI Series E - No 105; Eds. J L Figueiredo
and J A Moulign; Nijhoff, (1986), p 231.

34. PULLEN, J R:
"Catalytic Coal Gasification", IEA Report ICTIS/TR26, IEA Coal Research
London.
35. KAPTEYN, F; MOULIJN, J A:
"Carbon and Coal Gasification", NATO ASI Series E - No 105; Eds. J L Figueiredo
and J A Moulijn; Nijhoff, (1986), p 181.
36. WALKER Jnr, P L; SHELEF, M; ANDERSON, R A:
"Chemistry and Physics of Carbon", Eds. P L Walker Jr, P A Thrower; Marcel
Dekker, NY, (1968), vol 4, p 287.
37. MOORHEAD, R D; POPPA, H; HEINEMANN, K:
J of Vac Sci Tech, (1980), 17, 248.
38. GRAHAM, R G; BERGOUNEU, MA ; OVEREND, R P:
"Fast Pyrolysis of Biomass", J of Analytical and Applied Pyrolysis, (1984), vol 6,
pp 95-135.
39. SHAFIZADEH, F:
"Introduction to Pyrolysis of Biomass", J of Analytical and Applied Pyrolysis,
(1982), vol 3, pp 283-305.
40. RIJDHOLM, S A:
"Pulping Processes", Wiley International Science NY, (1965).
41. PETERSON, R C:
"Chemistry of Solid Wood", ACS Symposium Series, (1984), 207, p 57.
42. Emerging Technologies for Materials and Chemicals from Biomass;
ACS Symposium Series 476, Ch 23.

43. Wood Structure and Composition, vol 1, International Fibre Science; Eds. Menachem L, Goklstein I; Marcel, Dekker, (1984).
44. PEARL, I A:
"The Chemistry of Lignin", Marcel Dekker, NY, (1967).
45. "Thermal and System Design (Utility and I and M)", Mitsui Babcock Energy Limited Technical Manual, No. 1, p 02.03.BA4 11.8.94.
46. SUTCLIFFE, J F and BAKER, D A:
"Plants and Mineral Salts", Edward Arnold Limited, (1974).
47. ETEGNI, L and CAMPBELL, A G:
"Physical and Chemical Characteristics of Wood Ash", Bioresource Technology, (1991), 37, pp 173-178.
48. BRAUNSTEIN, H, et al:
"Biomass Energy Systems and the Environment", Pergaman Press, (1981).
49. LIVINGSTON, W R:
"Straw Ash Characteristics", Contractor Report, Babcock Energy Ltd, Renfrew, (1991).
50. GHALY, A E, et al:
"Physical and Thermochemical Properties of Cereal Straw", Energy Sources, (1990), vol 12, pp 131-145.
51. Encyclopedia of Material Science "Resource Recovery", (1986), 6, 4231-4238.
52. "Fundamental Studies into RDF Combustion", ETSU Contract Report B1229, (1991).

53. **LIVINGSTON, W R; BIRCH, M C:**
"The Combustion of Pelletised RDF", J of the Inst. of Energy, (1990), 63, pp 151-159.
54. "Slagging and Fouling in Combustion Plants", ETSU Contract Report 92012.
55. **AGRAWEL, R K:**
"A Rapid Technique for Characterisation and Proximate Analysis of RDF and its Implications for Thermal Conversion", Waste Management Research, (1988), 6, 271.
56. **SHAFIZADEH, F:**
"Pyrolysis and Combustion of Cellulosic Materials", Advances in Carbohydrate Chemistry, Eds. Korgram and Tippson; Pub. Academic Press, (1968), vol 23, pp 419-474.
57. **SHAFIZADEH, F and FU, Y:**
"Pyrolysis of Cellulose", Carbohydrate Research, (1973), vol 29, pp113-122.
58. **KILZER, F J; BROIDO, A:**
"Speculation on the Nature of Cellulose Pyrolysis Pyrodynamics", vol 2 pp 151-163, (1965).
59. **AGRAWEL, R K:**
"Kinetic Reactions Induced in the Pyrolysis of Cellulose II - The Modified Broido Model", Can. J of Chem Eng, (1988), vol 66, pp 413-448.
60. **ANTAL:, M J:**
Proc. Annual AIChE meet, Philadelphia, PA, June 1980, Am. Inst. Chem Eng., New York.

61. MADORSKY, S L; HART, V E and STRAWS, J:
"Thermal Degradation of Cellulosic Materials", Journal of Research National Bureau of Standards, (1958), vol 60, pp.343-349.
62. OREN, M; GUPTA, Y P; DAVID, G and MacKAY, M:
"Infra-red Study of Salt Free and Salt Treated Cellulose Pyrolysis Under a Nitrogen Atmosphere", Fuel, (1990), vol 69, pp 1561-1563, Short Communications.
63. SHAFIZADEH, F; LAH, Y Z and McINTYRE, C R:
"Thermal Degradation of 6-Chlorocellulose and Cellulose-Zinc Chloride Mixture", Journal of Analytical and Applied Pyrolysis, (1978), vol 22, pp 1183-1193.
64. SHAFIZADEH, F and CHEN, P P S:
"Preparation of 1, 6-Anhydro-3, 4 Dideoxy- β -D-glycero Hex-3-enopyranos-2-ulose (levoglucosenone) and some Derivatives Thereof", Carbohydrate Research, (1977), vol 58, pp 79-87.
65. DeGROOT, W F and SHAFIZADEH, F:
"The Influence of Ion Exchangeable Cation on the Carbonisation of Biomass", J of Analytical and Applied Pyrolysis; (1982), vol. 6, pp 217-232.
66. "Thermochemical Processing of Biomass", Ed. A V Bridgewater, Butterworth Scientific, Guildford, UK, (1984).
67. BRIDGEWATER, A V:
Pyrolysis Technologies and Costs : Energy from Biomass; 4th ed, Ed. G Grassi et al, Elsevier Applied Science, London (1989), pp 620-25.
68. MASCHIO, G; KOUFOPANOS, C and LUCCHESI, A:
"Pyrolysis a Promising Route for Biomass Utilisation", Bioresource Technology, (1992), vol 42, pp 219-231.

69. BRAME, J S S and KING, J G:
“Fuel - Solid Liquid and Gaseous”, Edward Arnold Ltd, London, (1955), p 239.
70. FIGUEIREDO, J L; VALENZUELA, C; BERNAITE, A and ENCINAR, J M:
“Pyrolysis of Holm Oak Wood: Influence of Temperature and Particle Size”, Fuel, (1989), 68, pp 1012.
71. KUMAN, N; GUPTA, R C:
“Influence of Carbonisation Conditions”, Transactions Indian Institute of Metals, (1993), vol 46, pt 6, pp 345-352.
72. SAVAGE, G:
Metals and Materials, (1988), 4, 544.
73. INGAKI, M; ITOCH, T, and NAKA, S:
“Graphitization and Sintering of Coals Under Pressure”, Fuel, (1979), 58, 741.
74. RUMSEY, J C V; PITT, G J:
“Some Techniques for the Characterization of Cokes and Graphites”, Fuel, (1978), 57, 155.
75. WIECKOWSKA, J; CMIELEWSKI, J:
“Characterisation of Petroleum Binders: Characterisation of Solid Products”, Fuel, (1980), 59, pp 185-189.
76. NEALY, J W:
Carbon, (1981), 19, 27.
77. RICHARDS, G N; ZHENG, N:
“Influence of Metal Ions and Salts on Products from the Pyrolysis of Wood : Applications to Thermochemical Processing of Newsprint and Biomass”, Journal of Analytical and Applied Pyrolysis; (1991), vol 21, pp 133-146.

78. ZAROR, C A:
“Studies of the Pyrolysis of Wood at Low Temperatures”, PhD Thesis, Dept. of Chem Eng, Imperial College, London University, (1982).
79. BRITT, P; BUCHANAN III, A C; ESKAY, T P; MUNGALL, W S:
“Mechanistic Investigations into the Decarboxylation of Aromatic Carboxylic Acids”, ACS Division of Fuel Chemistry Preprints, (1998), 44, 3, pp 533-510
80. STROMBERG, G; STRAWN, J; ARKENHAMMER, S:
J of Polymer Science, (1959), 35, 355.
81. ABBAS, K B and SOWICK, E M:
J of Appl. Sci, (1975), 19, 2991.
82. BRAUN, D; THALLMAIER, M:
Makromol Chem, (1966), 99, 59.
83. WINKLER, D E:
J of Polymer Science, (1959), 35, 3.
84. OUCHI, J:
J of Polymer Science, (1965), 2, 2685.
85. Encyclopedia of Chemical Technology:
Ed. Anthony Standen, Vol 14, 2nd Edition, Interscience Pub.
86. WOLKOBBER, P:
J of Polymer Science, (1962), 58, 1311.
87. MIMS, C A:
“Fundamental Issues in Control of Carbon Gasification Reactivity”, pp 393-407;
Eds. J Lahaye, P Ehrburger; 1091 Kluwer Academic Publishing.

88. SERIO, N A; SOLOMON, P R; BASSILAKES, R:
“The Effects of Minerals on Coal Reactivity”, Int. Conf on Coal Science, Tokyo, Oct. (1989).
89. FUNG, D P C; KIM, S D:
“Chemical Reactivity of Canadian Coal-Derived Chars”, Fuel, (1984), 63, 1197.
90. MORALES, I F; GARSON, F J L; PEINADO, A L:
“Study of Heat-Treated Spanish Lignites: Characterisation and Behaviour in CO₂ and O₂ Gasification Reactions”, Fuel, (1985), 64, 666.
91. HIPPO, E J; JENKINS, R G; WALKER, P L:
“Enhancement of Lignite Char Reactivity to Steam by Cation Addition”, Fuel, (1979), 58, 338.
92. LINARES-SOLANO, A; HIPPO E J; WALKER, P L:
“Catalytic Activity of Calcium for Lignite Char Gasification in Various Atmospheres”, Fuel, (1986), 65 776.
93. RADOVIC, L; WALKER, P L; JENKINS, R G:
“Effect of Lignite Pyrolysis Conditions on Calcium Oxide Dispersion and Subsequent Char REactivity”, Fuel, (1983), 62, 209.
94. De GROOT, W F; KANNAN, M P; RICHARDS, G N; TEANDER, O:
“Gasification of Agricultural Residues (Biomass): Influence of Inorganic Constituents”, J of Agricultural Food Chem, (1990), 38, pp 320-323.
95. De GROOT, W F; RICHARDS, G N:
“Influence of Pyrolysis Conditions and Ion-Exchanged Catalysts on the Gasification of Cottonwood Chars by Carbon Dioxide”, Fuel, (1988), 67, 352.

96. KANNAN, M P; RICHARDS, G N:
“Gasification of Biomass Chars in Carbon Dioxide: Dependence of Gasification Rate on the Indigenous Metal Content”, *Fuel*, (1990), 69, p 747.
97. WALKER Jnr, P L:
Fundamentals in Thermochemical Biomass Conversion; Eds. R P Overend, T A Milne and L K Mudge; Elsevier, New York, USA, (1985), 28 pp 485-509.

Chapter Three

Objectives

3.1 Objectives

The thermo-chemical processing of biomass and solid waste materials has been the subject of significant research and development efforts in North America, Japan and on continental Europe for over three decades. However, it is only in recent years that the subject has been given any serious consideration in Britain.

Most biomass and waste gasification systems are based on established technologies designed for the gasification of coal, which is now a fully commercial process. A number of integrated gasification combined cycle plant of reasonable size and which involve the gasification of coal at pressures up to 10 MPa (100 bar) are in operation around the world. There is therefore, a requirement for an improved understanding of how the design and operating parameters of coal gasification plant can be adapted to operate reliably and efficiently with a biomass and/or waste feed stock. This will require an improved knowledge of the characteristics and behaviour of the feedstock constituents, both organic and inorganic, in gasification systems. This forms the basis of the objectives for this study.

The principal objectives of this study can be stated as follows;

- (i) To provide data on the basic characteristics, relevant to gasification systems, of a range of biomass and waste materials in order to make direct comparisons with coal. The selected materials are listed below;
- Cereal straw
 - Wood - short rotation coppice (SRC)
 - waste wood (sawmill)
 - Municipal solid waste - RDF
- (ii) To provide information, at laboratory scale, on the behaviour of these materials during gasification by investigating relevant reactions, i.e. their behaviour during pyrolysis reactions and the reactivity of the resulting chars in oxygen.
- (iii) To provide information about the behaviour of the inorganic constituents of the biomass and waste feedstocks.
- (iv) To provide information about the interactions of the components of municipal waste by studying the behaviour of mixtures of these components during relevant thermal processes.

These objectives were established in order to provide a basic understanding of the behaviour during gasification, of the most commonly available biomass and waste resources in Britain.

Chapter Four

Experimental

4.1 Samples

4.1.1 Biomass Samples

In Britain, and in most northern European countries, the most important biomass materials which are relevant for use as fuels in combustion and gasification processes are;

- (i) Surplus cereal straws, and
- (ii) Wood materials, principally forestry and sawmill wastes, short rotation coppice wood crops, and industrial wood wastes.

In the course of the project, a number of samples of biomass materials were collected and these are listed below;

1. Cereal straw, obtained from Mitsui Babcock Technology Centre in Renfrew, who have been involved in the assessment of straw as a fuel for a number of years.

Wood Materials, including;

2. Danish pine roundwood, from Mitsui Babcock Technology Centre

Short rotation coppice wood from the Long Ashton Research Station, Bristol which were designated

3. Long Ashton I - mixed 1 year old poplar and willow,

4. Long Ashton II - 2 year old willow,

5. Long Ashton III - 3 year old willow, and

6. Long Ashton IV - mixed 3 and 4 year old poplar.

Short rotation coppice poplar sticks of 4 years old from the Silsoe Research Institute, Bedfordshire. This sample was separated into the following fractions;

7. Bark - separated outer stick material,

8. Sapwood - material beneath bark,

9. Twigs - new shoots from stick, and

10. Bulk - unseparated material.

The cereal straw and Danish pine wood materials had been dried and milled prior to reception and both of these materials had a grading of 2 mm top size. The four Long Ashton materials and the Silsoe material were received as chopped sticks. In order to maintain consistency and to ensure that representative samples of each material were analysed, all of the Long Ashton as well as all of the fractionated Silsoe materials were milled to have a top size of 2 mm.

4.1.2 Refuse Derived Fuels

One alternative to the mass burn incineration of municipal solid wastes is to pretreat the waste to produce a waste-derived fuel which can be combusted or

gasified in more conventional equipment. Two basic types of refuse-derived fuel can be prepared;

- (a) Coarse (floc)-type RDF, with a mass yield for the raw refuse in excess of 50 %, produced by a combination of screening ferrous metal extraction and shredding, and
- (b) densified or pelletised RDF, with a mass yield of less than 50 %, involving a high degree of sorting and pre-treatment.

The work reported in this study is concerned with pelletised RDF. A number of production plants were built in Britain to produce a pelletised and dried RDF. In this work samples were obtained from two of the RDF plants, which are still in operation, viz:

11. the *Byker* plant in Newcastle upon Tyne, and
12. the *Isle of Wight* plant.

These samples were obtained from Mitsui Babcock Technology Centre.

4.1.3 Acid-Washed Samples

In an attempt to study the influence of mineral matter on the behaviour of biomass and waste materials during thermal processing, selected samples were treated by ingestion in HNO₃ and HCl solutions. The materials treated were cereal straw, Danish pure wood, Byker RDF and Isle of Wight RDF. The procedure involved heating 0.2 litres of 1 M acid to 35-40 °C and adding 20 g of pre-dried sample. De-ionised water was added in order to create a slurry, the amount added dependant on the bulk volume of the sample, and this was continuously stirred for a period of 2 hours. Following this, the slurry was filtered and washed with de-ionised water to remove all the acid. This was carried out until the pH of the effluent water was identical to the original de-ionised water. The samples were

then dried in a vacuum oven at 60 °C. The samples prepared by acid washing were:

13. *HNO₃ washed straw,*
14. *HCl washed straw,*
15. *HNO₃ washed Danish pine,*
16. *HCl washed Danish pine,*
17. *HNO₃ washed Byker RDF,*
18. *HCl washed RDF,*
19. *HNO₃ washed Isle of Wight RDF,*
20. *HCl washed Isle of Wight RDF,*

4.1.4 RDF Model Composites

RDF materials have two main fractions.

- (i) Paper/board - cellulose-based material containing significant levels of binder/filler such as clays. This accounts for ~ 84 % wt of RDF (dry basis).
- (ii) Plastics - account for ~ 11 % wt (dry basis) of RDF. The main components of the plastic fraction are poly(ethene) and poly(vinylchloride) which represent 20 % and 8 % of the total plastic fraction respectively.

In order to study the interactions of the principal RDF components during thermal processing, model composite samples of cellulosic materials and plastic materials were prepared for analysis. The following materials were used;

Cellulosic Materials

1. Cereal Straw - milled with a top size of 2 mm
21. Cellulose powder - 20 micron, supplied from the Aldrich Chemical Company.

Plastic Materials

22. Poly(ethene) powder
23. Poly(vinylchloride) powder - (PVC), high molecular weight.
24. Saran powder - poly(vinylchloride)/poly(vinylidene chloride) copolymer.

All of the plastic materials were obtained from the Aldrich Chemical Company⁽⁵⁾.

The composite samples, which were prepared on a weight basis from these materials were:

25. 90 % Cellulose-10 % poly(ethene),
26. 50 % Cellulose-50 % poly(ethene),
27. 90 % Cellulose-10 % poly(vinyl chloride),
28. 50 % Cellulose-50 % poly(vinyl chloride),
29. 90 % Cellulose-10 % saran,
30. 50 % Cellulose-50 % saran,
31. 90 % Straw-10 % poly(vinyl chloride),
32. 50 % Straw-50 % poly(vinyl chloride),

4.2 Analysis Procedures

There are as yet no clearly defined standard procedures for the analysis of biomass and wastes, therefore for the purposes of this study, the British Standard methods for coal analyses were employed. This, with some minor modifications, is the procedure adopted in most fuel analysis laboratories, viz:

- (i) *Proximate Analysis* - i.e. the determination of moisture, volatile matter, ash and fixed carbon contents, of all of the raw samples were completed in accordance with BS 1016 part 104.
- (ii) *Ultimate Analysis* - i.e. the determination of the carbon, hydrogen, nitrogen, chlorine and oxygen (by difference) contents for all of the raw and char materials were completed in accordance with BS 1016 part 106.
- (iii) *Ash Analysis* - the compositions of the ash components of the samples were determined following BS 1016 part 14.

4.3 Thermal Decomposition of Samples in Air

The weight loss with increasing temperature increase for all of the materials were measured using a Stanton Redcroft TGA750 Thermogravimetric analyser. (A diagram of the TGA750 is presented in Figure 4.1). Typically ~ 10 mg of sample was loaded into a platinum crucible and placed into the cradle of the TG750 microbalance. The samples were then heated at a rate of 10 K min^{-1} , from ~ 293 K to 1173 K in order to obtain a complete temperature profile. At least two individual tests were performed in order to ensure reproducibility of results. An example of a weight loss profile, that for cellulose, is presented in Figure 4.2.

The first derivative of the weight loss dW_t/dT , i.e. the rate of weight loss with respect to temperature, was calculated for each sample. These data were plotted against temperature in order to determine the temperatures at which the rate of

weight loss peaked for each sample. An example graph, the rate of weight loss against temperature for straw, is presented in Figure 4.3.

4.4 Char Preparation

Chars were prepared by pyrolysing samples of material in a Stanton Redcroft tube furnace which was controlled by a Eurotherm Type 812 temperature controller. A diagram of the tube furnace apparatus is presented in Figure 4.4. The procedure involved loading a weight of sample, typically ~ 5 g into a silica boat which was then inserted into a silica tube contained within the tube furnace. The system was then purged with nitrogen at a rate of 1 litre minute⁻¹. The N₂ purge, was started 30 minutes before the sample was heated. The temperature was increased from room temperature, ~293 K to 1193 K at a rate of 10 K min⁻¹ and then left for 1 hour. The temperature inside the furnace was accurately measured using a Ni/Al Type K thermocouple which was connected to the Eurotherm Type 812 temperature control device. On completion, the samples were removed and weighed. The char preparation procedure was performed in duplicate for each sample to ensure reproducibility of results.

The actual char yields of the materials prepared under these conditions were calculated using the following equation:

$$\text{Char yield, (dry, ash free)} = \frac{W_o - W_c}{W_o} \times \frac{100}{1} \quad \text{equ 4.1}$$

W_o = weight of original material, corrected for ash and moisture content, and

W_c = weight of char, corrected for ash content.

In order to investigate the effects of possible interactions between components in the mixed cellulosic material - plastic material samples, the theoretical char yields were calculated. These were obtained using equation 4.8 shown below derived from first principles.

Let the char yield for a bi-component sample of weight fraction components a_1 and a_2 be

$$C_T = \frac{W_o - W_c}{W_o} \times \frac{100}{1} \quad \text{equ. 4.2}$$

then the char yield associated with component 1, C_1 , will be

$$C_1 = \frac{a_1 W_o - W_{f1}}{a_1 W_o} \quad \text{equ. 4.3}$$

where W_{f1} = final char weight fraction of component 1

Therefore the final weight fraction of component 1 and component 2 are;

$$W_{f1} = a_1 W_o - C_1 (a_1 W_o) \quad \text{equ. 4.4}$$

and
$$W_{f2} = a_2 W_o - C_2 (a_2 W_o) \quad \text{equ. 4.5}$$

The total final weight fraction, W_f can be calculated from the following equation,

$$W_f = W_{f1} + W_{f2} \quad \text{equ. 4.6}$$

This equation can be substituted into equation 4.2 to give an expression for the theoretical char yield C_T ;

$$C_T = \frac{[(a_1 W_o - a_1 W_o C_1) + (a_2 W_o - a_2 W_o C_2)]}{W_o} \quad \text{equ. 4.7}$$

and this can be simplified to

$$C_T = a_1 C_1 + a_2 C_2 \quad \text{equ. 4.8}$$

4.5 Char Reactivity Determination

The isothermal reactivity of the prepared chars to oxygen over a range of temperatures were determined using a Stanton Redcroft TGA750

thermogravimetric analyser. A diagram of this apparatus is presented in Figure 4.1. The experimental procedure involved loading an accurately weighed quantity of char sample, typically ~ 10 mg, into a platinum crucible which was subsequently placed on the TGA microbalance. The oxygen flow was set at 3 l h^{-1} and the sample was purged for a period of 15 minutes prior to heating. A heating rate of 10 K min^{-1} was used to heat the char sample to a required temperature, at which, the temperature was maintained to allow the char to react isothermally until a weight loss of more than 25 % had been achieved. The weight loss and temperature profiles were recorded on a Linseiss chart recorder. The experiments were repeated to ensure that results were reproducible. An example of the profiles of temperature and weight loss with respect to time are presented in Figure 4.5.

To provide a comparison between different chars, the reactivity values at a weight loss of 20 % were measured over a range of temperatures. The 20 % weight loss point was chosen for reactivity measurement since it was well inside the isothermal region for each char and this allowed results to be compared directly. The isothermal reactivity of the chars were calculated using the following equations.

The rate of reaction (r) was calculated from the slope of the weight loss curve at 20 % weight loss on a dry ash free basis.

$$r = \left(\frac{dW}{dt} \right) \quad \text{equ. 4.9}$$

r = Rate of reaction, g s^{-1}

dW/dt = Rate of weight loss at 20 %, g s^{-1} .

The reactivity was then calculated by substituting the rate of reaction into the following equation:

$$R = \left(\frac{1}{Wt} \right) \cdot r \quad \text{equ. 4.10}$$

R = Reactivity, $\text{g g}^{-1} \text{s}^{-1}$

W_t = Total weight of carbon burned off at 20 % (dry, ash free)

r = Rate of reaction, g s^{-1}

The estimated error of the data calculated from the experimental data is $\pm 5\%$.

The expected reactivity values of the bi-component composite materials' chars were calculated using the following equation;

$$R^l = R_1 a_1 + R_2 a_2 \quad \text{equ. 4.11}$$

R^l = Expected reactivity

R_1 = Reactivity of component 1

R_2 = Reactivity of component 2

a_1 = Weight fraction of component 1

a_2 = Weight fraction of component 2

The above equation was derived in a similar manner to equation 4.8, the equation for the calculation of the expected char yields produced from the prepared bi-component composites.

4.6 BET Surface Area Analysis

The surface areas of all of the chars were determined from 77K N_2 adsorption isotherms using the Brunauer, Emmett and Teller (BET) equation. Samples were weighed and deposited into flasks which were then securely fitted to a Micromeritics Accusorb 2100E adsorption apparatus. A schematic layout of the system used is presented in Figure 4.6. The samples were outgassed in-situ to a 10^{-2} Pa at a temperature of 398 K for a period of at least 12 hours. Initially, the

dead volume was determined using helium, since this gas has a low critical temperature (~ 5 K) and has no dipole or quadrupole and so does not adsorb on the sample. The sample was then outgassed prior to a series of 77 K N_2 adsorptions over an increasing range of pressures. This procedure involved filling a manifold of known volume to a set pressure, following which a valve was opened and the contents of the manifold flooded into the sample flask which was immersed in liquid N_2 . The system was then allowed to equilibrate. The valve was then closed and the procedure repeated until a required number of equilibrium pressures had been logged. The volume of the flasks and manifold were known and therefore the volume of adsorbed gas could be calculated. The surface area of a specific char sample was then determined from the volume of gas adsorbed at specific pressures using the BET equation.

The BET equation is derived from the Langmuir equation for adsorption. The Langmuir equation, which is based on monolayer adsorption, is expressed below:

$$p/V = p.V_m + 1/a.V_m \quad \text{equ. 4.12}$$

where

V = volume of gas adsorbed at equilibrium per unit mass of adsorbent,

p = pressure of the volume of gas,

V_m = volume of gas required to produce a complete monolayer, and

a = a constant dependent on temperature but independent of surface coverage.

Since the forces acting in physical adsorption are similar to those operating in liquefaction, physical adsorption is not limited to a monomolecular layer, but can continue until a multimolecular layer of liquid covers the adsorbent surface.

The BET equation is an extension of the Langmuir approach to allow for multilayer adsorption on non-porous surfaces. The BET equation is derived by

balancing the rates of evaporation and condensation for the various adsorbed layers, and is based on the simplifying assumption that a characteristic heat of adsorption ΔH_1 applies to the first monolayer, while the heat of liquefaction, ΔH_L , of the vapour in question applies to adsorption in the second and subsequent molecular layers. The equation is usually expressed as:

$$\frac{P}{V(p_0 - p)} = \frac{1}{V_m C} + \frac{(C-1) P}{V_m C P_0} \quad \text{equ. 4.13}$$

where

P_0 = saturation vapour pressure,

V_m = monolayer capacity, and

$C = \exp[(\Delta H_L - \Delta H_1)/RT]$.

The main purpose of the BET equation is to describe type II isotherms.

The expected surface area values of the chars prepared from the bi-component composite samples were calculated using the following equation.

$$S^1 = s_1 a_1 + s_2 a_2 \quad \text{equ. 4.14}$$

where

S^1 = Expected char surface area, $m^2 g^{-1}$,

s_1 = Char surface area of component 1,

s_2 = Char surface area of component 2,

a_1 = Weight fraction of component 1, and

b_1 = Weight fraction of component 2.

This equation was derived in a similar manner to equation 4.8, the equation for the calculation of the expected char yields prepared from bi-component composites.

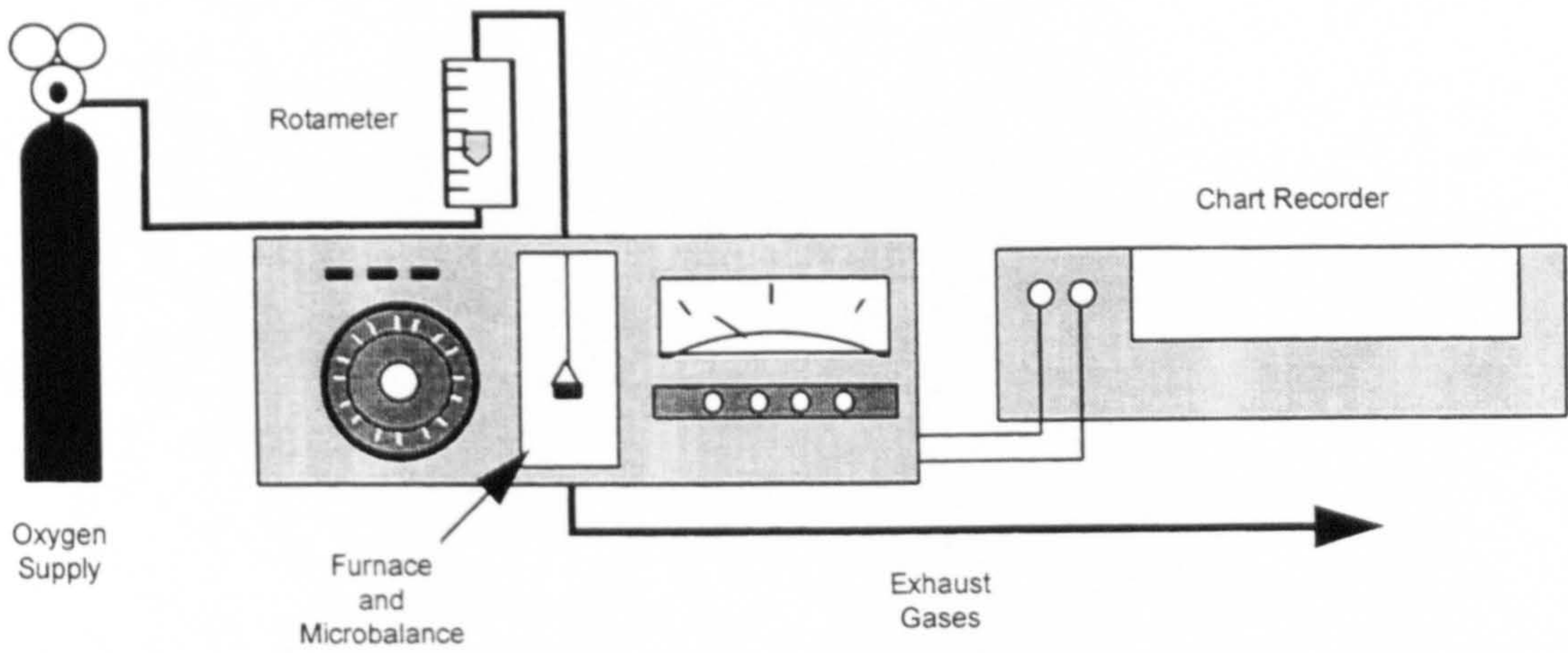


Figure 4.1 Illustration of Stanton Redcroft TGA750 TGA and Data Recording Equipment

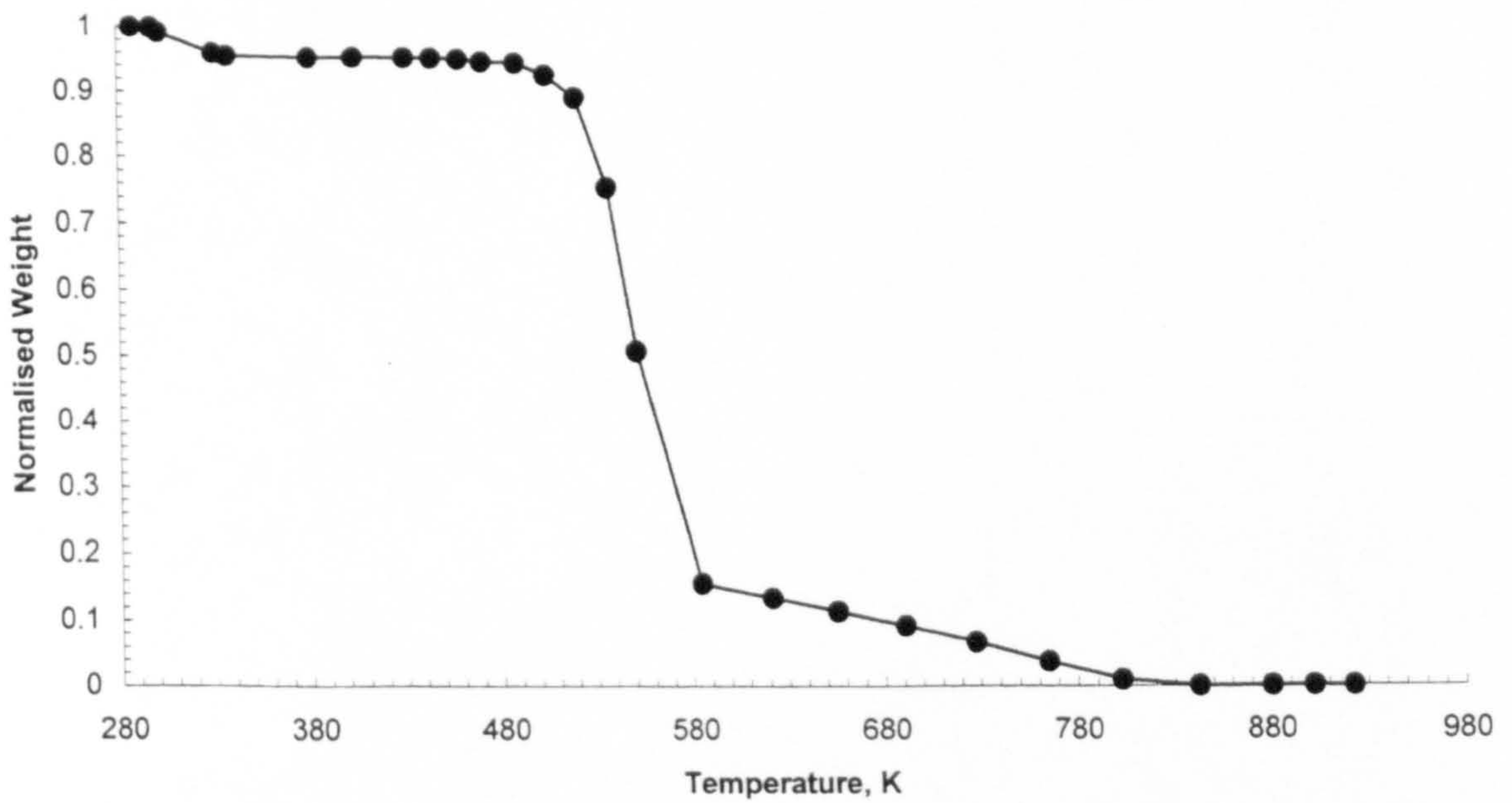


Figure 4.2 Normalised Weight Loss Profile of Cellulose, Heated at 10 K min^{-1} from 293-1173 K

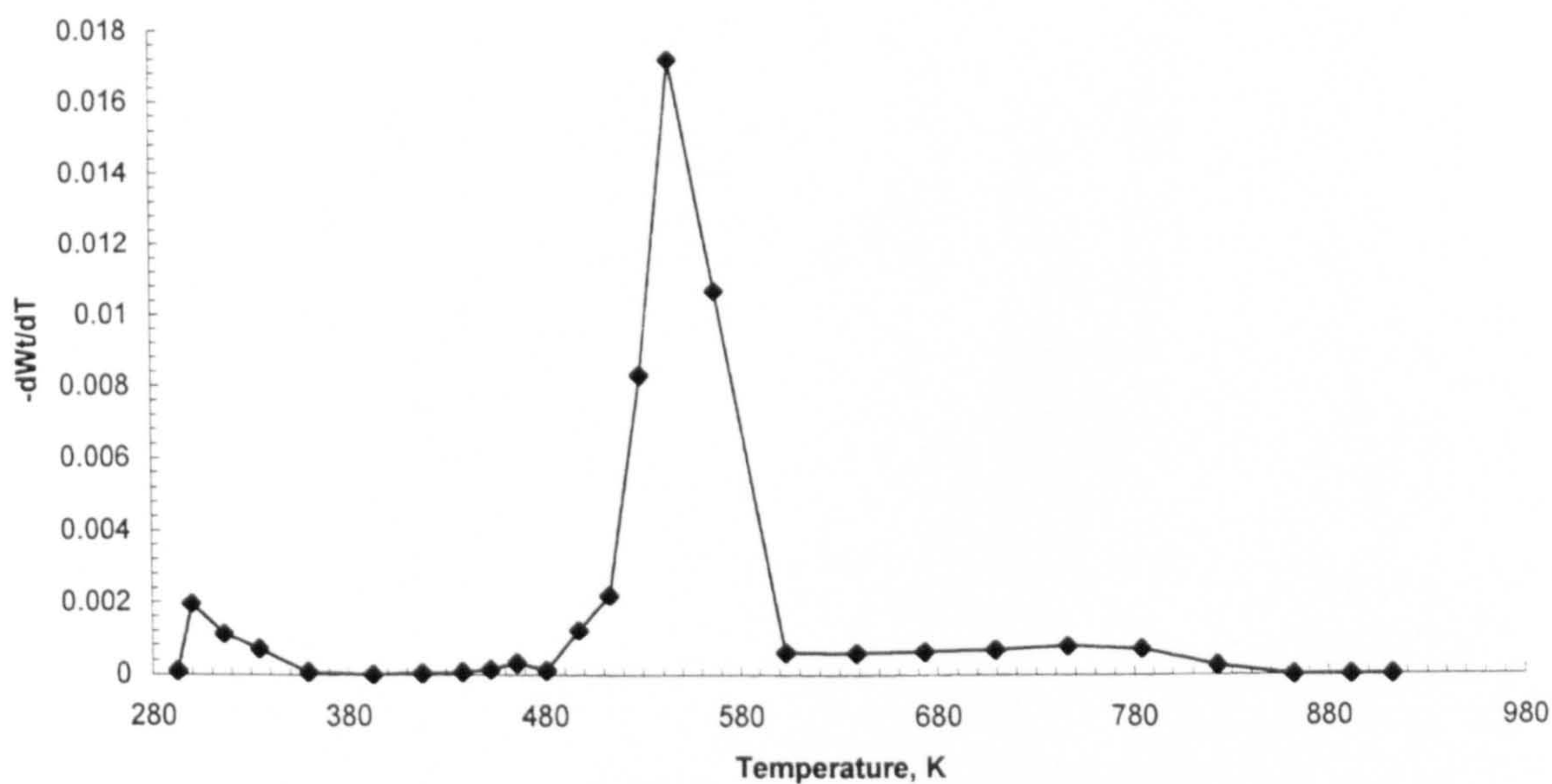


Figure 4.3 First Derivative Graph of Weight Loss with Respect to Temperature for Cellulose Heated at 10 K min^{-1} from 293-1173 K

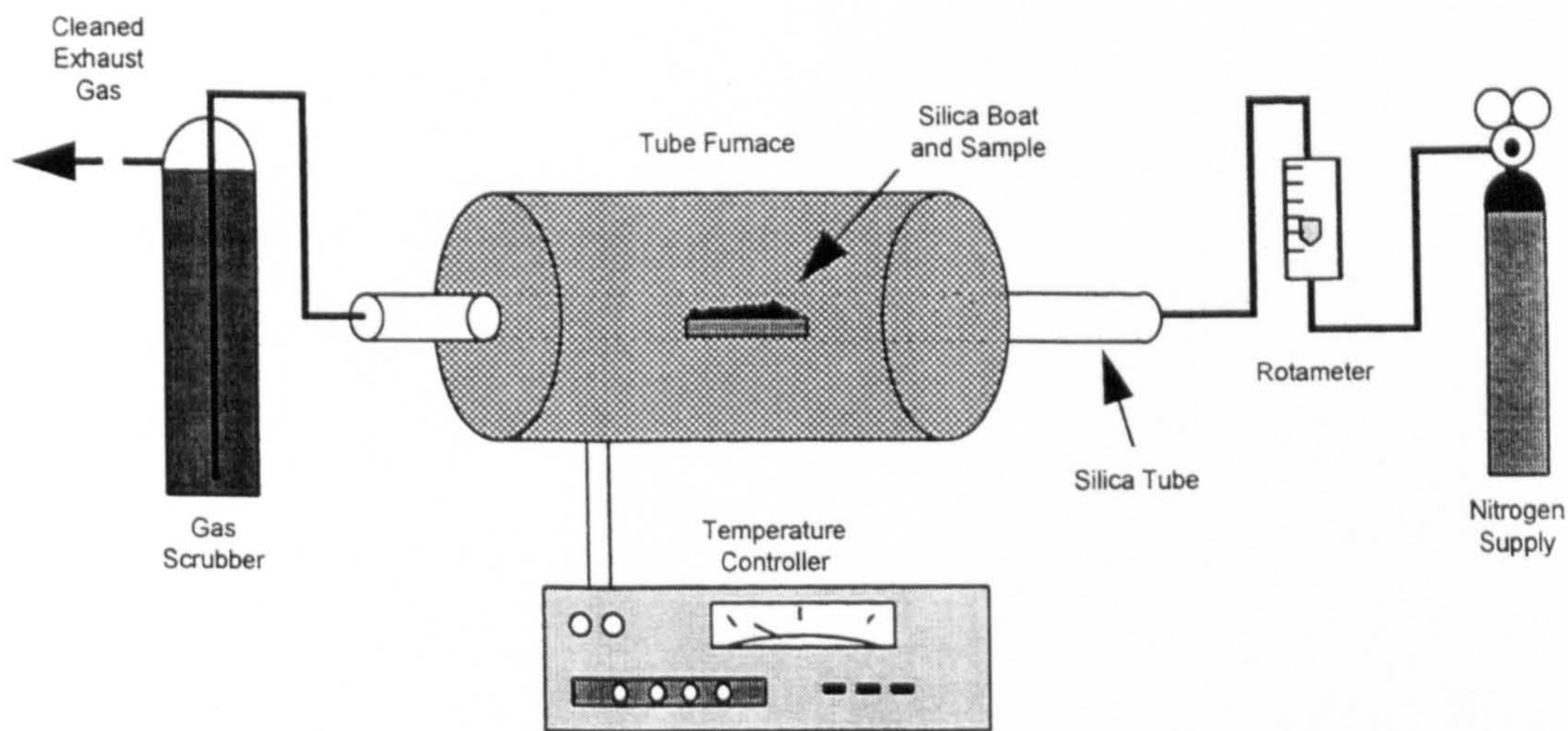


Figure 4.4 Illustration of Stanton Redcroft Tube Furnace and Eurotherm Type 812 Controller Used for Char Preparation

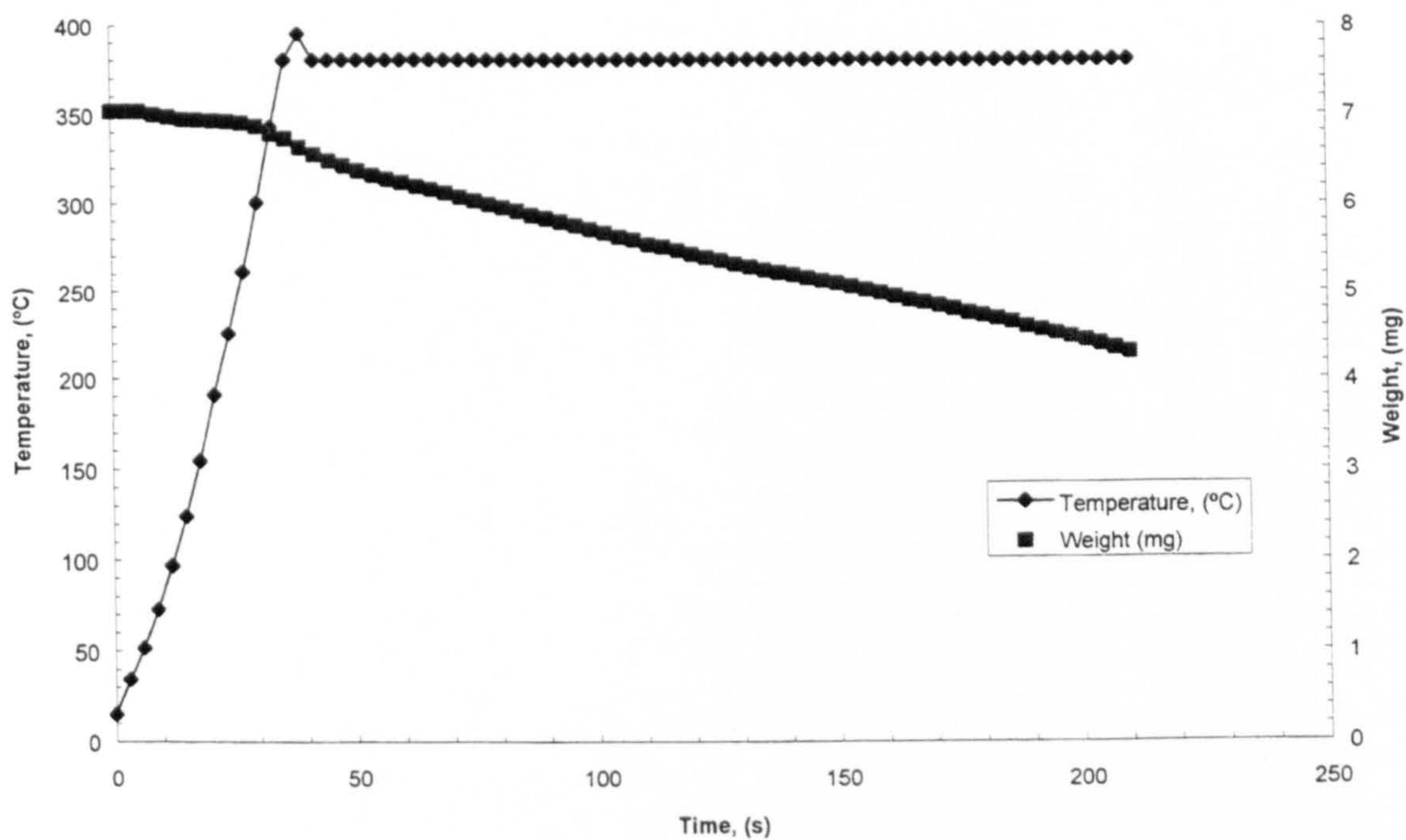


Figure 4.5 Graph of Isothermal Weight Loss for a Sample Char

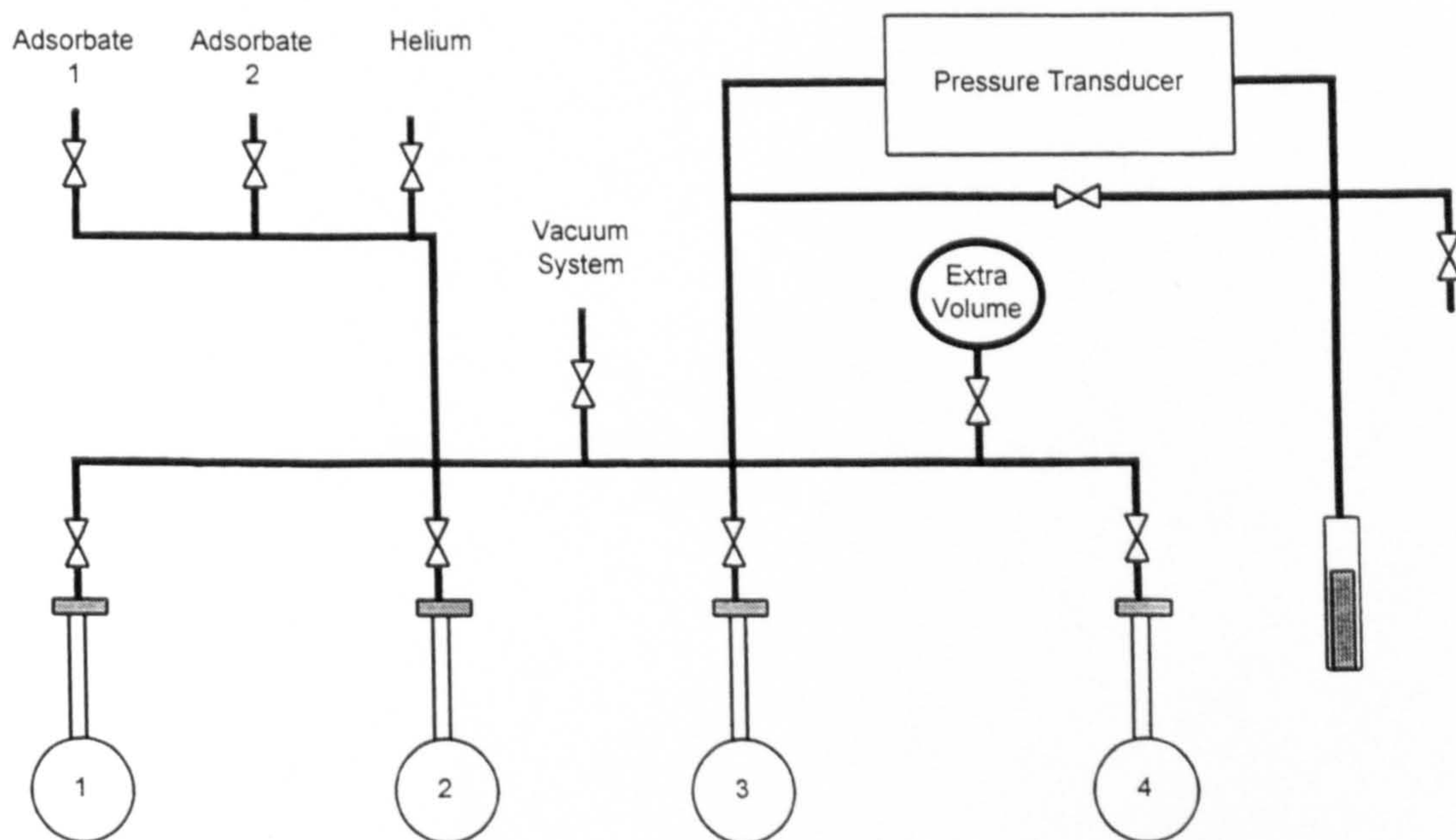


Figure 4.6 Illustration of Micromeritics Acusorb 2100E BET Surface Area Analysis Equipment Manifold

Chapter Five

Experimental Results

Biomass Materials

5.1 Analytical Data for the Biomass Samples

5.1.1 Proximate Analyses

The basic analysis data for the biomass samples are presented in Table 5.1. It is evident from the data that most of these samples had been pre-dried for storage purposes. Typically, freshly cut straw has a moisture content in the range 10-20 %, and newly harvested wood and short rotation coppice have moisture contents in the range 40-60 %. The exception is the Long Ashton III sample which has a moisture content of 41.3 %. This had not been pre-dried and the sample was clearly subject to microbiological degradation. In storage, biomass materials with moisture content in excess of around 20 % are subject to rapid microbial respiration.

The ash contents of all of the biomass materials are low. The ash content of the straw sample is fairly typical of cereal straws which commonly have ash contents in the range 3-6 %. The data for the fractionated short rotation coppice samples

from Silsoe show some interesting trends in that the bark fraction has the highest ash content, whereas the sapwood material has the lowest ash content. The bulk sample and the twig fraction, which contain both bark and sapwood, have intermediate ash contents. The Danish pine and Long Ashton samples all have ash contents less than 3 %.

The volatile matter contents of all of the biomass materials are high, in the range 80-90 %, on a dry basis. Again, the fractionated SRC samples from Silsoe show an interesting trend in that the bark sample has the lowest volatile matter content (80.8 %, dry basis), whereas the sapwood has the highest volatile matter content (91.2 %, dry basis). The bulk and twig samples have intermediate volatile matter contents since they contain both bark and sapwood.

5.1.2 Ultimate Analyses

The ultimate analysis data for all of biomass samples are fairly similar, with carbon contents in the range 40-45 % and hydrogen contents in the range 5.0-5.5 %. The nitrogen and chlorine contents of all of the samples are relatively low, except for the nitrogen content of the Danish pine sample, which is significantly higher than the others, for reasons which are not understood.

5.1.3 Ash Analyses

The ash analysis data for the biomass samples are presented in Table 5.2. Since there were insufficient quantities of some samples, the analyses were restricted to what are considered to be the more important components. The ash materials tend to be rich in SiO₂, CaO, K₂O and MgO with the SiO₂ and CaO concentrations varying considerably from sample to sample. The ash prepared from the straw sample is notable in that it has by far the highest SiO₂ concentration and lowest CaO concentration. The K₂O and MgO levels are reasonably similar, the only exception being the relatively low K₂O content of the Danish pine ash. Unlike coal ashes, the biomass ashes are not alumino-silicate systems. The inorganic fractions of the biomass materials consist of a mixture of simple inorganic

compounds principally SiO_2 as quartz or amorphous silica, and phosphates, sulphates and oxalates of the alkali and alkaline earth metals, and this is reflected in the ash analysis data.

5.2 Characteristics of the Chars Prepared from Biomass Samples

5.2.1 Char Yields

Chars were prepared from the biomass samples by heating in a fixed bed reactor, in a nitrogen atmosphere at 10 K min^{-1} , to 1173 K and holding at that temperature for a period of 1 hour. The char yield data for all of the samples are presented in Table 5.3. All of the biomass materials gave char yields in the range 22-29 %, with the straw being the lowest at 22 %. The Long Ashton samples were all very similar and gave char yields in the relatively narrow range 25.1-28.9 %. The data for the fractionated Silsoe samples are interesting in that the bark had the highest char yield at 26.6 % whereas the sapwood gave the lowest char yield at 22.5 %. The bulk material and the twigs, which contain both bark and sapwood gave intermediate char yields. Since the fractionated materials are all very similar chemically (see Table 5.1), it is most likely that the differences in char yields are due to the cell structures of the bark and sapwood materials.

5.2.2 Ultimate Analyses of Chars Prepared from Biomass Samples

The ash contents of the chars are presented in Table 5.3. These values reflect the ash contents of the parent materials, since the char yields are in a fairly narrow range.

The chemical compositions of the biomass chars are also presented in Table 5.3. When the data are compared to those for the original materials (see Table 5.1), it is evident that the pyrolysis process had the effect of increasing the carbon concentrations and decreasing the hydrogen and oxygen concentrations of the materials. The straw char is significantly different from the wood chars, in that it

has lower carbon and hydrogen contents. The chars prepared from the Long Ashton samples have fairly similar carbon, hydrogen and oxygen contents. There is an interesting trend, however, in the carbon contents of the chars produced from the fractionated Silsoe samples. The carbon contents in these chars were found to vary from 76.60-84.84 %. The bark char had the lower carbon content and the sapwood had the highest. The bulk material char and the twig char had intermediate values.

The nitrogen contents of the chars were found to vary considerably, from 0.31-1.91 %. The nitrogen contents of the Danish pine and straw were relatively high, at 1.91 and 1.83 % respectively. The nitrogen contents of the Long Ashton chars were relatively similar, and vary from 0.47-0.93 %. A trend is apparent in the nitrogen concentrations of the fractionated Silsoe chars. The bark char had the highest nitrogen content at 1.53 % and the sapwood char the lowest nitrogen content at 0.39 %. The bulkwood and twig chars had intermediate nitrogen contents.

The proportion of the nitrogen retained in the chars from the starting materials has been calculated, and these data are also presented in Table 5.3. The retained nitrogen was found to vary from 13 % for the Silsoe Sap char to 65 % for the Long Ashton I char. A trend is apparent for the Silsoe chars. The bark char had the highest proportion of retained nitrogen with 45 % and the sap char had the lowest proportion at 13 %. The twig char and the bulk char had intermediate values.

The chlorine concentrations of all the biomass materials had decreased to less than 0.1 % in the chars during pyrolysis.

5.2.3 Relationships Between the Biomass Char Yields with the Raw Sample and Char Characteristics

It is interesting to examine whether or not the char yields and char compositions can be related to the properties of the parent biomass materials. A plot of the char

yields against the fixed carbon contents of the biomass materials is presented in Figure 5.1a. Although there is a general upward trend, there is clearly no overall correlation for all of the biomass materials. However, when the data for the fractionated samples from Silsoe were plotted, (Figure 5.1b), a very good correlation was obtained. This indicates that the char yield increased linearly with increasing biomass fixed carbon content. The bark sample had the highest fixed carbon content and the highest char yield, and the sapwood sample had the lowest values.

No significant correlations were found between the biomass material carbon contents and char yields, and this is illustrated in Figure 5.2.

It is also instructive to investigate the relationships between the char yields and the chemical composition of the resultant char. A plot of the char carbon concentrations against the char yields for all of the biomass materials is presented in Figure 5.3a. There is no overall trend. However, as is illustrated in Figure 5.3b, there is an excellent correlation for the Silsoe fractionated samples. The sapwood yielded the lowest quantity of char, with the resultant char having the highest carbon concentration, while the bark produced the highest char yield with the resultant char having the lowest carbon content. The bulk and twig samples were found to have intermediate values.

The char nitrogen content data was plotted against char yield and this graph is presented in Figure 5.4a. There was no overall correlation for all of the samples, however, there was another clear trend for the fractionated Silsoe samples and this is illustrated in Figure 5.4b. This trend indicates that the nitrogen content of the chars increased linearly with increasing char yield. The sapwood char had the lowest nitrogen content and lowest char yield, the char prepared from the bark had the highest nitrogen content and highest char yield, and the bulk and twig materials had intermediate values.

The proportion of the nitrogen retained in the chars was calculated for each sample, and these values were also plotted against char yield. It is evident from the graph, which is presented in Figure 5.5a, that there is a relationship for these materials, with the sole exception of the straw. This relationship suggests that, for the wood materials, the proportion of nitrogen retained in the char increased with increasing char yield. The separated Silsoe data are presented in Figure 5.5b and it is clear that these data conform to the trend.

5.3 Thermal Decomposition Analyses of the Biomass Samples

The weight losses from the biomass materials in air with increasing temperature were measured in a Thermal Analyser over the temperature range 280-1170 K, at a temperature increase rate of 10 K min⁻¹. The weight loss profile for the straw sample is reproduced in Figure 5.6 and the first derivative curve, dWt/dT against T, is reproduced in Figure 5.7. The curves for all of the biomass materials are very similar and three peaks are evident, these were:

Peak 1 due to moisture loss from the sample,

Peak 2 due to devolatilisation of the biomass, and

Peak 3 due to burnout of the residual char material.

The characteristic peak temperatures for all of the biomass materials are listed in Table 5.4. It is clear from these data that the characteristic peak temperatures for all of the biomass materials are very similar and occur within the following ranges:

1. Moisture loss 300-340 K,
2. Devolatilisation 490-550 K, and
3. Char burnout 620-710 K.

One point of note concerns the devolatilisation and char burnout peak temperatures for the fractionated Silsoe SRC samples. In both cases, the bark material has the lowest peak temperatures and the sapwood material the highest. The peak temperatures for the bulk and twig samples are intermediate. These trends are similar to those observed in the char yield data.

5.4 The Reactivities of the Biomass Chars in Oxygen

Chars were prepared from all of the biomass materials by heating to 1173 K in a nitrogen atmosphere. The reactivities of these chars in oxygen were measured in a thermal analyser, by measurement of the isothermal rate of weight loss (at 20 % weight loss) over a range temperatures. The reactivity-temperature curves for all of the samples are reproduced in Figure 5.8. The reactivity-temperature curves for all of the chars have the same basic shape. At 570 K and below the reactivity values are very low. At higher temperatures, where the reactivity of a char exceeded $5-10 \times 10^{-4} \text{ g g}^{-1} \text{ s}^{-1}$ it was difficult to obtain an accurate measurement. In order to allow direct comparisons between the chars, the reactivity data at 613 and 633 K are listed in Table 5.5.

5.4.1 Relationships of Biomass Char Reactivity with Raw Sample and Char Characteristics

It is interesting to examine whether or not the char reactivities are related to the properties of the parent materials. A plot of the char reactivities at 613 and 633 K against the fixed carbon contents of the parent biomass materials is presented in Figure 5.9a. It is clear from the graph that there is no overall trend for all the biomass materials. There are however, reasonable correlations for the Silsoe fractionated samples. These correlations, shown in Figure 5.9b, indicate that the char reactivity increased linearly with increasing biomass fixed carbon content. The bark had the highest fixed carbon content and its char had the highest reactivity values, while the sapwood, with the lowest fixed carbon, produced a

char with the lowest reactivity values. The bulk and twig char samples yielded intermediate values.

No significant correlation was found between the char reactivities and the carbon contents of the parent biomass materials, and this is illustrated in Figure 5.10.

A plot of the char reactivities against the char yields is presented in Figure 5.11a. There was no overall trend for all of the samples, however, as illustrated in Figure 5.11b, it is evident that there were excellent correlations for the Silsoe fractionated samples. The bark yielded the highest quantity of char, with the resultant char having the highest reactivity, while the sapwood produced the lowest yield of char with the resultant char being the least reactive. The bulk and twig samples had intermediate values.

The biomass reactivity data were also plotted against the carbon contents of the chars. From the graph presented in Figure 5.12a, it is evident that there is no overall trend, however there was another strong correlation for the Silsoe fractionated material. This trend, clearly shown in Figure 5.12b, indicates that the char reactivity increased linearly with decreasing carbon concentration. The bark chars with the lowest carbon content had the highest reactivity, and the sapwood chars, which is the least reactive, had the highest carbon concentration.

It is clear therefore, that for the Silsoe fractionated samples, the char reactivity was a function of the fixed carbon content of the parent material, of the char yield and of the carbon contents of the char. The bark material had the highest fixed carbon content, gave the highest char yield and the resultant char had the lowest carbon content and the highest reactivity. The sapwood had the lowest fixed carbon content, gave the lowest char yield, and the resultant char had the highest carbon content and the lowest reactivity. The bulk and twig samples, which contain both bark and sapwood gave intermediate results.

5.5 BET Surface Area Determinations of the Biomass Chars

The BET surface areas of all the char samples were measured and the data are presented in Table 5.6. The surface area of the straw char sample is significantly higher than those of the wood materials. The Danish pine and Silsoe sapwood chars had very similar surface areas, while the values of the other chars were somewhat lower. There is a trend apparent in the surface areas of the Silsoe fractionated chars, the sapwood char having the highest measured surface area, the bark char having the lowest surface area. The bulk and the twig chars had intermediate values.

5.5.1 Relationships of the Surface Area of the Biomass Chars with Raw Sample and Char Characteristics

A plot of the surface areas against the fixed carbon contents of the biomass materials is presented in Figure 5.13a. There is clearly no overall correlation for all of the biomass materials, however there is a reasonable trend for the samples of fractionated SRC from Silsoe. This trend, shown in Figure 5.13b indicates that the surface area of the chars decreased linearly with increasing sample fixed carbon content. The sapwood with the lowest fixed carbon content has the highest char surface area while the bark with the highest fixed carbon content has the lowest surface area. No correlation was found for the carbon content of the biomass materials and the char surface area data, this is shown in Figure 5.14.

It is clear from the data for the Silsoe samples that the materials with the highest volatile matter content produced a char with the highest surface area and vice versa.

The surface area data were plotted against the char yield, and this is presented in Figure 5.15a. There was clearly no correlation between the surface area and char yield data for all the biomass materials, however, as illustrated in Figure 5.15b, there was a good linear correlation for the Silsoe samples. This indicates that the char surface area decreased with increasing char yield. The biomass char surface

area data was also plotted against the carbon content of the chars. As shown in Figure 5.16a, there was no overall relationship. There was, however, a good relationship for the Silsoe fractionated samples. This can be seen in Figure 5.16b. The char surface area values increased linearly with increasing char carbon concentrations. The bark char, with the lowest carbon concentration, had the lowest surface area value and the sapwood char with the highest carbon concentration had the highest char surface area. The twig and bulk char data were of intermediate values.

5.6 Relationship of Char Surface Area with the Reactivity of the Biomass

Chars

The biomass char reactivity data at 613 and 633 K were plotted against the char surface area values. This graph is presented in Figure 5.17. There was no obvious trend.

It is reasonable to expect that the char reactivity is controlled by the carbon content of the char and the surface area available for reaction. Char material with a high carbon content is expected to be less reactive but this material also has a high surface area. It may be that the carbon content and surface area effects on the char reactivity are competing.

5.7 Relationships of Ash Components with Biomass Char Characteristics and Reactivity

It has been reported in literature that the mineral matter, and in particular the calcium compounds, have an influence on the reactivity of char materials to air and other gases at temperatures below 900 K, (see for instance Hengel and Walker 1984, Lineras-Salano et al 1986, Levendis et al 1989 and Raveendram et al 1995).

It is interesting, therefore, to investigate whether the ash content and CaO content of the biomass materials have any influence on the char yields and char reactivities.

5.7.1 Relationships Between Ash Components with Biomass Char

Characteristics

In order to study the influence of ash content on the measured biomass fixed carbon contents, the data have been plotted in Figure 5.18a. There was no apparent trend for all of the samples, however, as illustrated in Figure 5.18b, there is an excellent correlation for the fractionated Silsoe samples. This indicates that there was a linear relationship, with the fixed carbon content increasing with increasing ash content. The sapwood material had the lowest ash content and also the lowest fixed carbon content while the bark which had the highest ash content also had the highest fixed carbon content. The bulk and twig materials have intermediate values.

The influence of ash content on the yields of char obtained was also investigated. A plot of char yield against ash content is presented in Figure 5.19a. There was no overall trend for all of the biomass samples, however, as illustrated in Figure 5.19b, there was a clear trend for the Silsoe sample data. The sapwood material which had the lowest ash content was found to give the lowest char yield while the bark material with the highest ash content was found to give the greatest char yield. The bulk and twig materials which have intermediate ash contents gave intermediate char yields.

The influence of ash content on the biomass char carbon concentrations was also investigated. A graph of char carbon concentration against ash content is presented in Figure 5.20a. There was evidence of a reasonable trend between the biomass char carbon concentrations and sample ash content for all of the materials as well as another good trend for the Silsoe samples. This trend is clearly illustrated in Figure 5.20b. The sapwood material which has the lowest ash content produced a char which had the highest carbon concentration while the bark

material produced a char with the lowest carbon concentration. The twig and bulk materials were found to have intermediate values.

5.7.2 Relationships Between the Ash Components with Biomass Char Reactivity

The effect of ash on char reactivity was studied and Figure 5.21 shows the reactivities of all the biomass chars at 613 K and 633 K plotted against the char ash contents. Reasonable trends can be seen at both temperatures with the char reactivities increasing linearly with increasing ash content. The exception was the straw char which does not conform. The straw ash was different however, from the wood ash in that it is rich in SiO_2 and had a low CaO content. When a similar plot was prepared of the char reactivities against the CaO content of the chars, which is presented in Figure 5.22, remarkably good correlations were obtained at both temperatures. This represents fairly compelling evidence of a significant effect of the CaO content of the char over the range 1.0-5.5 % in increasing char reactivity. In this case the straw conforms to the correlation.

5.8 Summary of the Observed Behaviour of the Studied Biomass Materials During Gasification Processes

It is clear from the data presented above that there are a number of interesting correlations between the basic physical and chemical properties of the biomass materials and their behaviour in gasification processes, i.e. the char yields when heated to 1173 K in the absence of oxygen and the characteristics of the resultant char materials. This is particularly true for the fractionated SRC wood materials provided by the Silsoe Research Institute. Four fractions were prepared, viz:

- a) sapwood,
- b) bark,

- c) small twigs, and
- d) the bulk material.

The behaviour of these materials reflect, in the main, the characteristics of the bark and the sapwood. The small twigs and the bulk material contain both sapwood and bark, and accordingly have intermediate properties. The principal differences between the bark and sapwood are that the bark has a higher fixed carbon content and the higher ash content.

With these fractionated materials, the following correlations were observed,

1. the char yields increased linearly with increasing char yield,
2. the char carbon contents decreased linearly with increasing char yield,
3. the char reactivity in oxygen at low temperatures increased linearly with increasing char carbon content,
4. the char reactivity in oxygen decreased linearly with increasing char carbon content,
5. the char surface area decreased linearly with increasing char yield, and the char surface area increased with increasing char carbon content.

The effects of the ash constituents of the biomass materials on their behaviour has also been investigated, and a number of interesting correlations, again principally for the fractionated Silsoe SRC wood samples, have been observed, viz:

6. the char yields for the Silsoe samples increased linearly with increasing ash content,
7. the char carbon contents decreased with increasing ash content, for all of the biomass materials tested,

8. the char reactivities in oxygen at low temperatures increased linearly with increasing ash content for all the biomass materials, except for the wheat straw, and
9. the char reactivities in oxygen at low temperatures increased linearly with increasing CaO content of the char for all of the biomass materials, including the wheat straw.

It is clear from the observations that both the characteristics of the organic fraction and the inorganic constituents of the biomass materials have an influence on their behaviour in pyrolysis and gasification reactions. These observations will be discussed in more detail in Chapter 7.

5.2 Analytical Data for the HNO₃ and HCl Acid-Washed Biomass Samples

5.2.1 Proximate and Ultimate Analyses

In an attempt to investigate further the mineral matter effects, the straw and Danish pine samples were treated by digestion in 1 M HNO₃ and HCl solutions at 35-40 °C for two hours followed by washing in distilled water until the washings were neutral. The intention was to artificially reduce the ash contents of the biomass materials.

The proximate and ultimate analysis data for the raw and acid treated samples are presented in Table 5.7. Acid treatment of delicate biomass materials is commonly practised by experimentalists, however, it may have significant effects on the organic matter as well as the mineral material. It is instructive, therefore, to examine the effects on the biomass materials. Looking first at the proximate analysis data, it is clear that the ash contents of the acid treated materials had been reduced, as expected, but also that the fixed carbon contents had been reduced significantly. This was found to be greater with the nitric acid than the hydrochloric acid, which is not surprising in view of the fact that nitric acid is a

powerful oxidant, the effectiveness being dependent on the concentration. This effect was also evident in the ultimate analysis data, which shows that the oxygen content of the materials treated with nitric acid had increased. It is also apparent from the data that the HCl treatment was very effective in removing the nitrogen from the biomass. This is due to the aqueous HCl breaking down the proteins present in these materials by the hydrolytic cleavage of their amide bonds to give soluble amino acids. Both acid treatments effectively reduced the chlorine content.

The principal effect of the acid washing treatment was to reduce the ash content of the biomass materials from 4.5 to around 2.8-3.0 % for the straw and from 1.7 to around 0.5-0.6 % for the Danish pine. The effect on the ash composition can be seen in Table 5.8. It is clear from the data that the main effect of the treatment was to reduce the CaO, MgO, K₂O and Na₂O contents to very low levels in both cases. This is very much as expected. The Fe₂O₃ concentrations of both the straw and Danish pine ash were significantly reduced in the HCl washed samples.

5.10 Analytical Data of Chars Prepared from HNO₃ and HCl Acid-Washed Biomass Samples

5.10.1 Char Yields and Ultimate Analyses of HNO₃ and HCl Acid-Washed Biomass Sample Chars

The char yield and ultimate analysis data for the chars (1173 K in N₂), prepared from the raw and acid-treated biomass materials, are presented in Table 5.9.

The chemical compositions of the chars prepared from the acid treated samples differ significantly from the chars prepared from the parent materials in that they have higher concentrations of hydrogen, oxygen and nitrogen. These differences were found to be greater for the chars prepared from the nitric acid-treated samples. The chlorine content of all the chars were very low, at < 0.10 %.

5.10.2 Relationships Between the HNO₃ and HCl Acid-Washed Biomass

Sample Char Yields with the Precursor Sample and Char Characteristics

The relationships between the char yields and char compositions and the properties of the precursor materials were examined. A plot of the char yields against the fixed carbon content of the precursors are presented in Figure 5.23. There were distinct trends for both the straw and the Danish pine samples. The trends, which were similar for both sample groups, indicated that the char yields increased linearly with increasing fixed carbon content. In both cases, the samples treated with nitric acid had the lowest fixed carbon contents and the lowest char yields. The untreated materials had the highest fixed carbon contents and the highest char yields.

The carbon contents of the chars prepared from the raw and acid treated biomass were plotted against the char yields, and this graph is presented in Figure 5.24. There were excellent trends for the straw and Danish pine data. In both cases, the char yield was found to decrease linearly with increasing char carbon content, with the char prepared from nitric acid-treated biomass having the lowest char yield and the char prepared from the untreated biomass materials having the highest char yield.

The char nitrogen contents were plotted against char yields, and this graph is presented in Figure 5.25. There were excellent individual trends for both the straw and Danish pine data. These trends both clearly indicate that there is a linear relationship, with the nitrogen contents of the chars increasing with char yield. The untreated materials produced chars with the highest yield and highest nitrogen levels, while the chars produced from the nitric acid-treated materials had the lowest char yield and also the lowest nitrogen contents.

5.11 Thermal Decomposition Analyses of HNO₃ and HCl Acid-Washed Biomass Samples

The weight losses from the biomass and acid-treated biomass materials in air with increasing temperature were measured in a Thermal analyser over the temperature range 280-1170 K, at a temperature increase rate of 10 K min⁻¹. The weight loss profile for the straw sample is reproduced in Figure 5.6 and the first derivative curve, dWt/dT against T, is reproduced in Figure 5.7. The curves for all of the samples were very similar and a general description of the profiles is presented in Section 5.3. The characteristic peak temperatures of the biomass and acid-treated biomass samples are listed in Table 5.10.

The main observation is that the devolatilisation and char burn-out peak temperatures were significantly higher for both the acid-treated straw and Danish pine. The HNO₃ washed samples had the highest devolatilisation peak temperatures, while the HCl washed samples had the highest char burn-out peak temperatures in each group of samples.

5.12 Reactivity Measurements of HNO₃ and HCl Acid-Washed Biomass Sample Chars in Oxygen

The reactivities of the chars prepared from the acid washed biomass materials were measured in an oxygen atmosphere over a range of temperatures using the same procedure employed for the biomass char reactivity determination. The reactivity-temperature curves for all of the chars prepared from the acid-treated biomass samples are reproduced in Figure 5.26. It is clear that the chars prepared from untreated biomass materials were significantly more reactive than the chars prepared from the acid-washed samples. They also had lower burn-out temperatures. The reactivities of the untreated biomass chars were measurable from 610-670 K while the reactivities of the chars prepared from the acid washed samples were measurable from 630-730 K. It is also evident from these data that

the chars prepared from the HCl washed biomass samples were less reactive than those prepared from the HNO₃ washed samples. The char prepared from the HCl washed straw had the lowest measured reactivity over the temperature range measured. In order to allow direct comparisons between the chars, the reactivity data at 633 and 633 K are listed in Table 5.11.

5.12.1 Relationships Between the Reactivities of HNO₃ and HCl Acid-Washed Biomass Sample Chars in Oxygen with the Precursor Material and Char Characteristics

A plot of the char reactivity values at 633 K against the fixed carbon contents of the untreated acid-washed biomass materials is presented in Figure 5.27. The reactivities of the chars prepared from the acid-washed materials were all very much lower than those of the chars prepared from the untreated materials. There was no clear relationship, however, between the char reactivities and the fixed carbon contents of the parent materials.

Similar results were obtained when the char reactivity data were plotted against the char carbon contents, presented in Figure 5.28 and 5.29.

5.13 BET Surface Area Determination of HNO₃ and HCl Acid-Washed Biomass Sample Chars

The BET surface areas of the chars prepared from the acid-treated biomass samples were measured and the results are presented in Table 5.12. The chars prepared from the acid treated materials had lower surface areas than those prepared from the untreated biomass. The surface area values of the straw char and acid-washed straw chars range from 20-29 m² g⁻¹, while the Danish pine char and acid-washed Danish pine chars range from 2-19 m² g⁻¹. In both groups of samples the char prepared from the HNO₃ treated biomass had the lowest measured surface area values.

5.13.1 Relationships Between the Surface Area of HNO₃ and HCl Acid-Washed Biomass Sample Chars with the Precursor Material and Char Characteristics

A plot of the char surface area data parent material fixed carbon contents is presented in Figure 5.30. There were excellent trends for the two groups of samples with the surface area values increasing linearly with increasing fixed carbon content. In each case, the untreated parent material char had the highest fixed carbon content and also the largest surface area. The chars prepared from the HNO₃ washed samples had the lowest fixed carbon contents and the lowest surface areas.

The surface area data were plotted against the char yields, and the graph is presented in Figure 5.31. There are excellent trends for both materials with the surface areas increasing with increasing with char yield. The HNO₃ washed biomass materials produced chars with the lowest yields and lowest char surface areas. The untreated biomass yielded the most char, and the resultant chars had the highest surface areas.

The surface area data were also plotted against the char carbon content values, and as can be seen in Figure 5.32, there are excellent trends for both the straw and Danish pine groups of samples. In both cases the char carbon content increases with decreasing char surface area. The chars prepared from the untreated biomass had the highest surface areas and lowest char carbon concentrations, and the chars prepared from the HNO₃ washed biomass materials had the highest char carbon concentrations and the lowest surface area values.

5.14 Relationships of Char Surface Area with Reactivity of HNO₃ and HCl

Acid-Washed Biomass Chars

The reactivity data measured at 653 K for all of the sample chars were plotted against the char surface area values. It is clear from the graph presented in Figure [5.33](#) that there is no discernible trend in the data.

5.15 Relationships Between the Ash Contents of the HNO₃ and HCl Acid-Washed Biomass Samples with the Precursor Material Characteristics, and Char Characteristics

In order to study the influence of reducing the ash concentrations on the measured biomass fixed carbon contents, the data have been plotted in Figure [5.34](#). There was no trend for all of the data, however there was an excellent correlation for the Danish pine data. This trend indicates that there was a linear relationship, with the fixed carbon content increasing with increasing ash content. The untreated Danish pine had the highest ash and the highest fixed carbon contents while the HNO₃ washed Danish pine had the lowest values.

The effects of the ash content on char preparation and char characteristics were also investigated. A plot of char yield against ash content for the straw and Danish pine samples is presented in Figure [5.35](#). There was a reasonable trend for the Danish pine and acid-washed Danish pine samples. This trend indicates that char yield increased with increasing ash content, the untreated Danish pine has the highest ash content and highest char yield. The HNO₃ washed Danish pine had the lowest ash content and lowest char yield.

The char carbon concentrations were plotted with the ash contents, and as is clearly illustrated in Figure [5.36](#), there was an excellent correlation for all of the data. This trend indicates that the concentration of carbon in char decreased with increasing ash content. The untreated straw had the highest ash content and the

resultant char has the lowest carbon content, while the HNO₃ washed Danish pine had the lowest ash content and the resultant char had the highest carbon content. The other samples had intermediate values.

5.16 Relationships of Ash Concentrations and Components of HNO₃ and HCl Acid-Washed Biomass with Char Reactivity

In order to investigate the relationship between char reactivity and ash concentrations, the reactivity data were plotted against the char ash contents, and this graph is presented in Figure 5.37. It can be seen that there was no overall trend. When the reactivity data were plotted against the char CaO contents, there was no correlation for all of the data, but there were similar trends for both groups of samples. These trends, illustrated in Figure 5.38 suggest that the reactivity of the chars increased linearly with increasing char CaO content.

5.17 Summary of the Effects of HNO₃ and HCl Acid-Washing on Biomass Sample Characteristics and Char Characteristics

The effects of the treatment of the straw and Danish pine samples with HNO₃ and HCl can therefore be summarised as follows:

1. The hydrogen, nitrogen and chlorine concentrations in the treated samples were lower than those of the untreated materials. The materials which were washed in HNO₃ also had higher oxygen concentrations, resultant from the oxidising nature of the acid.
2. The volatile matter contents were significantly increased and the ash contents were reduced. The principle effects on the ash were reductions in the CaO, MgO, K₂O and Na₂O, to very low levels

3. The char yields for the acid treated samples were significantly lower. These chars had lower of hydrogen, nitrogen and oxygen contents and had higher carbon contents than the chars prepared from the untreated materials.
4. When the char reactivities were measured in oxygen, the chars prepared from acid treated biomass were found to be significantly less reactive than those prepared from the parent materials.

Proximate Analysis (%, as received)	Cereal Straw	Danish Pine	Long Ashton				Silsoe			
			I	II	III	IV	Bulk	Sap	Bark	Twig
Moisture	6.1	8.0	6.5	6.7	41.3	10.1	6.8	6.8	6.6	6.7
Volatile Matter	78.9	71.6	80.0	81.8	45.4	76.3	82.8	85.0	75.5	76.9
Fixed Carbon	10.7	18.9	11.8	10.0	11.8	10.9	9.4	7.5	13.9	13.2
Ash	4.2	1.6	1.7	1.4	1.5	2.7	1.0	0.7	4.1	3.3
Ultimate Analysis (%, as received)										
Moisture	6.1	8.0	6.5	6.7	41.3	10.1	6.8	6.8	6.6	6.7
C	39.1	41.6	42.4	41.6	26.5	38.9	43.8	44.5	43.2	42.5
H	5.5	5.9	5.0	5.0	3.1	4.8	5.1	5.2	5.2	5.3
N	0.6	1.4	0.3	0.4	0.2	0.4	0.6	0.6	0.9	0.7
Cl	0.75	0.1	0.01	0.11	0.08	0.11	0.12	0.13	0.11	0.12
O (by difference)	43.7	41.5	44.2	44.8	27.4	43.0	42.5	42.0	39.9	41.4
Ash	4.2	1.6	1.7	1.4	1.5	2.7	1.0	0.7	4.1	3.3

Table 5.1 Basic Analytical Data for the Biomass Samples

Ash Analysis (%)	Cereal Straw	Danish Pine	Long Ashton				Silsoe			
			I	II	III	IV	Bulk	Sap	Bark	Twig
SiO ₂	71.3	34.6	4.2	18.0	5.2	5.5	8.8	7.4	12.8	9.2
Al ₂ O ₃	1.0	19.8	-	-	-	-	-	-	-	-
Fe ₂ O ₃	0.8	4.3	1.3	1.7	1.4	0.3	2.2	1.7	2.2	0.9
CaO	10.3	29.3	31.4	26.8	32.4	39.4	35.3	28.6	33.9	14.3
MgO	1.9	2.1	5.0	4.9	8.9	5.4	6.0	5.9	4.2	4.2
TiO ₂	-	0.6	-	-	-	-	-	-	-	-
K ₂ O	11.4	3.4	16.3	14.6	16.0	14.1	11.9	19.3	15.1	17.9
Na ₂ O	0.4	1.4	0.6	0.5	1.1	1.1	1.1	0.5	0.4	0.5
P ₂ O ₅	3.0	2.2	-	-	-	-	-	-	-	-
SO ₃	-	-	-	-	-	-	-	-	-	-
Ash Content (%, dry basis)	4.5	1.7	1.8	1.5	2.6	3.0	1.1	0.8	4.4	3.5

Table 5.2 Ash Analysis Data for the Biomass Samples

	Cereal Straw	Danish Pine	Long Ashton				Silsoe			
			I	II	III	IV	Bulk	Sap	Bark	Twig
Char Yield (%, dry, ash free)	22.0	24.2	28.9	25.2	28.3	25.1	24.2	22.5	26.6	24.7
Char Ash Content (%, dry)	20.5	7.0	6.2	6.0	9.2	12.0	4.5	3.6	16.5	14.2
Ultimate Analysis (%, dry ash free)										
C	73.3	88.3	80.5	85.2	83.7	80.3	81.7	84.8	76.6	79.7
H	2.0	0.5	0.5	0.5	0.5	0.5	0.3	0.3	0.5	0.4
N	1.8	1.9	0.7	0.5	0.8	0.9	0.6	0.4	1.5	1.2
Cl	< 0.1	< 0.1	< 0.1	< 0.1	< 0.1	< 0.1	< 0.1	< 0.1	< 0.1	< 0.1
O (by difference)	22.8	9.2	18.2	13.7	15.0	18.2	17.2	14.3	21.3	18.6
% of Original Nitrogen Retained in Char	56.1	30.3	64.6	27.5	56.6	50.8	23.4	12.9	44.9	39.2

Table 5.3 The Char Yields, Char Ash Contents and the Ultimate Analysis of Chars Prepared from the Biomass Samples at 10 K min^{-1} to 1173 K in a Nitrogen Atmosphere

Peak Temperatures, (K)	Cereal Straw	Danish Pine	Long Ashton				Silsoe			
			I	II	III	IV	Bulk	Sap	Bark	Twig
Peak 1, (Moisture)	310	340	300	300	310	310	310	300	300	310
Peak 2 (Devolatilisation)	500	550	550	530	540	530	530	540	490	530
Peak 3 (Char Burn-out)	710	710	690	700	680	660	660	690	620	650

Table 5.4 The Temperatures for the Peak Rate of Weight Loss Associated with Moisture Loss, Devolatilisation, and Char Burn-out for the Biomass Materials

Char Reactivity ($\text{g g}^{-1} \text{s}^{-1} \times 10^{-4}$)	Cereal Straw	Danish Pine	Long Ashton				Silsoe			
			I	II	III	IV	Bulk	Sap	Bark	Twig
at 613 K	0.80	0.72	0.62	0.43	1.19	2.28	0.43	0.10	2.43	1.05
at 633 K	1.74	1.70	1.47	1.00	2.29	4.60	0.79	0.17	5.01	2.05

Table 5.5 The Reactivity Data for Chars Prepared from the Biomass Samples at 10 K min^{-1} to 1173 K in a Nitrogen Atmosphere

	Cereal Straw	Danish Pine	Long Ashton				Silsoe			
			I	II	III	IV	Bulk	Sap	Bark	Twig
Char 77 K N ₂ BET Surface Area, (m ² g ⁻¹)	29	19	5	7	11	8	7	18	4	7

Table 5.6 The BET Surface Area Data for Chars Prepared from the Biomass Samples at 10 K min⁻¹ to 1173 K in a Nitrogen Atmosphere

Proximate Analysis (%, dry basis)	Cereal Straw			Danish Pine		
	Raw	HNO ₃ Washed	HCl Washed	Raw	HNO ₃ Washed	HCl Washed
Volatile Matter	84.0	93.6	88.9	77.8	91.9	89.6
Fixed Carbon	11.4	3.4	8.3	20.5	7.6	9.8
Ash	4.5	3.0	2.8	1.7	0.5	0.6
Ultimate Analysis (%, dry, ash free)						
C	43.4	44.1	47.6	46.2	44.6	49.1
H	6.2	4.9	5.0	6.3	5.6	5.4
N	0.7	0.4	0.3	1.5	0.8	0.6
Cl	0.8	< 0.1	< 0.1	0.1	< 0.1	< 0.1
O (by difference)	49.0	50.5	47.0	45.7	48.9	45.4

Table 5.7 The Proximate and Ultimate Analysis Data for the Untreated, and HNO₃ and HCl Acid-Washed Biomass Samples

Ash Analysis (%)	Cereal Straw			Danish Pine		
	Raw	HNO ₃ Washed	HCl Washed	Raw	HNO ₃ Washed	HCl Washed
SiO ₂	71.3	90.2	89.7	34.6	42.6	39.4
Al ₂ O ₃	1.0	-	-	19.8	-	-
Fe ₂ O ₃	0.78	0.8	<0.1	4.3	4.1	2.5
CaO	10.3	0.4	0.5	29.4	8.3	5.7
MgO	1.9	0.1	0.2	2.1	2.0	1.9
TiO ₂	-	-	-	0.6	-	-
K ₂ O	11.4	0.3	0.1	3.4	1.8	1.0
Na ₂ O	0.4	0.1	0.1	1.4	0.3	0.5
P ₂ O ₅	3.02	-	-	2.2	-	-
SO ₃	-	-	-	-	-	-

Table 5.8 The Ash Analysis Data for the Untreated and HNO₃ and HCl Acid-Washed Biomass Samples

	Cereal Straw			Danish Pine		
	Raw	HNO ₃ Washed	HCl Washed	Raw	HNO ₃ Washed	HCl Washed
Char Yield (%, dry, ash, free)	22.0	14.6	15.9	24.2	21.3	22.9
Char Ash Content (%, dry)	20.5	20.5	17.6	7.0	2.3	2.6
Ultimate Analysis (%, dry, ash free)						
C	73.3	81.7	79.5	88.3	92.1	90.8
H	2.0	0.6	0.8	0.5	0.4	0.4
N	1.8	1.0	1.2	1.9	1.8	1.8
Cl	< 0.1	< 0.1	< 0.1	< 0.1	< 0.1	< 0.1
O (by difference)	22.8	16.6	18.4	9.2	5.6	6.9
% of Original Nitrogen Retained in Char	56	51	67	30	43	64

Table 5.9 The Char Yields, Char Ash Contents and Ultimate Analysis Data for Chars Prepared from the Untreated, and HNO₃ and HCl Acid-Washed Biomass Samples at 10 K min⁻¹ to 1173 K in a Nitrogen Atmosphere

	Cereal Straw			Danish Pine		
	Raw	HNO ₃ Washed	HCl Washed	Raw	HNO ₃ Washed	HCl Washed
Peak Temperatures (K)						
Peak 1, (Moisture)	310	310	310	340	320	330
Peak 2 (Devolatilisation)	500	530	520	550	570	560
Peak 3 (Char Burn-out)	710	770	790	710	780	800

Table 5.10 The Temperatures for the Peak Rate of Weight Loss Associated with Moisture Loss, Devolatilisation, and Char Burn-out for the Untreated, and HNO₃ and HCl Acid Washed Biomass Samples

	Cereal Straw			Danish Pine		
	Raw	HNO ₃ Washed	HCl Washed	Raw	HNO ₃ Washed	HCl Washed
Char Reactivity (g g⁻¹ s⁻¹ x 10⁻⁴)						
at 633 K	1.74	0.13	0.05	1.70	0.18	0.06
at 653 K	3.90	0.26	0.13	3.48	0.36	0.13

Table 5.11 The Reactivity Data for Chars Prepared from the Untreated, and HNO₃ and HCl Acid-Washed Biomass Samples at 10 K min⁻¹ to 1173 K in Nitrogen Atmosphere

	Cereal Straw			Danish Pine		
	Raw	HNO ₃ Washed	HCl Washed	Raw	HNO ₃ Washed	HCl Washed
Char 77 K N ₂ BET Surface Area, (m ² g ⁻¹)	29	20	25	19	2	10

Table 5.12 The BET Surface Area Data for Chars Prepared from the Untreated, and HNO₃ and HCl Acid-Washed Biomass Samples Prepared at 10 K min⁻¹ to 1173 K in a Nitrogen Atmosphere

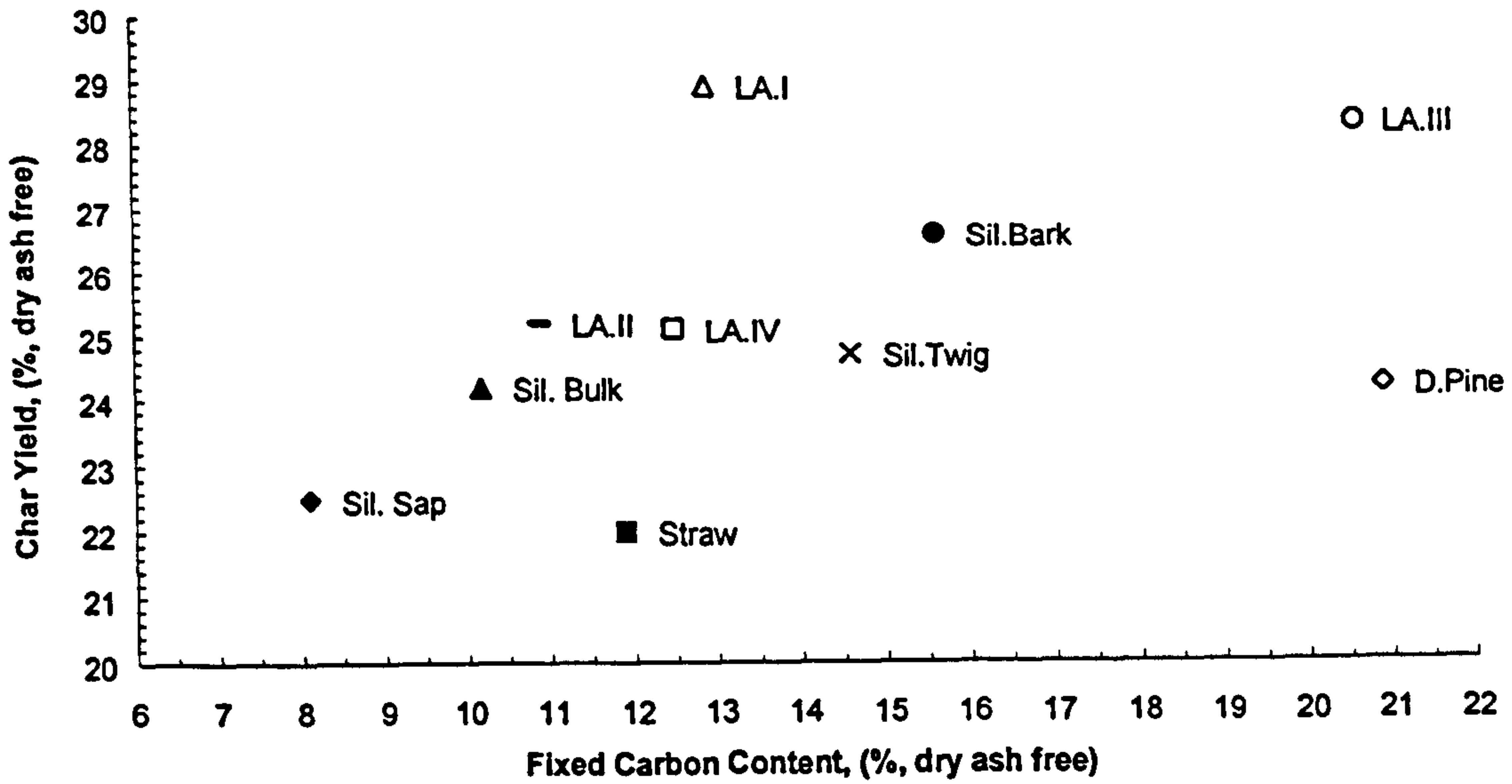


Figure 5.1a The Biomass Sample Char Yields Plotted Against Fixed Carbon Contents of the Parent Materials

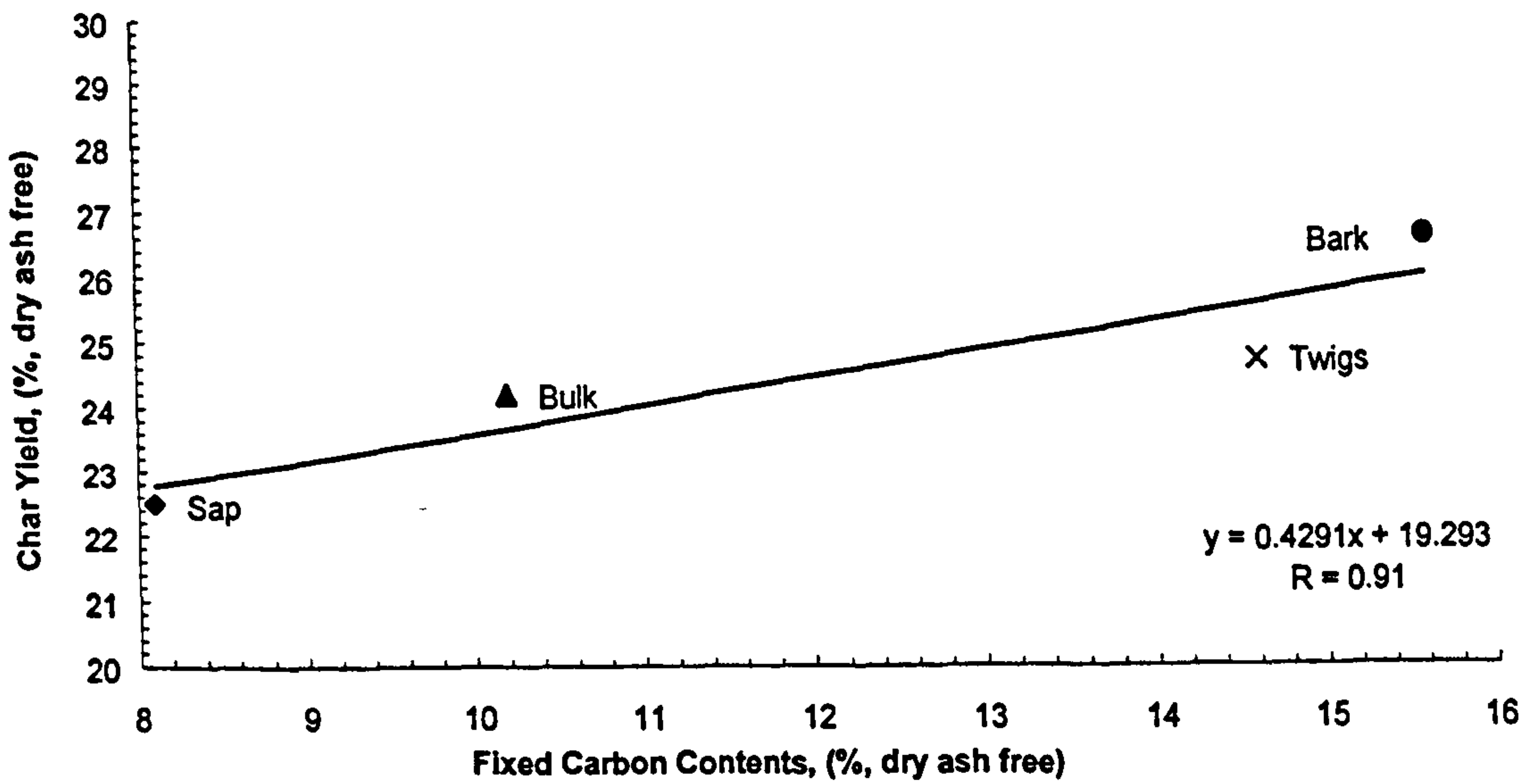


Figure 5.1b The Char Yields for the Fractionated Silsoe Samples Plotted Against their Fixed Carbon Contents

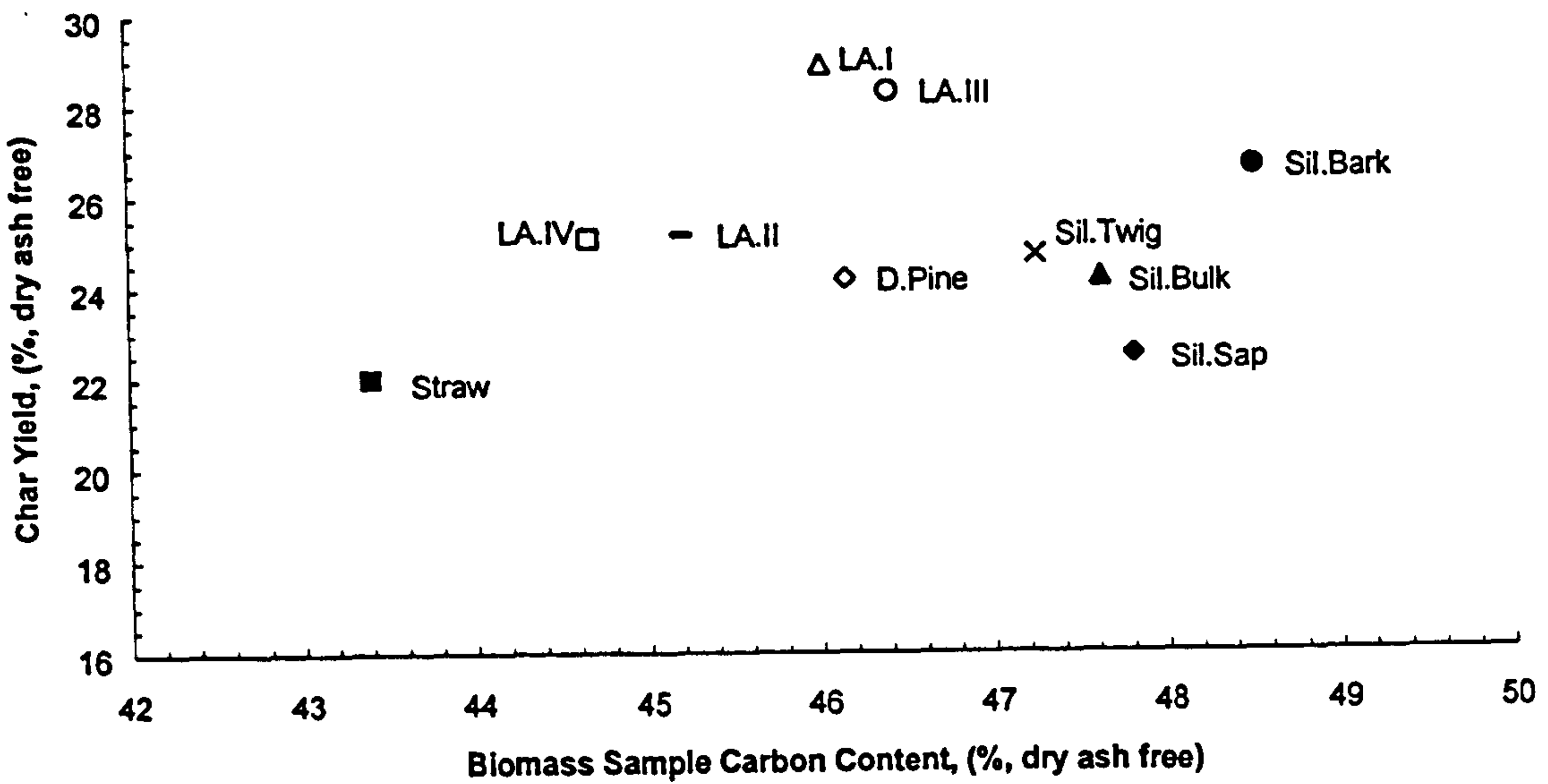


Figure 5.2 The Char Yields of the Biomass Materials Plotted Against the Carbon Content

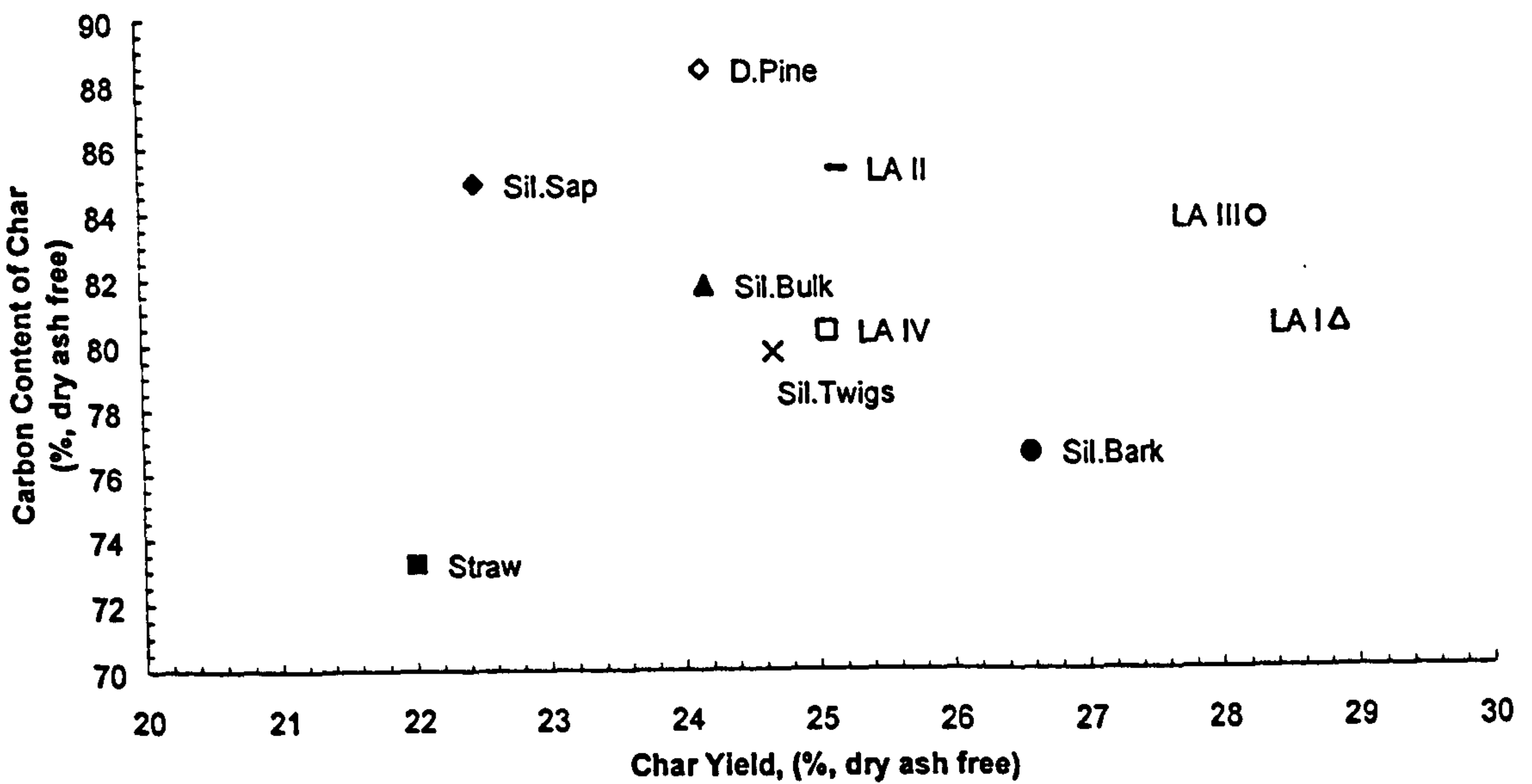


Figure 5.3a The Biomass Char Carbon Content Plotted Against the Char Yields

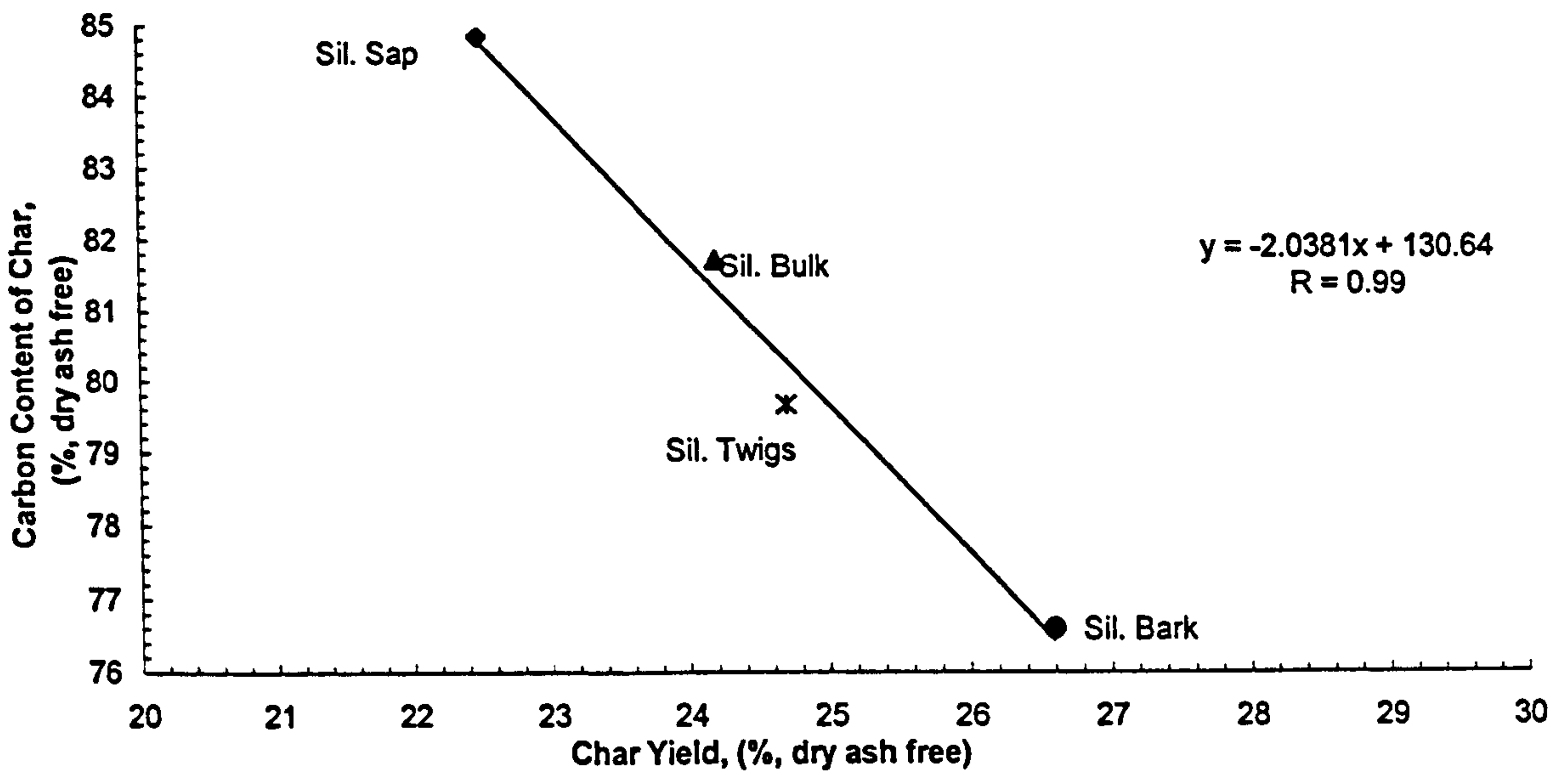


Figure 5.3b The Silsoe Fractionated Sample Char Carbon Contents Plotted Against the Char Yields

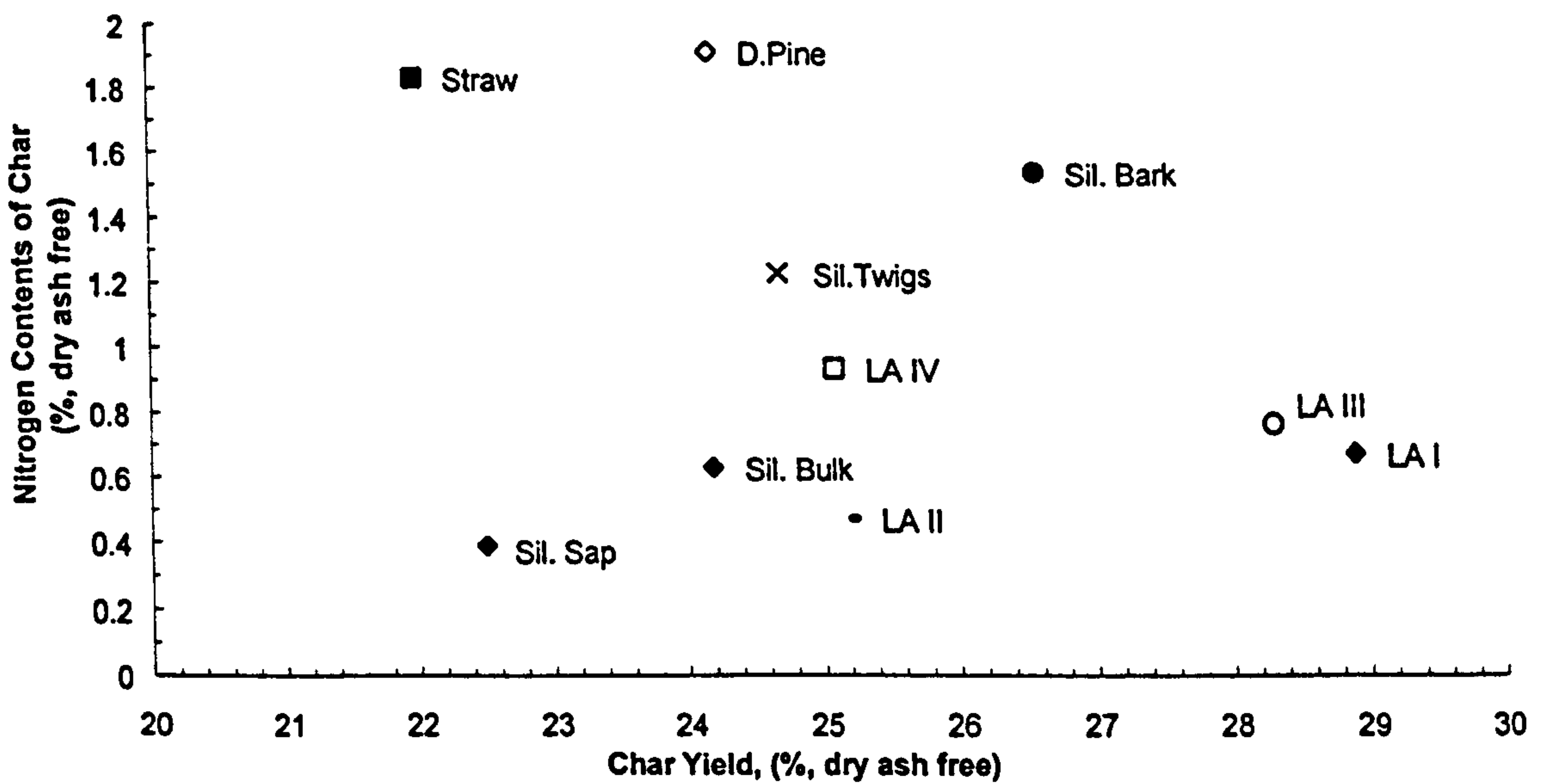


Figure 5.4a The Biomass Sample Char Nitrogen Contents Plotted Against the Char Yields

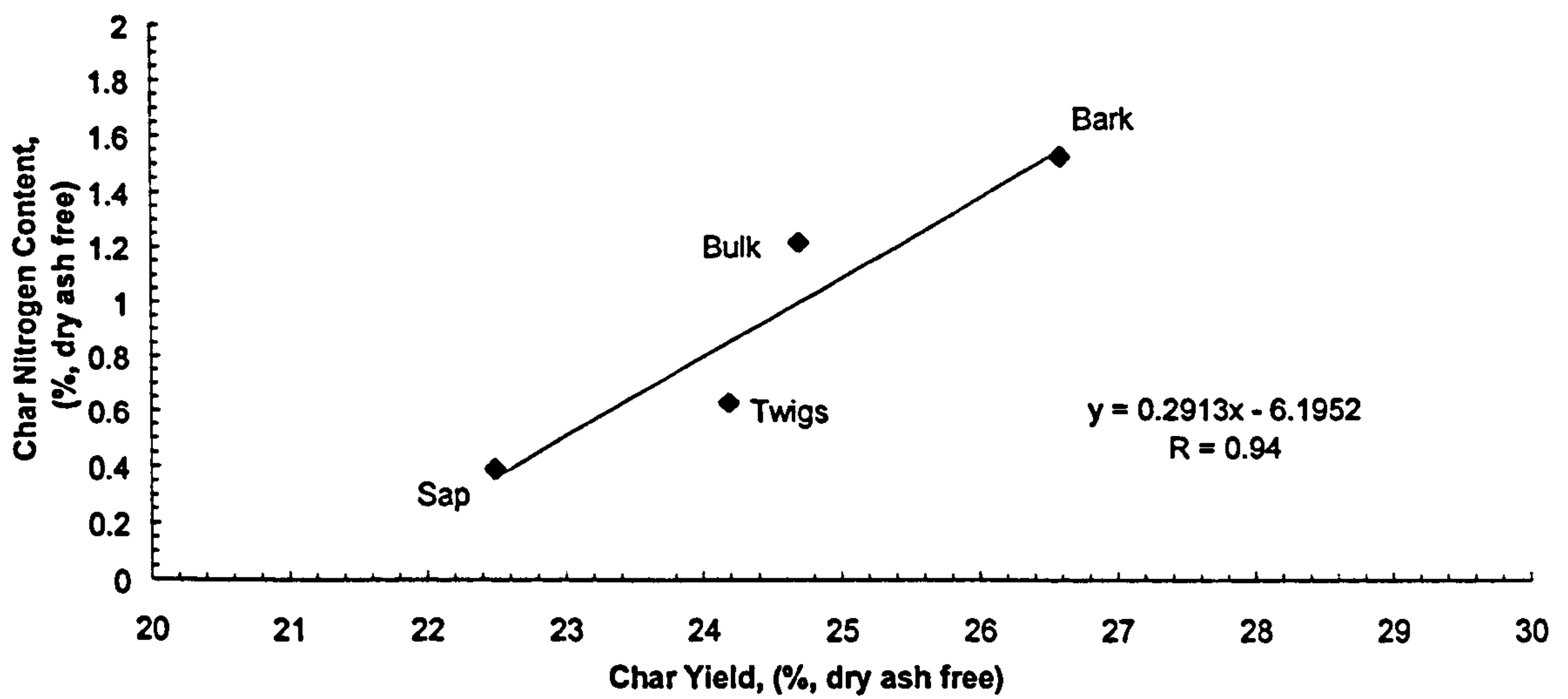


Figure 5.4b The Fractionated Silsoe Samples Char Nitrogen Contents Plotted Against their Char Yields

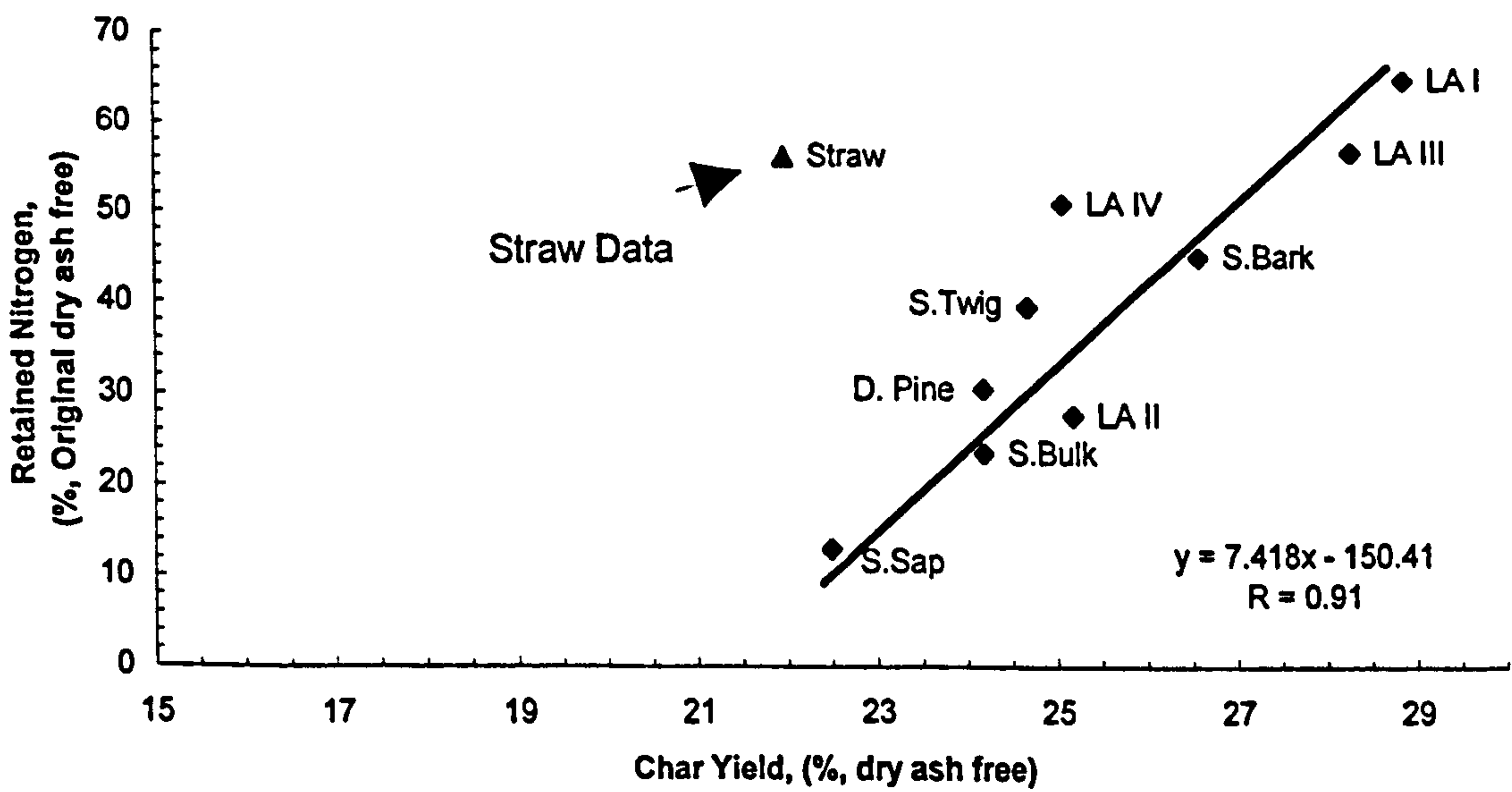


Figure 5.5a The Retained Nitrogen in Biomass Chars Plotted Against the Char Yields

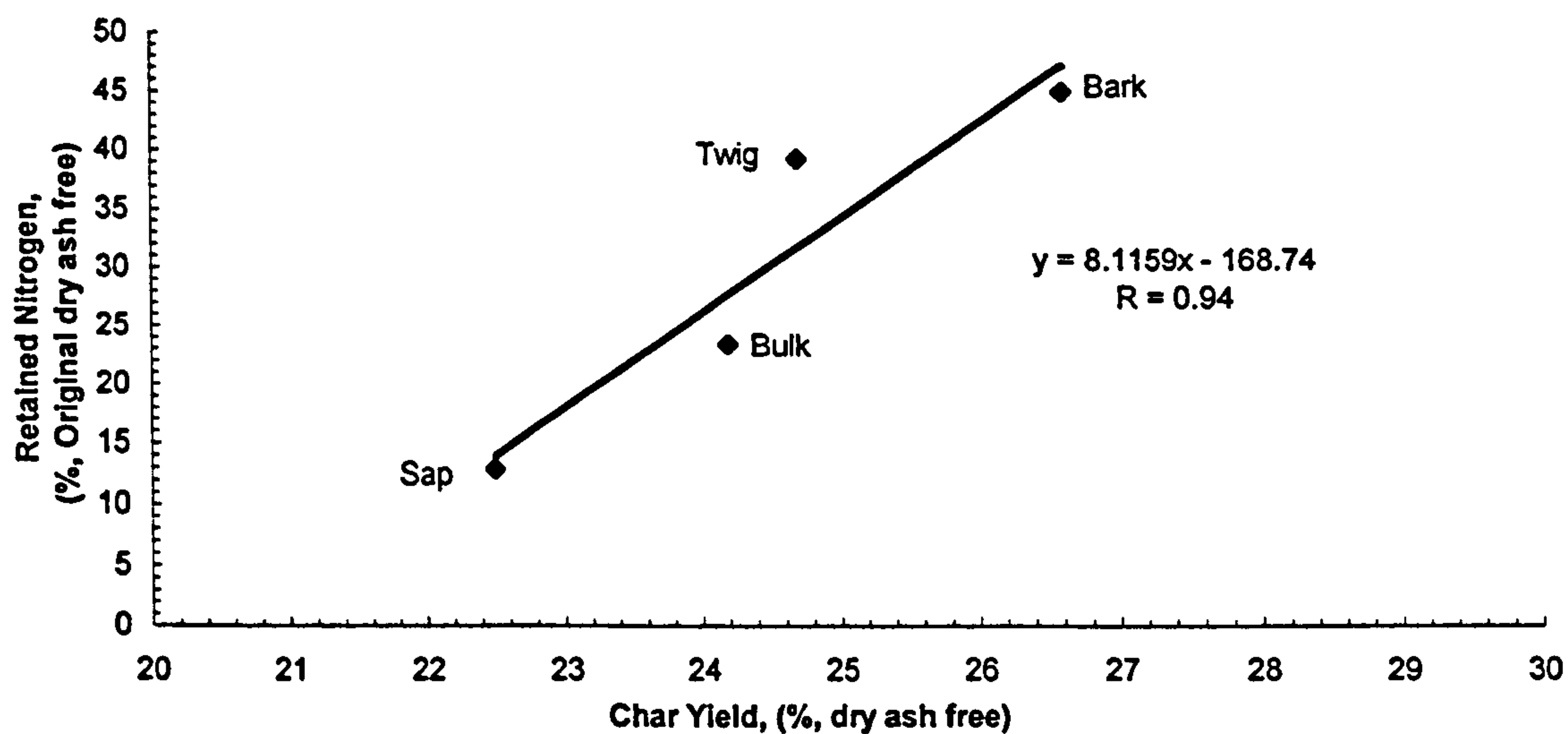


Figure 5.5b The Fractionated Silsoe Samples Retained Nitrogen in Char Plotted Against the Char Yields

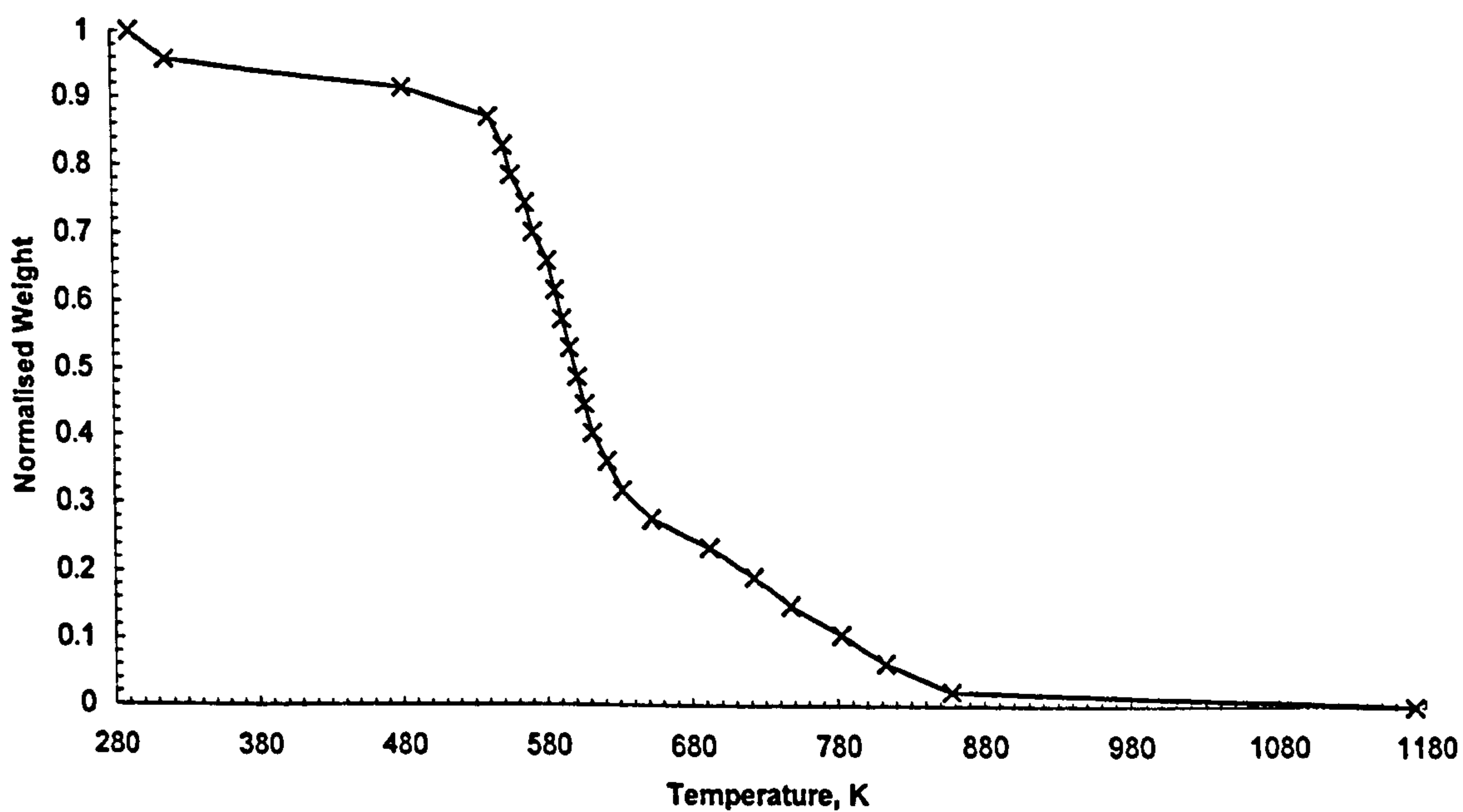


Figure 5.6 The Weight Loss Profile of Straw, Heated at 10 K min^{-1} from 293-1173 K, Normalised for Ash Content

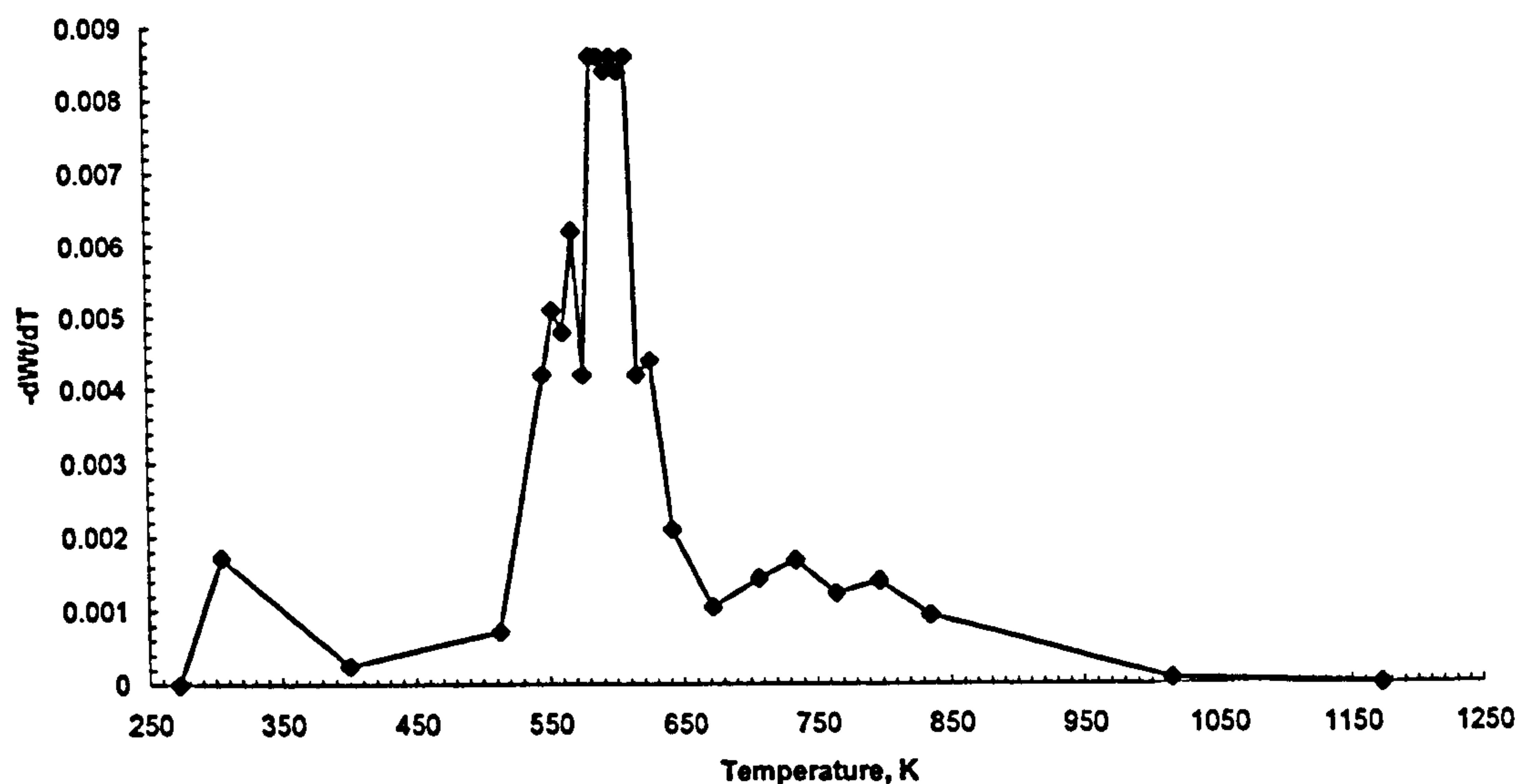


Figure 5.7 The First Derivative Weight Loss Profile of Straw ($-dWt/dT$), Heated at 10 K min^{-1} from 293-1173 K, Normalised for Ash Content

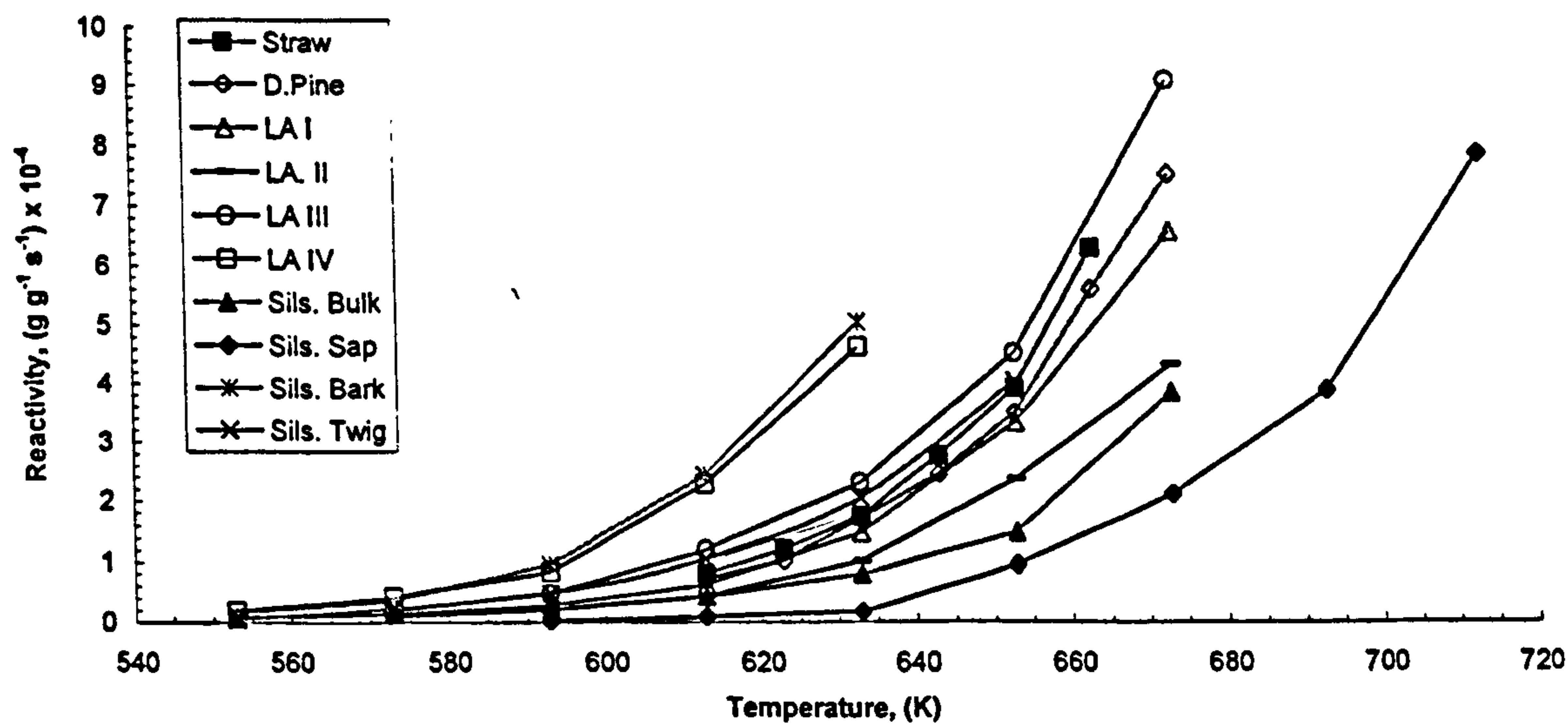


Figure 5.8 The Biomass Sample Chars Isothermal Reactivity in O_2 (3 l h^{-1}) Data in the Temperature Range 553-713 K

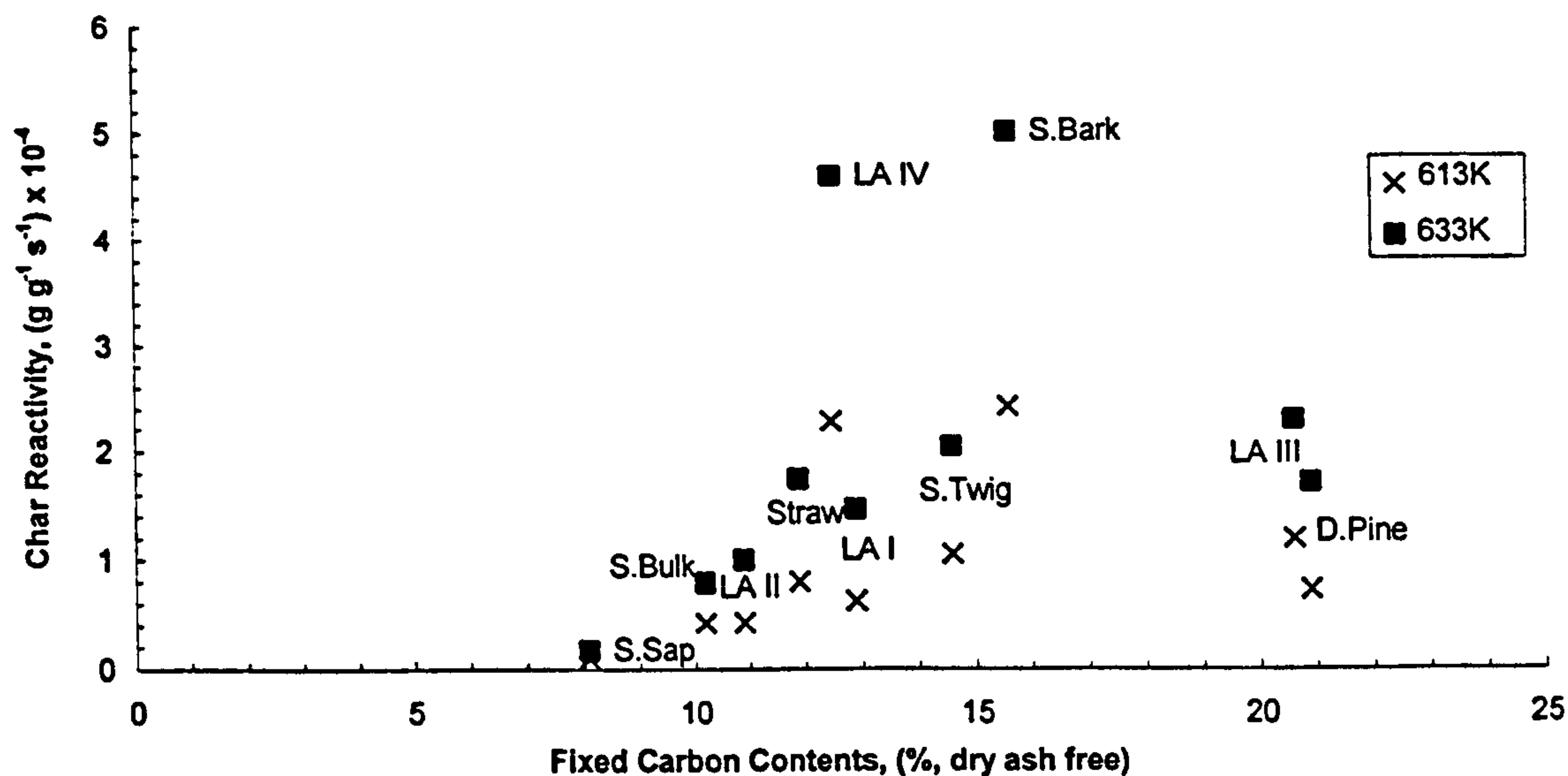


Figure 5.9a The Biomass Sample Chars Isothermal Reactivities in O_2 (3 l h^{-1}) at 613 and 633 K, Plotted Against the Fixed Carbon Contents of the Parent Materials

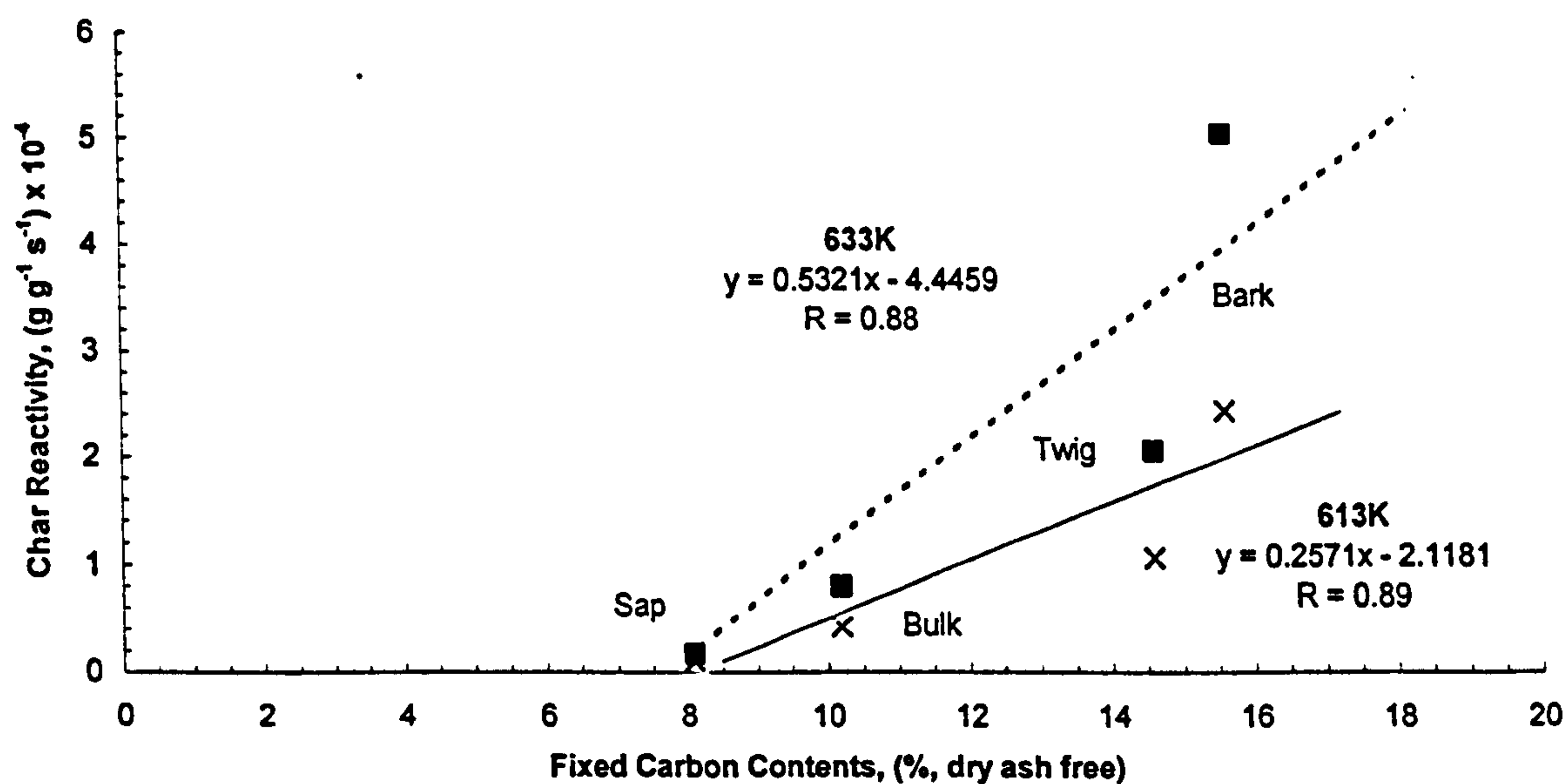


Figure 5.9b The Fractionated Silsoe Sample Chars Isothermal Reactivities in O_2 (3 l h^{-1}) at 613 and 633 K, Plotted Against Sample Fixed Carbon Contents

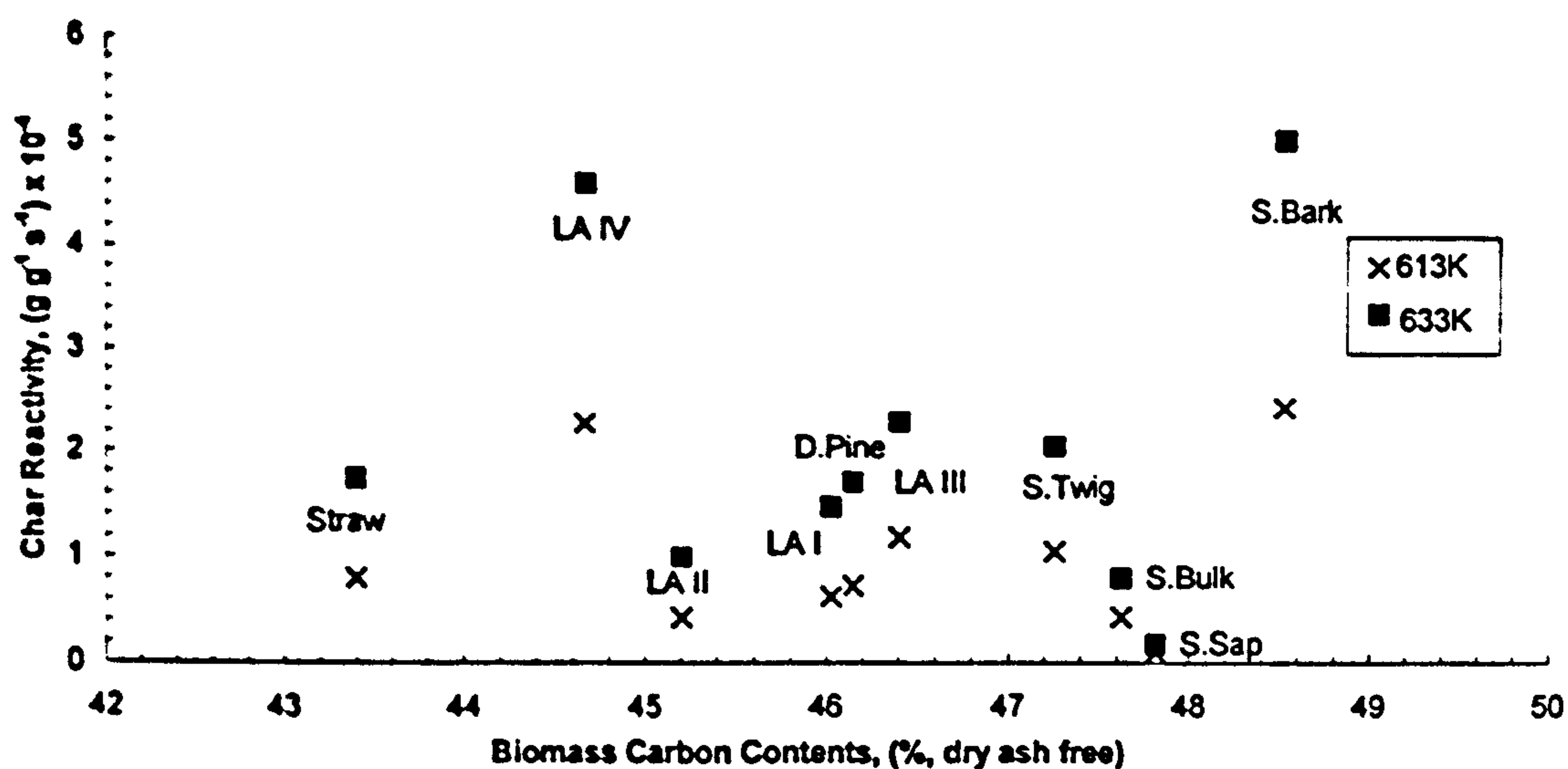


Figure 5.10 The Biomass Chars Isothermal Reactivities in O_2 (3 l h^{-1}) at 613 and 633 K, Plotted Against the Carbon Contents of the Parent Materials

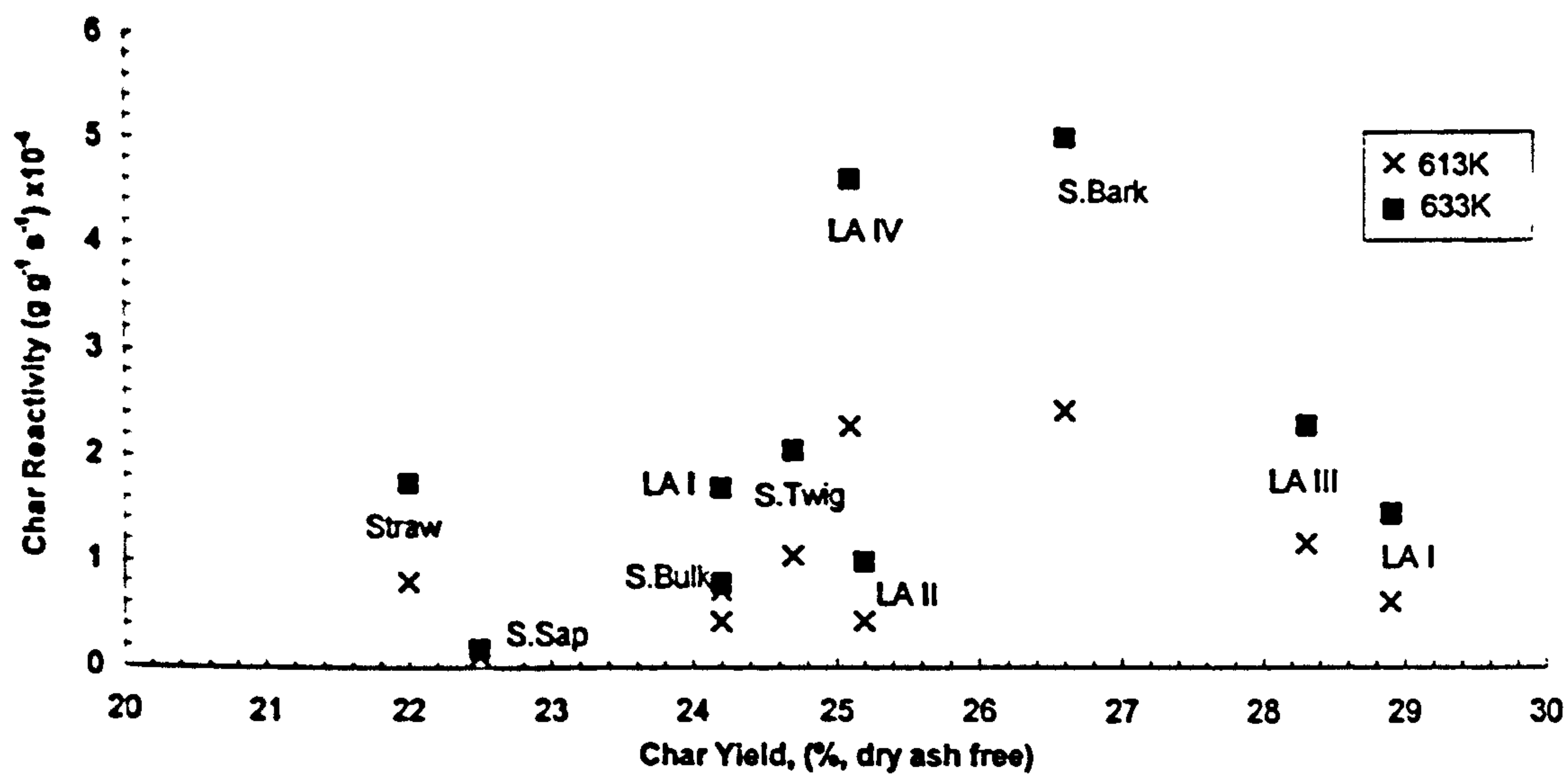


Figure 5.11a The Biomass Chars Isothermal Reactivities in O_2 (3 l h^{-1}) at 613 and 633 K, Plotted Against Char Yield

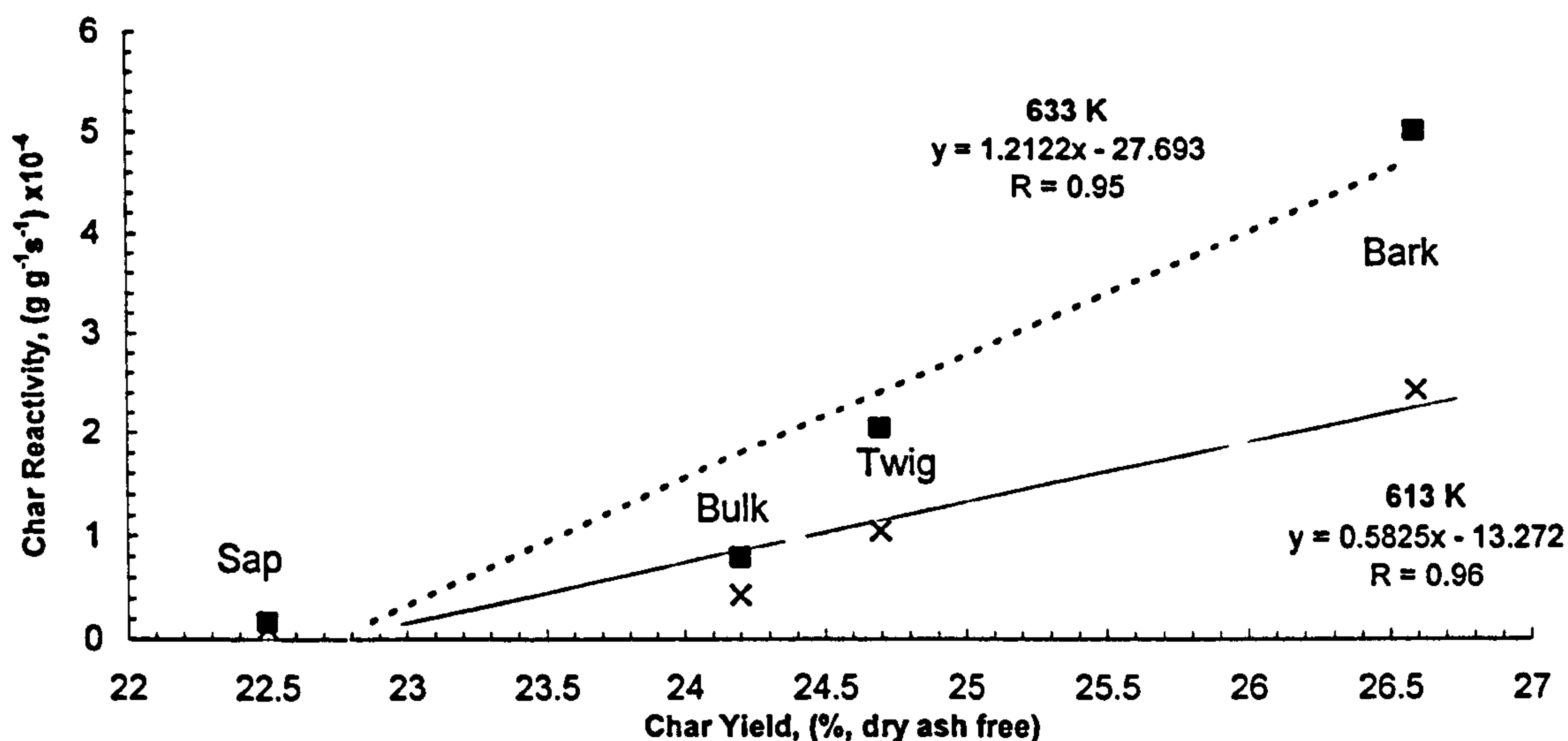


Figure 5.11b The Isothermal Reactivities in O_2 (3 l h^{-1}) at 613 and 633 K, of the Chars Prepared from the Fractionated Silsoe Samples, Plotted Against Char Yield

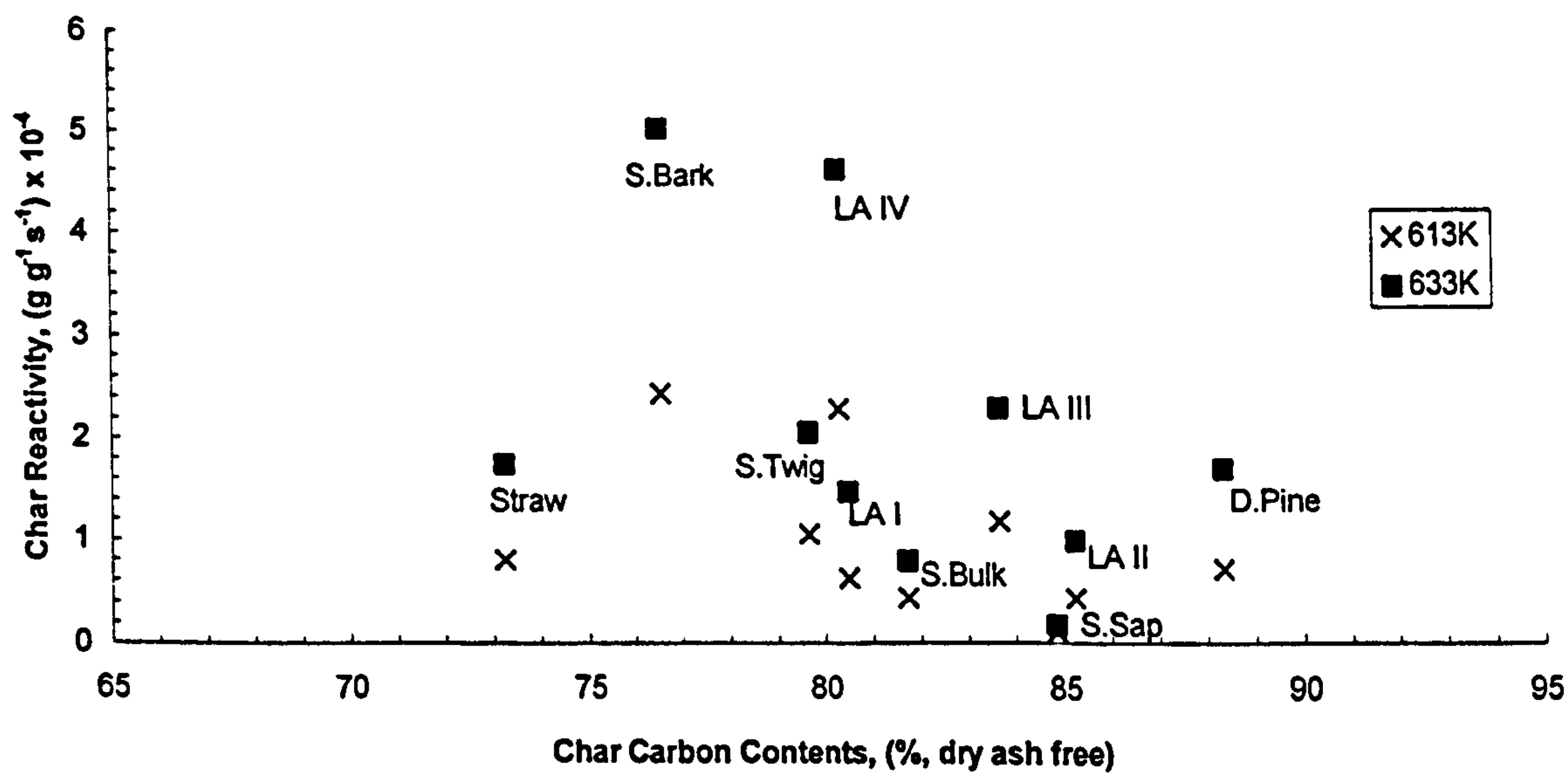


Figure 5.12a The Isothermal Reactivities in O_2 (3 l h^{-1}) at 613 and 633 K, of all the Biomass Chars, Plotted Against the Char Carbon Content

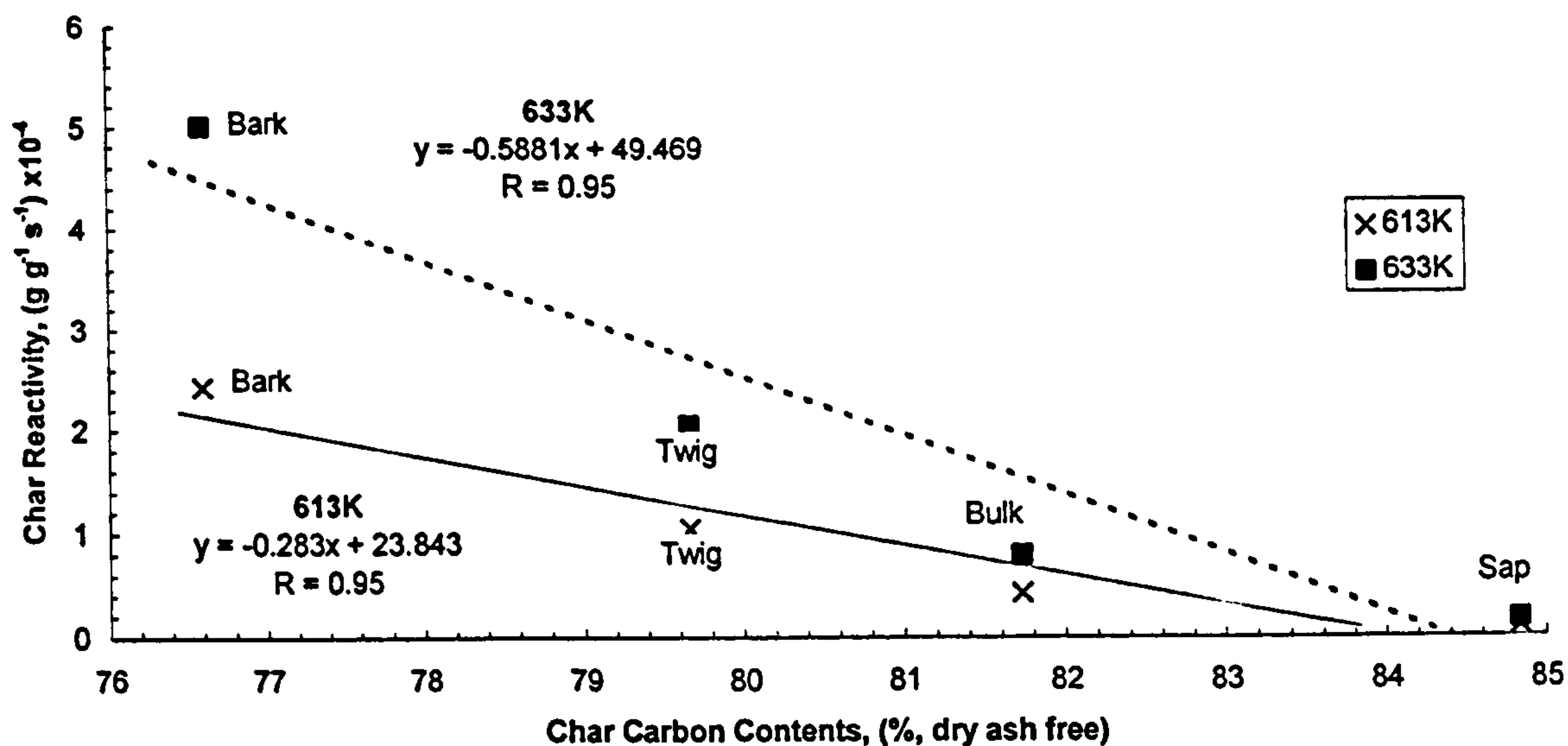


Figure 5.12b The Isothermal Reactivities in O_2 (3 l h^{-1}) at 613 and 633 K, of the Chars Prepared from the Fractionated Silsoe Samples, Plotted Against the Char Carbon Content

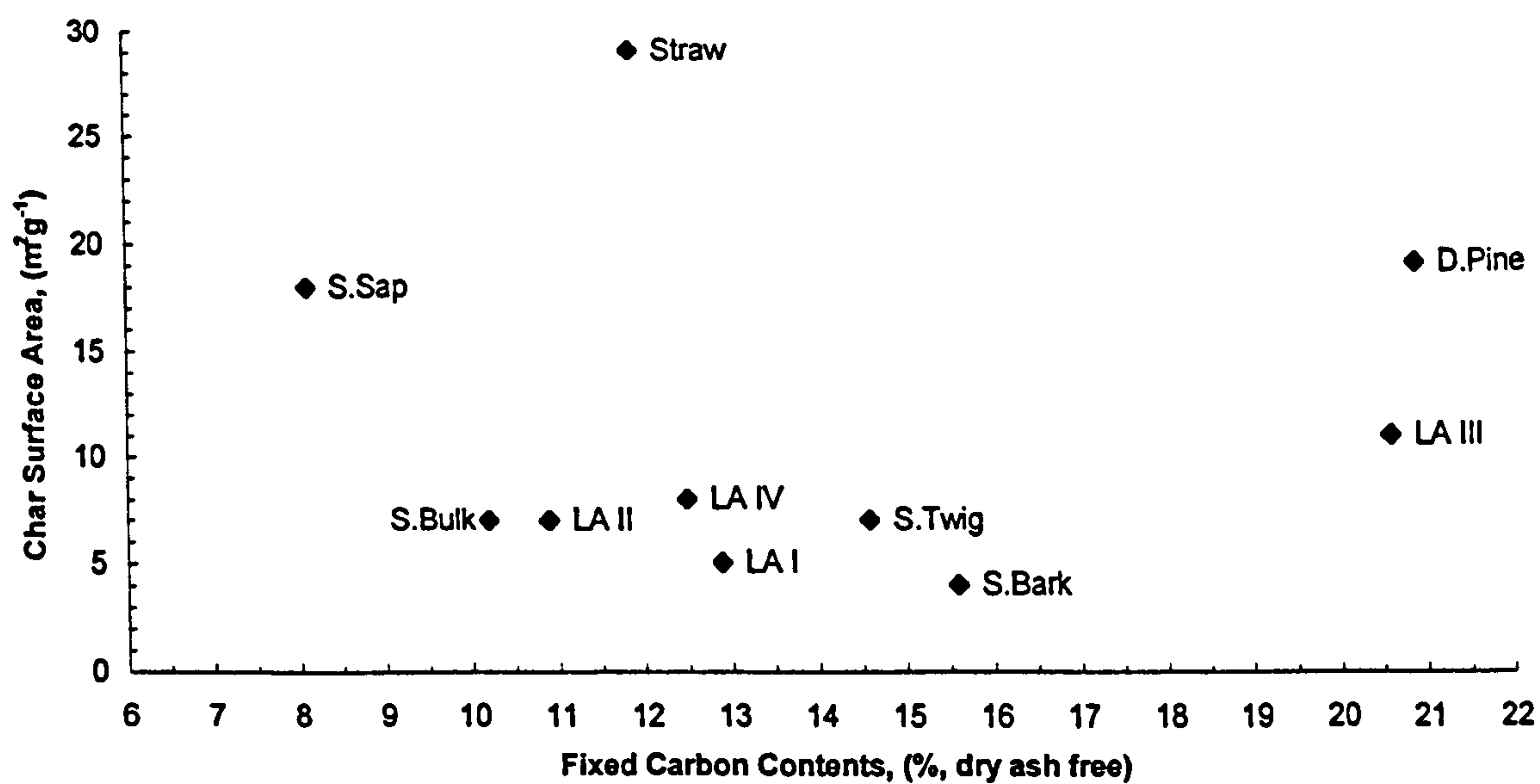


Figure 5.13a The Surface Areas of the Biomass Chars Plotted Against the Fixed Carbon Content of the Parent Materials

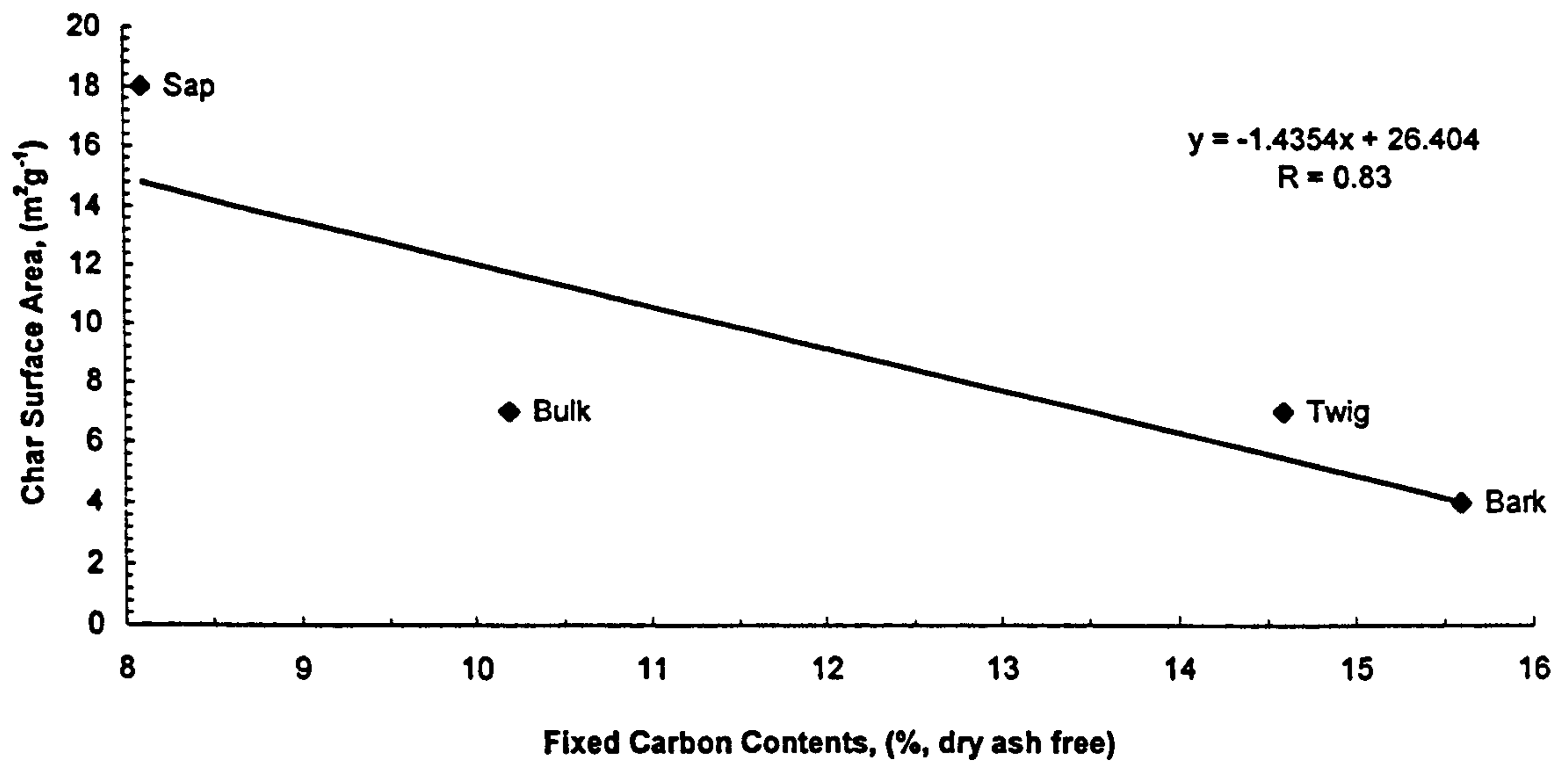


Figure 5.13b The Surface Areas of the Chars Prepared from the Fractionated Silsoe Samples Plotted Against the Fixed Carbon Content of the Parent Materials

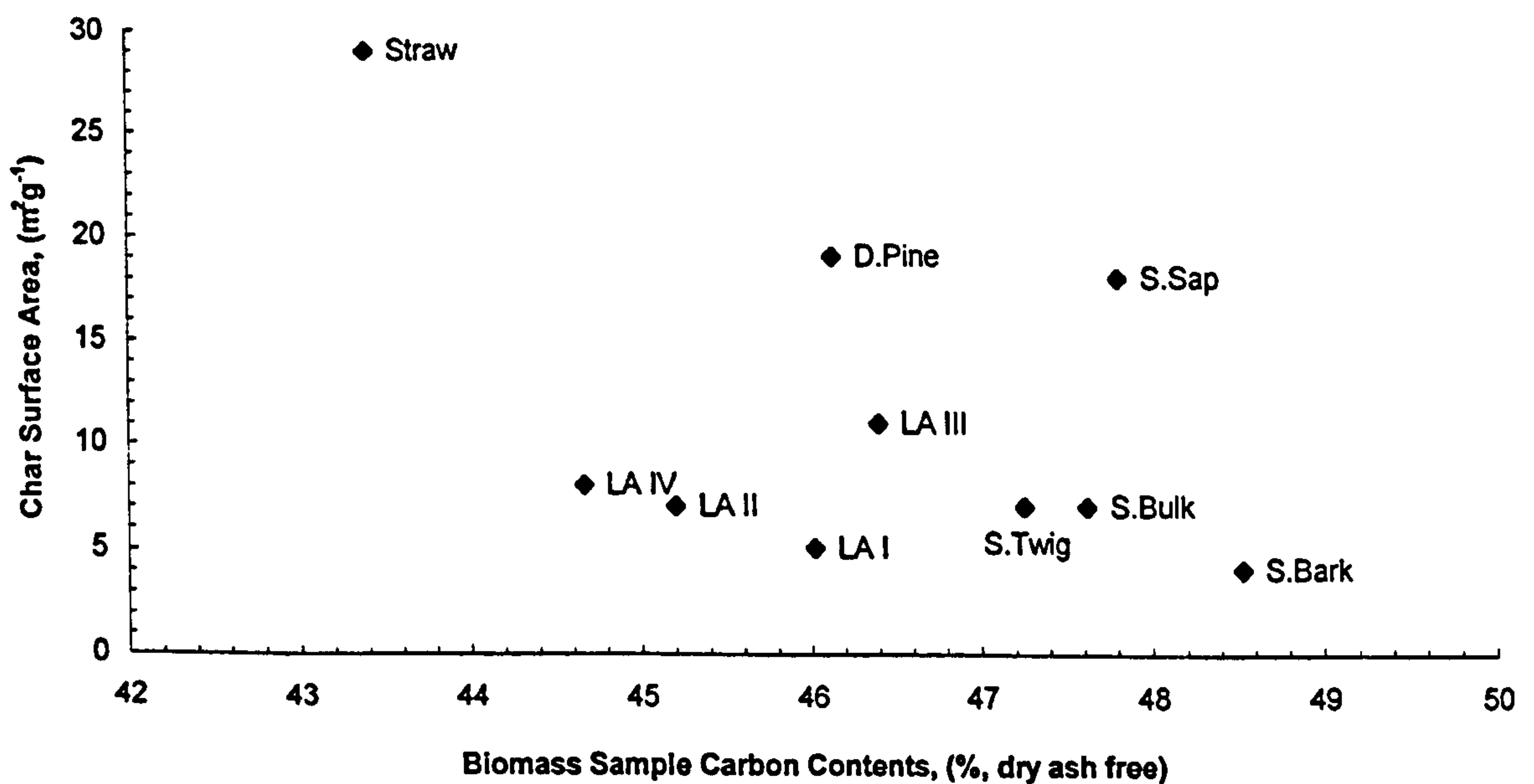


Figure 5.14 The Carbon Content of the Biomass Chars Plotted Against the Char Surface Area

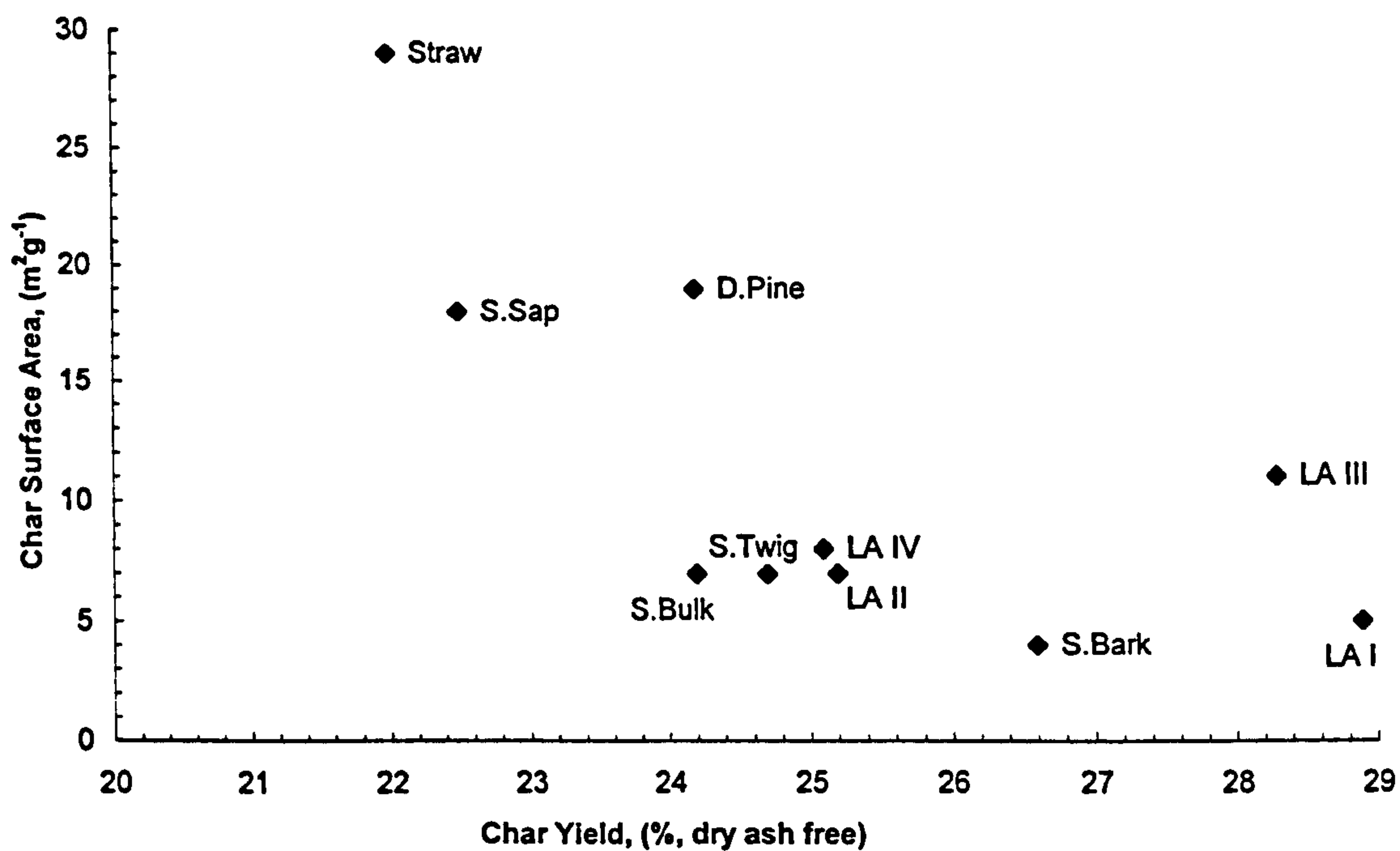


Figure 5.15a The Surface Areas of the Biomass Chars Plotted Against Char Yield

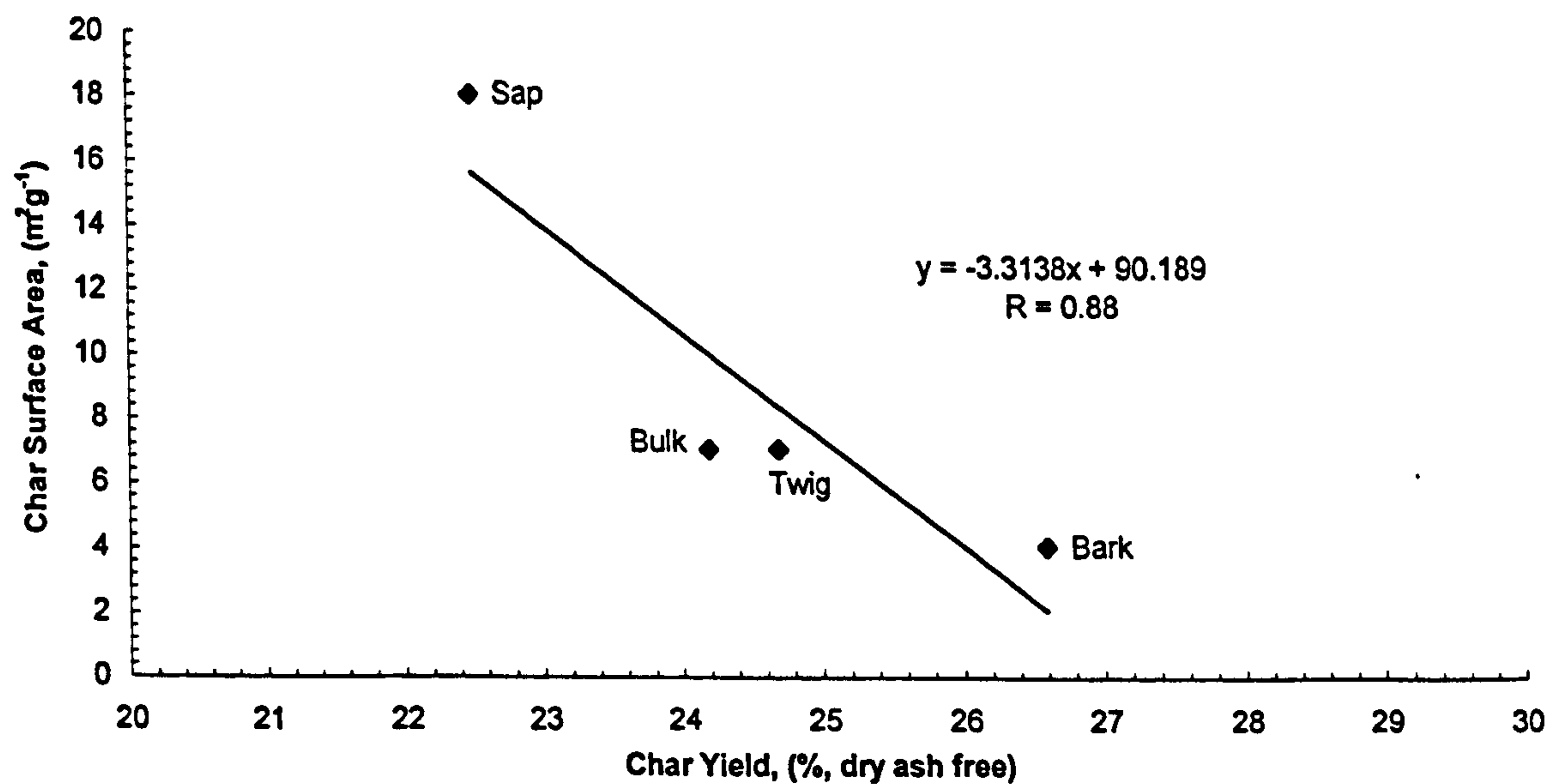


Figure 5.15b The Surface Areas of the Chars Prepared from the Fractionated Silsoe Samples Plotted Against Char Yield

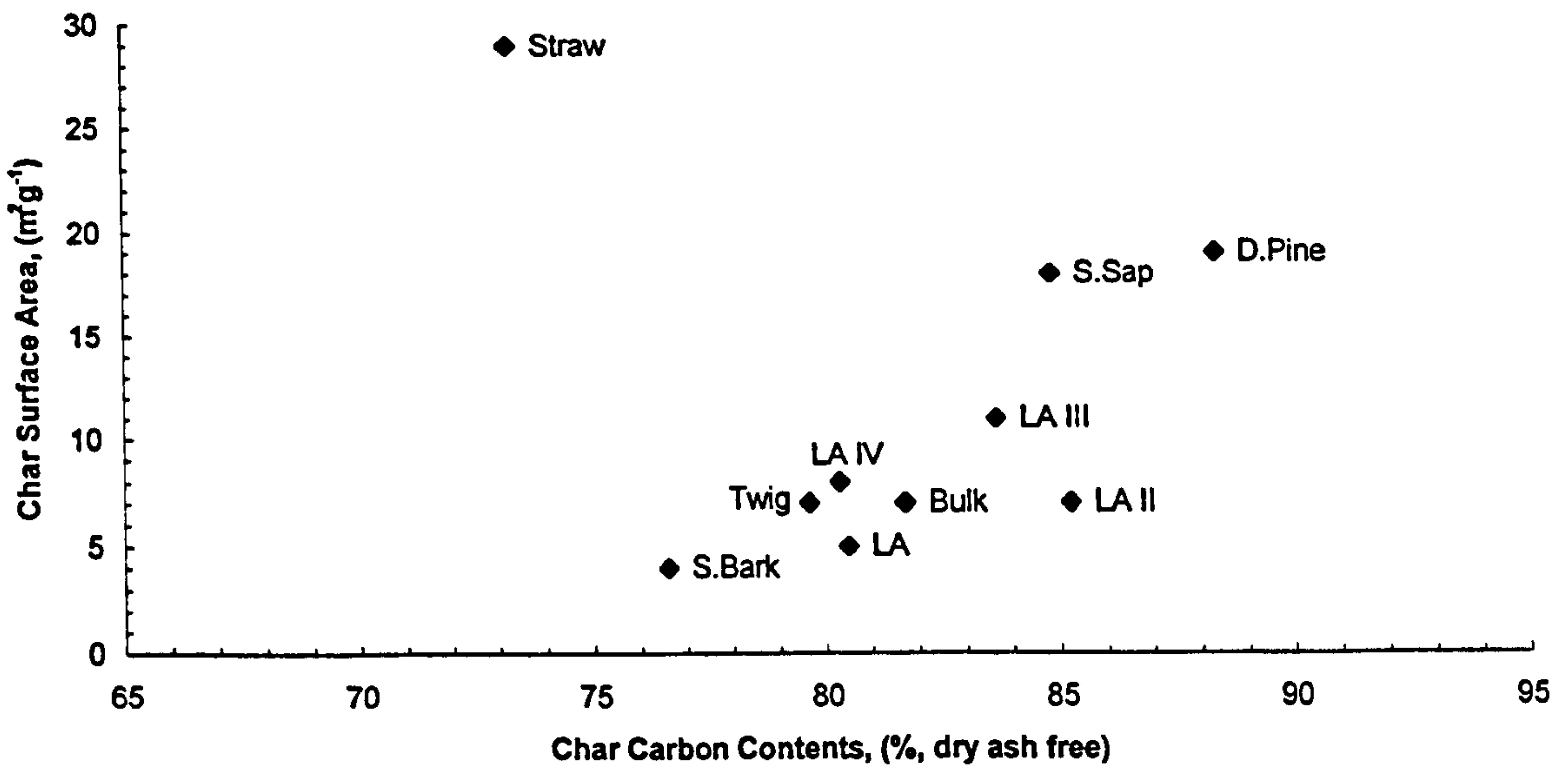


Figure 5.16a The Surface Areas of the Biomass Chars Plotted Against Char Carbon Content

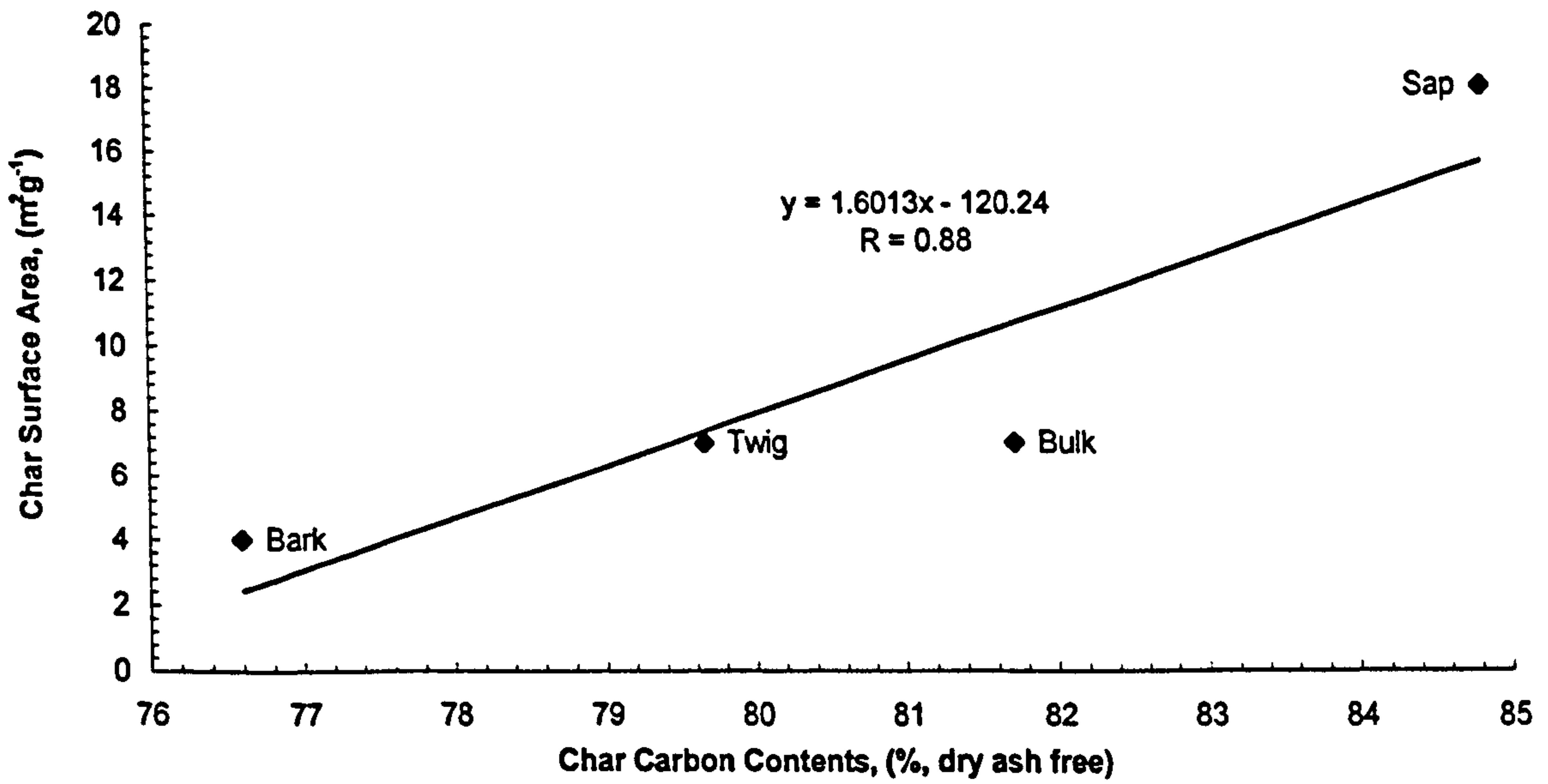


Figure 5.16b The Surface Area of the Chars Prepared from the Fractionated Silsoe Samples Plotted Against Char Carbon Content

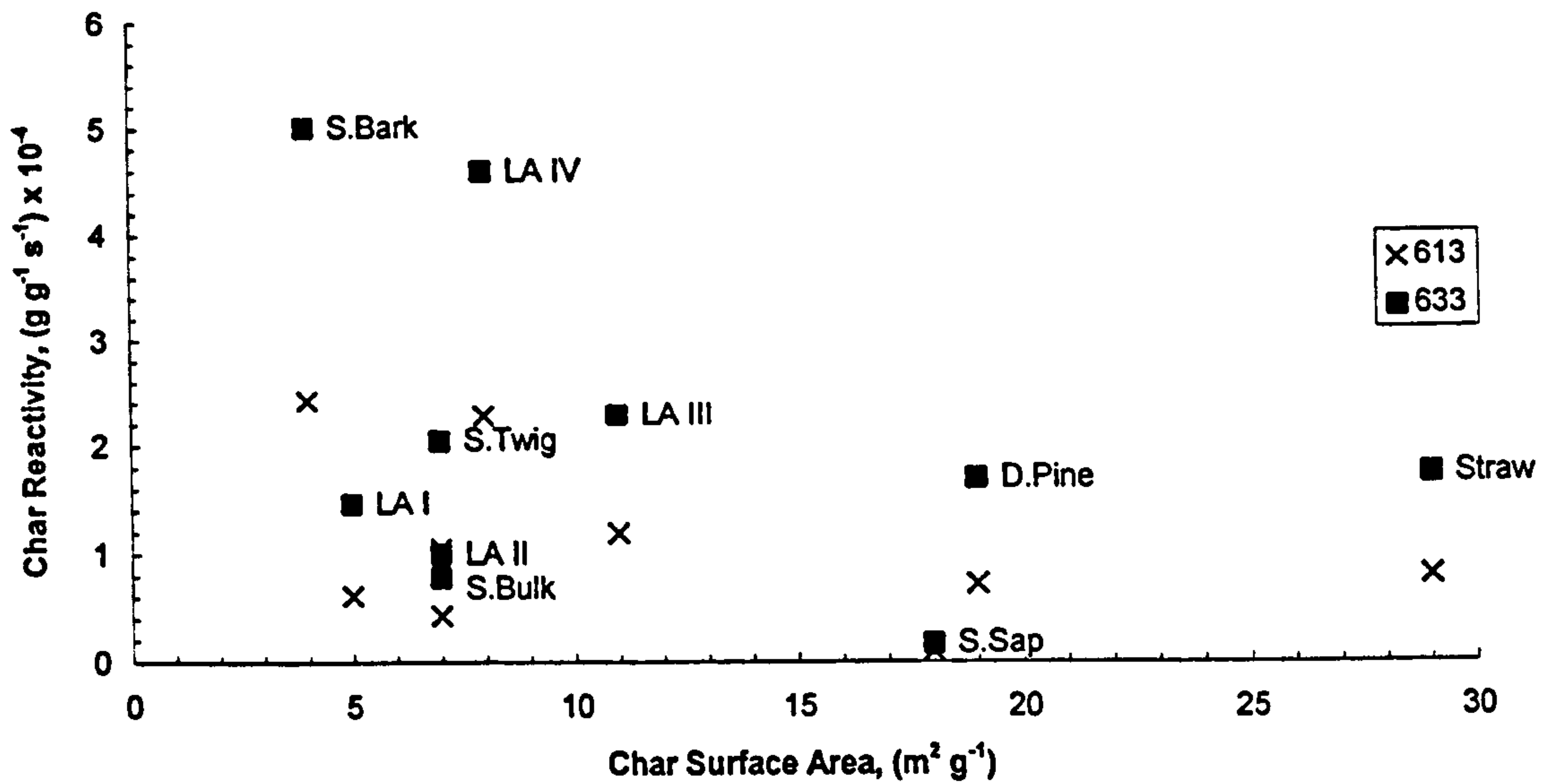


Figure 5.17 The Isothermal Reactivities in O₂ (3 l h⁻¹) at 613 and 633 K, of the Biomass Chars, Plotted Against Char Surface Area

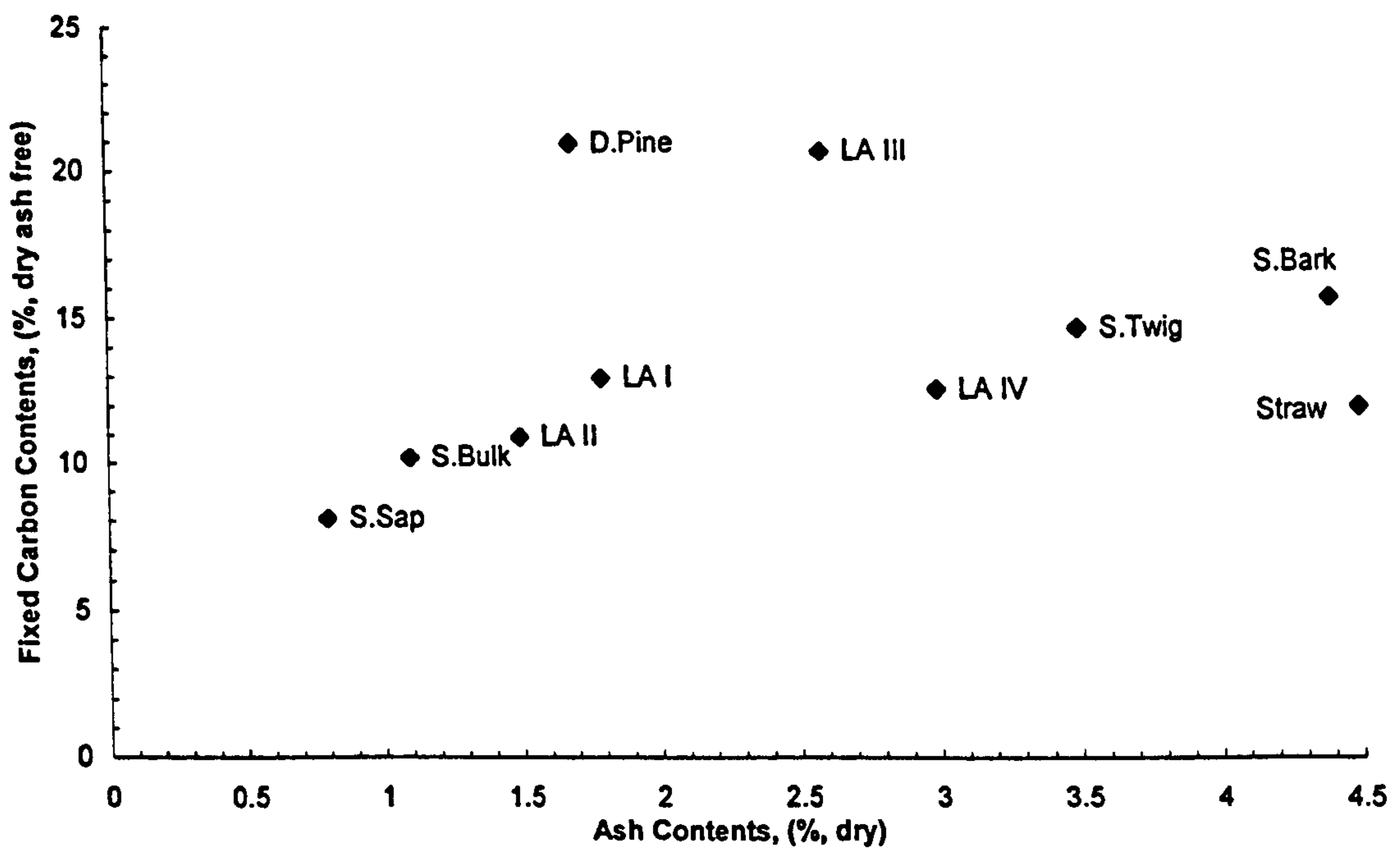


Figure 5.18a The Biomass Fixed Carbon Contents Plotted Against Ash Content

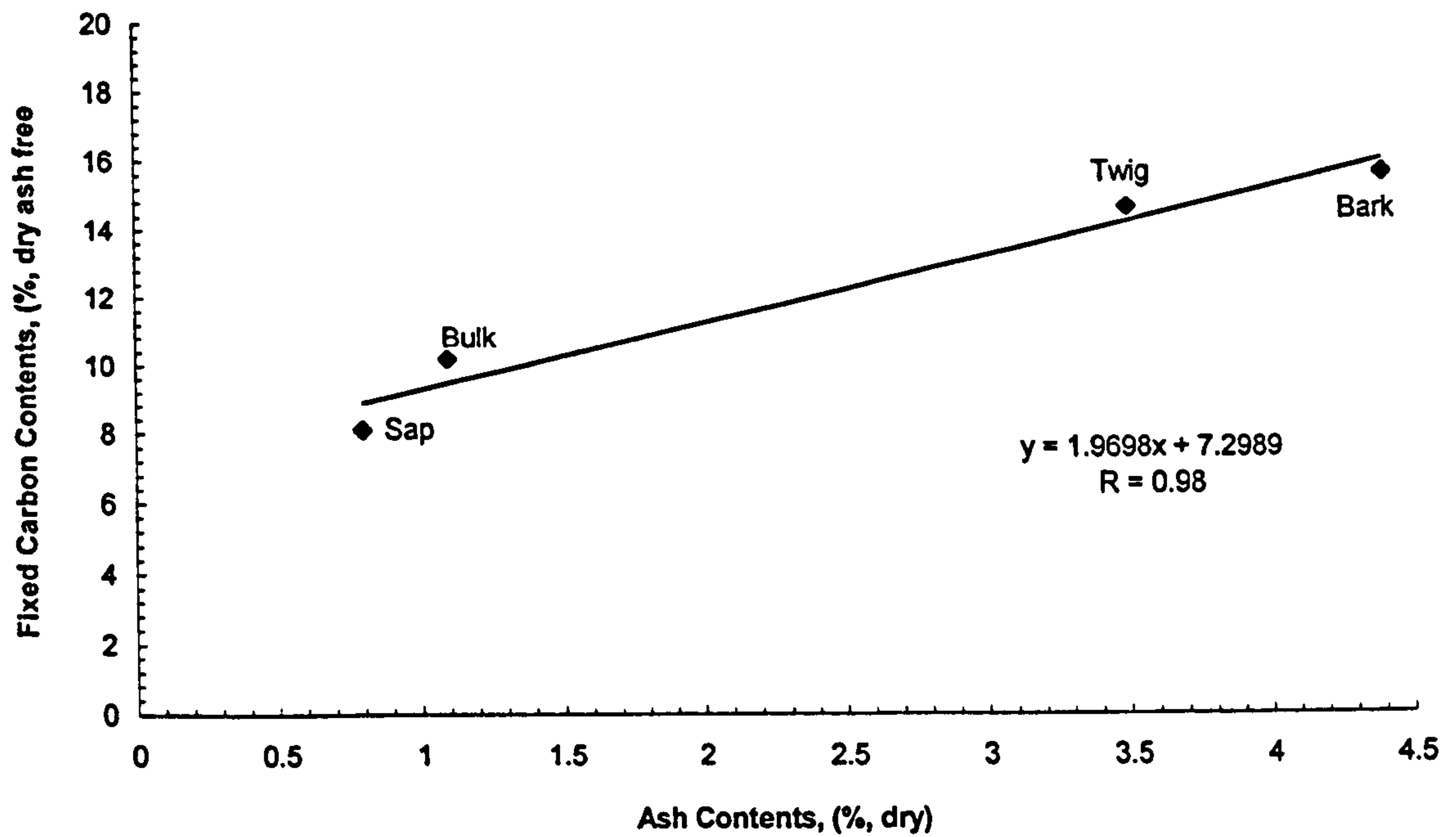


Figure 5.18b The Fixed Carbon Contents of the Fractionated Silsoe Samples Plotted Against Ash Content

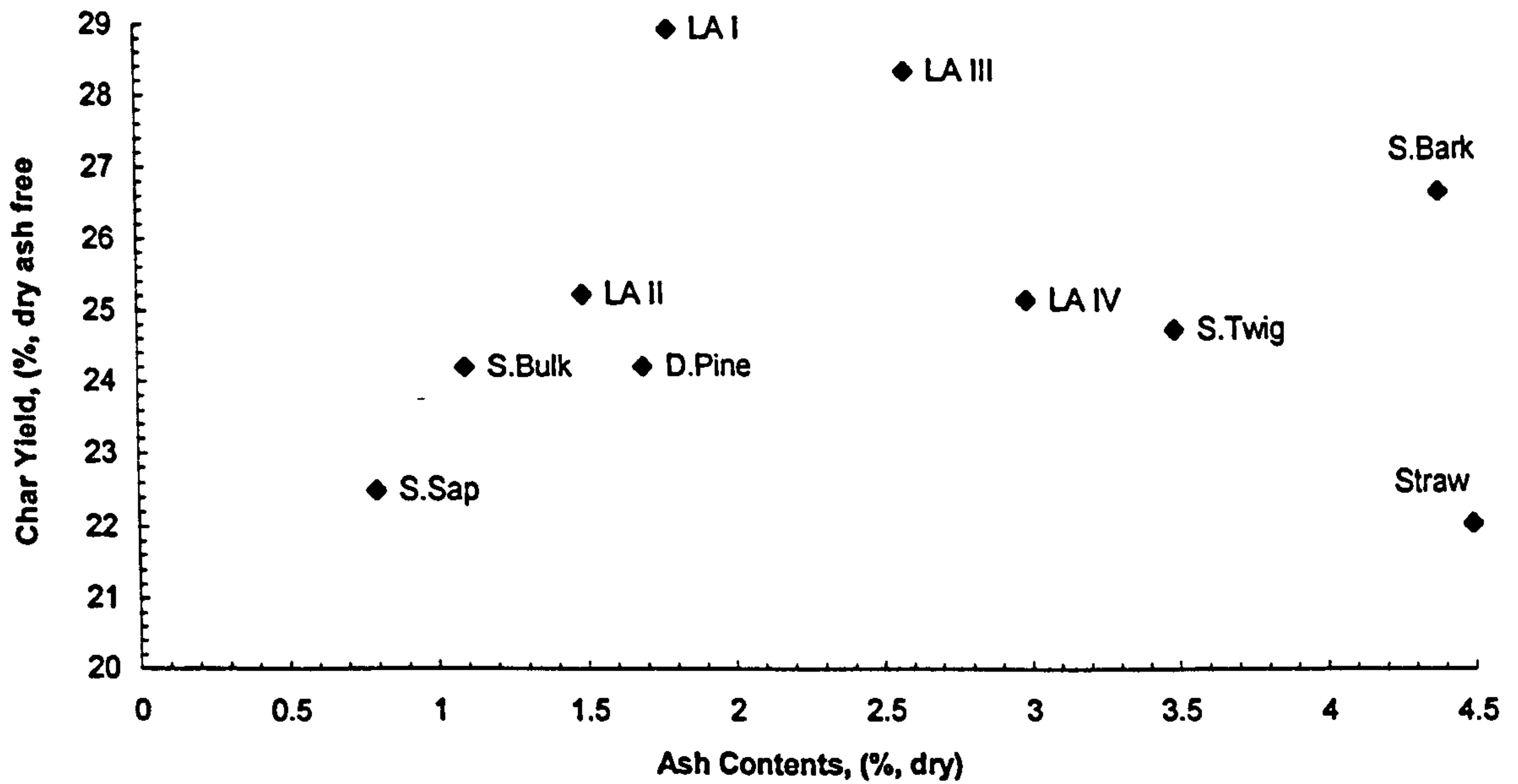


Figure 5.19a The Yields of Char Prepared from of the Biomass Materials Plotted Against Ash Content

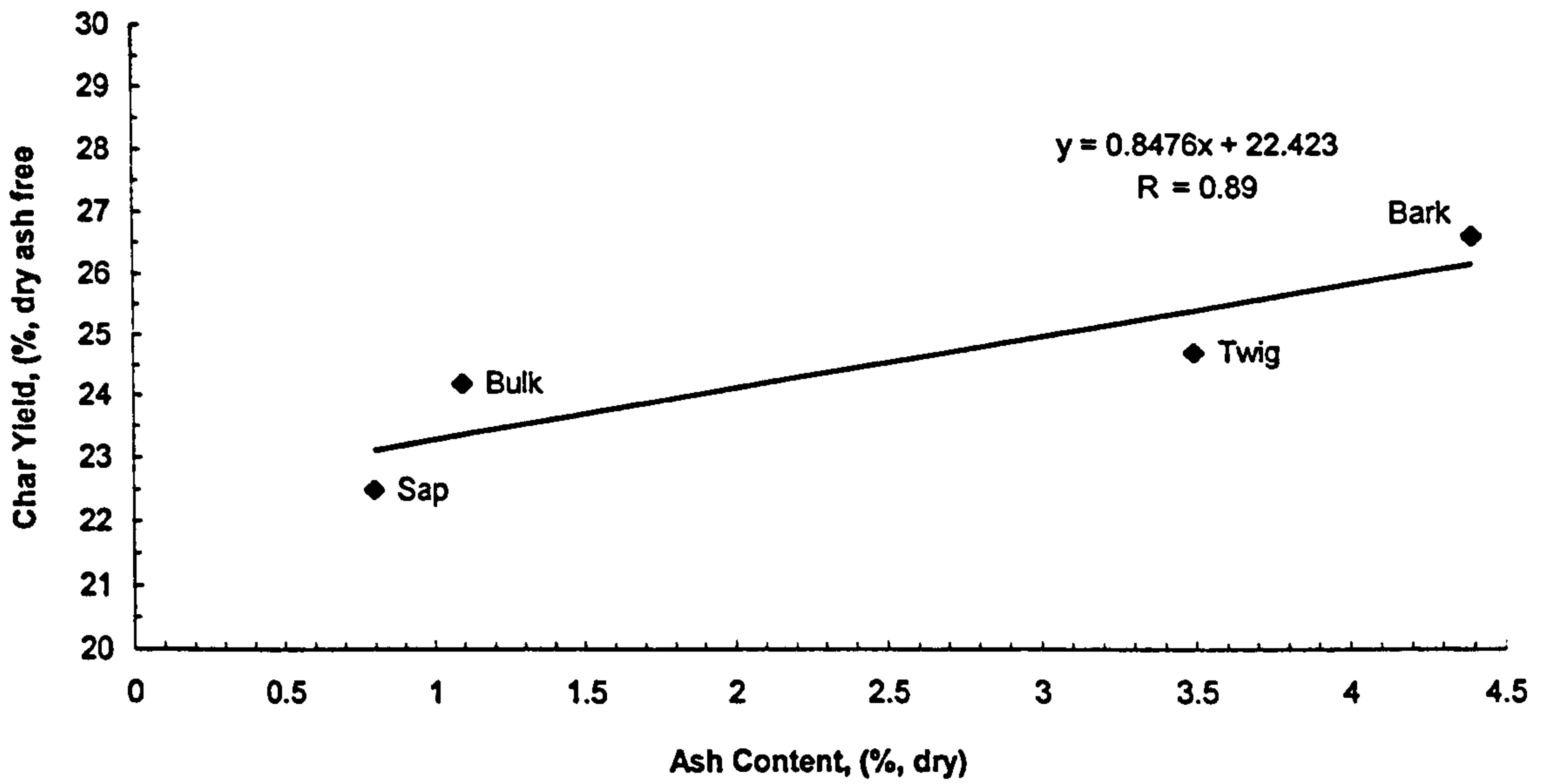


Figure 5.19b The Yields of Char Prepared from the Silsoe Fractionated Materials Plotted Against Ash Content

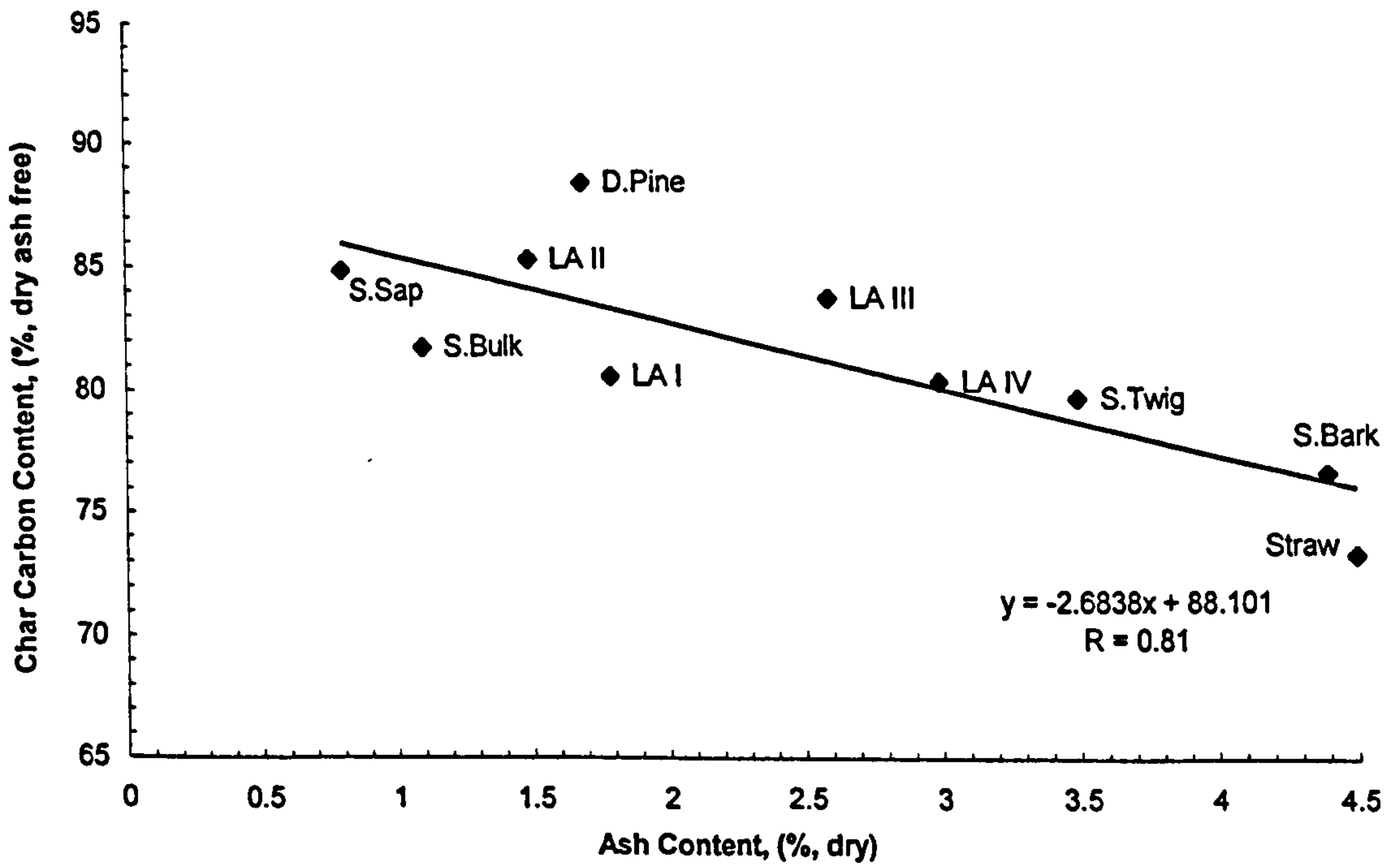


Figure 5.20a The Biomass Chars Carbon Content Plotted Against Ash Content

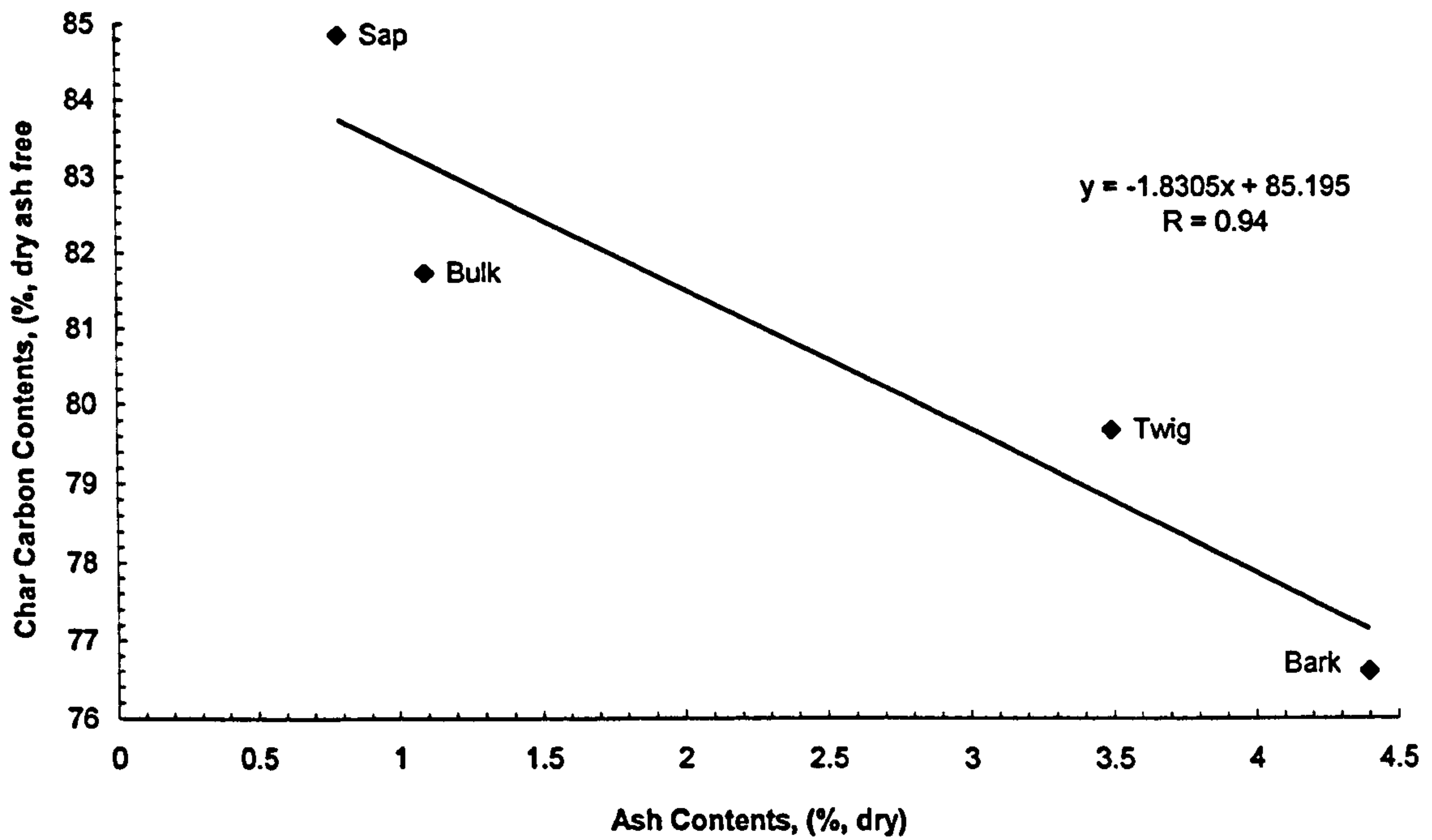


Figure 5.20b The Carbon Content of the Chars Prepared from the Fractionated Silsoe Materials Plotted Against Ash Content

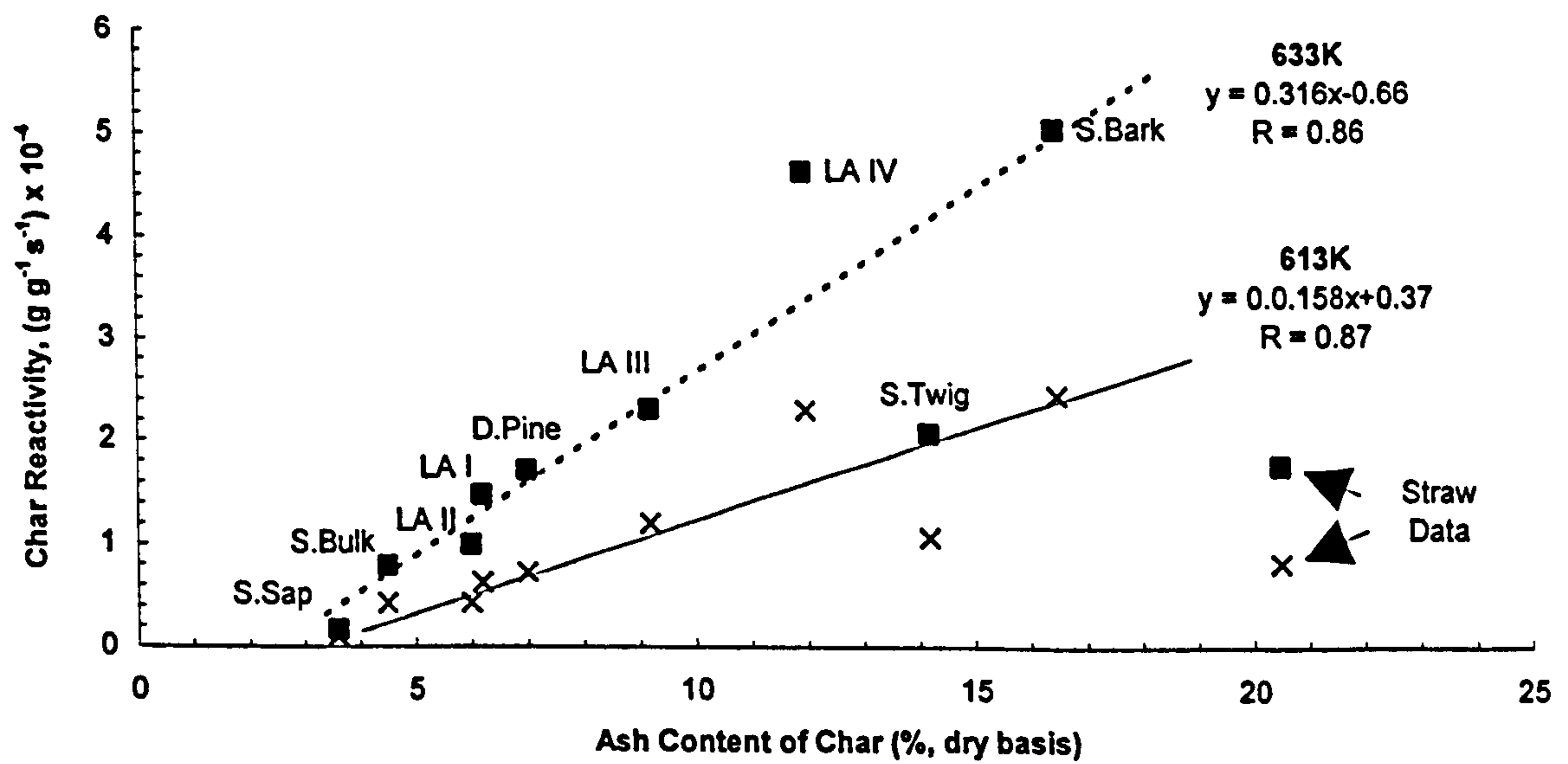


Figure 5.21 The Isothermal Reactivities in O_2 (3 l h^{-1}) at 613 and 633 K of the Biomass Chars, Plotted Against Char Ash Content

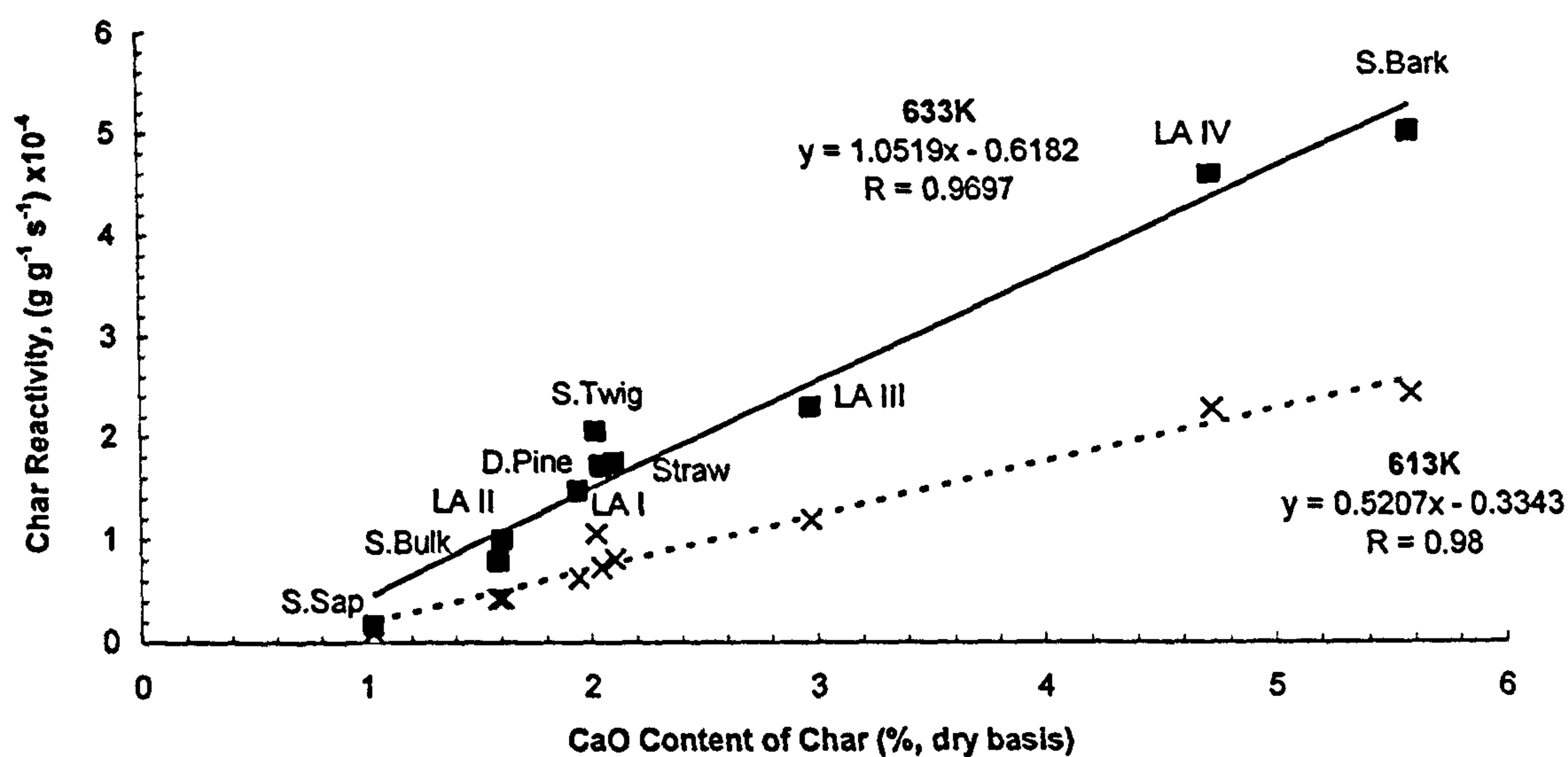


Figure 5.22 The Isothermal Reactivities in O_2 (3 l h^{-1}) at 613 and 633 K of the Biomass Chars, Plotted Against Char CaO Contents

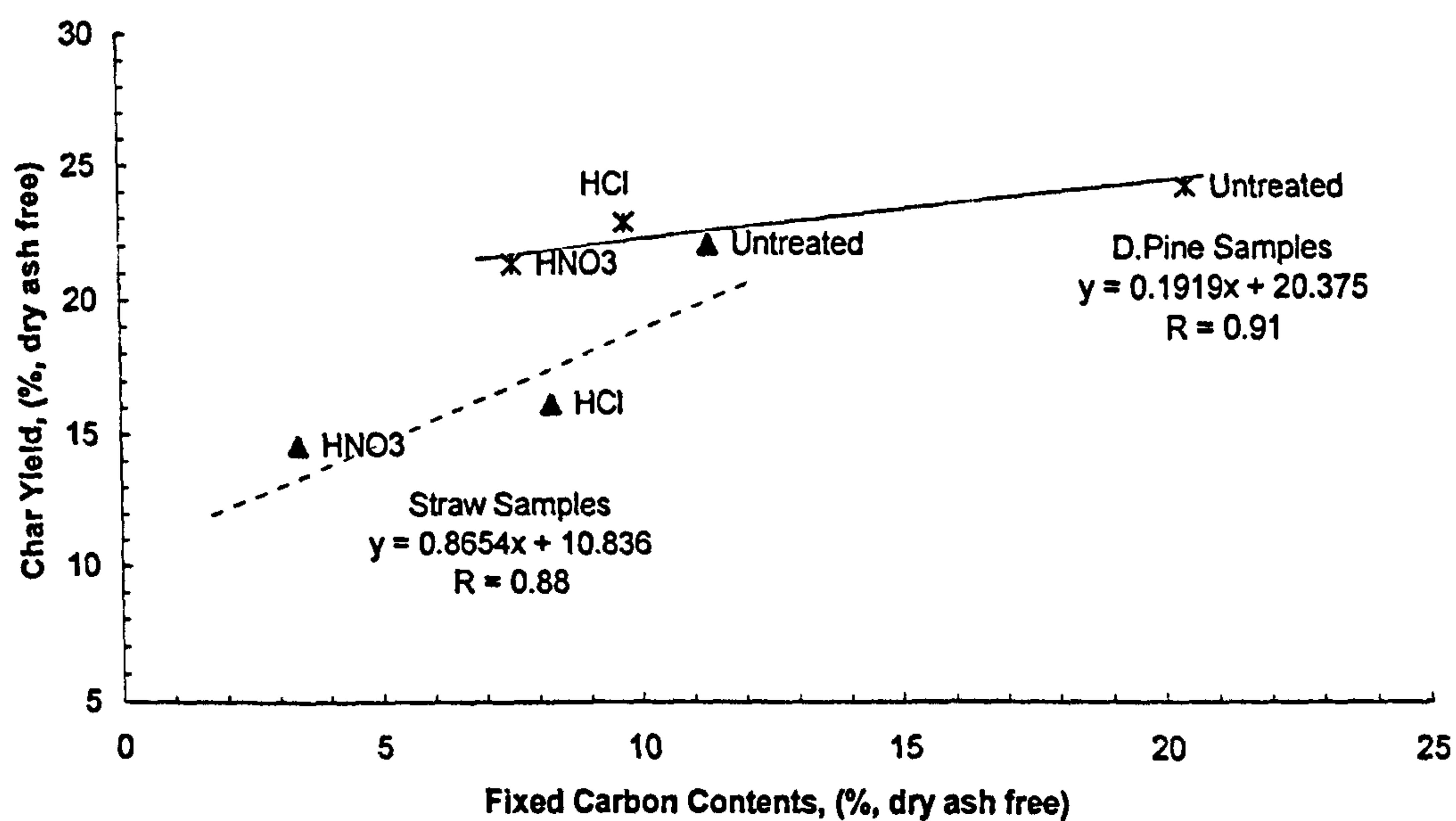


Figure 5.23 The Char Yields Plotted Against Fixed Carbon Content for the Untreated and Acid-Washed Straw and Danish Pine Samples

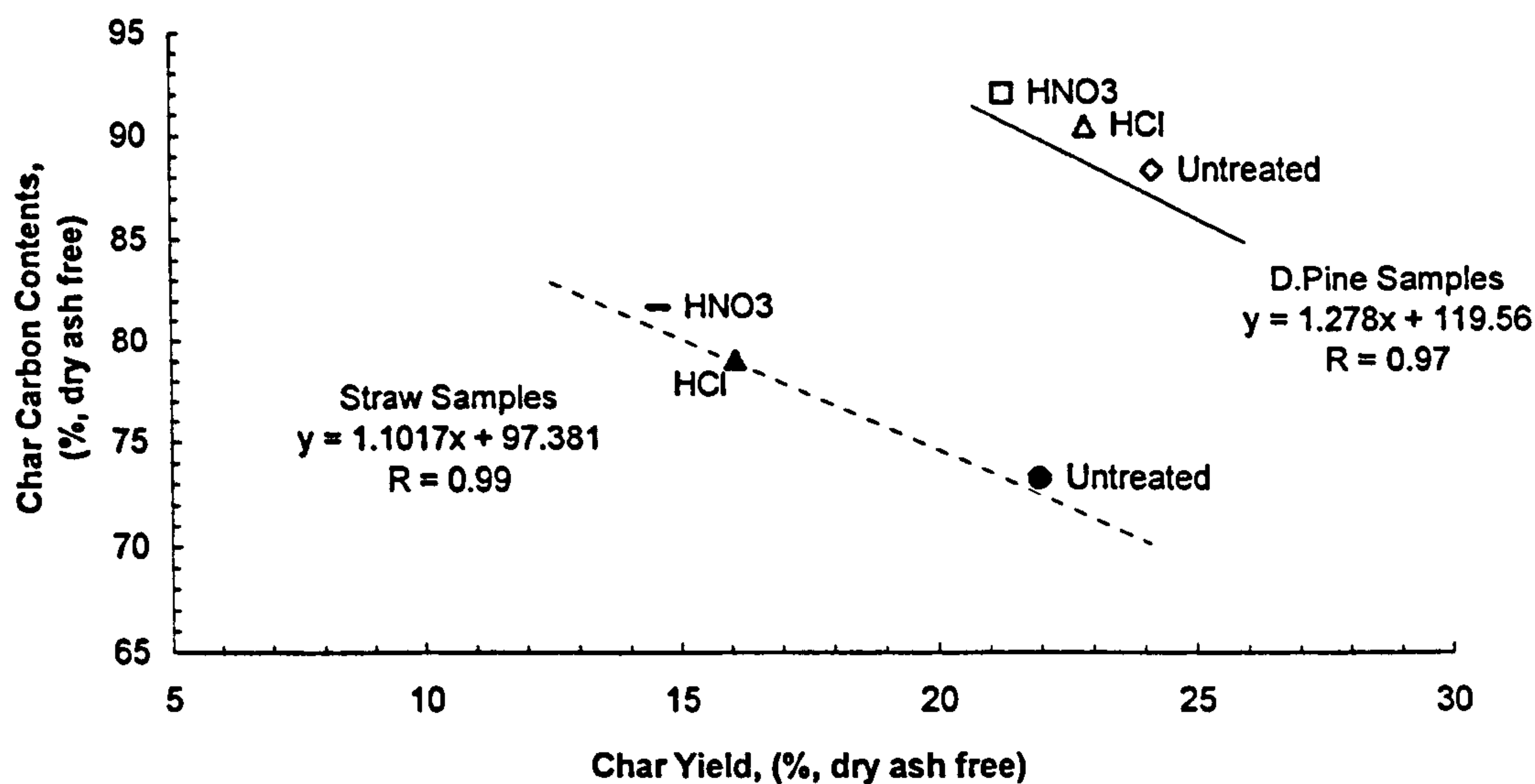


Figure 5.24 The Char Carbon Contents Plotted Against Char Yields for the Untreated and Acid-Washed Straw and Danish Pine Samples

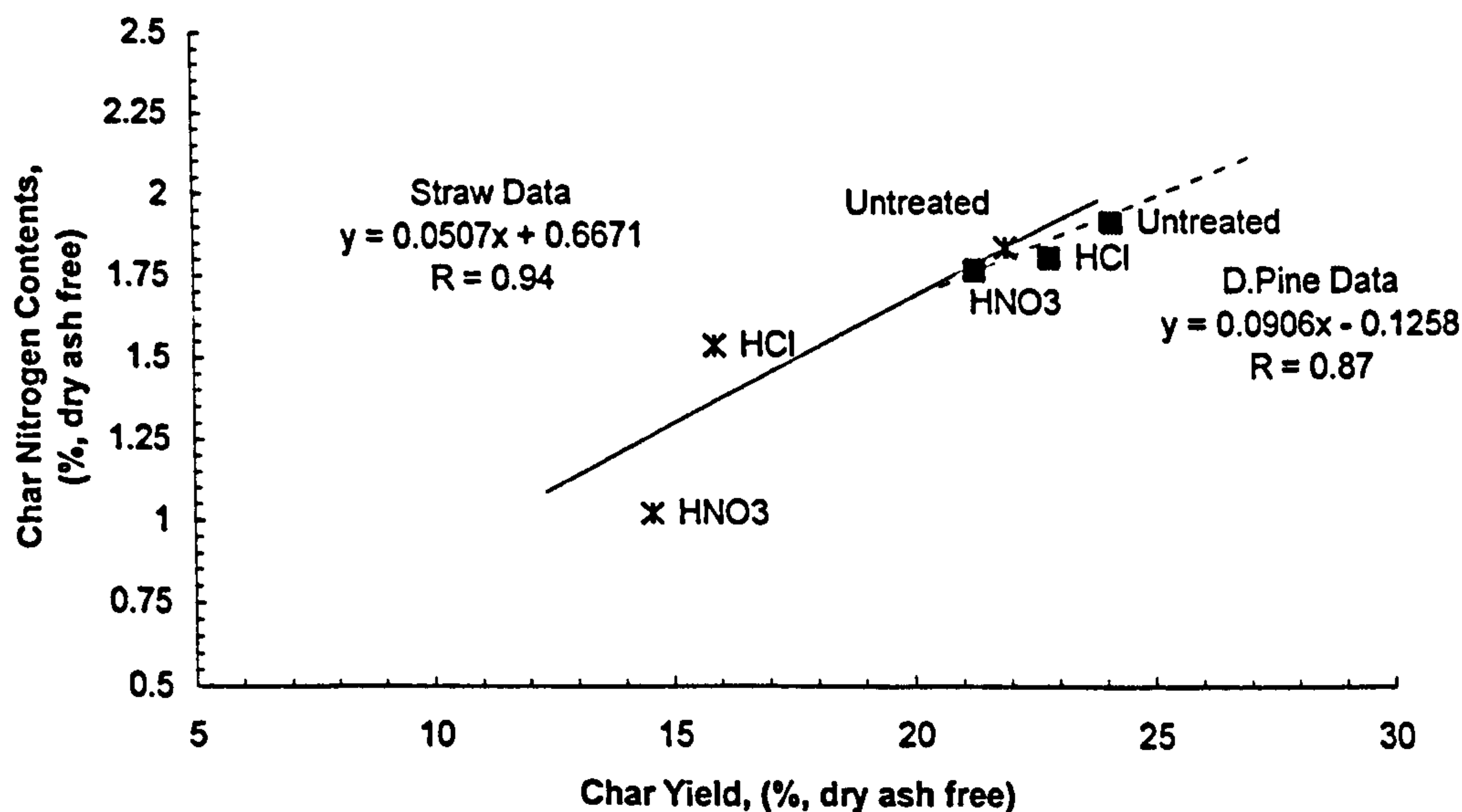


Figure 5.25 The Char Nitrogen Contents Plotted Against Char Yields for the Untreated and Acid-Washed Straw and Danish Pine Samples

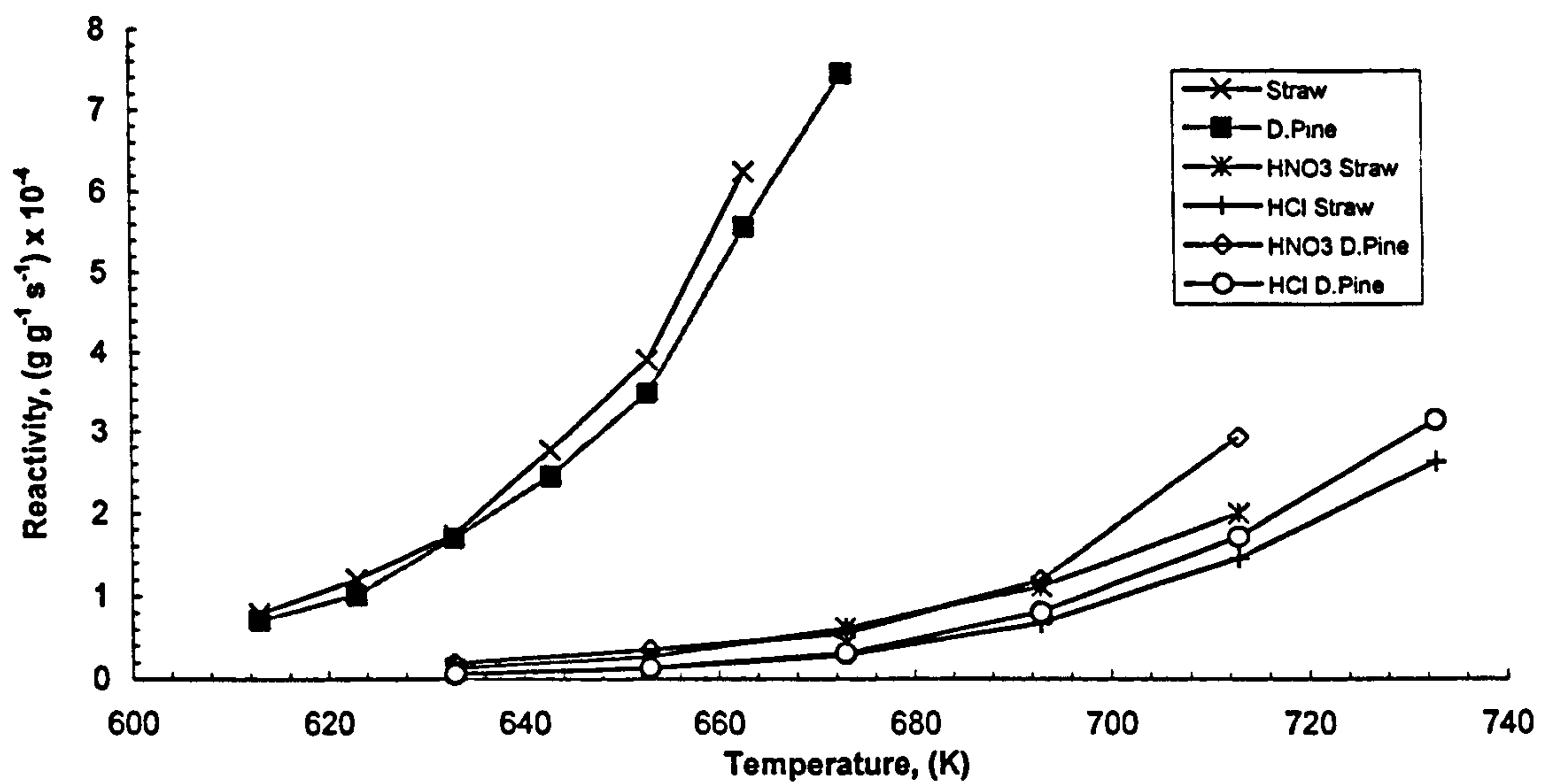


Figure 5.26 The Isothermal Reactivity in O_2 (3 l h^{-1}), in the Temperature Range 613 to 733 K, of the Chars Prepared from the Untreated and Acid-Washed Biomass Samples

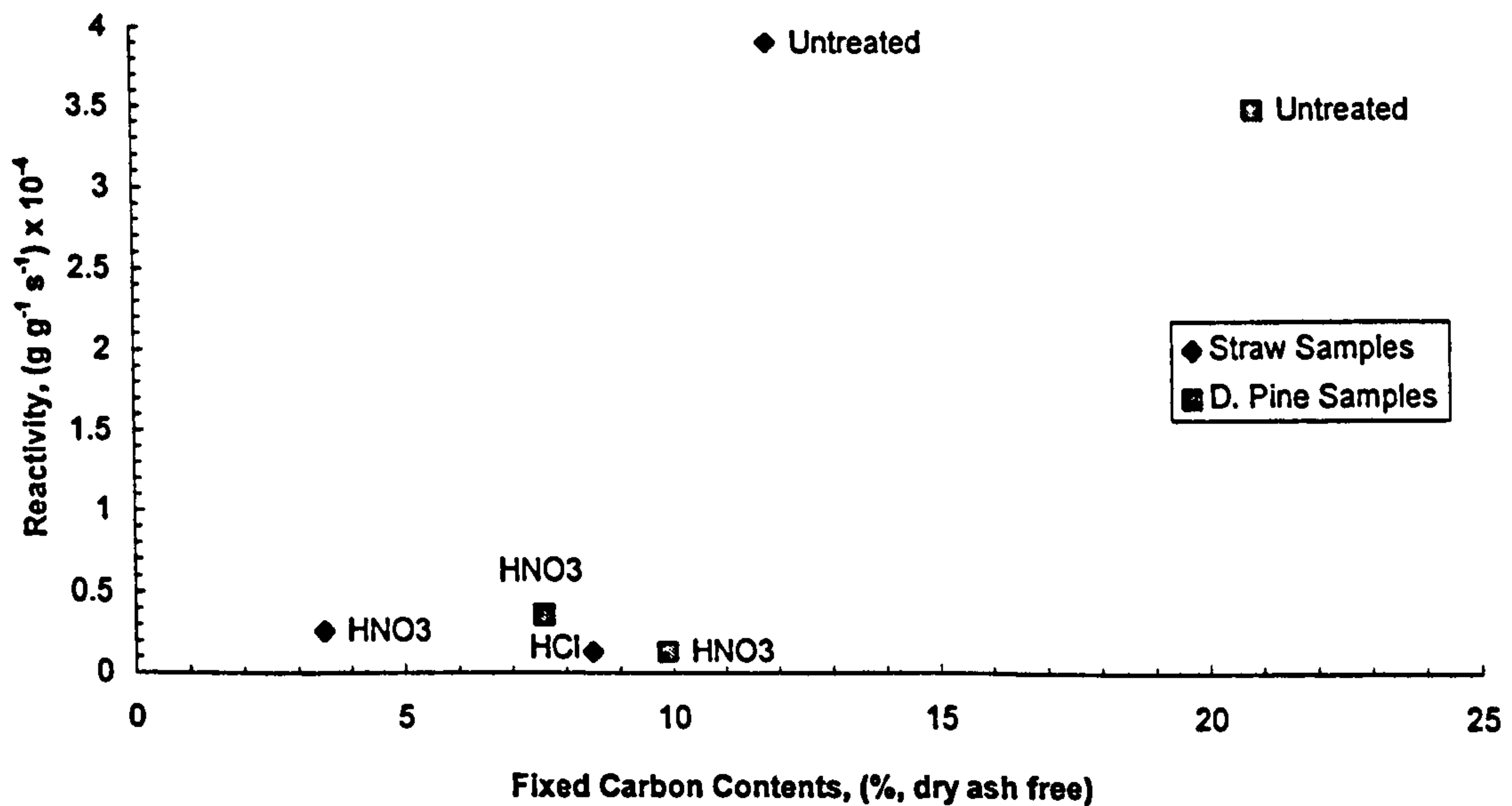


Figure 5.27 The Isothermal Reactivity in O_2 (3 l h^{-1}) at 633 K, of the Chars Prepared from the Untreated and Acid-Washed Biomass Samples Plotted Against Fixed Carbon Contents

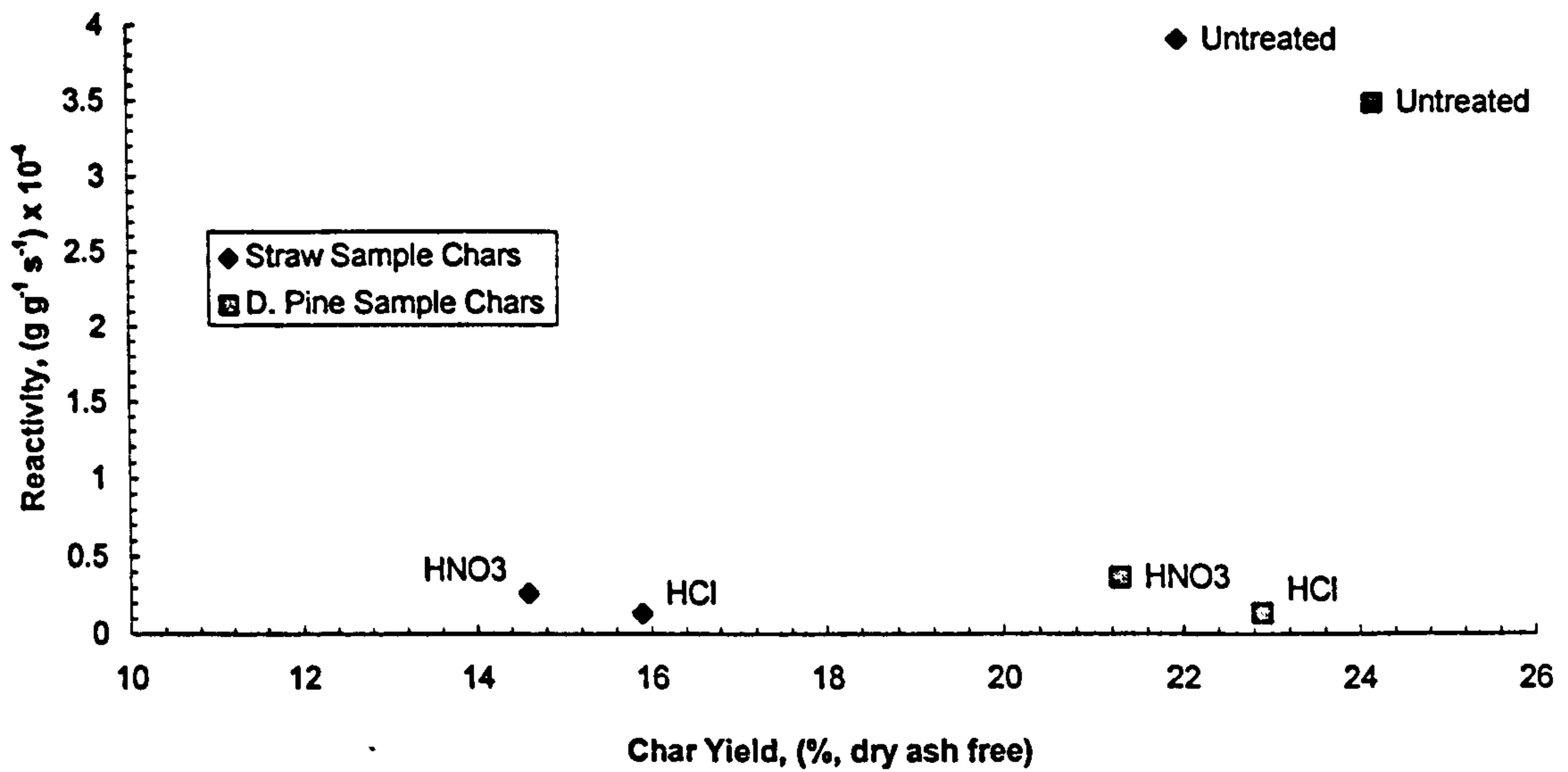


Figure 5.28 The Isothermal Reactivity in O_2 (3 l h^{-1}) at 633 K, of the Chars Prepared from the Untreated and Acid-Washed Biomass Samples Plotted Against Char Yield

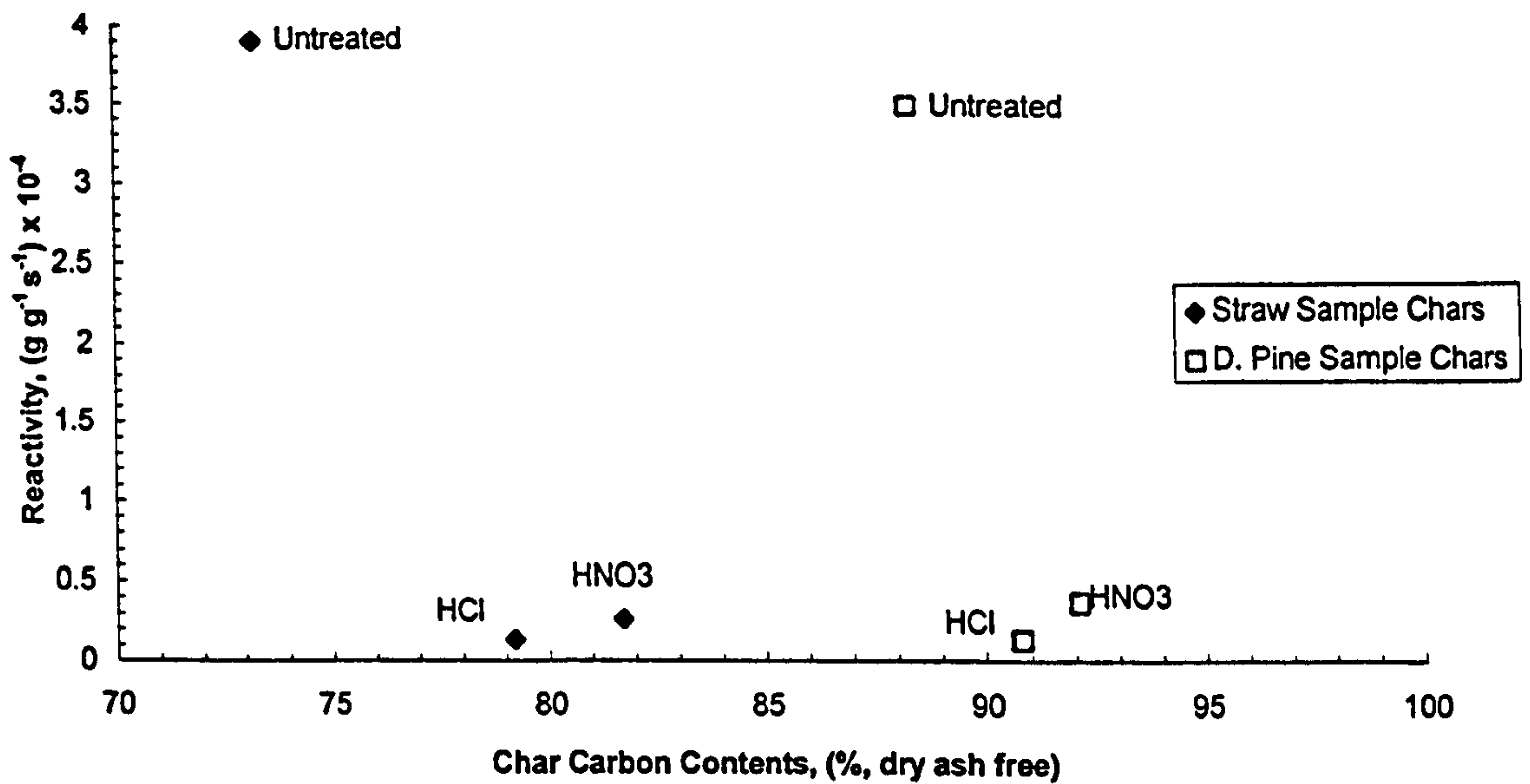


Figure 5.29 The Isothermal Reactivity in O_2 (3 l h^{-1}) at 633 K, of the Chars Prepared from the Untreated and Acid-Washed Biomass Samples Plotted Against Char Carbon Content

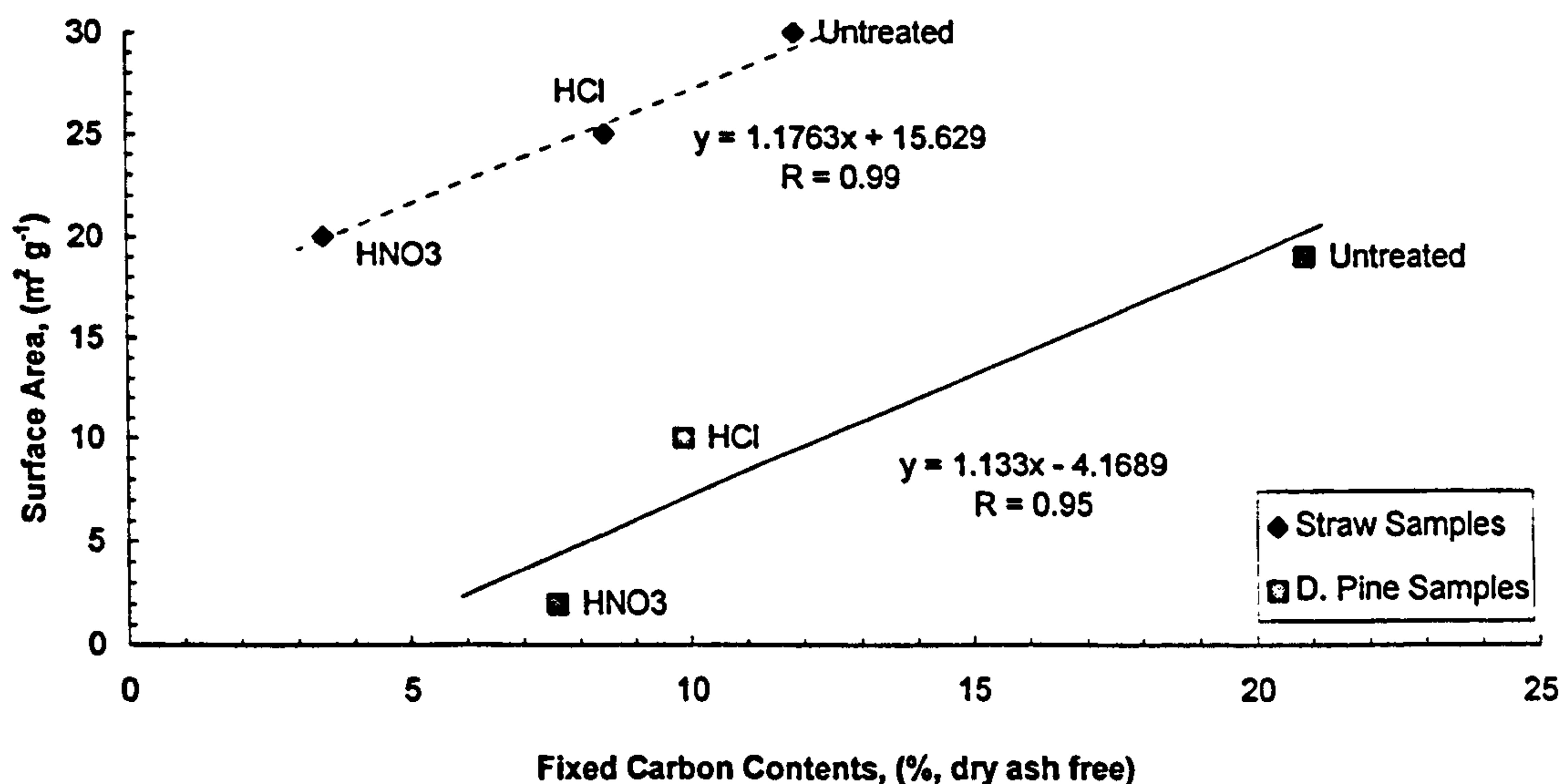


Figure 5.30 The Surface Areas of the Chars Prepared from the Untreated and Acid-Washed Biomass Samples Plotted Against Fixed Carbon Content

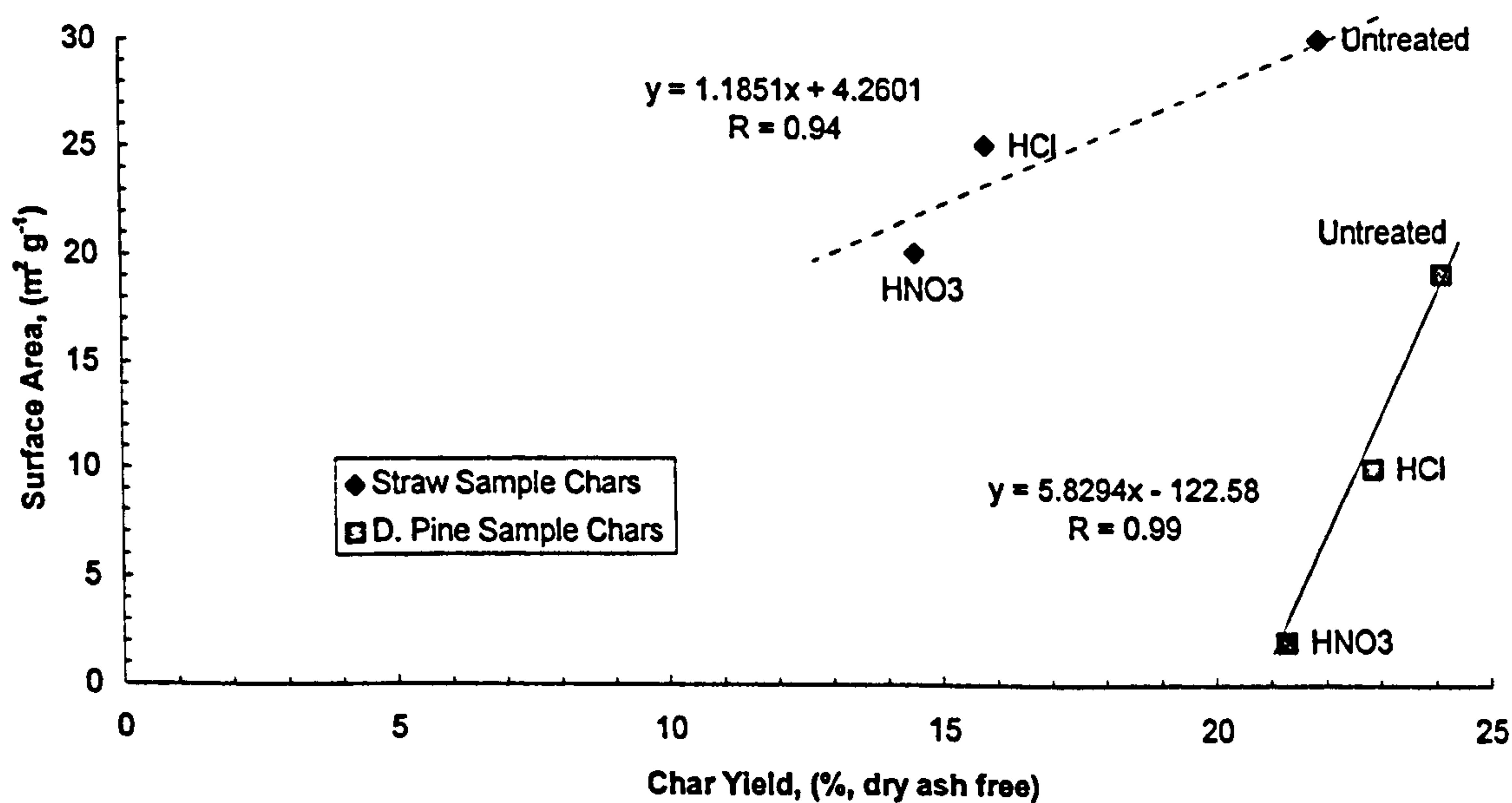


Figure 5.31 The Surface Areas of the Chars Prepared from the Untreated and Acid-Washed Biomass Samples Plotted Against Char Yield

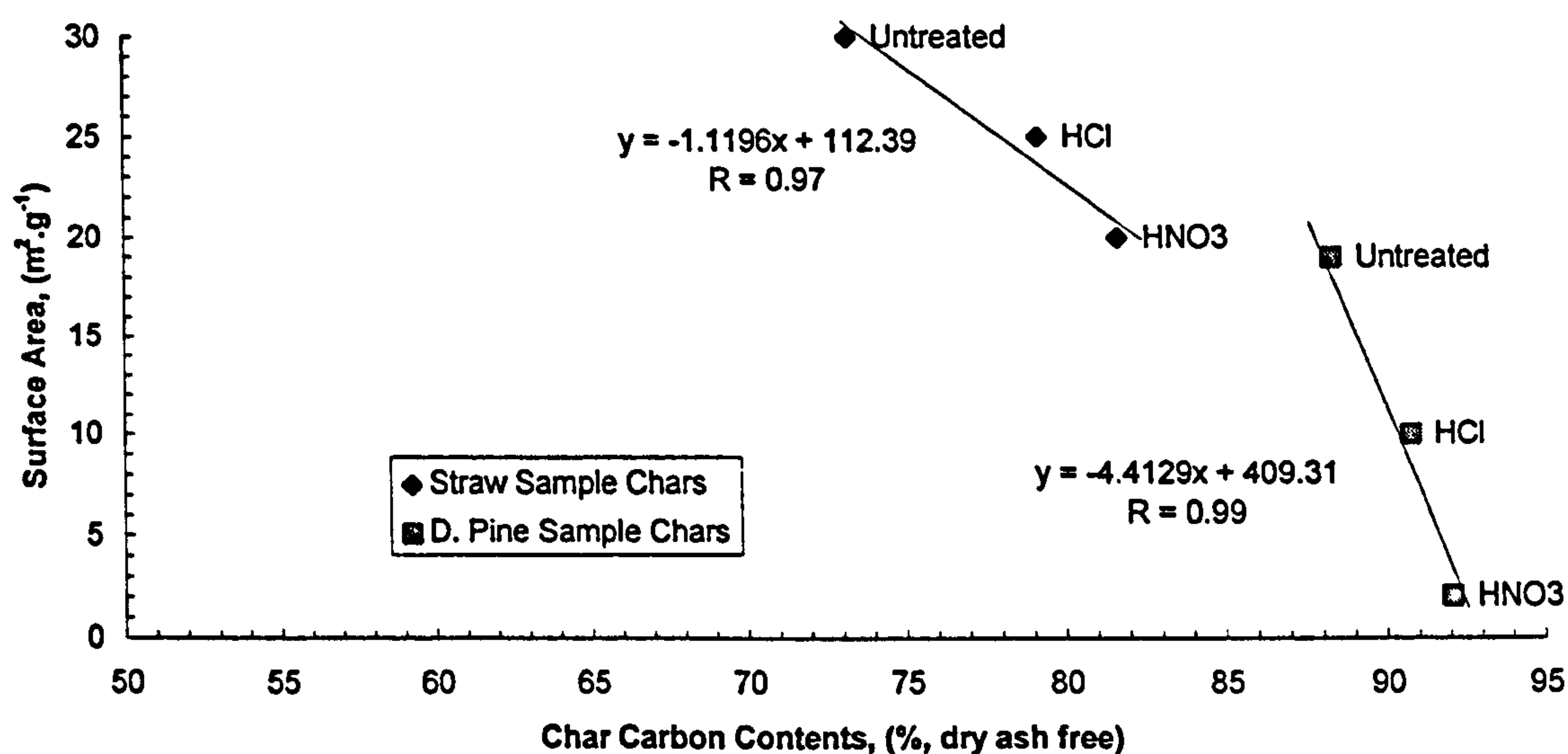


Figure 5.32 The Surface Areas of the Chars Prepared from the Untreated and Acid-Washed Biomass Samples Plotted Against Char Carbon Content

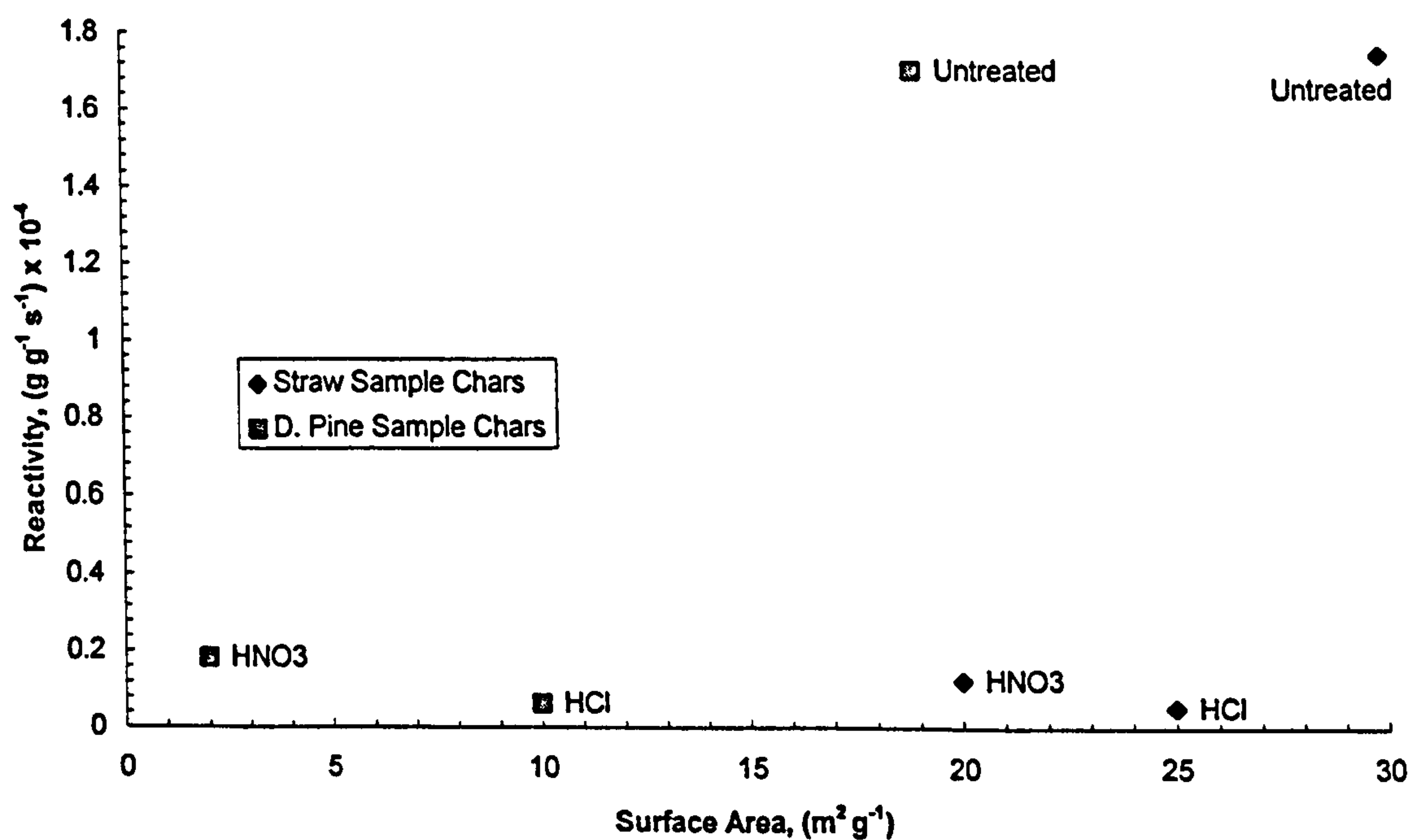


Figure 5.33 The Isothermal Reactivities in O₂ (3 l h⁻¹) at 633 K, of the Chars Prepared from the Untreated and Acid-Washed Biomass Samples Plotted Against Char Surface Area

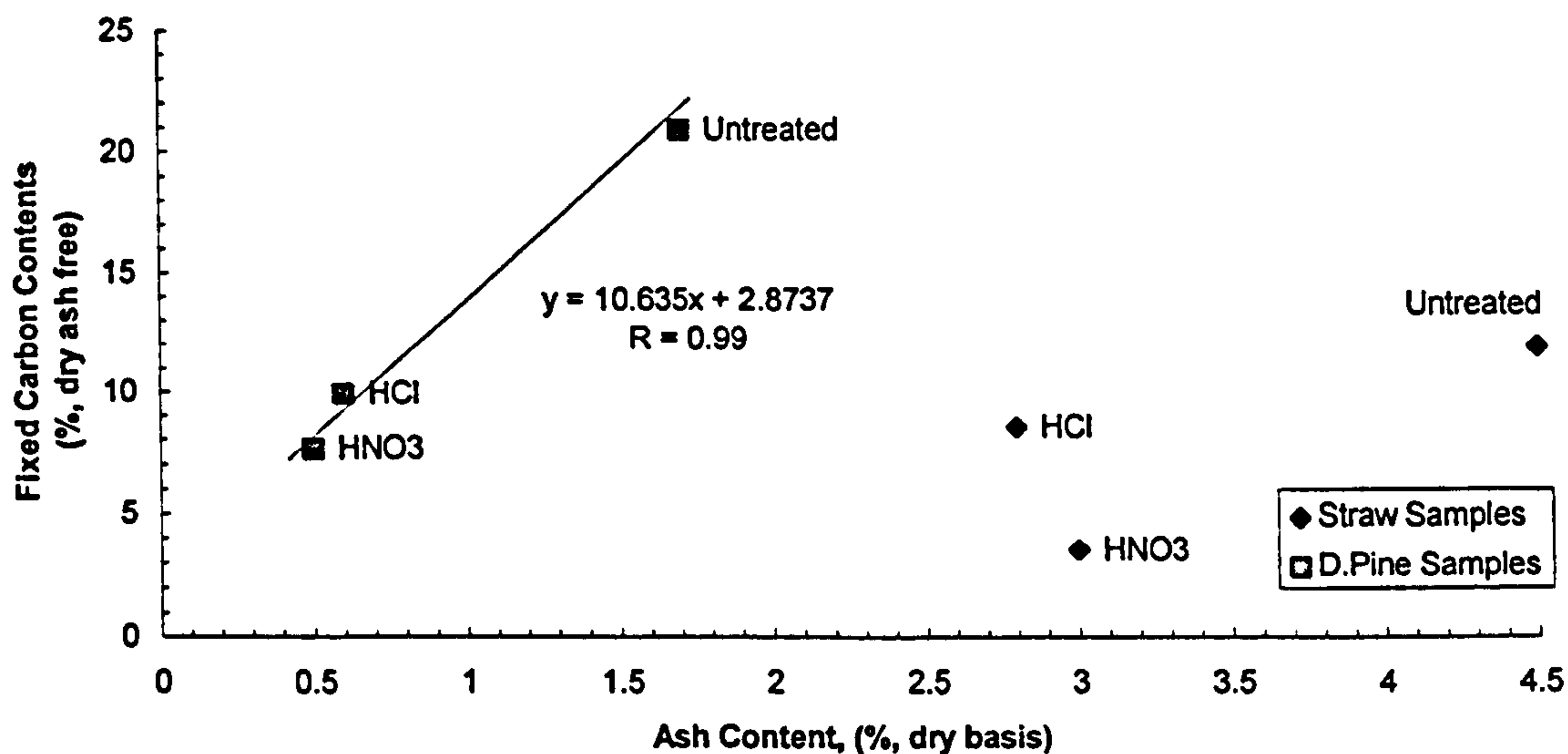


Figure 5.34 The Fixed Carbon Contents of the Untreated and Acid-Washed Biomass Samples Plotted Against Ash Content

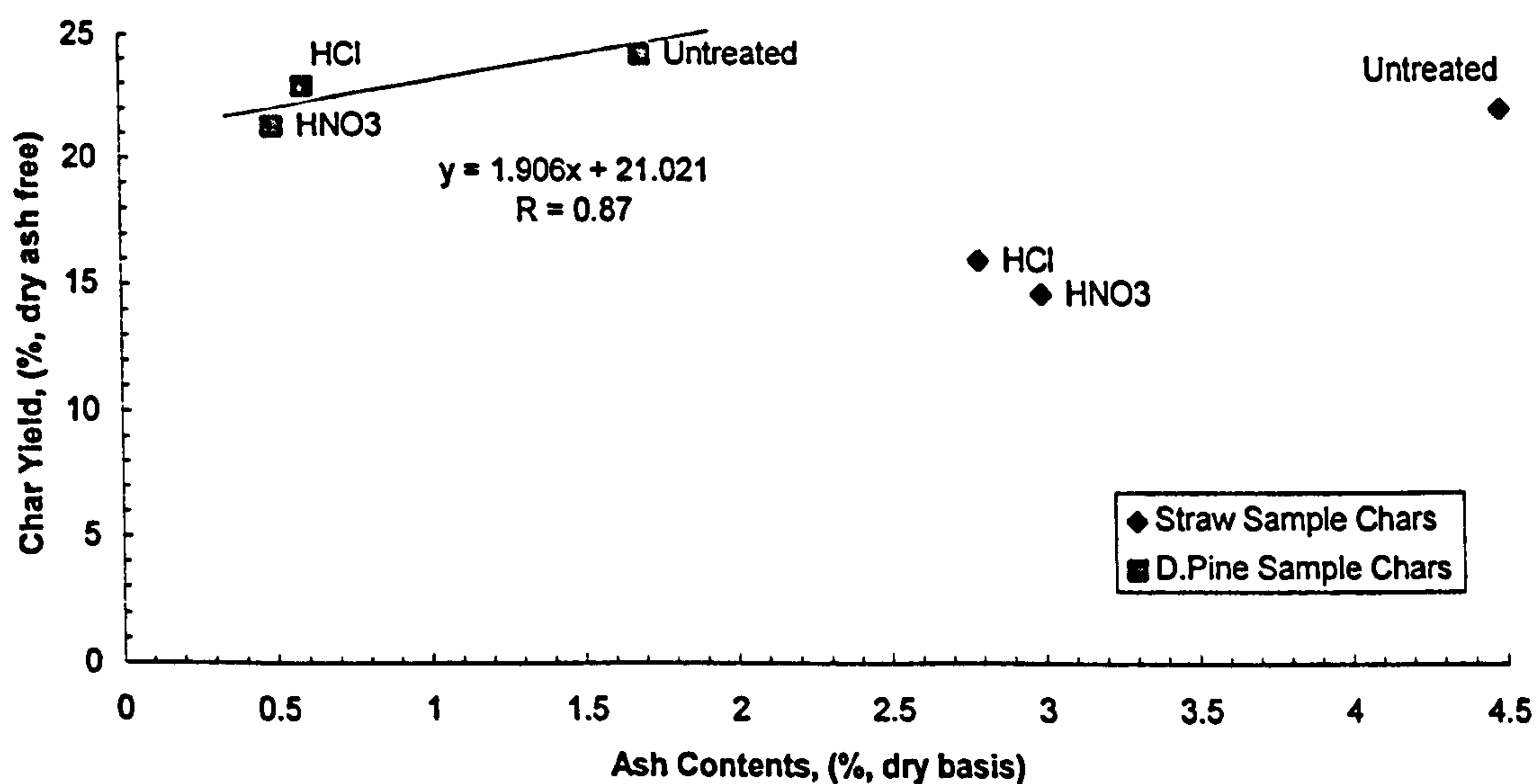


Figure 5.35 The Yields of Char Prepared from the Untreated and Acid-Washed Biomass Samples Plotted Against Ash Content

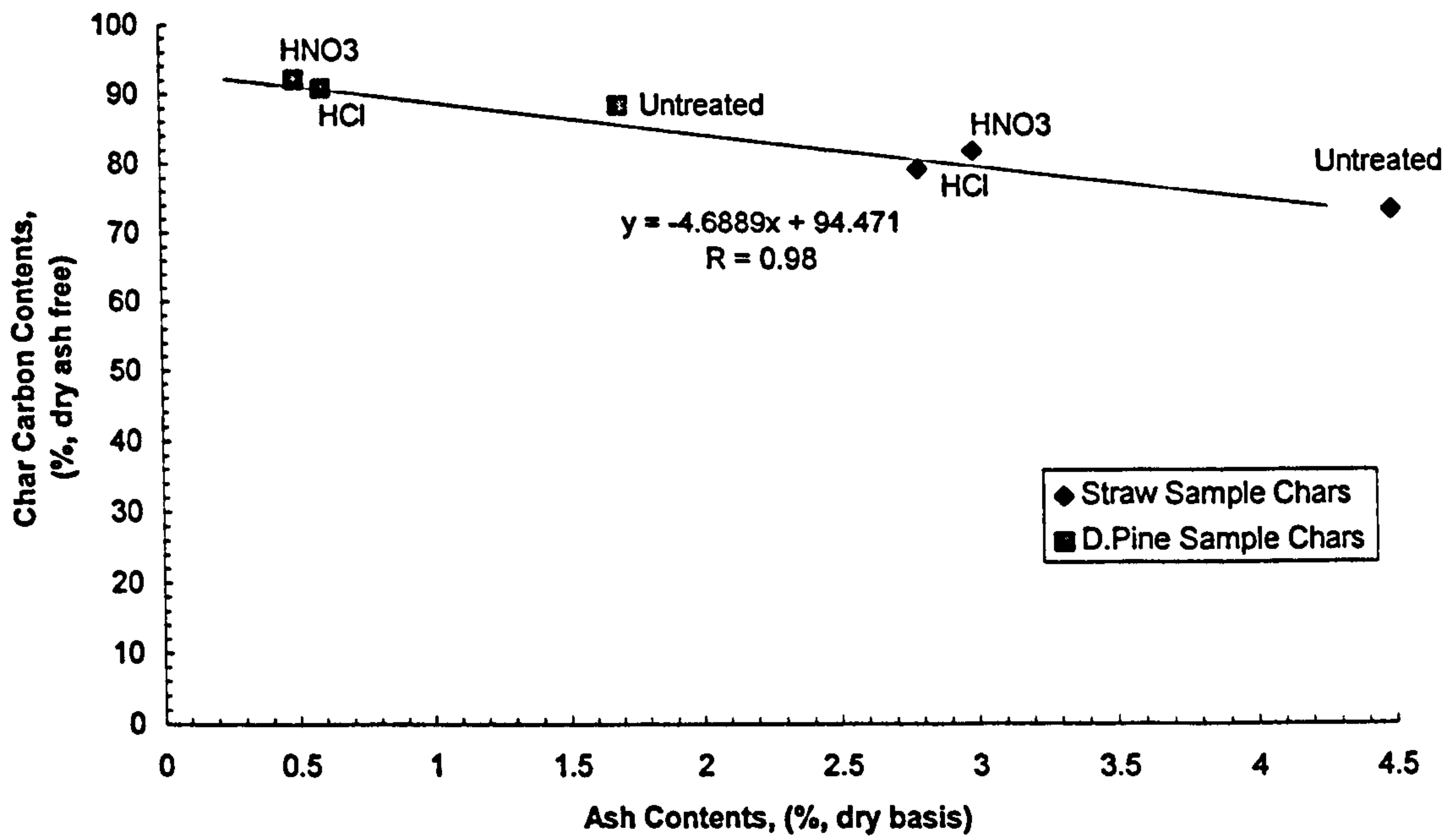


Figure 5.36 The the Untreated and Acid Washed Biomass Sample Char Carbon Contents Plotted Against Ash-Content

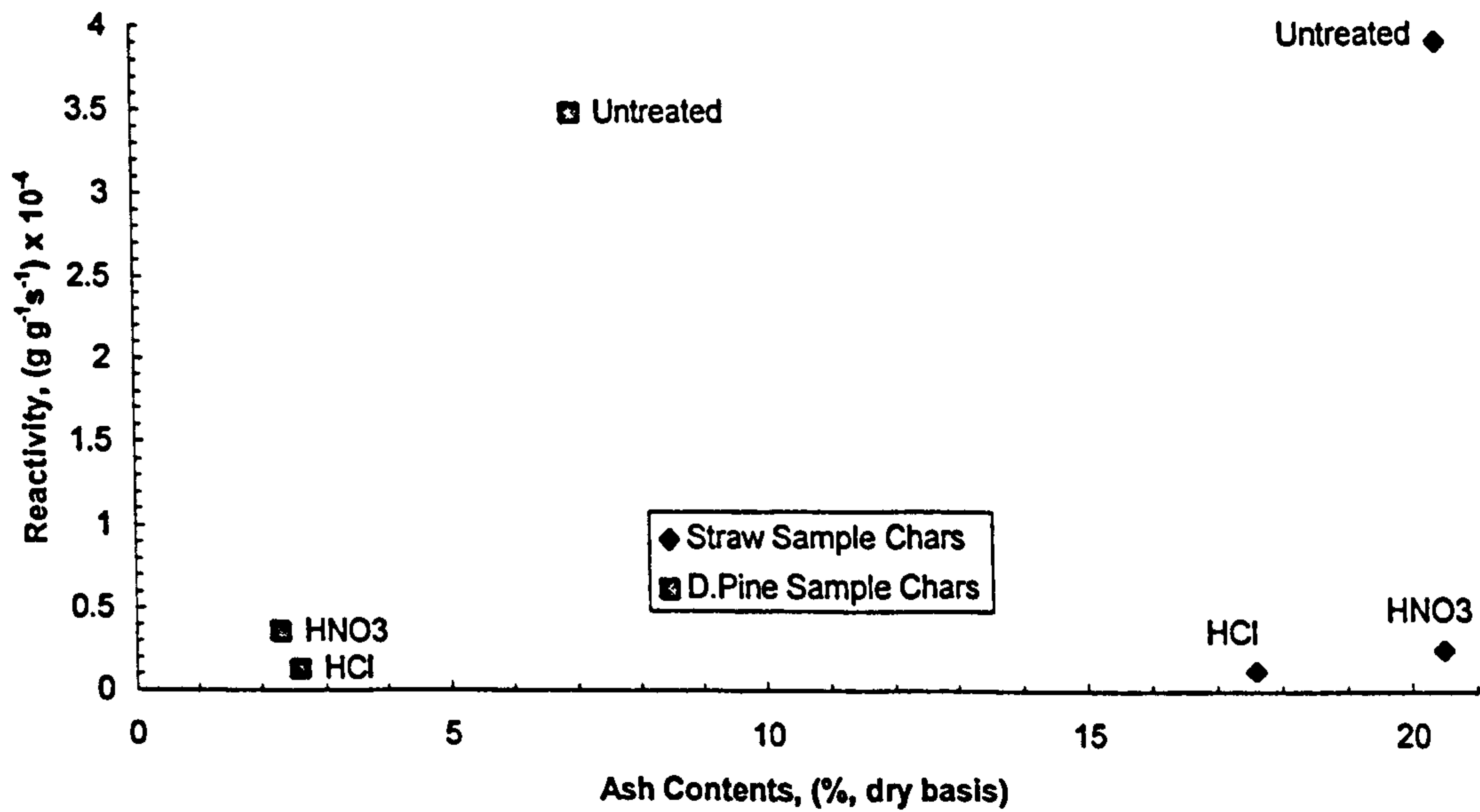


Figure 5.37 The Isothermal Reactivity in O_2 (3 l h^{-1}) at 633 K, of the Chars Prepared from the Untreated and Acid Washed Biomass Samples Plotted Against Ash Content

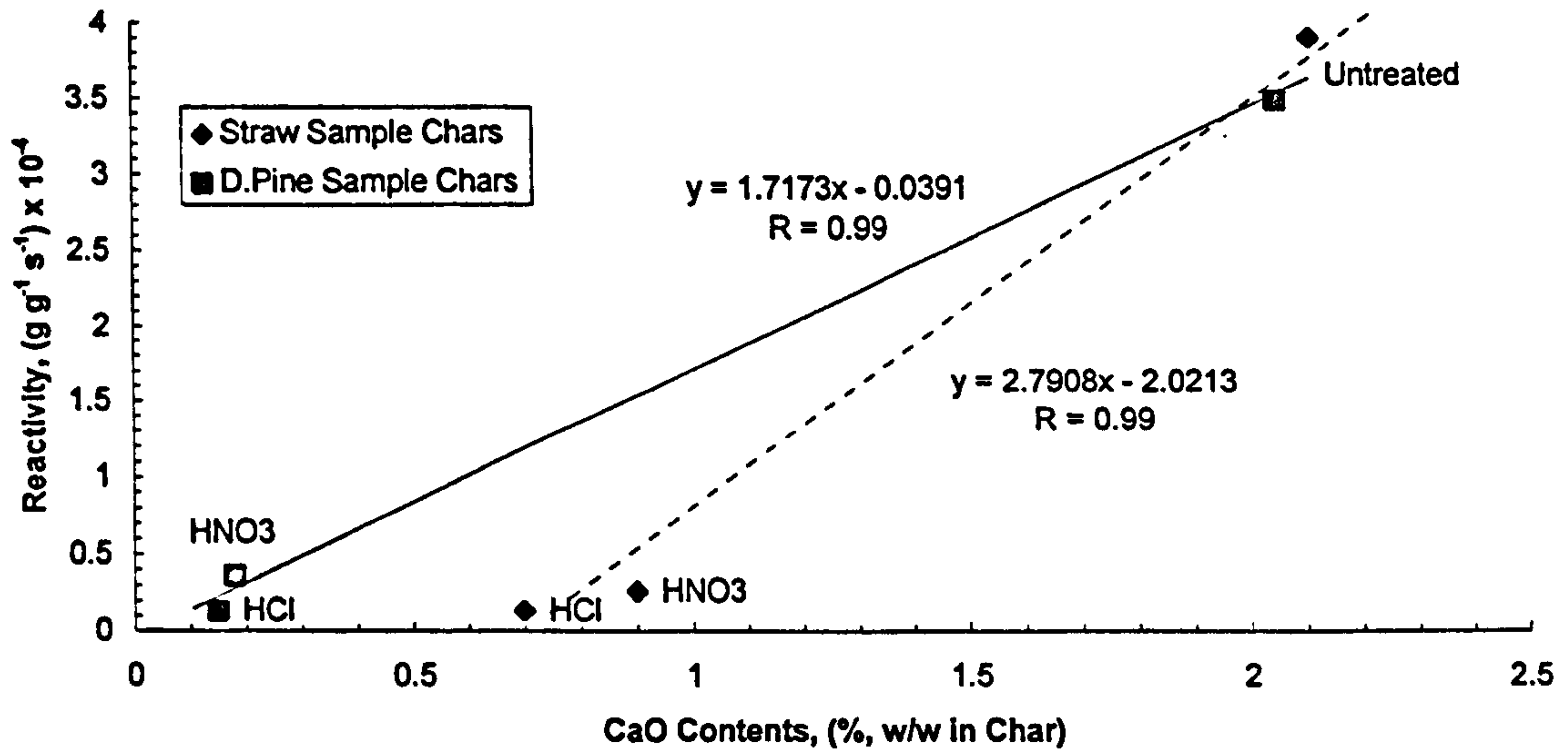


Figure 5.38 The Isothermal Reactivity, in O₂ (3 l h⁻¹) at 633 K, of the Chars Prepared from the Untreated and Acid-Washed Biomass Samples Plotted Against Char CaO Content

Chapter Six

Experimental Results

Refuse Derived Fuel Materials

6.1 Analytical Data for the Raw, HNO₃ and HCl Acid-Washed RDF Samples

A similar approach to that applied to the biomass materials has been adopted in the study of pelletised refuse-derived fuels. These are produced commercially in a number of plants in Britain by the processing of municipal solid wastes and are marketed as industrial fuels. Samples of products from two such plants at Byker in Newcastle upon Tyne and on the Isle of Wight have been studied.

6.1.1 Proximate and Ultimate Analyses of RDF Samples

The basic analysis data for the two RDF samples are presented in Table 6.1. The major constituents of the RDF are paper/board and sheet plastics and this is reflected in the analysis data. Both samples have high volatile matter content (73-76 %, dry basis) and low fixed carbon contents (10-14 %, dry basis). The Byker material has the higher ash content, 15.6 % as compared to 10.8% for the Isle of Wight sample. An ash content of around 15 % is fairly typical of the earlier RDF

plants such as Byker. The Isle of Wight plant is relatively new and lower ash contents can be achieved in the more modern plants.

The ultimate analysis data for the two RDF samples are fairly similar, 49-51 % carbon, ~ 8% Hydrogen and 40-42 % oxygen, on a dry basis, and these values are consistent with the composition of the major constituents. The nitrogen contents are 1.11 and 0.59 % (dry basis) for the Byker and Isle of Wight samples respectively, and the chlorine contents are ~ 0.3-0.35 %. These values are fairly typical of those for the RDF materials produced by the British plants, although, in some cases chlorine contents up to 1 % or so have been reported.

6.1.2 Proximate and Ultimate Analyses of HNO₃ and HCl Acid-Washed RDF Samples

The RDF samples were acid treated in the same fashion as the biomass materials described in Chapter 5, and the basic analysis data are also presented in Table 6.1. In both cases the acid treatment resulted in a reduction in the ash content and an increase in the volatile matter content. This is reflected in the ultimate analysis data which shows significant increases in the oxygen contents of the acid treated materials. The HNO₃ treatment was found to be particularly effective in extracting the chlorine from both RDF samples and both acid treatments also resulted in a reduction in the nitrogen contents of both RDF materials.

6.1.3 Ash Analyses of Raw, HNO₃ and HCl Acid-Washed RDF Samples

The ash compositions of the RDF and acid treated RDF were determined, and this is presented in Table 6.2. Typically the major ash constituents of RDF are inorganic fillers used in the manufacture of paper and board, i.e. kaolinite (Al₂O₃.2SiO₂.2H₂O) and calcium carbonate (CaCO₃), while the minor constituents are tinfoil, titania, and the salts of the alkali metals. This was found to be the case for the ash of the Byker and Isle of Wight samples.

The major effect of the acid treatments was to produce a significant reduction of the CaO contents of the ashes in both cases.

6.2 Analytical Data for Chars Prepared from Raw, HNO₃ and HCl Acid-Washed RDF Samples

6.2.1 Char Yields and Ultimate Analyses of Raw, HNO₃ and HCl Acid-Washed RDF Sample Chars

Chars were prepared from the RDF and acid-treated RDF samples by heating in a fixed bed reactor at 10 K min⁻¹ in a nitrogen atmosphere to 1173 K and holding at that temperature for a period of 1 hour. The char yields, ash contents and ultimate analyses of the prepared chars are presented in Table 6.3. It should be noted that the char yields for the two raw RDF materials are very similar at around 20.5 % (dry, ash free), and that the char yields for the acid-washed materials were lower than those for the raw RDF samples.

6.2.2 Relationships Between the Char Yields with the Raw Sample and Char Characteristics for the Untreated and Acid-Washed RDF Materials

A plot of the char yield against the fixed carbon contents of the untreated and acid-washed RDF materials is presented in Figure 6.1. A reasonably good positive, linear correlation was obtained, which suggests that the char yield increased linearly with increasing fixed carbon content of the parent RDF materials.

The char yield data were also plotted against the carbon contents (dry, ash free) of the parent RDF materials. It is evident from the graph, which is presented in Figure 6.2, that there was a reasonably good positive correlation. This trend suggests that the char yield increases linearly with increasing carbon content of the parent materials.

It is also instructive to investigate the relationships between the char yield and chemical composition of the resultant char. A plot of the char carbon concentrations against the char yields for the untreated and acid-washed RDF materials is presented in Figure 6.3. A good correlation obtained which indicates that the char carbon contents decreased linearly with increasing char yield.

6.3 Reactivity Measurements of Raw, HNO₃ and HCl Acid-Washed RDF

Sample Chars in Oxygen

The reactivities of the chars were measured using the technique described in Chapter 4, Section 4.5, and the reactivity-temperature curves are reproduced in Figure 6.4. The reactivity values for the RDF and acid treated RDF chars, at 683 K, are listed in Table 6.4. It is clear from these data that the reactivities of the chars prepared from the original RDF materials were significantly higher than those for the acid treated materials, and in both cases, the chars prepared from the HCl treated materials, had significantly lower reactivities than those chars which had been prepared from the HNO₃ treated material.

6.4 BET Surface Area Determination of Raw, HNO₃ and HCl Acid-Washed RDF Sample Chars

The surface areas of the char materials were measured, using the method described in Chapter 4, Section 4.6, and the results are presented in Table 6.5. It is evident from these data that the surface areas of the chars prepared from the original RDF materials were similar (25-30 m² g⁻¹), and were higher than those for the chars prepared from the acid washed samples. For both groups of samples, the chars prepared from the HNO₃ washed RDF materials had slightly lower surface area than those of the HCl washed samples.

6.4.1 Relationships Between Char Surface Area with Precursor Characteristics and Char Reactivities for the Raw, HNO₃ and HCl Acid-Washed RDF Samples

The char surface area values have been plotted against the fixed carbon contents of the parent materials and the char yields, and these are presented in Figure 6.5 and Figure 6.6. It is clear that the surface area increased linearly with increasing fixed carbon content and char yield. The reactivity data for the chars at 683K were also plotted against the measured char surface areas, and as illustrated in Figure 6.7, there is no apparent overall relationship between these parameters.

6.5 Relationships Between the Ash Compositions of Raw, HNO₃ and HCl Acid-Washed RDF Sample Chars and their Reactivity in Oxygen

One of the major effects of acid treatment was to decrease the ash contents and, in particular, the lime contents of the RDF's. It is interesting to examine the relationship of these parameters to the char reactivities, in a manner analogous to that employed with the biomass materials. The char reactivities have been plotted against the char ash content in Figure 6.8. It should be noted that the ash content of the Byker RDF is significantly higher than that of the Isle of Wight RDF and so in this respect the materials are not directly comparable. For each material there is a reasonable positive linear relationship between the char reactivity and the char ash content, although these are only based on three data points. Similar correlations were found between the char reactivities and the CaO content of the chars for both groups of samples and these are illustrated in Figure 6.9.

6.6 Summary of the Effects of HNO₃ and HCl Acid-Washing on the RDF

Samples

The results of the RDF and acid washed RDF can therefore be summarised as follows;

1. The proximate and ultimate analyses of the Byker and Isle of Wight samples were generally similar, the only difference being that the Byker sample had a higher ash content.
2. Acid washing effectively increased the volatile matter content of the RDF samples and reduced the amounts of ash, mainly the CaO components. Both acids were effective at reducing the nitrogen contents and the HNO₃ washing was particularly effective in extracting Cl.
3. The untreated RDF samples produced similar char yields of ~ 20% (daf) during pyrolysis at 10 K min⁻¹ to 1173 K in N₂. The char yields produced from the acid washed samples under identical conditions were lower, the lowest yields being obtained for the HNO₃ washed samples.
4. The isothermal reactivities of the chars measured in oxygen were greater for those prepared from the untreated samples. For both sample types, the chars prepared from the HCl washed materials were the least reactive over the temperature range studied.
5. The 77 K N₂ BET surface area measurements of the chars produced from the untreated RDF samples were similar at ~ 25 m² g⁻¹. These were significantly higher values than those of the chars prepared from the acid washed RDF materials. The chars prepared from the HNO₃ washed samples had the lowest surface area values for both types of RDF.
6. The char surface area values for the untreated and acid washed samples were found to increase linearly with both fixed carbon content and char yield.

6.7 Analytical Data of the RDF Model Composites

In order to study further the carbonisation behaviour of mixed materials such as municipal solid waste and RDF, a number of artificial mixtures containing cellulosic materials and synthetic polymers were prepared. The basic components of these mixtures are as follows:

- (a) laboratory-grade cellulose powder,
- (b) finely chopped straw,
- (c) laboratory-grade poly (ethene),
- (d) laboratory-grade, high molecular weight poly(vinyl chloride), (PVC) powder, and
- (e) laboratory-grade Saran powder. Saran is a poly(vinylchloride)-poly (vinylidenechloride) copolymer.

The pure compounds and mixtures were analysed using the approach adopted from the biomass and RDF materials.

6.7.1 Proximate and Ultimate Analyses of RDF Model Composites

The proximate analysis data for the pure compounds and the mixtures are presented in Table 6.6. Only the straw sample had a significant ash content, and both the cellulose and straw samples had small but significant moisture contents. The pure materials had fixed carbon contents which vary between 0% for the poly(ethene) and nearly 30 % for the Saran. The fixed carbon contents of the PVC and Saran were significantly different, at around 5 % and 30 % respectively. These materials are similar chemically, however their decomposition pathways are significantly different. The thermal decomposition of PVC involves the elimination of HCl, considered to occur by a free radical chain mechanism, and the formation of linear sequences conjugated double bonds. At higher temperatures,

gaseous products, principally alkenes, are evolved. Saran has a greater tendency to cross-linking during the dehydrochlorination process, providing a more thermally stable product.

The measured fixed carbon contents of the mixtures showed some interesting behaviour. For the poly(ethene)/cellulose mixtures, the values were approximately additive, whereas for the PVC/cellulose, Saran/cellulose and PVC/straw mixtures, the measured fixed carbon contents were significantly higher than would be predicted by calculation based on simple proportion, i.e. assuming additive behaviour. There was clearly some interaction between the components of these mixtures which acted to inhibit the release of volatile material. The nature of these interactions will be discussed in more detail in Chapter 7.

The ultimate analysis data for the pure materials and the mixtures are presented in Table 6.7. The compositions of the pure materials are very similar to the theoretical compositions, and the data for the mixtures indicate simple additive behaviour. These data also confirm that the mixtures were prepared in the correct proportions.

It is interesting to note that Saran has a significant nitrogen content, which originates from an additive used in manufacturing to initiate polymerisation.

6.8 Analytical Data of the Chars Prepared from RDF Model Composites

Chars were prepared from the pure materials and mixtures in a fixed bed reactor at 10 K min^{-1} in a nitrogen atmosphere to 1173 K, and holding at that temperature for a period of 1 hour. The yields and ultimate analysis data of these prepared chars are presented in Table 6.8.

6.8.1 RDF Model Composites Char Yields and Char Proximate and Ultimate Analyses

The char yields for the pure materials were found to vary from zero for the poly(ethene) to around 32 % for the Saran and these are roughly in the same order as the measured fixed carbon contents. There was again a notable difference in the PVC and Saran values, the char yield of PVC, at 10 %, was found to be much less than that for Saran despite their relatively similar compositions. The char yields for the poly(ethene)-cellulose mixtures were simply additive, but for the mixtures containing chlorinated polymers the char yields were higher than those calculated from the mixture compositions.

The relationship between the char yields and the measured fixed carbon contents for the pure materials and mixtures is illustrated in Figure 6.10. These data indicate that there was a reasonably good linear correlation between the char yields and fixed carbon contents for all of the samples. The only data point which is significantly different is that for pure poly(ethene) which gave zero values for both fixed carbon and char yield.

The ultimate analysis data for the chars are also presented in Table 6.8. Under the experimental conditions described above, carbonisation of the materials had not gone to completion, and the chars contained significant hydrogen and oxygen contents, in most cases. The chars prepared from the pure cellulose, PVC and Saran materials had carbon contents around 95 % or higher, and low hydrogen and oxygen contents. The char yields for the cellulose-poly(ethene) mixtures were found to be additive and the char hydrogen and oxygen contents were similar, both close to that of the pure cellulose char. The mixtures of cellulose with chlorine-containing polymers showed very different behaviour. The char yields were higher than expected and the hydrogen and oxygen contents of the chars were also much higher than expected. This suggests that the presence of chlorine had a significant impact on the carbonisation behaviour of the cellulose-polymer mixtures.

The influence of chlorine on the pyrolysis behaviour of cellulosic materials has previously been reported by Essig et al (1988) and Oren (1990). In these cases increases in the char yields were also observed in the presence of chlorine.

The char yields obtained from the PVC-straw mixtures were also higher than expected and these chars had higher hydrogen and oxygen contents. The data indicate that significant levels of nitrogen were retained within the chars but that the chlorine had largely been released during the carbonisation process.

6.9 Thermal Decomposition Analyses of RDF Model Composites

The results of the Thermogravimetric Analysis of the pure materials and mixtures are presented in Table 6.9. The experimental procedure is described in Section 4.3 above. In most cases, three peaks on the Differential Thermogravimetric Analysis curves were apparent, viz;

- (a) a moisture loss peak at around 300 K for those samples containing significant moisture,
- (b) a volatile peak at temperatures in the range 470-650 K, and
- (c) a char burnout peak at temperatures in the range 740-860 K.

Looking in the first instance at the data for the decomposition of the poly(ethene), it can be seen that the devolatilisation peak was at temperatures around 650 K, and that there was no char burnout peak. The decomposition of poly (ethene) requires the breaking down of aliphatic C-C bonds to allow the formation of volatile species of low molecular weight, hence the relatively high peak temperature. With increasing temperature, all of the poly(ethene) was released in volatile form and no char residue was formed. There was, therefore, no char burnout peak for poly(ethene).

The devolatilisation peaks for the cellulose and straw samples were at 540 and 590 K respectively. The value for straw was a little higher than that for cellulose because of the significant level of lignin in straw. In both cases, a char residue was produced which oxidised at similar temperatures, around 740-780 K.

The decomposition of PVC and Saran involves the elimination of HCl. In the case of Saran, which has two Cl atoms bonded to single bonded to the single C atoms, devolatilisation occurred at lower temperatures than for PVC, which has only one. In both cases, the residue of devolatilisation is a carbon skeleton, which oxidised at relatively high temperatures, around 860 K.

The data for the cellulose-poly(ethene) mixtures are also presented in Table 6.9, and it can be seen that the devolatilisation of the mixtures was dominated by the behaviour of the cellulose component, with the major devolatilisation peak at around 540 K and the char burnout peak at around 750-780 K.

The devolatilisation peaks for the PVC-cellulose mixtures were at temperatures in the region 470-530 K, and this is significantly lower than those of the constituents i.e. PVC at 600 K and cellulose at 550 K. The char burnout peaks for the mixtures were broad and at temperatures around 780 K, which is intermediate between those of the constituent materials.

Reduced devolatilisation temperatures were also observed for the PVC-straw mixtures, i.e. 540-580 K compared to around 590-600 K for the constituent materials. The char burnout peaks were broad at temperatures around 840 K, i.e. between those of the straw and PVC.

The Saran-cellulose mixtures exhibited two peaks at around 470-480 K and 530-540 K, i.e. at temperatures close to those of the constituents. The char burnout peaks were broad and at temperatures around 750-800 K, i.e. intermediate between those of the constituents.

It is clear from the discussion presented above that the DTG data for the pure materials and the mixtures can be understood in terms of the materials involved. There was some evidence, however, of reduced devolatilisation temperatures for the PVC-cellulose and PVC-straw mixtures, which may be a result of the presence chlorinated species reducing the devolatilisation temperatures of cellulose. This was not observed for the Saran-cellulose mixtures, however, in this case Saran had the lower devolatilisation temperature of the two-component mixture.

6.10 Reactivity Measurements of RDF Model Composite Chars in Oxygen

The char reactivity data, measured using the technique described in Chapter 4, Section 4.5, are presented in Table 6.10 and are plotted in Figure 6.11. Looking first at the reactivity data for the chars produced from the pure materials, these are best compared using the data collected at 653 K. The straw char was by far the most reactive material. The least reactive was the PVC, with the cellulose and Saran chars having intermediate reactivity values. The poly(ethene) produced no char.

The reactivity values for the chars produced from the poly(ethene)-cellulose mixtures were very similar to those of the cellulose char. This indicates that when the mixtures were heated the poly(ethene) was released as a volatile material leaving a char comprising only of residue from the cellulose. This agrees with the observation, that the char yields for these mixtures were additive.

The char reactivity data for the PVC-cellulose and the PVC-straw mixtures have been plotted in Figures 6.12 and 6.13. The data are compared to the additive line and in both cases it is clear that the measured reactivities were significantly less than additive. In both cases, the addition of only 10 % by weight of PVC resulted in sharp decreases in the reactivities of the resultant chars.

Similar data for the Saran-cellulose mixtures are presented in Figure [6.14](#), and these data show very different behaviour. In this case, the char reactivities were significantly higher than additive. The addition of only 10% by weight of Saran produces a significant increase in the char reactivity than would be expected if the reactivities were additive.

6.11 BET Surface Area Determination of RDF Model Composites Sample

Chars

The surface areas of the char materials were measured using a BET N₂ method as described in Chapter 4, Section 4.6. The experimental data are listed in Table [6.11](#) and the calculated values for the composite blend chars are also listed. The cellulose char had the highest surface area at around 300 m² g⁻¹. The Saran and straw chars had similar surface area values. The PVC char had a very low value, indicating that the material had melted during the pyrolysis process.

The surface areas of the chars prepared from the poly(ethene)-cellulose mixtures were found to be very similar to that of the cellulose char. These data further suggested that the poly(ethene) component of the blends completely devolatilise during pyrolysis leaving the cellulose char residue.

The data for the PVC-cellulose and PVC-straw mixture chars showed reduced surface areas. These data are illustrated in Figures [6.15](#) and [6.16](#) respectively. The measured values are presented in comparison to the additive line, and it is evident that the addition of only 10 % by weight of PVC produced significant reductions in the surface areas of the prepared chars.

The surface area data for the Saran-cellulose chars in comparison to the additive line is presented in Figure [6.17](#). In this case, the char surface area values were a little higher than expected.

6.12 Summary of RDF Model Composites Experimental Results

The results experimental data for the RDF model composites can therefore be summarised as follows;

1. The proximate analysis results data for the PVC and saran samples were notably different despite both having similar chemical composition. The fixed carbon content of PVC was $\sim 5\%$ while the value was 30% for saran.
2. The ultimate analysis data for the pure compounds were very close to the theoretical values and the data for the mixtures were additive, which confirmed that they were prepared in the correct proportions.
3. The yields of char produced from PVC and saran when heated at 10 K min^{-1} to 1173 K in N_2 were similar to their fixed carbon values. PVC produced a char yield of 10% while that for saran was $\sim 32\%$.
4. The char yields produced from the mixtures containing chlorinated polymers were greater than expected and these chars also contained more hydrogen and oxygen contents than expected.
5. The char yields of all the polymers and composite mixtures were found to increase linearly with increasing carbon content.
6. The straw char had the highest reactivity to O_2 over the measured temperature range. The PVC char was the least reactive.
7. The measured reactivity of the poly(ethene)/cellulose mixture chars were very similar to that of the pure cellulose char.
8. The measured reactivities of the PVC/straw and PVC/cellulose mixtures were lower than expected, while the reactivity of the saran/cellulose chars were higher than expected.

9. The char prepared from cellulose was determined had the highest surface area and the char prepared from PVC had the lowest.

10. The surface area values for the poly(ethene)/cellulose mixture chars were very similar to the value for the pure cellulose char.

11. The measured surface areas of the PVC/cellulose and PVC/straw chars were lower than expected while those for the saran/cellulose mixture chars were higher than expected.

Proximate Analysis (%, dry basis)	Byker RDF			Isle of Wight RDF		
	Raw	HNO ₃ Washed	HCl Washed	Raw	HNO ₃ Washed	HCl Washed
Volatile Matter	73.8	80.9	79.2	75.8	84.5	83.3
Fixed Carbon	10.5	7.0	9.1	13.4	7.8	9.6
Ash	15.6	12.1	11.7	10.8	7.6	7.1
Ultimate Analysis (%, dry, ash free)						
C	49.5	46.5	49.0	49.6	47.6	48.0
H	8.5	6.6	6.7	7.9	6.3	7.4
N	1.1	0.8	0.4	0.6	0.4	0.5
Cl	0.3	< 0.1	0.3	0.4	< 0.1	0.3
O (by difference)	40.6	46.0	43.7	41.6	45.6	44.8

Table 6.1 Analytical Data for the Raw and Acid-Washed Byker and Isle of Wight RDF Samples

Ash Analysis (%)	Byker RDF			Isle of Wight RDF		
	Raw	HNO ₃ Washed	HCl Washed	Raw	HNO ₃ Washed	HCl Washed
SiO ₂	43.2	60.9	-	39.7	60.0	-
Al ₂ O ₃	31.1	25.6	-	32.6	26.5	-
Fe ₂ O ₃	2.4	3.4	2.1	1.9	3.2	2.0
CaO	15.4	3.6	1.0	15.8	3.7	1.7
MgO	2.5	2.1	2.1	2.1	1.8	1.9
TiO ₂	2.8	1.5	-	2.9	1.7	-
K ₂ O	1.6	0.6	0.9	0.4	0.4	0.3
Na ₂ O	2.6	1.9	1.9	3.4	2.3	1.3
P ₂ O ₅	1.0	0.4	-	1.0	0.4	-
SO ₃	< 0.1	< 0.1	-	0.2	0.1	-

Table 6.2 Ash Analyses Data for the Raw and Acid-Washed Byker and Isle of Wight RDF Samples

	Byker RDF			Isle of Wight RDF		
	Raw	HNO ₃ Washed	HCl Washed	Raw	HNO ₃ Washed	HCl Washed
Char Yield (%, dry, ash free)	20.7	18.1	19.3	20.3	17.7	19.2
Char Ash Content (%, dry)	75.4	66.9	60.6	53.2	42.9	37.0
Ultimate Analysis (%, dry, ash free)						
C	84.2	89.7	87.7	82.2	90.7	88.5
H	0.7	0.5	0.5	1.0	0.5	0.7
N	1.4	1.9	1.8	1.0	1.7	1.4
Cl	0.9	< 0.1	< 0.1	0.5	< 0.1	< 0.1
O (by difference)	13.0	7.9	9.9	15.3	7.0	9.3

Table 6.3 The Char Yields, Char Ash Contents and Ultimate Analysis of Chars Prepared from the Raw and Acid Washed Byker and Isle of Wight RDF Samples at 10 K min⁻¹ to 1173 K in a Nitrogen Atmosphere

	Byker RDF			Isle of Wight RDF		
	Raw	HNO ₃ Washed	HCl Washed	Raw	HNO ₃ Washed	HCl Washed
Char Reactivity (g g ⁻¹ s ⁻¹ x 10 ⁻⁴)						
at 683 K	3.51	1.01	0.48	9.49	0.81	0.10

Table 6.4 The Reactivity Data of Chars Prepared of Chars Prepared from the Raw and Acid Washed Byker and Isle of Wight RDF Samples at 10 K min⁻¹ to 1173 K in a Nitrogen Atmosphere

	Byker RDF			Isle of Wight RDF		
	Raw	HNO ₃ Washed	HCl Washed	Raw	HNO ₃ Washed	HCl Washed
Char 77 K N ₂ BET Surface Area (m ² g ⁻¹)	30	9	14	25	8	11

Table 6.5 BET Surface Area Data of Chars of Chars Prepared from the Raw and Acid Washed Byker and Isle of Wight RDF Samples at 10 K min⁻¹ to 1173 K in a Nitrogen Atmosphere

Proximate Analysis (%, as analysed)	Moisture	Volatile Matter	Fixed Carbon	Expected Fixed Carbon	Ash
Cellulose	3.9	94.8	1.3	-	-
Ploy(ethene)	0.0	100	0.0	-	-
1/9 Poly(ethene)/Cellulose	0.0	95.2	1.2	1.2	-
1/1 Poly(ethene)/Cellulose	1.9	97.4	0.7	0.7	-
PVC	0.0	95.2	4.8	-	-
1/9 PVC/Cellulose	3.3	88.5	8.2	1.7	-
1/1 PVC/Cellulose	2.1	88.3	9.6	3.1	-
Saran	0.0	70.4	29.6	-	-
1/9 Saran/Cellulose	3.8	83.0	13.2	4.1	-
1/1 Saran/Cellulose	1.9	74.1	24.0	15.5	-
Straw	6.1	78.9	10.7	-	4.2
1/9 PVC/Straw	7.6	68.8	19.9	10.1	3.7
1/1 PVC/Straw	3.6	78.2	16.0	7.8	2.2

Table 6.6 The Proximate Analyses Data for Cellulose, Poly(ethene), PVC, Saran, Straw and the Composite Mixtures

Ultimate Analysis (%, as analysed)	C	H	N	Cl	O (by difference)
Cellulose	41.8	5.9	0.0	0.0	52.3
Poly(ethene)	85.7	14.3	0.0	0.0	0.0
1/9 Poly(ethene)/Cellulose	46.0	7.0	0.0	0.0	47.1
1/1 Poly(ethene)/Cellulose	64.0	10.2	0.0	0.0	25.1
PVC	38.2	4.8	0.0	56.4	0.0
1/9 PVC/Cellulose	41.4	5.9	0.0	5.6	47.2
1/1 PVC/Cellulose	40.1	5.4	0.0	28.1	26.3
Saran	33.7	2.2	5.4	58.7	0.0
1/9 Saran/Cellulose	41.0	5.5	0.5	5.9	47.1
1/1 Saran/Cellulose	37.7	4.0	2.7	29.3	26.2
Straw	43.6	6.2	0.71	0.8	48.7
1/9 PVC/Straw	43.2	6.1	0.6	6.5	43.7
1/1 PVC/Straw	40.9	5.5	0.3	28.6	24.6

Table 6.7 The Ultimate Analyses Data for Cellulose, Poly(ethene), PVC, Saran, Straw and the Composite Mixtures

	Char Yield (%, dry, ash free)	Expected Char Yield (%, dry ash free)	C	H	N	Cl	O (by difference)
Cellulose	18.3	-	95.0	0.1	-	-	4.5
Poly(ethene)	No Char Formed	-	-	-	-	-	-
1/9 Poly(ethene)/ Cellulose	16.4	16.5	94.9	0.6	-	-	4.5
1/1 Poly(ethene)/ Cellulose	9.3	9.2	94.9	0.6	-	-	4.5
PVC	10.0	-	98.8	0.6	-	0.5	-
1/9 PVC/Cellulose	21.0	17.5	86.1	1.7	-	< 0.1	12.1
1/1 PVC/Cellulose	17.7	14.2	86.0	1.8	-	0.1	12.1
Saran	31.8	-	95.0	0.4	4.4	0.2	-
1/9 Saran/Cellulose	24.7	19.7	81.7	1.9	0.5	< 0.1	15.7
1/1 Saran/Cellulose	29.8	25.1	79.9	2.6	2.2	< 0.1	15.3
Straw	22.0	-	73.3	2.0	1.8	< 0.1	22.8
1/9 PVC/Straw	27.4	20.8	74.1	2.1	2.0	0.1	21.7
1/1 PVC/Straw	23.5	16.0	80.5	1.7	1.3	0.3	16.3

Table 6.8 The Char Yields, Expected Char Yields and Ultimate Analyses Data for Chars Prepared from Cellulose, Poly(ethene), PVC, Saran, Straw and the Composite Mixtures at 10 K min^{-1} to 1173 K in Nitrogen Atmosphere

	Peak 1 (Moisture, K)	Peak 2 (Devolatilisation, K)	Peak 3 (Char Burn-Out, K)
Cellulose	300	550	750-780 (broad)
Poly(ethene)	-	650	-
1/9 Poly(ethene)/ Cellulose	300	540	780 (broad)
1/1 Poly(ethene)/ Cellulose	300	540	750
PVC	-	600	860
1/9 PVC/Cellulose	300	520	780
1/1 PVC/Cellulose	300	470/530	(broad)
Saran	-	480	860
1/9 Saran/Cellulose	300	470/540	750 (broad)
1/1 Saran/Cellulose	300	480/530	800 (broad)
Straw	300	590	740
1/9 PVC/Straw	300	540	840 (broad)
1/1 PVC/Straw	300	540/580	(broad)

Table 6.9 The Temperatures for the Peak Rate of Weight Loss Associated with Moisture, Devolatilisation and Char Burn-out for Cellulose, Poly(ethene), PVC, Saran, Straw and the Composite Mixtures

	Char Reactivity ($\text{g g}^{-1} \text{s}^{-1} \times 10^{-4}$)									
	613 K	633 K	643 K	653 K	663 K	673 K	683 K	693 K	713 K	733 K
Cellulose	-	0.07	-	0.28	-	0.43	-	0.84	1.54	2.8
Poly(ethene)	No Char Produced									
1/9 Poly(ethene)/Cellulose	-	-	-	0.27	-	0.39	-	0.80	1.49	2.86
1/1 Poly(ethene)/Cellulose	-	-	-	0.29	-	0.44	-	0.86	1.51	2.69
PVC	-	0.02	0.04	0.05	0.07	0.10	-	0.19	0.28	-
1/9 PVC/Cellulose	-	0.09	-	0.18	-	0.28	-	0.60	1.11	2.25
1/1 PVC/Cellulose	-	-	-	0.12	-	0.22	-	0.46	0.85	1.62
Saran	-	0.25	-	0.52	-	0.99	-	2.28	3.73	-
1/9 Saran/Cellulose	-	0.19	-	0.37	-	0.61	-	1.26	2.54	-
1/1 Saran/Cellulose	-	0.25	-	0.48	-	0.88	-	1.93	3.41	-
Straw	0.80	1.74	2.75	3.90	6.24	-	-	-	-	-
1/9 PVC/Straw	-	1.11	1.59	1.94	2.95	5.05	-	-	-	-
1/1 PVC/Straw	-	0.39	0.53	0.89	1.51	2.40	3.37	4.78	-	-

Table 6.10 The Reactivity Data for Chars Prepared from Cellulose, Poly(ethene), PVC, Saran, Straw and the Composite Mixtures at 10 K min^{-1} to 1173 K in Nitrogen Atmosphere

	Char 77 K N ₂ BET Surface Area (m ² g ⁻¹)	Expected Char 77 K N ₂ BET Surface Area (m ² g ⁻¹)
Cellulose	300	-
Poly(ethene)	No Char Formed	
1/9 Poly(ethene)/ Cellulose	302	300
1/1 Poly(ethene)/ Cellulose	297	300
PVC	1	-
1/9 PVC/Cellulose	193	270
1/1 PVC/Cellulose	14	150
Saran	38	-
1/9 Saran/Cellulose	286	274
1/1 Saran/Cellulose	184	158
Straw	30	-
1/9 PVC/Straw	20	27
1/1 PVC/Straw	3	16

Table 6.11 The BET Surface Area Data for Chars Prepared from Cellulose, Poly(ethene), PVC, Saran, Straw and the Composite Mixtures at 10 K min⁻¹

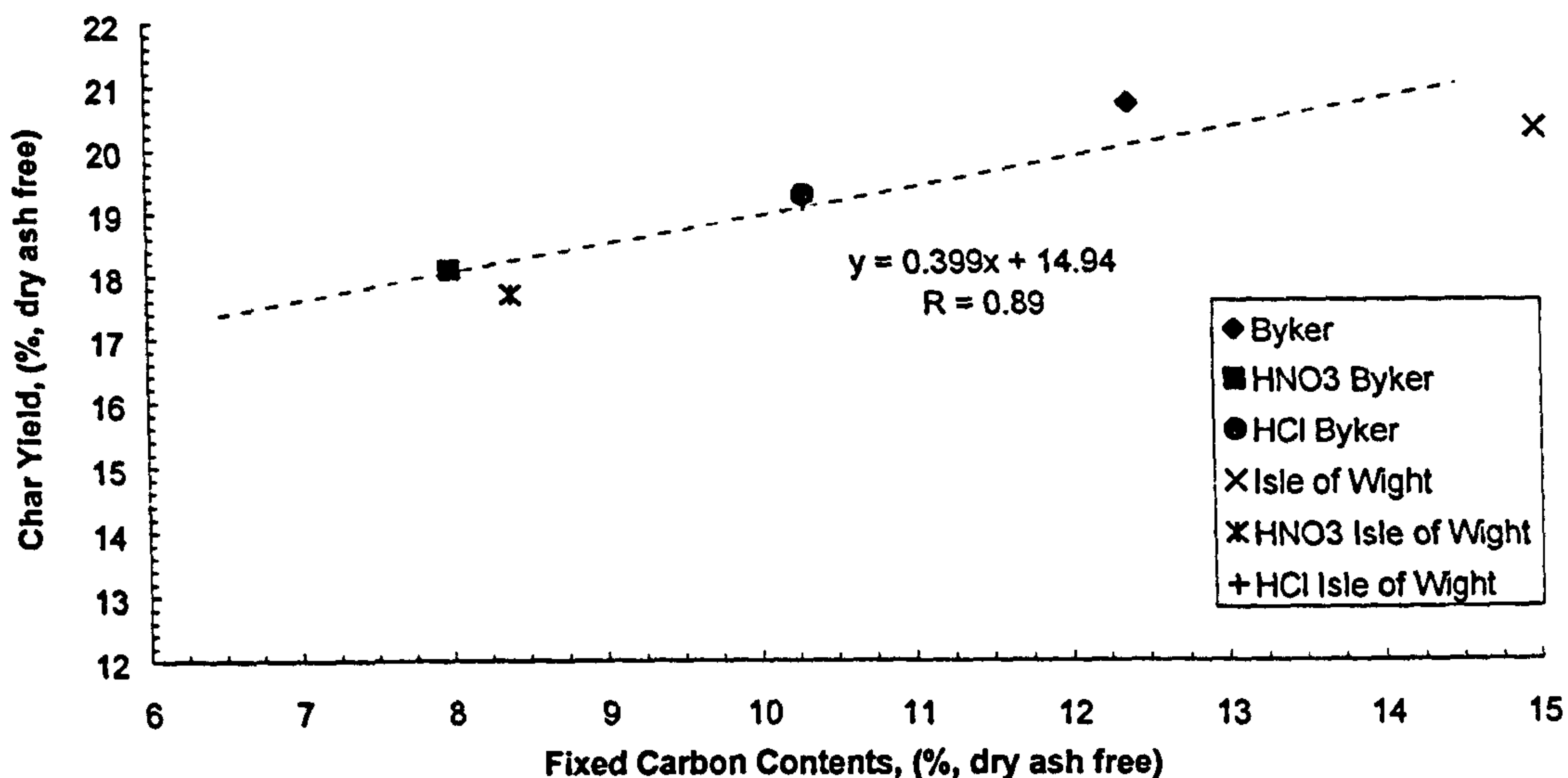


Figure 6.1 The Raw and Acid-Washed Byker and Isle of Wight RDF Sample Char Yields Plotted Against Fixed Carbon Contents

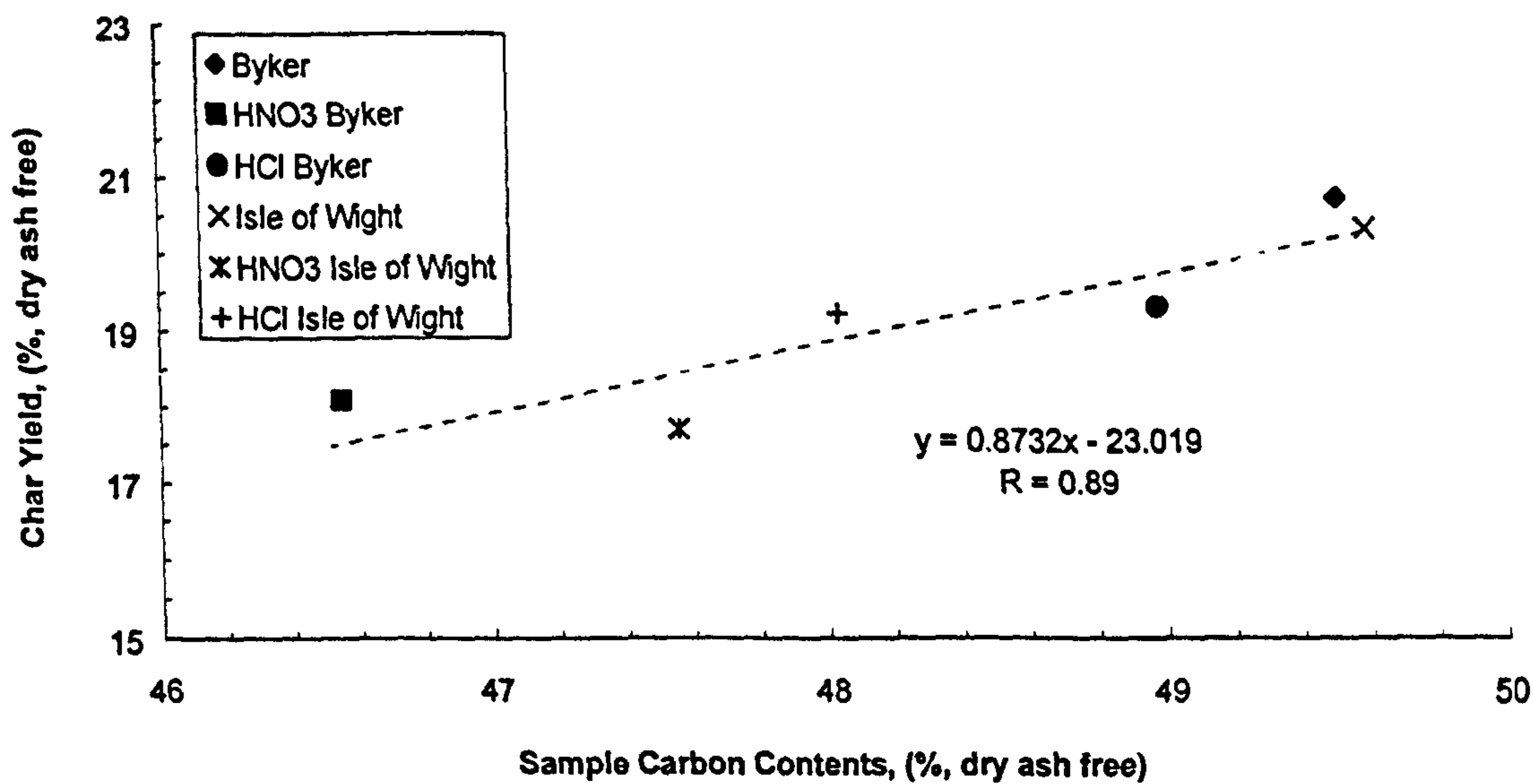


Figure 6.2 The Raw and Acid-Washed Byker and Isle of Wight Sample Char Yields Plotted Against Sample Carbon Contents

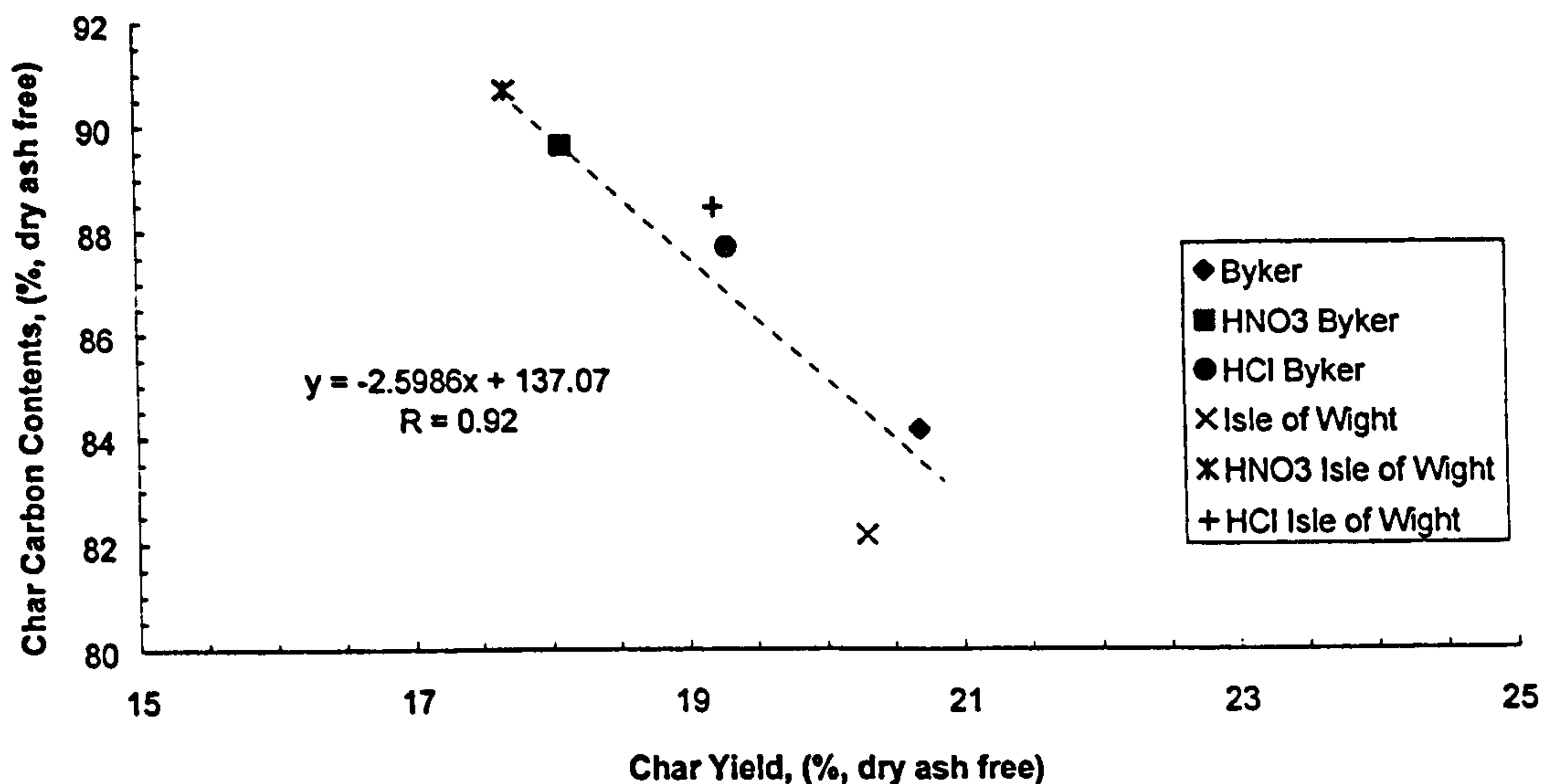


Figure 6.3 The Raw and Acid-Washed Byker and Isle of Wight Sample Char Carbon Contents Plotted Against Char Yield

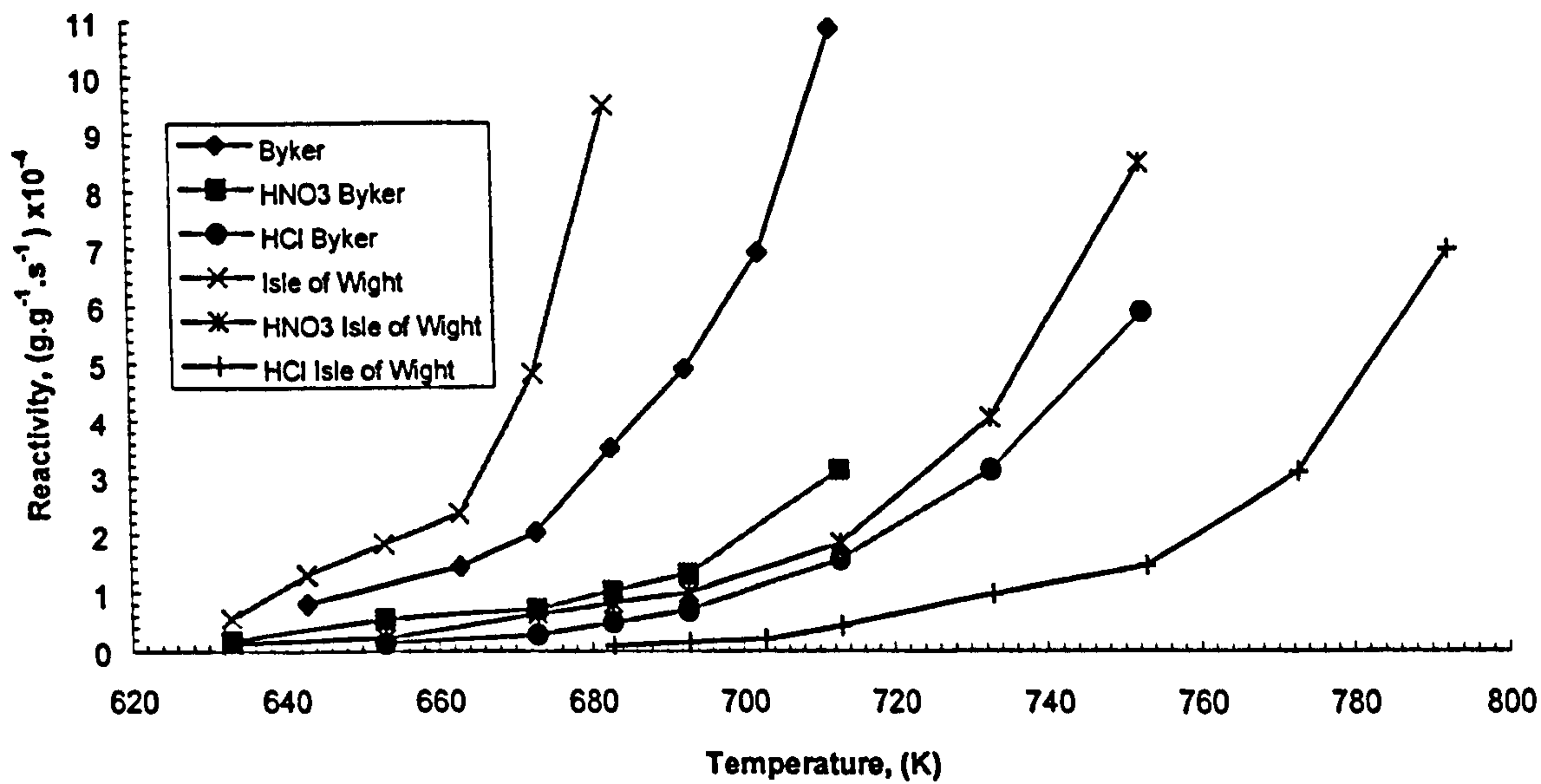


Figure 6.4 The Raw and Acid-Washed Byker and Isle of Wight RDF Sample Chars Isothermal Reactivity in O_2 (3 l h^{-1}) from 633 and 793 K

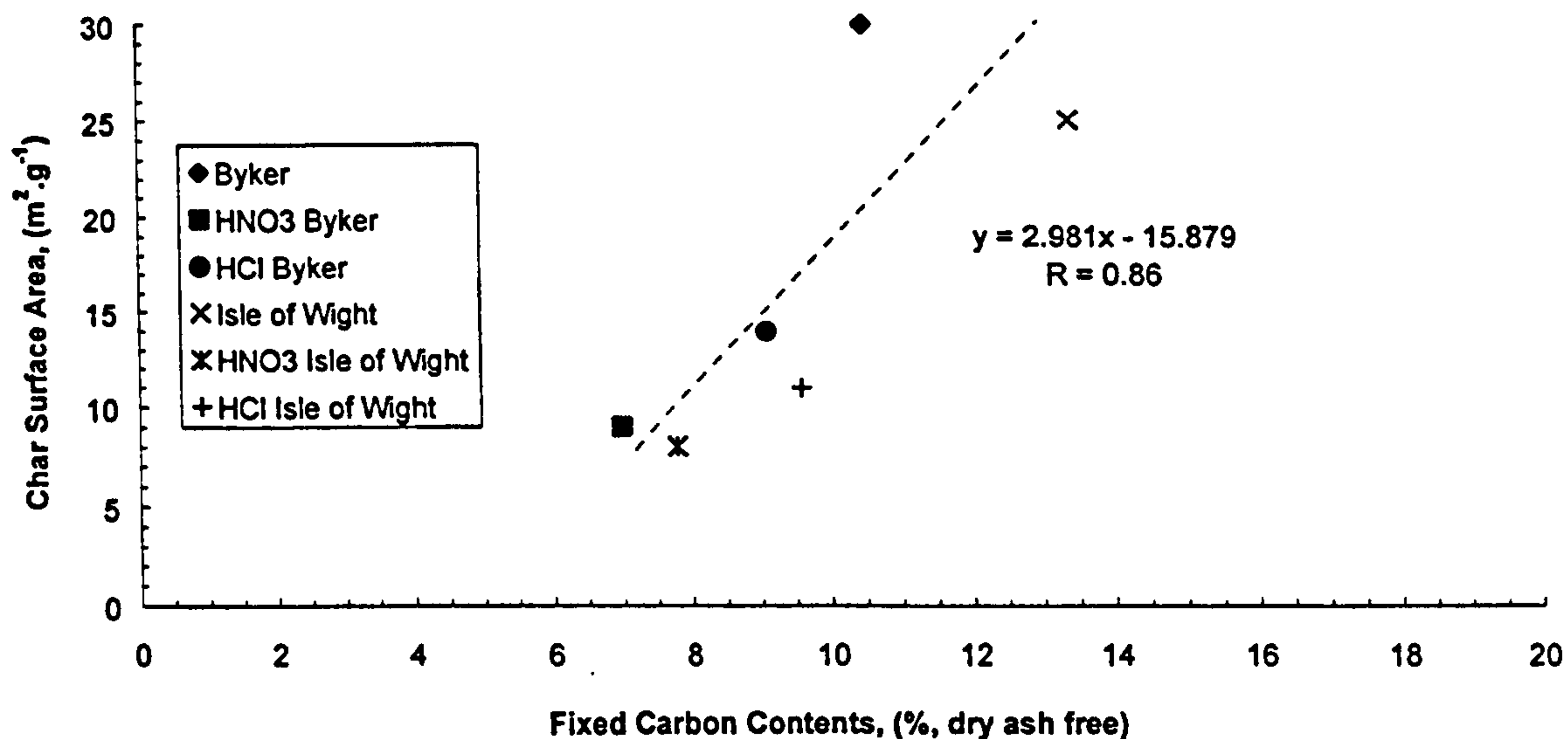


Figure 6.5 The Raw and Acid-Washed Byker and Isle of Wight Sample Char Surface Area Data Plotted Against Fixed Carbon Contents

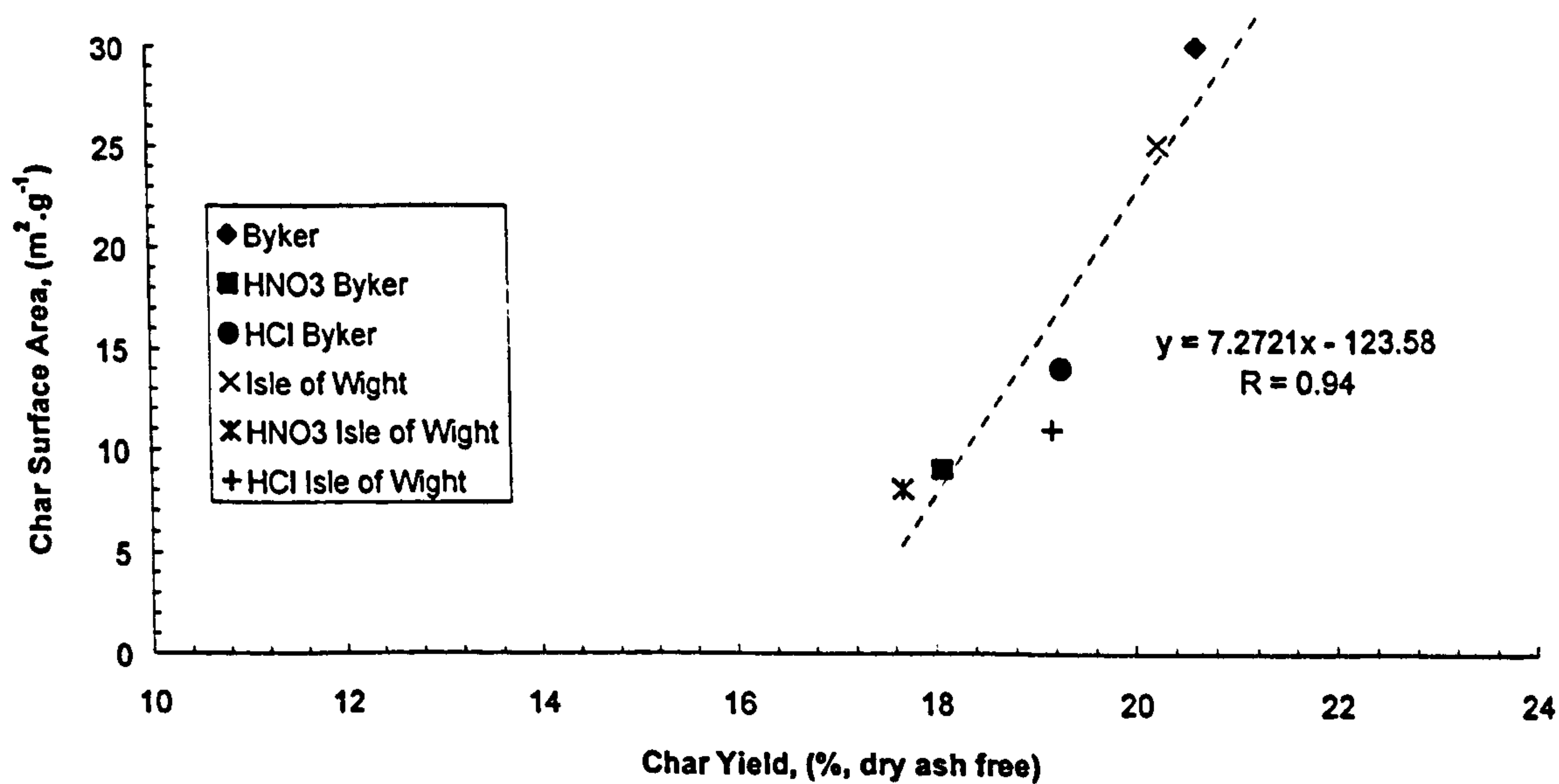


Figure 6.6 The Raw and Acid-Washed Byker and Isle of Wight Sample Char Surface Area Data Plotted Against Char Yield

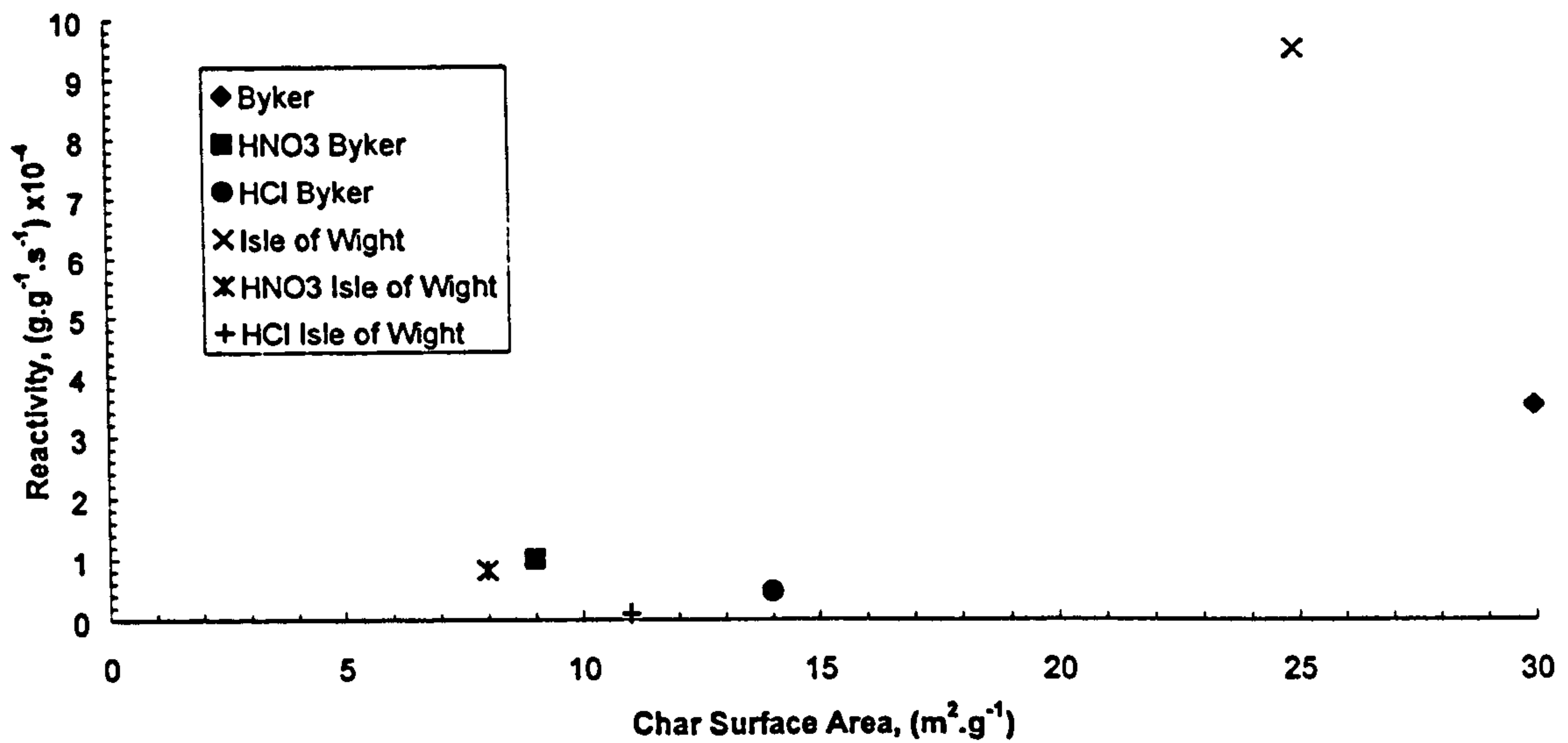


Figure 6.7 The Raw and Acid-Washed Byker and Isle of Wight Sample Char Reactivity in O₂ (3 l h⁻¹) Data at 683 K Plotted Against Char Surface Area

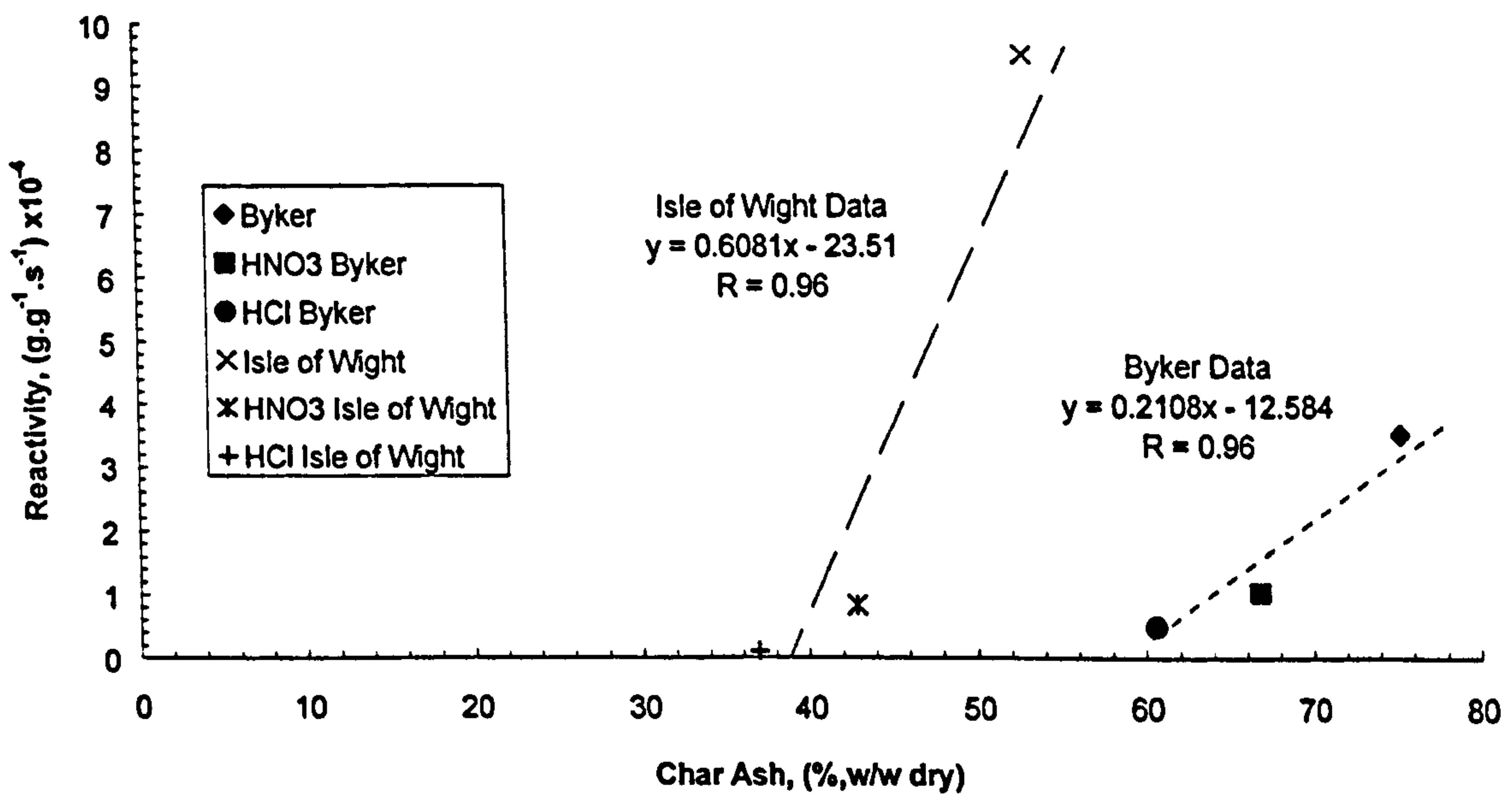


Figure 6.8 The Raw and Acid-Washed Byker and Isle of Wight Sample Char Reactivity in O₂ (3 l h⁻¹) Data at 683 K Plotted Against Char Ash Content

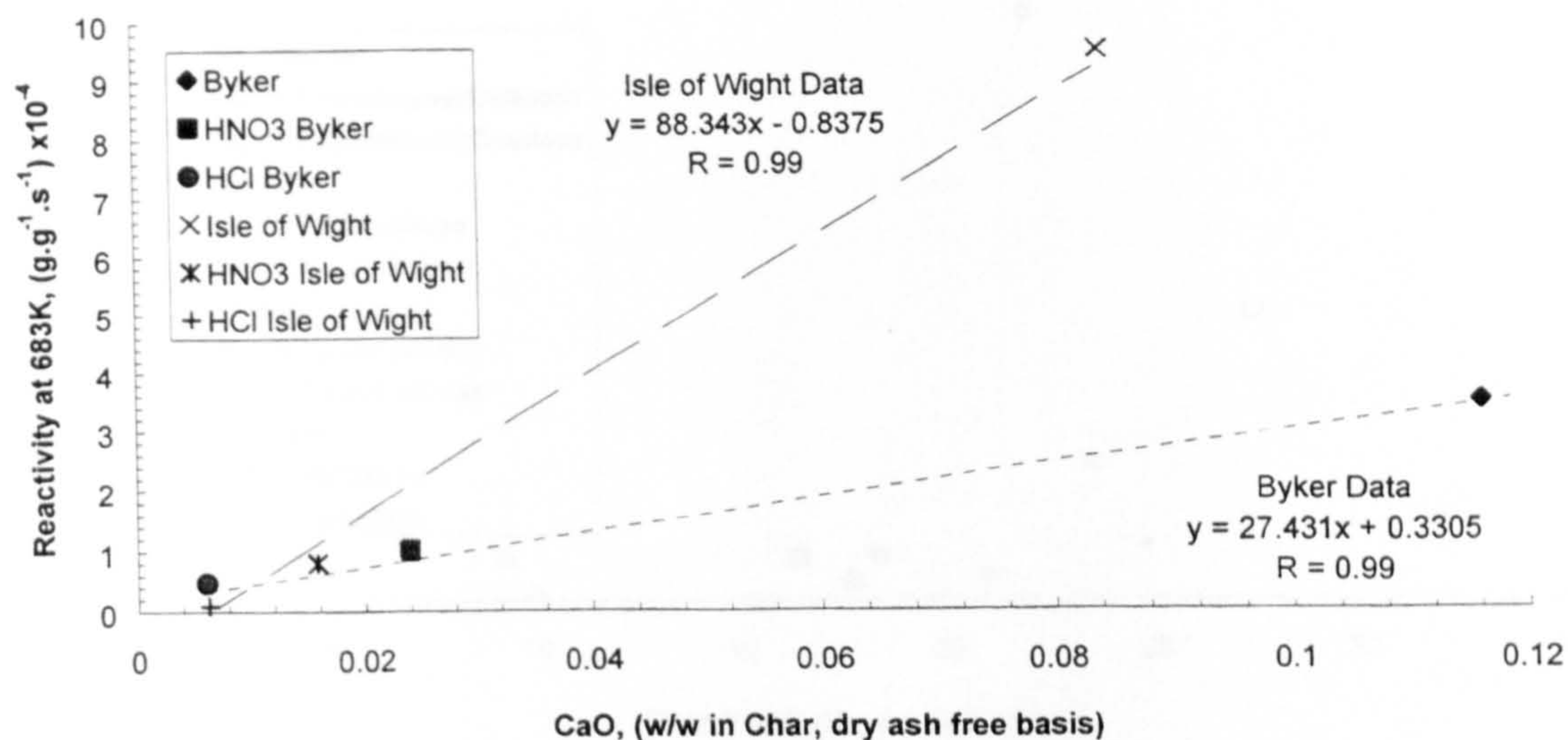


Figure 6.9 The Raw and Acid-Washed Byker and Isle of Wight Sample Char Reactivity in O₂ (3 l h⁻¹) Data at 683 K Plotted Against Char CaO Content

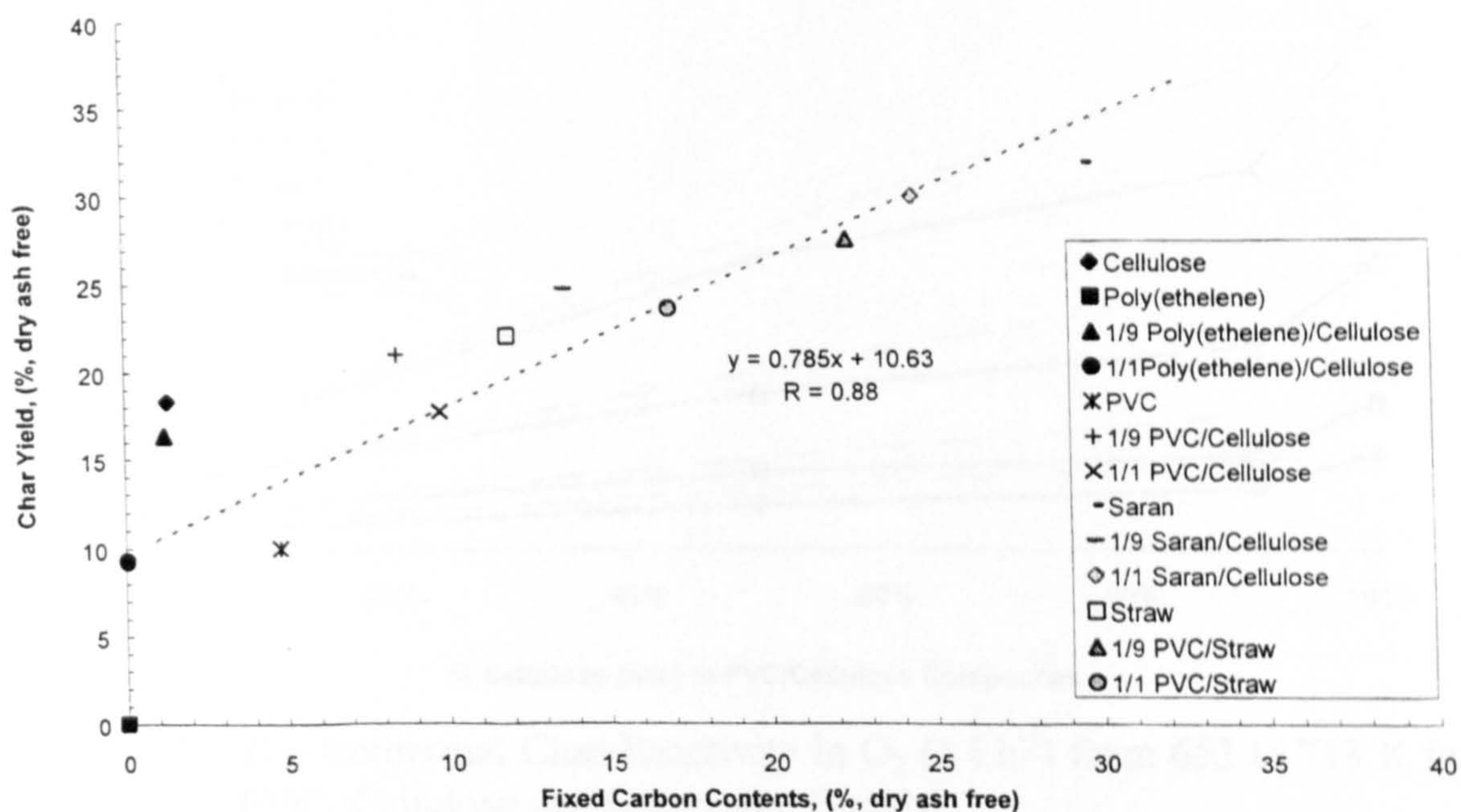


Figure 6.10 The Char Yield Data for Cellulose, Poly(ethene), PVC, Saran, Straw and Composite Blends Plotted Against Fixed Carbon Contents

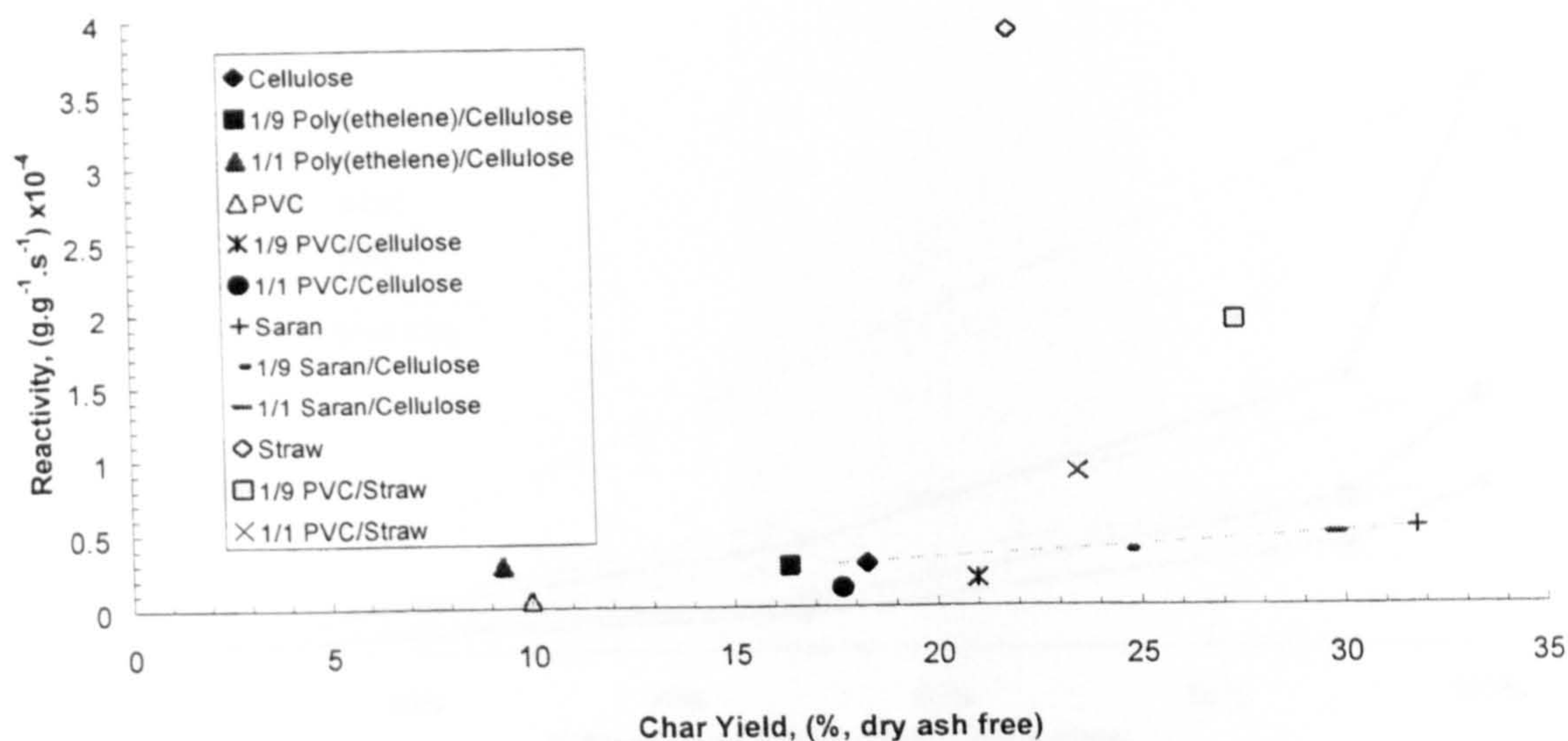


Figure 6.11 The Isothermal Char Reactivity in O_2 (3 l h^{-1}) Data at 653 K Against Char Yields for Cellulose, Poly(ethene), PVC, Saran, Straw and Composite Blends

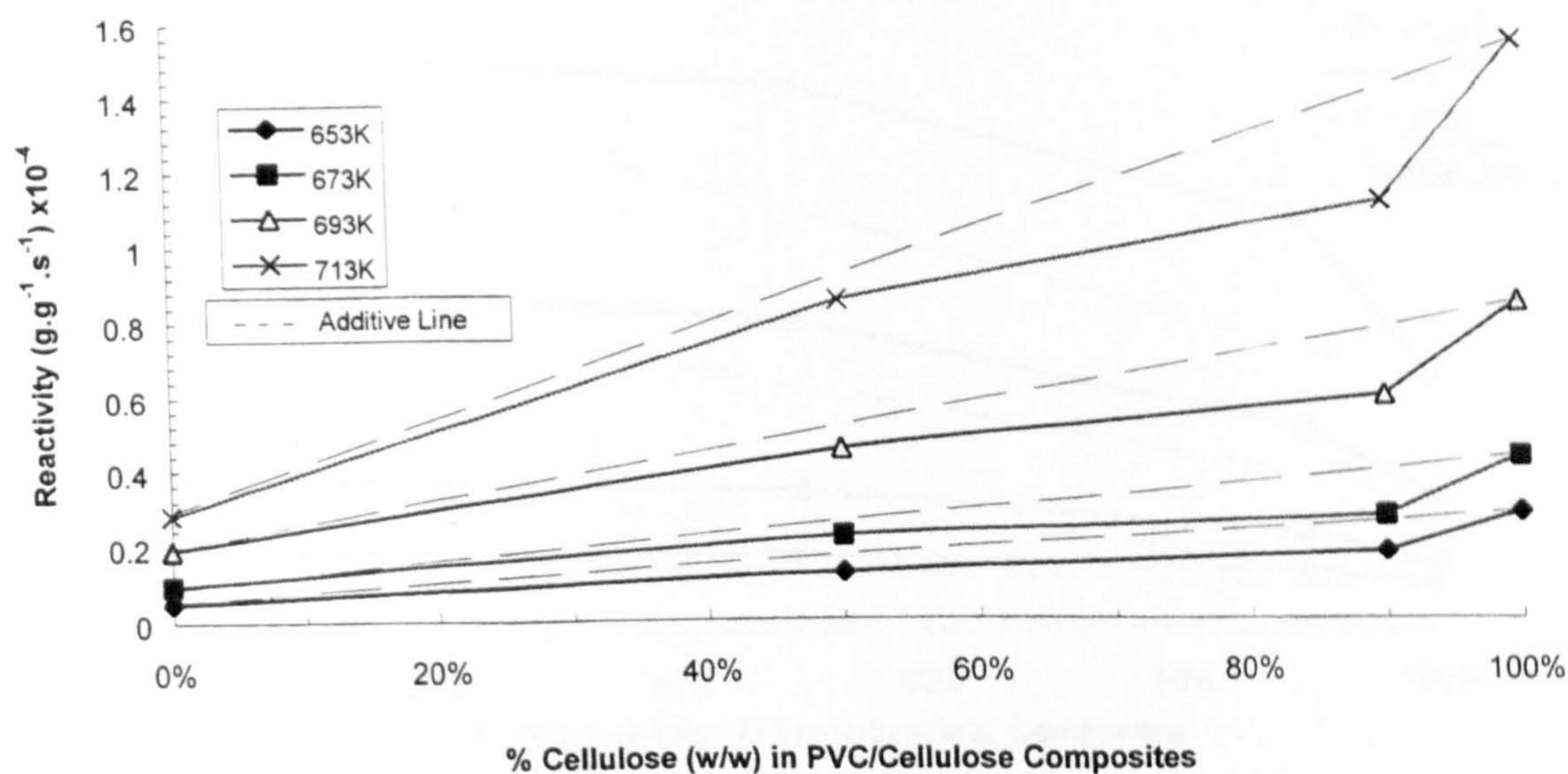


Figure 6.12 The Isothermal Char Reactivity in O_2 (3 l h^{-1}) from 653 to 713 K for PVC, Cellulose and Composite Blends

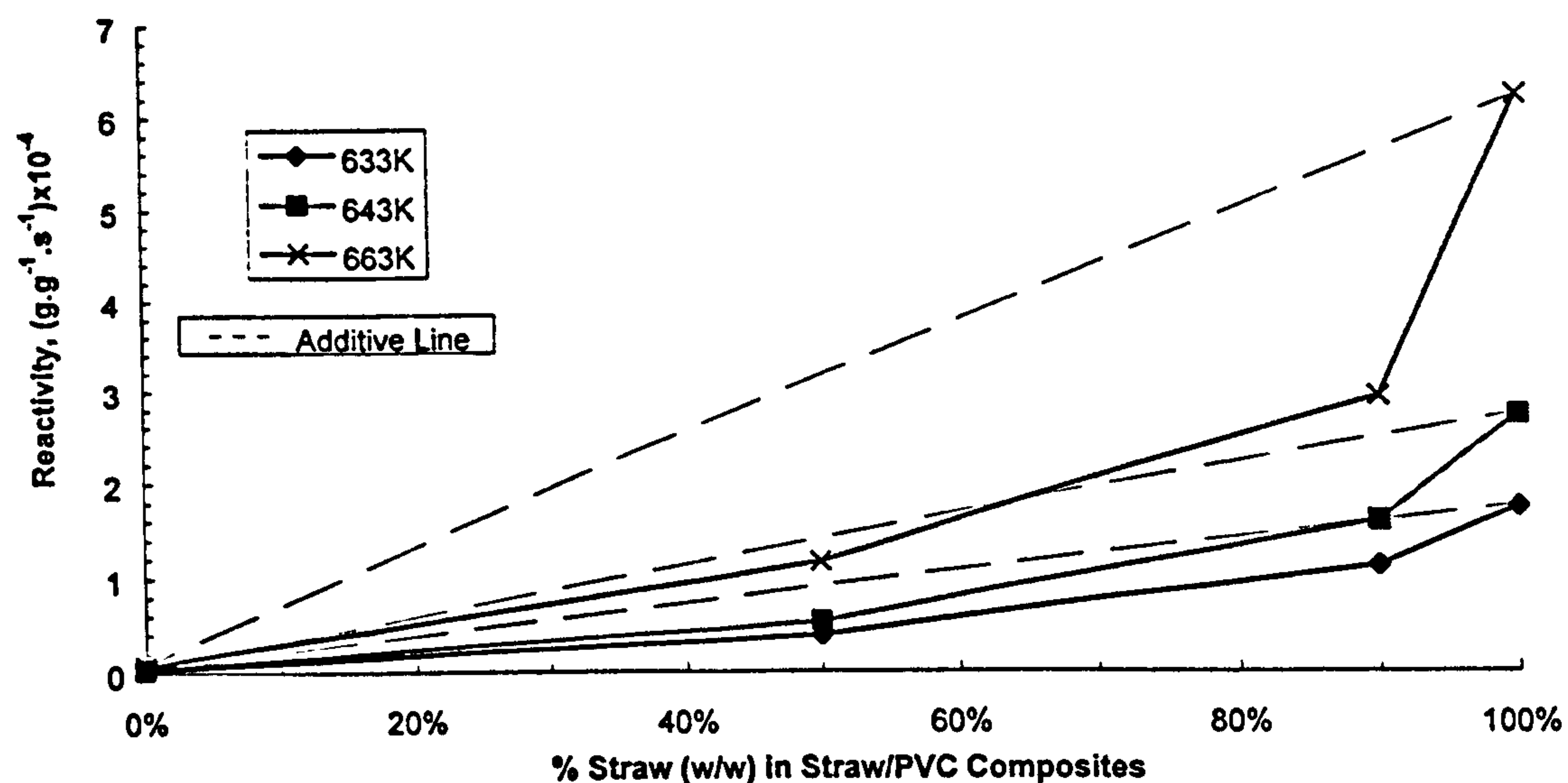


Figure 6.13 The Isothermal Char Reactivity in O_2 (3 l h^{-1}) from 633 to 663 K for Straw, PVC and Composite Blends

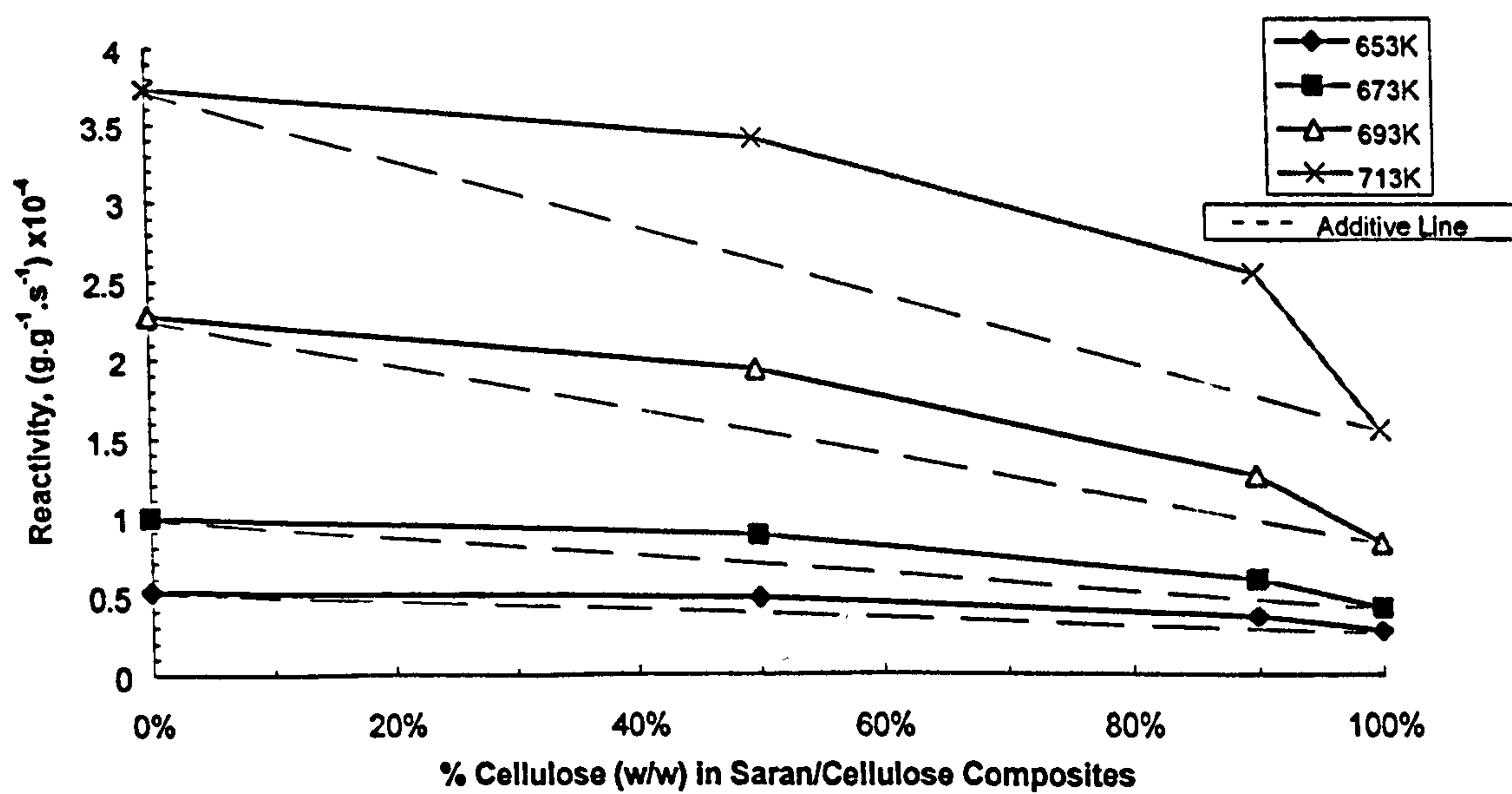


Figure 6.14 The Isothermal Char Reactivity in O_2 (3 l h^{-1}) from 653 to 713 K for Saran, Cellulose and Composite Blends

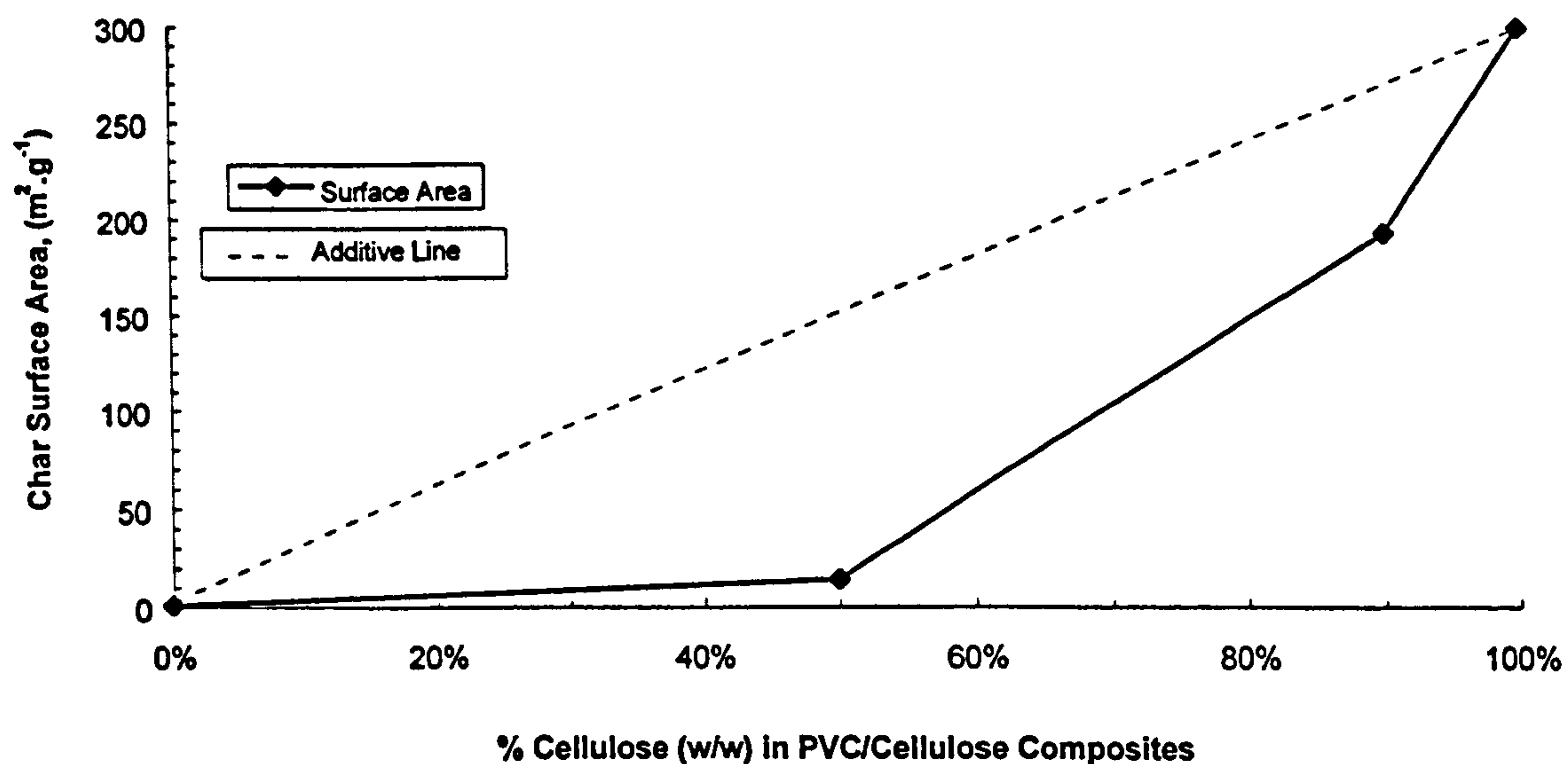


Figure 6.15 The Char Surface Area Data for PVC, Cellulose and Composite Blends

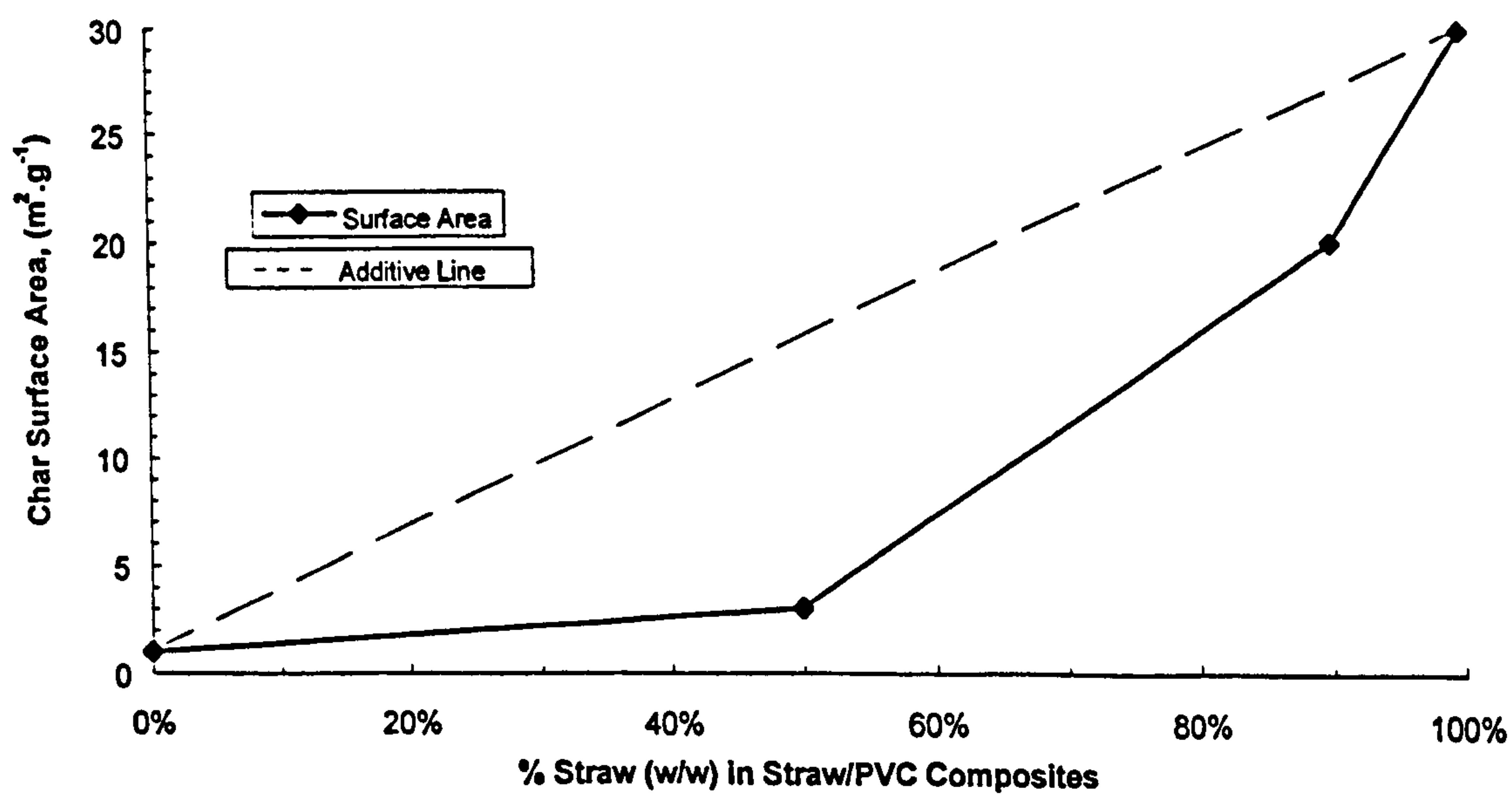


Figure 6.16 The Char Surface Area Data for Straw, PVC and Composite Blends

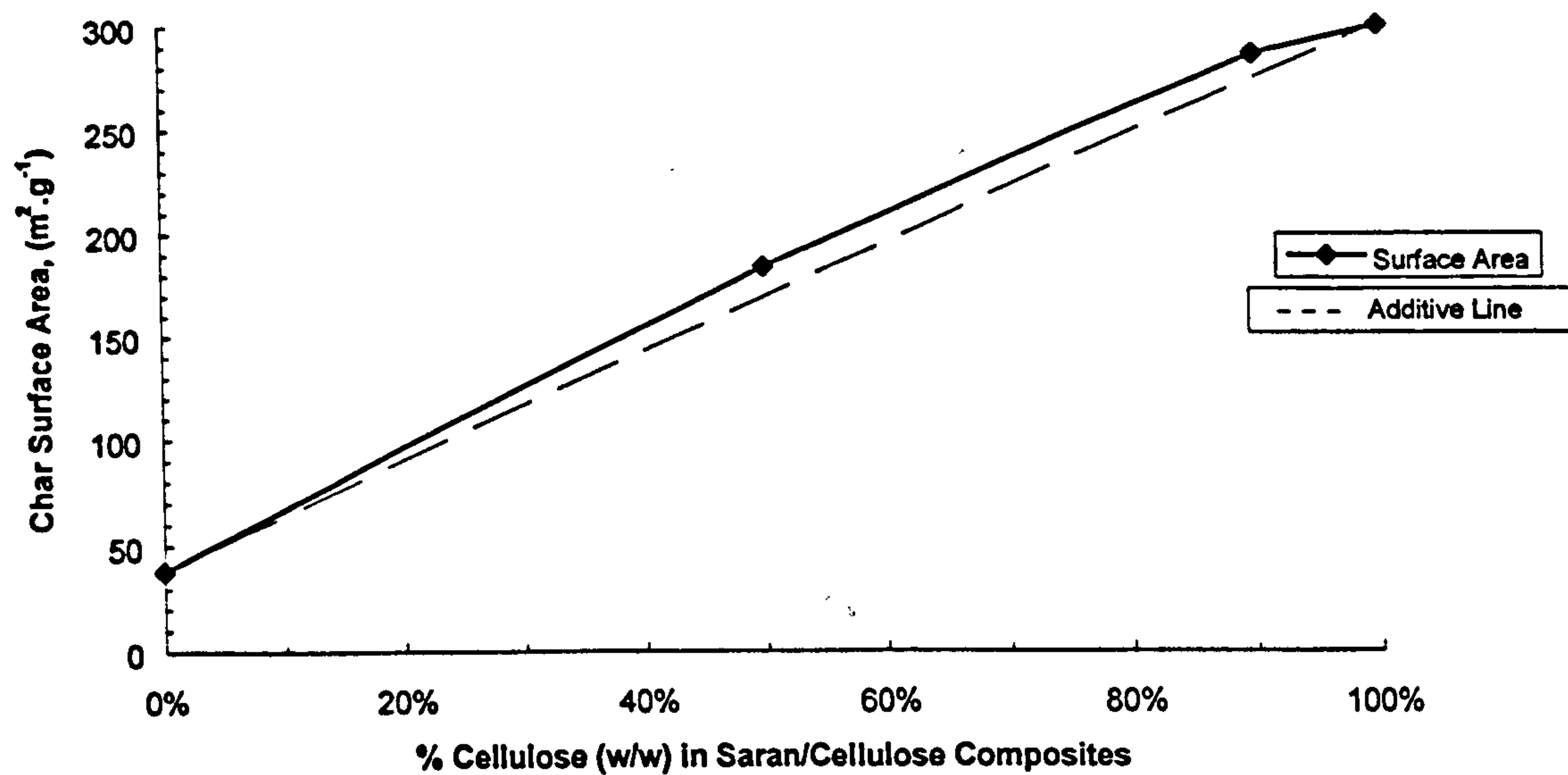


Figure 6.17 The Char Surface Area Data for Saran, Cellulose and Composite Blends

Chapter Seven

Discussion

7.1 Discussion

The principal objectives of this project, as described in Chapter 3, were to provide information about the nature of a wide range of biomass and waste materials, and to study at laboratory-scale, the behaviour of these materials in pyrolysis and gasification reactions. The data which was presented in Chapters 5 and 6, provides information about

- (a) the physical and chemical characteristics of a range of biomass and waste materials,
- (b) the char yields in pyrolysis reactions,
- (c) the isothermal reactivities of the chars in oxidation reactions at temperatures in the range 280-440 °C, and
- (d) the influence of the feed material ash constituent on these reactions.

In this chapter these issues will be discussed under the following subject areas,

1. The influence of the basic characteristics of the biomass and waste materials on their behaviour in industrial fuel handling and gasification systems.
2. The behaviour of the biomass and waste materials during pyrolysis reactions.
3. The isothermal reactivities of the chars prepared from the biomass and waste materials in oxygen and the kinetics of these reactions.
4. The influence of mineral matter on the behaviour of the biomass and waste materials during pyrolysis and the reactivities of the resultant char materials.
5. The effects of component interaction on pyrolysis behaviour and resultant char characteristics for RDF materials.
6. The relevance and application of the results to large-scale biomass and waste gasification.

7.2 The Influence of the Basic Characteristics of Biomass and Wastes on their Behaviour in Industrial Fuel Handling and Gasification Systems

The emergence of fossil fuels as the dominant fuel resources has been attributable in the main to their physical characteristics. Coal, oil and gas can be considered as being high quality fuel forms. They have high GCV, and are readily extracted from source, transported to site, stored, processed and fired in large volume. The physical characteristics and properties of a variety of fuels are presented in Table 7.1⁽¹⁻⁵⁾. Over the years, the infrastructures for the supply of a number of these materials and a technical base for their processing have become well established. This has resulted in the use of fossil fuels for energy production forming the basis of all modern economies.

Generally, when the potential use of biomass and wastes materials for energy production on an industrial scale is discussed, the supply, handling and processing

of these materials need careful consideration. If these materials are to be exploited as fuel stocks, then the following issues must be resolved, viz.;

- (i) the establishment of a market which will be able to provide a sustainable supply of material of known quality, and at acceptable cost,
- (ii) the establishment of a reliable and guaranteed delivery system which can supply fuel in a usable form, and
- (iii) the development of reliable and efficient methods of pre-processing the delivered materials to a condition which satisfies the demands of a particular thermal processing application.

The main characteristics which make fossil fuel usage advantageous are that they are all highly calorific, most have high bulk energy density and all are easily handled and processed. Natural gas is an exception in that it has relatively low bulk energy density, $(39.2 \text{ MJ Nm}^{-3})^{(1)}$, however unlike coal and oil it can be delivered directly to site and used without significant processing. Fuel oils are liquids of variable viscosity. Residual fuels are most commonly employed for power generation and these have high viscosity. They require heated storage and must be filtered and heated to elevated temperatures to ensure effective atomisation and efficient combustion. Coals require milling and drying prior to combustion and gasification. Both oil and coal can be stored for long periods of time without significant deterioration in quality.

As solid fuels, biomass and waste materials are clearly most similar to coal, however, most biomass and waste materials have more onerous storage and pre-processing requirements than coal, and these are summarised in Table 7.1. They have lower calorific value on both a weight and volumetric basis, and this leads to higher storage and transportation costs. Biomass and waste materials which have moisture contents greater than about 15-20 %, such as green wood and domestic refuse, are not suitable for long-term storage since they are subject to microbial respiration, and significant deterioration in quality. Green wood can be stored for

periods up to 12 months but it has to be kept cool. This is inconvenient and expensive, particularly for larger volume applications.

Biomass and waste materials of lower moisture content ($< 20\%$ w/w) such as dried, densified RDF and straw, can be stored for long periods of time without loss of material or deterioration in quality provided they are kept dry^(2, 5).

Some of the biomass and waste materials, such as chipped wood and pelletised RDF can be handled as a bulk solid in a fashion similar to that used for coal. They are however, subject to physical damage during handling and this leads to the generation of excessive levels of fines⁽⁵⁾. Straw is stored and transported in baled form and specialised equipment is required for the handling and breaking of the bales⁽²⁾.

All of the biomass and waste materials require significant pre-processing prior to combustion or gasification. This may include pre-drying, as in the case of green wood, and in most cases, comminution, i.e. shredding in the case of straw and other baled materials, and milling in the case of chipped or pelletised materials. In most cases, commercial equipment, demonstrated under power station conditions, is not readily available for these applications⁽²⁻⁵⁾.

Most commercial gasification processes have been designed and developed for coal. There are essentially three basic types of process;

- (a) high temperature, pressurised, oxygen blown, entrained flow gasifiers for large power plant which require a milled fuel feed,
- (b) fluidised bed gasifiers for smaller scale applications which require a chipped fuel, and
- (c) fixed bed gasifiers which operate with lump material which has low fines content.

In general terms, there are limitations to the scale of operation of biomass and waste energy conversion plants which are imposed by the logistics of the fuel supply chain and by the physical characteristics of the fuel. These can be illustrated by using two simple examples. A 50 MWe wood gasification power plant operating at an energy conversion efficiency of 35 % would have a total fuel requirement (dry basis) of $\sim 200,000$ tonnes p.a.. At an annual yield of ~ 10 tonnes ha^{-1} (dry basis), this means that the plant would have a requirement in excess of 20,000 ha of short rotation coppice in cultivation.

Since the short rotation coppice is only harvested in a relatively short period in the winter, the great majority of this material (200,000 tonnes) would have to be stored for periods of up to a year. At a bulk density of 125 kg m^{-3} (dry, chipped form) this means that the plant would require a total storage capacity of the order of 1.6 million cubic meters⁽³⁾. To supply the plant, the fuel requirement is $25.6 \text{ tonnes h}^{-1}$ or $\sim 205 \text{ m}^3 \text{ h}^{-1}$. This would require 3 deliveries per hour by tipper lorry of 65 m^3 capacity per 24 hour day⁽³⁾.

Similarly, if a 50 MWe gasification plant was operating at 35% energy conversion efficiency was to use municipal solid waste, 400,000 tonnes p.a. would be required. The annual arising of MSW is ~ 0.5 tonnes per person, therefore the refuse from 800,000 people would be required.

These considerations apply to the logistics of the supply of most other biomass and waste materials, i.e. there is a natural upper limit of the equivalent of 30-50 MWe for energy conversion plant, whether these plant involve firing these fuels alone or the co-firing of these materials with more conventional fuels.

Large coal-fired gasification plant is based on high temperature, pressurised, oxygen blown combined cycle gasification technology which is appropriate for that scale of operation. It is possible to introduce a small quantity of alternative materials such as waste, biomass sewage etc. into these systems. However, for plant dedicated to the conversion of biomass and waste at smaller scale (≤ 50

MWe) it is more appropriate to employ simpler, less expensive technologies based on atmospheric pressurised, air blown, circulating fluidised bed gasification technologies, or at very small scale the fixed bed gasification systems. A description of the appropriate gasification technologies for biomass and waste conversion is presented in Chapter 1 and a more detailed description is given by W H Blackadder et al⁽⁹⁾.

7.3 The Behaviour of Biomass and Waste Materials During Pyrolysis Reactions

The design and operation of industrial gasification plant are controlled by the basic characteristics of the fuel, and principally

- (a) the char yields and reaction kinetics of the char materials, and
- (b) the chemistry and fusion behaviour of the ash material.

Most gasification systems have been designed for the processing of bituminous coals, which are the most common type of fuels used in gasification plant world-wide. Lignites and brown coals are also used in some parts of the world. The properties of these fuels are, in many ways, intermediate between those of bituminous coals and biomass materials.

Biomass and waste materials are, in general, more reactive in gasification processes than are bituminous coals and lignites. The char yields are relatively low and the char particles that are produced tend to be more open in structure and more reactive than coal chars. A comparison of the relative volatile matter content of bituminous coals, lignite and brown coals and biomass materials is represented in Table 7.2⁽⁶⁻⁸⁾.

The carbon conversion levels in fluidised bed gasifiers firing bituminous coals are restricted by the relatively high char yields in these systems whereas the carbon conversion in biomass gasification are very much higher under comparable

conditions. This is shown in Table 7.2⁽⁶⁻⁸⁾ which lists the char yields prepared by pyrolysis to 900 °C for the study biomass samples and for bituminous, lignite and brown coals. The coal sample values were found in literature. These data indicate that at 900 °C the char yields of the biomass and waste material were much lower than those of the coals, with an average yield of 25 % compared to char yields of > 50 % for bituminous coals. In gasification systems however, the amount of char material produced is lower due to reaction with oxidising gases. The biomass materials produce chars which are more reactive than coal chars and therefore, to obtain high carbon conversions, less severe conditions are required compared to those for coal. Biomass materials can be gasified in simple air-blown fixed or fluidised bed systems operated at atmospheric pressure, and under these conditions can produce carbon conversion in excess of 95 %. In the case of coal which produces larger quantities of less reactive char, more severe conditions are required. Generally coal is gasified at higher temperatures in oxygen and the system may be operated under pressure. In most situations, there is still a significant quantity of char material produced and a char combustor is needed to increase the efficiency of fuel usage.

7.4 The Isothermal Reactivities of Chars Prepared from Biomass and Waste Materials in Oxygen and the Kinetics of these Reactions

The reaction of the chars prepared from the biomass materials with oxygen, were studied using a Stanton Redcroft TGA750 thermogravimetric analyser. These chars were prepared from the parent biomass materials, by heating samples in a fixed bed reactor at 10 K min⁻¹, to 900 °C (1173 K), in a nitrogen atmosphere and holding at that temperature for a period of one hour.

A typical graph of isothermal weight loss in oxygen for Silsoe Sap char at 380 °C (753 K), is reproduced in Figure 7.1.

The rate of weight loss data for Long Ashton and the Silsoe sample chars, were used to the study reaction kinetics. The "Differential Method" by J H Van't Hoff⁽¹⁰⁾ was used, viz.;

$$\frac{-dc}{dt} = k c^n, \quad \text{equ. 7.1}$$

c = concentration at any instant, and n is the order of reaction with respect to carbon

For two different concentrations,

$$\frac{-dC_1}{dt} = k C_1^n \quad \text{and} \quad \frac{-dC_2}{dt} = k C_2^n \quad \text{equ. 7.2}$$

and by taking logarithms, it is easily shown that

$$n = \frac{\log\left(\frac{-dC_1}{dt}\right) - \log\left(\frac{-dC_2}{dt}\right)}{\log C_1 - \log C_2}$$

equ. 7.3

The order of reaction, is independent of the units employed to express the concentrations, i.e. it is dimensionless.

The data for Silsoe Sap char reactions in oxygen over the temperature range 360-440 °C were analysed, using equation 7.3, to calculate the order of reaction for the char. The data used for these calculations, is presented in Table 7.3, together with the calculated order of the reaction values.

It is clear from the calculated order data, that the isothermal reaction of Silsoe Sap char over the temperature range 360-440 °C, was approximately first order. The calculated reaction orders were found to range from 0.8 to 1.19 and the average value was 1.00. These values are in good agreement with the data reported by I Smith⁽¹¹⁾. The data for all of the Silsoe and Long Ashton chars were then investigated. The first order rate law is presented below in its two useful forms:

$$\ln\left(\frac{C_t}{C_o}\right) = -kt \quad \text{equ. 7.4}$$

and

$$C_t = C_o e^{-kt} \quad \text{equ. 7.5}$$

where $C_o =$ Initial Concentration of Reactant,

$C_t =$ Concentration of Reactant at time, t, and

$k =$ Rate Constant, s^{-1} .

The Silsoe and Long Ashton char isothermal reaction data were plotted using equation 7.4, and an example of a typical graph obtained, that for Silsoe Sap char at 440 °C, is presented in Figure 7.2. It is evident from this graph, that the reaction between this particular char and oxygen did follow first order kinetics, since a good linear correlation was obtained. This behaviour was also found for the other chars investigated. The calculated rate constants and correlation coefficients over the range of temperatures studied, are presented in Table 7.4. As expected, the rate constants were found to increase with increasing temperature for all of the chars.

The reaction rate values, over a range of temperatures, were used to calculate the activation energy of each char. The activation energy, which is independent of temperature was calculated using the Arrhenius equation. The Arrhenius equation is presented below in its two useful forms:

$$\ln k = \ln A - \frac{E_a}{RT} \quad \text{equ. 7.6}$$

and

$$k = Ae^{\frac{-E_a}{RT}}$$

equ. 7.7

k = Rate Constant at Temperature, $T = s^{-1}$

R = Universal Gas Constant, = $J K^{-1} mol^{-1}$

E_a = Activation Energy, and = $J mol^{-1}$

A = Pre-exponential term = s^{-1}

The activation energy for each char was calculated, using equation 7.6, by plotting $\ln k$ against $1/T$. An example graph, that for the Silsoe Sap char between 340-440 °C is presented in Figure 7.3. The activation energy values for each char were calculated from the slopes of the plots, and these values, together with the correlation coefficient for each suite of char data, are presented in Table 7.5. The activation energy values for the chars were found to range from 91 $kJ mol^{-1}$ to 137 $kJ mol^{-1}$. The activation energies of a wide range of char materials to oxygen were reported by I W Smith⁽¹¹⁾. For impure and natural forms of carbon, i.e. cokes produced from coals and various types of petroleum cokes, the activation energy values are of the order of 100-170 $kJ mol^{-1}$. The values measured in this work for the chars produced from biomass and waste materials are toward the lower end of this range. This is as much as would be expected for highly disordered and impure forms of carbonaceous material.

The activation energy values were compared with char reactivity values measured at 340 and 360 °C (613 and 633 K), and a plot of reactivity values against activation energy values is presented in Figure 7.4. It is clear from the graph that there was a reasonable linear relationship between the activation energy values and reactivity values of the chars, the reactivity values increasing with decreasing activation energy.

7.5 The Influence of Mineral Matter on the Behaviour of Biomass and Waste Materials During Pyrolysis and the Reactivities of the Resultant Char Materials

It is well documented in the literature that the reactivities of char materials, during gasification and combustion processes, is greatly influenced by the quantity and type of mineral matter present. This was found to be the case for the biomass chars in this study. As previously indicated in Section 5.7.2 and illustrated in Figure 5.20, the measured reactivities of the majority of biomass chars, at 613 and 633 K increased with increasing ash content. The cereal straw char data was the only exception to this trend. Studies by De Groot et al⁽¹²⁾ on the gasification of agricultural residues in CO₂ produced similar findings. They suggested that the reactivity of their biomass chars, with the exception of a cereal straw, increased with increasing ash content. The deviation from the trend for the wheat straw char was considered to be due to the high concentration of silica in this char.

An excellent relationship between the char reactivity and the CaO content was found for all of the biomass chars, i.e. that the reactivity increases linearly with increasing char CaO concentration. The isothermal reactivity values were found to range from 0.1-2.4 x 10⁻⁴ g g⁻¹ s⁻¹ at 613 K and from 0.2-5.0 x 10⁻⁴ g g⁻¹ s⁻¹ at 633 K for CaO concentrations between 1.0-5.6 % w/w in the sample chars. This correlation was also previously illustrated, in Figure 5.21.

The influence of other char ash components was also investigated. When the char ash concentrations of SiO₂ and K₂O, major components of all of the biomass chars, were plotted against the reactivity data, no correlations were found. These graphs are presented in Figure 7.5 and 7.6 respectively.

The influence of CaO on the reactivity of the biomass chars, under the particular conditions used in this study, was further investigated by plotting the calculated activation energy data against the char CaO concentrations. It is evident from this graph, reproduced in Figure 7.7, that a reasonable, overall relationship exists

which suggests that the activation energy of the chars decreases with increasing CaO concentration. The trend is clearly non-linear, however it can be defined by two distinct regions. From 0.01 to 0.02 % w/w CaO, the activation energy decreases sharply from 138 to 105 kJ mol⁻¹, while from 0.02 to 0.06 % w/w CaO, the decrease in activation energy is much less, from 105 to 92 kJ mol⁻¹.

The effects of inherent mineral matter on reactivity was further investigated by ingesting the Danish pine and straw samples in 1 M HNO₃ and 1M HCl solutions. As mentioned previously, in Section 5.8.1, the principal effect of these procedures was to reduce the ash content of the materials, from 4.5 to 2.8-3.0 % for the straw and from 1.7 to 0.5-0.6 % for the Danish pine. In all cases, the main result was a reduction in CaO, MgO, K₂O and Na₂O contents of the ash, and for the HCl washed samples, the Fe₂O₃ concentrations were also greatly reduced. When the reactivity data of the chars prepared from the acid washed and parent materials are plotted against the char ash content, as previously shown in Figure 5.36, no correlation was found. However, it is clear that the chars prepared from the acid washed materials were less reactive than those prepared from the parent materials.

The reactivity data for these chars was also plotted against char CaO concentrations, as shown in Figure 5.37, and correlations were found for the straw and Danish pine suites of samples individually. These trends indicated that for each group of chars the reactivity decreased with decreasing CaO concentration. The acid washed char reactivity and CaO concentration data have been plotted with the other biomass char reactivity and CaO concentration data, and this graph is presented in Figure 7.8. It can be seen from this plot that the acid washed material data clearly fits the trend which was previously established for the biomass char data. This further suggests that for the biomass chars studied, the reactivity behaviour at low temperatures was greatly influenced by the CaO contents of the char materials.

The postulation that Ca containing mineral compounds are amongst the most active during biomass gasification has been presented by a number of experimentalists⁽¹²⁻

¹⁴⁾ Kinetic studies at low to intermediate temperatures, 500-1600 K have shown that the extent of activity does not only rely on the concentration, but also the chemical form^(15,16), inclusion^(17,18) size and uniformity of dispersion⁽¹⁹⁾.

7.6 The Effects of Component Interaction on Pyrolysis Behaviour and Resultant Char Characteristics for RDF Materials

There is currently a growing interest in the combustion and gasification of waste materials, such as municipal wastes, refuse-derived fuels and general industrial wastes. These materials are widely available at low or negative cost and have a reasonable calorific value of 8-16 MJ kg⁻¹(as received). Also, landfill disposal of these materials is becoming less popular for environmental reasons, and more expensive.

General waste materials are complex mixtures of a variety of components which can vary with time and location. For simplicity, they can be considered as being a mixture of biomass materials, synthetic polymers and inorganic materials, and these are described, generally, below;

- (i) Biomass materials - cellulose and lignin derived materials such as green vegetable material, wood, straw, paper and board.
- (ii) Synthetic polymers - polymeric materials such as PVC, poly(ethylene), poly(etheneterephthalate) etc.
- (iii) Inorganic materials - materials such as ceramics, metals, glass, paper and plastic filler materials etc.

A more detailed description and component assays of a number of waste materials are given in Chapter 2.

A knowledge of the behaviour of these complex mixed materials in pyrolysis and gasification systems is required. For waste materials, this not only involves having an understanding of how the components behave individually, but also, more importantly, having an understanding of any interactions that may be important during co-processing. In this study, simple bi-component mixtures containing cellulosic and synthetic polymer materials were prepared to allow investigation of the interactions between some of the major components of waste materials. The composition of the blends, on a w/w basis (dry), are presented below.

- (i) 1/9 Poly(ethene)/Cellulose,
- (ii) 1/1 Poly(ethene)/Cellulose,
- (iii) 1/9 PVC/Cellulose,
- (iv) 1/1 PVC/Cellulose,
- (v) 1/9 Saran/Cellulose,
- (vi) 1/1 Saran/Cellulose,
- (vii) 1/9 PVC/Straw, and
- (viii) 1/1 PVC/Straw.

The techniques which were employed for basic material analyses, char preparation and analyses, and char isothermal reactivity in oxygen determination are described in detail in Chapter 4.

It is clear from the results presented and described in Chapter 6 that the different blends behaved differently during thermal processing. For instance, if the fixed carbon and char yield data (Tables 6.6 and 6.8) are considered, it can be seen that the values obtained for the poly(ethene)/cellulose mixtures are close to those expected, a result which suggests that no component interaction occurred during

thermal processing. Conversely, the fixed carbon and char yield data of the blends containing either of the chlorinated polymers (PVC or Saran) were found to be greater than expected and obviously some form of interaction between the components did take place. The measured and expected fixed carbon values and char yields of the blends and blend component materials are presented in Table 7.6. From these data, it is interesting to note that the 1/9 PVC/Cellulose and 1/9 Saran/Cellulose blends, which have a similar composition to RDF (10 % synthetic polymer and 90 % cellulosic material), appeared to roughly model the RDF fixed carbon values and char yields. These particular blends had fixed carbon values which ranged from 9-14 % and char yields of 21-25 %, while the Byker and Isle of Wight RDF materials had produced fixed carbon values of 12-15 % and produced char yields of ~ 20 %.

The measured increases in fixed carbon values and char yields for these blends may be due to the interaction of HCl, which is evolved from the chlorine containing polymers, and the cellulosic material, a phenomenon which has been described by Shafizadeh⁽²⁰⁾. In a study of the effects of ZnCl₂ on cellulose pyrolysis, Shafizadeh⁽²⁰⁾ suggested that the increase in the char yields was due to the formation of HCl, a major product of PVC and Saran pyrolysis⁽²²⁾. It was proposed that HCl could initiate the acid catalysed dehydration reactions and could also catalyse the condensation reactions of the intermediate products. The condensation reactions would give rise to products which can no longer escape from the heated zone by evaporation, and thus, they would remain to be roasted and charred.

The chars which were produced from the blends were found to have a variety of characteristics. Considering, in the first instance, the poly(ethene)/cellulose blend chars, the measured surface area and reactivity values, measured isothermally in oxygen, were close to the expected values, which indicates that there was little or no interaction between the components during thermal processing. The char surface area and reactivity values for the blends containing the chlorinated polymers were not as expected. The chars produced from the PVC/cellulose and

saran/cellulose blends were found to have very different characteristics. The PVC/cellulose chars were found to be less reactive in oxygen than expected and they also had a lower surface area. The chars prepared from the saran/cellulose blends were more reactive in oxygen and had an increased surface area. The relative increases and decreases in surface area and reactivity for both sets of blends are illustrated in Figures 6.12, 6.14, 6.15 and 6.17 in Chapter 6. The PVC/straw blend chars had similar characteristics to the PVC/cellulose chars and these are also illustrated in Chapter 6, in Figures 6.13 and 6.16.

The differences between the PVC/cellulose and Saran/cellulose blend chars are due to the differences in behaviour of the PVC and Saran components during pyrolysis. As PVC is heated, it passes through a fluid phase to produce a non-porous char with low surface area. Saran does not pass through a fluid phase, but alternatively, undergoes extensive cross linking to produce a char of high porosity, and surface area. As previously suggested, cellulose, when in the presence of HCl during pyrolysis, will produce an increased quantity of char material which is more reactive. During the pyrolysis of PVC/cellulose blends the increase in reactivity is not detected since the PVC fuses and encloses the cellulose char. The reactive surface area of the resultant char is reduced. During saran/cellulose blend pyrolysis, the saran does not fuse, and an increased char reactivity is measured.

Some of the blends were prepared to be comparable in composition to a typical RDF material, in an attempt to model the behaviour during thermal processing, and the resultant char characteristics. These were the 1/9 poly(ethene)/cellulose, 1/9 PVC/cellulose, 1/9 Saran/cellulose and 1/9 PVC/cellulose blends.

In the first instance, the success of these blends at modelling RDF behaviour during thermal processing was considered. From the char yield values presented in Table 7.7, it is clear that only the 1/9 PVC/cellulose blend with a char yield of 21 %, was comparable to the Byker and Isle of Wight RDF materials. The 1/9 Saran/cellulose blend, despite having a chlorine content similar to that of the 1/9 PVC/cellulose blend, had a lower char yield of 17.5 %. This is due to the fact

that unlike PVC, Saran does not fluidise and coat the cellulosic material during heating. The 1/9 poly(ethene)/cellulose blend, which contained no chlorine, produced the lowest yield of char at 16.4 %. The 1/9 PVC/straw blend produced a higher yield of char than the RDF material, with 27.4 %. The reason for the greater yield could be due to a combined chlorine and mineral matter effect. Further evidence for this was apparent in the char yield data obtained for the acid-washed RDF materials. These had both reduced ash and chlorine contents compared to the untreated RDF materials, and they produced lower char yields.

When the effectiveness of the blends at modelling RDF char reactivity was considered, only the reactivity value for the 1/9 PVC/straw char, which is also presented in Table 7.7, was similar to those of the RDF chars. The reactivity values for other blend chars were much lower than those of the RDF chars. This could possibly be due to the effect of the presence of the ash component of the 1/9 PVC/straw blend. This suggestion is supported by the observation that these blend chars which did not have an ash component, had reactivity values close to those of the chars prepared from the acid-washed RDF materials.

7.7 The Relevance and Application of Results to Industrial-Scale Biomass and Waste Gasification Systems

Overall, the results of the work reported in this document provide fundamental information about the physical and chemical characteristics of a range of the more important biomass materials, and about their behaviour in pyrolysis and gasification systems. Data on the char yields in pyrolysis reactions over a range of temperatures up to 900 °C, and on the reactivities of the resultant chars with oxygen at temperatures up to 450 °C, have been presented. Biomass and waste materials are relatively complex, and all have significant levels of ash and other inorganic constituents. The influence of these constituents on the yields of char and char reactivities has been studied in some detail, and an attempt has been made

to simulate the behaviour of the RDF materials using synthetic mixtures of their major organic constituents.

The experimental work has been performed at small scale in the laboratory, and in the case of the char reactivity measurements, at relatively low temperatures. The industrial-scale gasification of biomass and waste materials will be carried out in a number of ways depending principally on the scale of operation, viz.;

- (a) at small scale, up to 10 MW_{th}, in purpose designed, fixed bed reactors,
- (b) at medium scale, up to 100 MW_{th}, in purpose designed, fluidised bed reactors,
and
- (c) at large scale, by co-gasification with coal and other fuels.

In all cases, the design and operation of industrial-scale plant will require laboratory and test-scale procedures for the characterisation of the behaviour of the different feedstocks and methods for the prediction of the behaviour of these materials in operating plant.

One of the key requirements is the information on the reactivity of the feedstock and the conversion efficiency in gasification systems, and the results of the experiment work presented herein provides a means of obtaining relevant information. Both fluidised bed and fixed bed gasifiers are designed to cope with a range of fuel size distribution and reactivities, by providing longer residence times for larger and less reactive particles. The energy losses due to unreacted carbonaceous material are thereby reduced to a few percent of the energy input. The unreacted material reports to the ash take-off from the gasifier and the solid rejects from the cyclones and filters in the gas clean-up system. There may also be energy losses in the discards from the tar scrubbing system. The overall energy conversion efficiency is also dependant on the operating temperatures within the gasifier, which are generally in excess of 750 °C, and these are dependent largely on the fusion characteristics of the fuel ash.

In industrial gasification systems, therefore, the energy losses due to unreacted carbonaceous material are significantly lower than those measured in the laboratory experiments, however they are dependant on the basic fuel characteristics, and principally the char yield and char reactivity. For example, in fluidised bed or spouted bed, air/steam-blown gasifiers for coal, the char yields with high volatile bituminous coals of volatile matter content in the range 35-40 % (dry, ash free) are commonly in the range 25-35 %, or around 40-50 % of the measured fixed carbon contents. In air-blown fluidised bed gasifiers using wood as a fuel, the heat losses are commonly in the range 5-10 %, and the char yields are generally less than 5 % of the fuel input. This is less than 25 % of the char yields measured in the laboratory pyrolysis experiments, due to the high reactivity of the wood chars and the relatively high air:fuel ratios used in these systems.

In general terms, therefore, the biomass and waste materials are relatively attractive as feed materials for gasification systems, because of their low char yields and high char reactivities, particularly compared to coal. Within the range of biomass and waste materials studied in the present work, the lowest char yields of the materials at 900 °C were measured for the RDF materials, at around 20 % (dry, ash free), compared to 20-29 % for the SRC wood materials. The RDF char materials also had relatively high char reactivity values. In principal, therefore, the conversion efficiency of the RDF materials should be higher than that of the SRC wood materials in industrial gasification systems.

The findings of the present work on the relative char yields and char reactivities of different components of the fractionated SRC wood samples from the Silsoe Research Station are also of interest in this context. The production and utilisation of SRC wood as a fuel is expanding in many northern European countries, and its utilisation as a fuel in gasification systems will increase significantly over the next few years. SRC wood fuel is known to behave differently from soft roundwood materials both in terms of the carbon conversion levels and the ash behaviour. The distinct trends observed in the present work may be of value to plant designers

and operators in helping to explain some of the behaviour of these materials in industrial plant.

One of the more important findings of the current project is the relationship between the char reactivities of a wide range of materials and their CaO content. This result is potentially of interest to the designers and operators of industrial gasifiers, and may be of value in the development of predictive process models of these systems. CaO is an important ash constituent of many biomass and waste materials, and CaO compounds are commonly used as catalyst materials for tar cracking in industrial gasifier, both in the gasifier and in separate tar cracking units. Information of the type present herein, on the relationship between the CaO content of the fuel and the basic kinetic data presented herein on the biomass and waste char reactions with oxygen at low temperatures are also likely to be of value to engineers involved in the development of computer simulations of combustion and gasification processes.

One of the important difficulties encountered in the processing of many waste materials is associated with their heterogeneous nature and the possibility of unpredicted interactions between individual constituents. The results of the experimental work on the behaviour of model composites of synthetic polymers and cellulose materials, and in particular the influence of chlorinated polymers on the char yields and char reactivities of the mixtures, maybe of benefit in helping elucidate the behaviour of complex mixed wastes. For instance, the relatively low reactivities of the chars prepared from mixtures containing PVC is considered to be due to the melting of the PVC during pyrolysis and the physical masking of the cellulose char surfaces. The behaviour of the poly(ethene) and Saran in these mixtures was very different from that of the PVC, in ways that can be described in terms of the behaviour of the different polymers during the pyrolysis process. These findings were consistent with the results of the char surface area measurements of the chars.

Fuel	Physical Form	Moisture (%)	Ash (%)	GCV		Storage	Transport	Handling	Processing Requirements
				(wt) MJ/kg (daf)	(vol) KJ/m ³ (daf)				
Natural gas	Gaseous	-	-	50.7	39.2	Large pressure vessels	Pipeline or by road/rail in pressure vessel	Easy to pump	None
Fuel Oil	Viscous Liquid	< 0.2	< 0.1	42.9	41 x 10 ³	Large heated tankage (30 -50 °C)	Heated bulk transport	Easy to pump when heated	Filtration and heating to temps > 100 °C prior to atomisation
Lignitic Coals	Friable Solid	Variable ≤ 60	Variable < 50	13-17	(8-14) x 10 ³	Uncovered in stockpiles (short term)	Large container on train or lorry	By conveyor belt or by mechanical grab devices	Milling and drying
	Brittle Solid	Variable ≤ 20	Variable < 50	24-33	(16-30) x 10 ³	Uncovered stockpiles	Large container on train or lorry	" "	Milling and drying
	Brittle Solid	≤ 3	Variable < 50	35-37	(16-35) x 10 ³	Uncovered stockpiles	Large container on train or lorry	" "	Milling and drying
Straw	Solid with high aspect ratio	≤ 20	≤ 10	16.2	1.9 x 10 ³ (large bales)	Stockpiled in baled form (short term)	By train or lorry	In baled form	Bale breaking and shredding by scarifier
Wood	Sub 24mm chips	Variable ≤ 60	≤ 5	19.5-21.8	(2-3) x 10 ³	Stockpiled in chipped form (short term)	By train or lorry	In loose form	Drying perhaps and milling
Municipal Waste	Irregular	20-40	~ 30	13.0	1.3 x 10 ³	Cannot be stored in raw form	In containers by train or lorry	By conveyor belt or by mechanical grab devices	High degree of sorting and milling
	Pellet (densified)	< 20	< 20	20	8 x 10 ³	Stockpiled in short term	In containers by train or lorry	In pellet chipped form	Milling

Table 7.1 Comparative Physical Characteristics and Handling and Processing Requirements of Fossil Fuels and Biomass and Waste Materials⁽¹⁻⁵⁾

Material	Volatile Matter, (% daf)	Fixed Carbon, (% daf)	Char Yield, Prepared at 900 °C, (% daf)
Cereal Straw	88.1	11.9	22.0
Danish Pine	79.1	20.9	24.2
Long Ashton I	87.1	12.9	28.9
II	89.1	10.9	25.2
III	79.4	20.6	28.3
IV	87.5	12.5	25.1
Silsoe Bulk	89.8	10.2	24.2
Sap	91.9	8.1	22.5
Bark	84.4	15.6	26.6
Twig	85.4	14.6	24.7
Byker RDF	87.6	12.4	20.7
Isle of Wight RDF	85.0	15.0	20.3
Lignite/Brown Coal	40-50 ^(6, 7)	50-60 ^(6, 7)	30-40 ⁽⁸⁾
Bituminous Coal	20-40 ^(6, 7)	60-80 ^(6, 7)	~50 ⁽⁸⁾

Table 7.2 Proximate Analysis Data and 900 °C (1173 K) Char Yields for Biomass and Selected Coals

	Temp. (°C)	C ₁ (mg)	dC ₁ (mg)	dt ₁ (s)	C ₂ (mg)	dC ₂ (mg)	dt ₂ (s)	n
1	440	7.449	0.877	1080	7.287	0.715	900	1.00
2	440	7.287	0.272	360	6.868	0.515	720	1.09
3	440	7.449	0.291	360	6.868	0.399	540	1.09
1	420	6.474	0.697	540	6.203	0.223	180	0.99
2	420	6.203	0.223	180	5.777	0.416	360	0.97
3	420	6.474	0.494	360	5.777	0.222	180	0.95
1	400	7.262	1.134	1800	6.974	0.657	1080	0.90
2	400	7.262	2.069	3600	6.974	1.781	3240	1.13
3	400	7.262	1.305	2160	6.317	0.189	360	1.01
1	380	6.436	1.232	5040	6.278	0.918	3960	1.13
2	380	6.436	1.373	5760	6.278	1.215	5400	0.93
3	380	6.436	1.232	5040	5.509	0.304	1440	1.09
1	360	7.004	0.911	7200	6.708	0.615	5040	0.80
2	360	7.107	1.104	7920	7.004	0.398	2880	0.80
3	360	7.107	0.104	720	6.708	0.1027	720	1.19
AVERAGE								1.00

Table 7.3 Calculated Rate Data and Reaction Order Values for Silsoe Sap Char Isothermal Reaction in Oxygen

Temp (°C)	LONG ASHTON				SILSOE			
	I k_1 (s ⁻¹)	II k_1 (s ⁻¹)	III k_1 (s ⁻¹)	IV k_1 (s ⁻¹)	Bulk k_1 (s ⁻¹)	Sap k_1 (s ⁻¹)	Bark k_1 (s ⁻¹)	Twig k_1 (s ⁻¹)
	R	R	R	R	R	R	R	R
280				7.0x10 ⁻⁶			1.15x10 ⁻⁵	3x10 ⁻⁶
300	4.0x10 ⁻⁶	3.0x10 ⁻⁶	7.0x10 ⁻⁶	1.5x10 ⁻⁵	0.914		2.x10 ⁻⁵	6x10 ⁻⁶
320	1.0x10 ⁻⁵	6.0x10 ⁻⁶	2.0x10 ⁻⁵	3.0x10 ⁻⁵	0.986		4x10 ⁻⁵	2x10 ⁻⁵
340	2.0x10 ⁻⁵	1.5x10 ⁻⁵	3.0x10 ⁻⁵	6.0x10 ⁻⁵	0.989	3x10 ⁻⁶	8x10 ⁻⁵	3x10 ⁻⁵
360	4.0x10 ⁻⁵	3.0x10 ⁻⁵	6.0x10 ⁻⁵	1.0x10 ⁻⁴	0.993	8x10 ⁻⁶		5x10 ⁻⁵
380	8.0x10 ⁻⁵	6.0x10 ⁻⁵	1.1x10 ⁻⁴		0.999	1.5x10 ⁻⁵		
400					0.999	3.5x10 ⁻⁵		
420						7x10 ⁻⁵		
440						2x10 ⁻⁴		

Table 7.4 Rate Constant Values and Linear Correlation Coefficients for Long Ashton and Silsoe Material Char Reaction in O₂ Over the Temperature Range 280-440 °C (553-713 K)

Material Char	Ea (kJ mol ⁻¹)	A (s ⁻¹)	R	Reactivity	
				613K (340 °C) (g g ⁻¹ s ⁻¹ x 10 ⁻⁴)	633K (360 °C) (g g ⁻¹ s ⁻¹ x 10 ⁻⁴)
Long Ashton I	114 x 10 ³	8.08 x 10 ⁻⁶	0.999	0.621	1.468
II	118 x 10 ³	5.83 x 10 ⁻⁶	0.999	0.428	0.995
III	103 x 10 ³	6.21 x 10 ⁻⁵	0.993	1.185	2.291
IV	96 x 10 ³	5.47 x 10 ⁻⁴	0.999	2.276	4.60
Silsoe Bulk	119 x 10 ³	5.47 x 10 ⁻⁶	0.999	0.425	0.791
Sap	137 x 10 ³	6.28 x 10 ⁻⁷	0.999	0.100	0.171
Bark	91 x 10 ³	2.07 x 10 ⁻⁴	0.997	2.425	5.01
Twig	105 x 10 ³	3.27 x 10 ⁻⁵	0.987	1.047	2.052

Table 7.5 Arrhenius Data, Data Correlation Coefficients and Measured Isothermal Reactivity Values for Long Ashton and Silose Sample Chars

Material	Fixed Carbon %, (daf)	Expected Fixed Carbon %, (daf)	Char Yield %, (daf)	Expected Char Yield %, (daf)	Char Reactivity at 653 K (380 °C) ($\text{g g}^{-1} \text{s}^{-1} \times 10^{-4}$)
Poly(ethene)	0.0	-	0.0	-	-
Celulose	1.35	-	18.3	-	0.282
PVC	4.80	-	10.0	-	0.051
Saran	29.60	-	31.8	-	0.519
Straw	11.93	-	22.0	-	3.901
1/9 Poly(ethene)/ Celulose	1.20	1.22	16.4	16.5	0.270
1/1 Poly(ethene)/ Cellulose	0.71	0.68	9.3	9.2	0.285
1/9 PVC/Cellulose	8.48	1.70	21.0	17.5	0.180
1/1 PVC/Cellulose	9.81	3.98	17.7	14.2	0.122
1/9 Saran/Cellulose	13.72	4.18	24.7	19.7	0.369
1/1 Saran/Cellulose	24.46	15.48	29.8	25.1	0.479
1/9 PVC/Straw	22.44	11.22	27.4	20.8	1.936
1/1 PVC/Straw	16.99	8.37	23.5	16.0	0.888
Byker RDF	12.44	-	20.7	-	1.12
Isle of Wight RDF	15.02	-	20.3	-	1.83

Table 7.6 Experimental and Theoretical Fixed Carbon and Char Yields, and Measured Char Isothermal Reactivity Values for RDF Models and Components

Material	Char Yield, (% daf)	Reactivity, at 653 K (380 °C) ($\text{g g}^{-1} \text{s}^{-1} \times 10^{-4}$)	Comment
Byker RDF	20.7	1.12	Ash and Cl component
Isle of Wight RDF	20.3	1.83	Ash and Cl component
1/9 Poly(ethene)/cellulose	16.4	0.27	No ash, no Cl
1/9 PVC/cellulose	21.0	0.18	Cl component
1/9 Saran/cellulose	17.7	0.37	Cl component
1/9 PVC/straw	27.4	1.94	Ash and Cl component
HNO ₃ Byker RDF	18.1	0.55	Reduced ash and Cl component
HCl Byker RDF	19.3	0.13	Reduced ash and Cl component
HNO ₃ Isle of Wight RDF	17.7	0.22	Reduced ash and Cl component
HCl Isle of Wight RDF	19.2	0.02	Reduced ash and Cl component

Table 7.7 The Char Yield Data and Char Reactivity Data for the Untreated and Acid-Washed Byker and Isle of Wight RDF and the RDF Model Blends

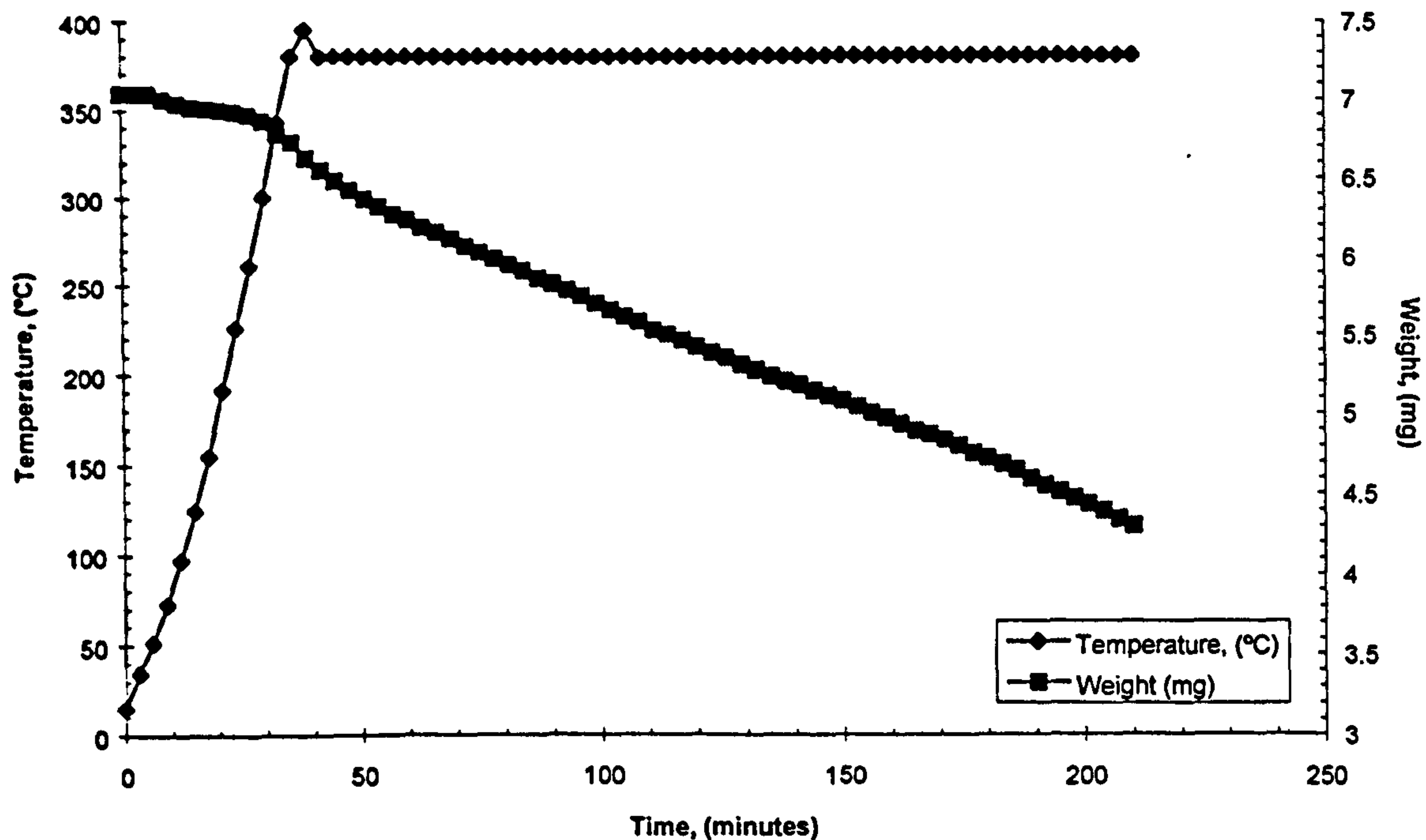


Figure 7.1 The Isothermal Weight Loss for Silsoe Sap 900 °C (1173 K) Char Reacting in Oxygen (3 l h^{-1}) at 380 °C (653 K)

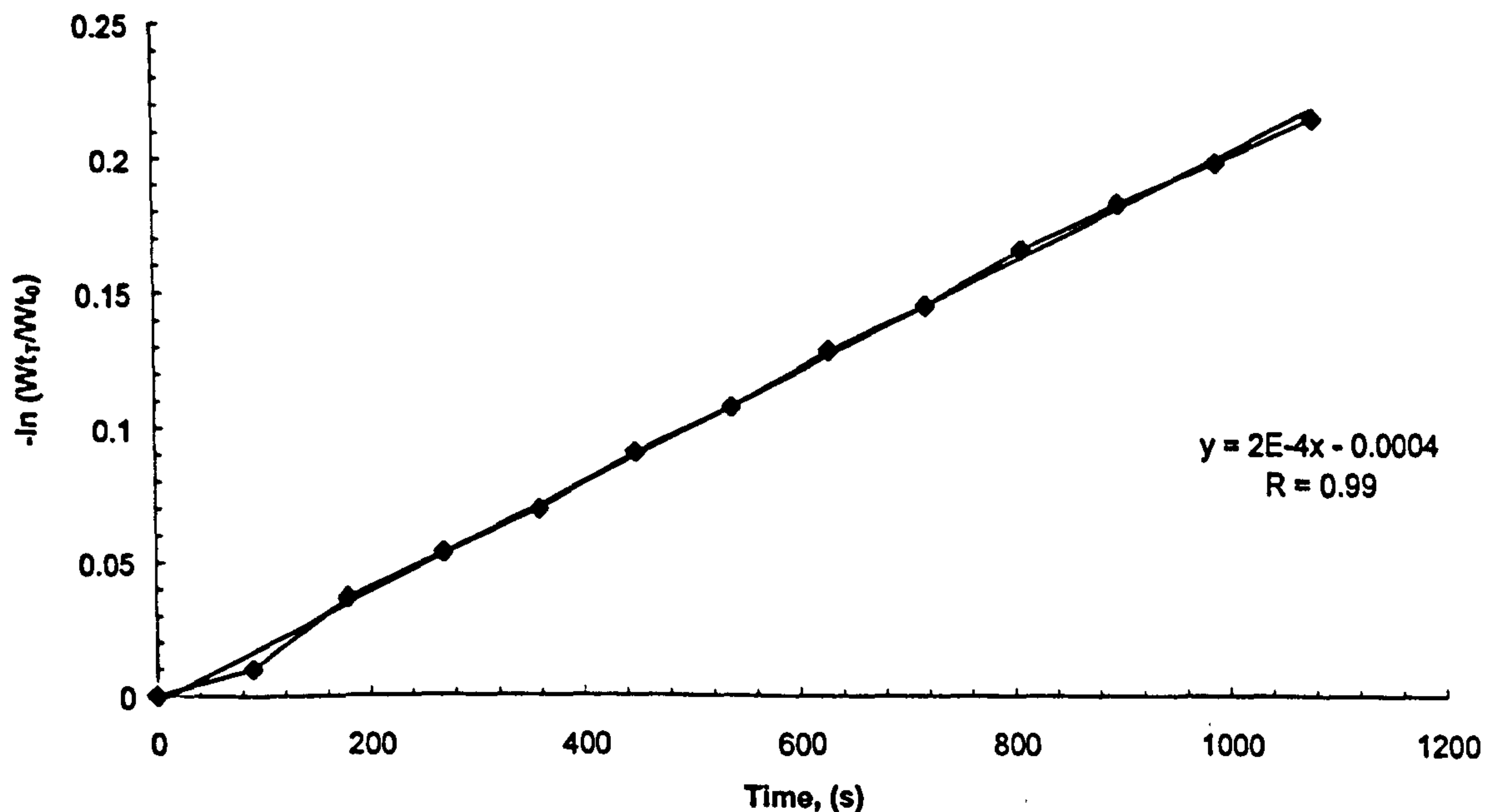


Figure 7.2 Plot of $-\ln(W_t/W_o)$ Versus Time for Silsoe Sap 900 °C (1173 K) Char Isothermal Reaction in Oxygen at 440 °C (713 K)

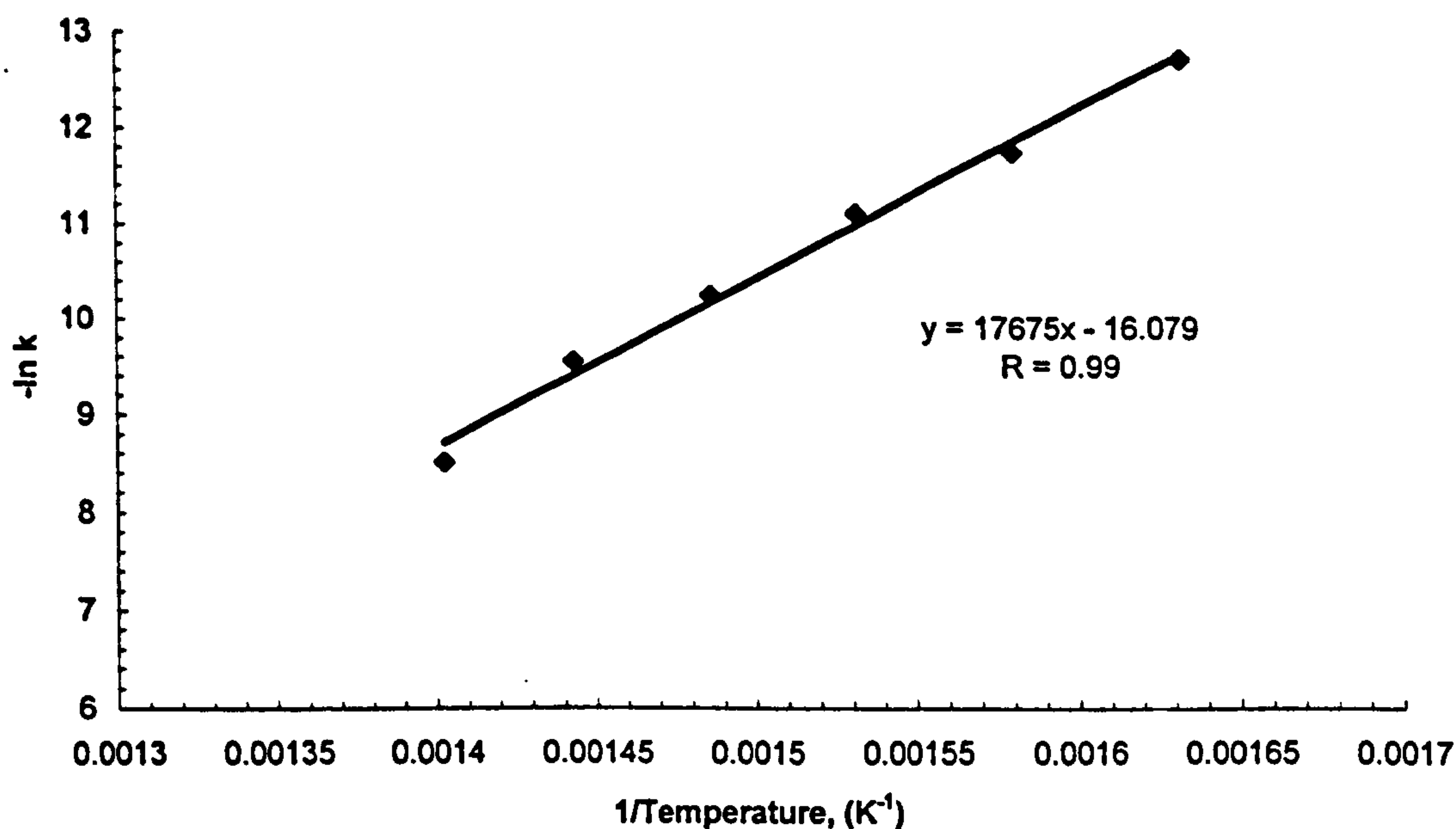


Figure 7.3 Plot of the $-\ln(\text{Rate Constant})$ Data Plotted Against $(\text{Temperature})^{-1}$ for the Silsoe Sap 900 °C (1173 K) Char Isothermal Reactions in the Temperature Range 340–440 °C (613–713 K)

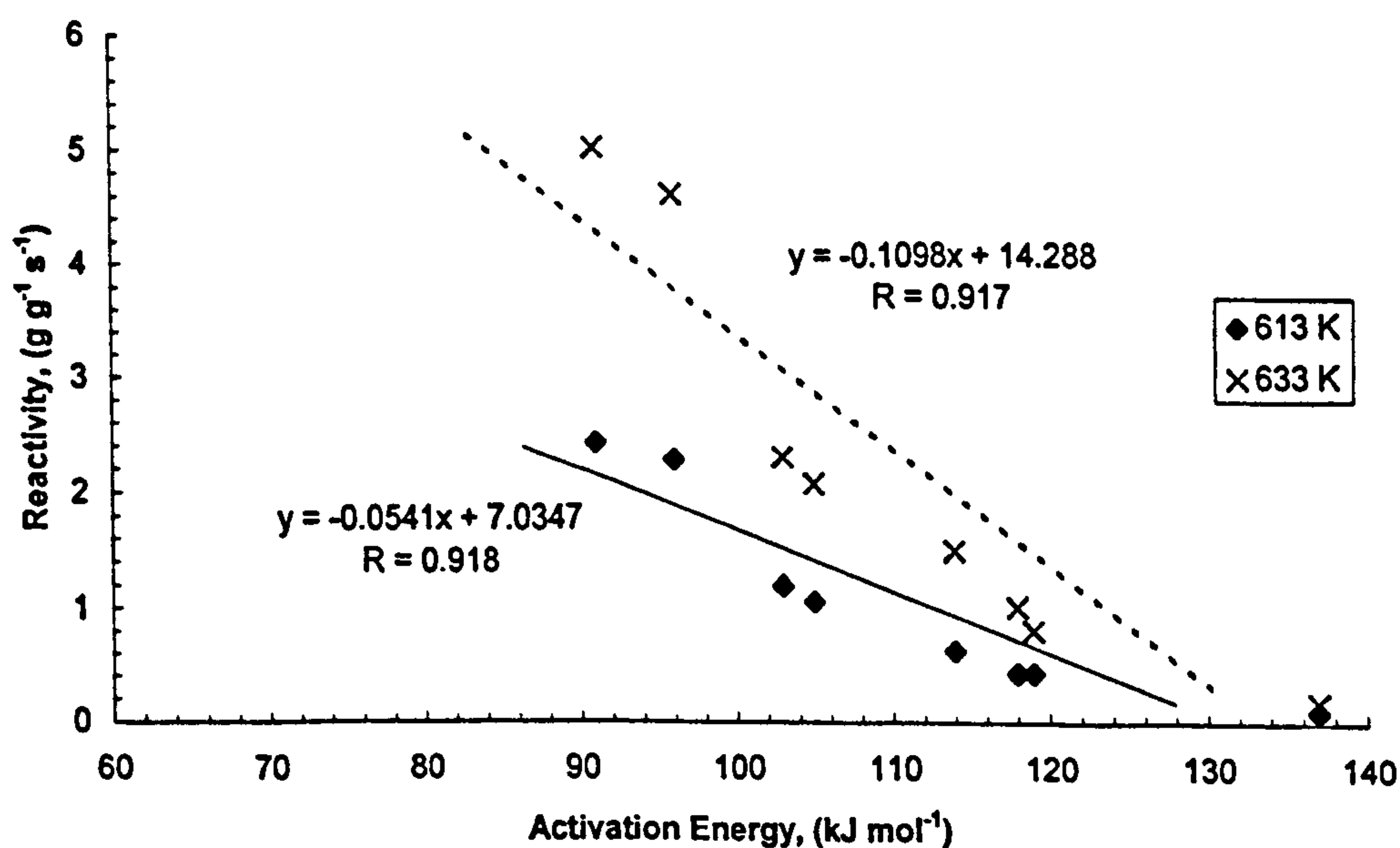


Figure 7.4 Plot of the 900 °C (1173 K) Char Isothermal Reactivities in Oxygen Data Determined at 340 and 360 °C (613 and 633 K) Plotted Against the Determined Char Activation Energy Data for the Long Ashton and Silsoe Materials

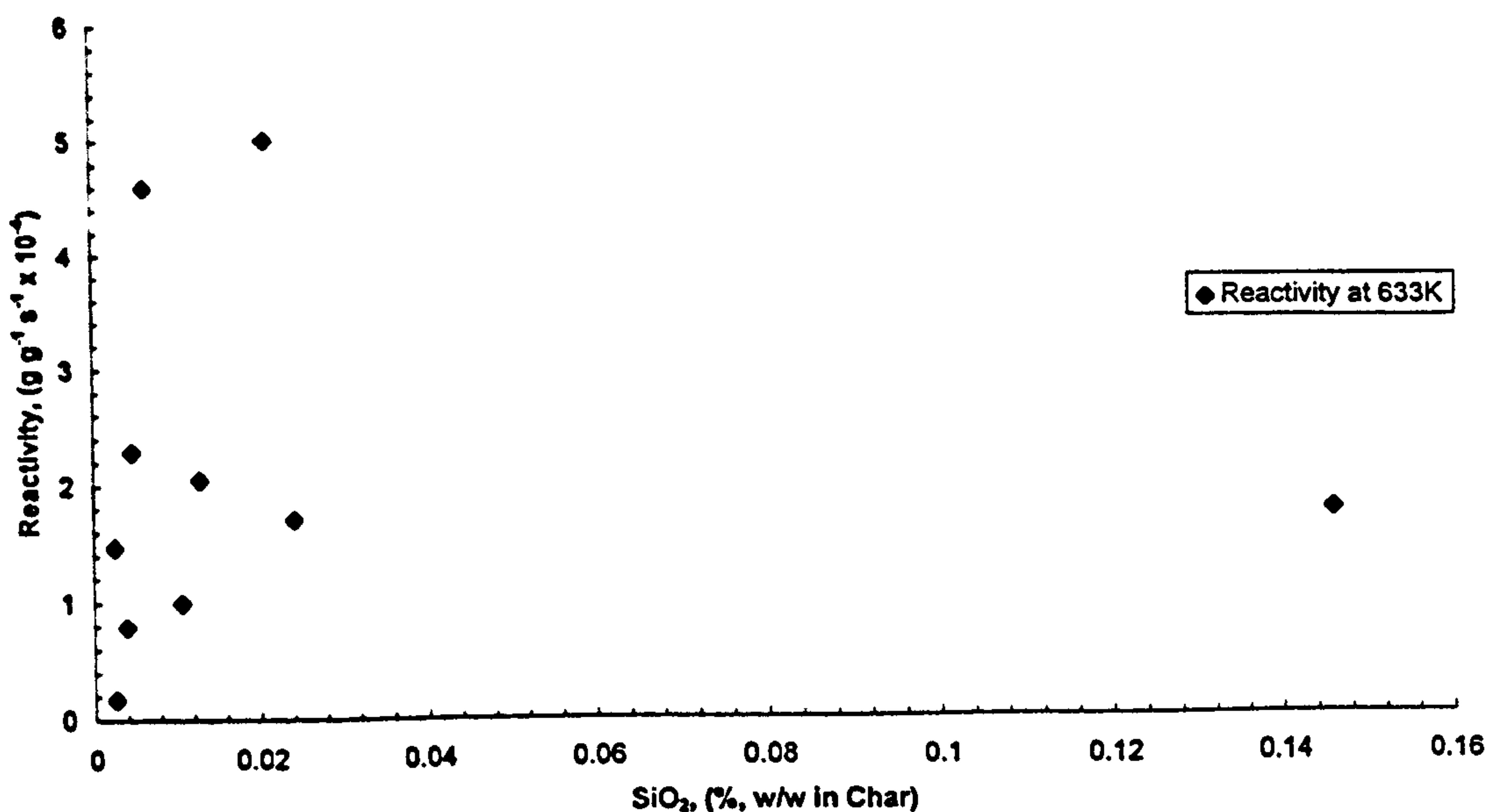


Figure 7.5 Plot of the 900 °C (1173 K) Char Isothermal Reactivity in Oxygen Determined at 360 °C (633 K) Versus Char SiO₂ Concentration for the Long Ashton and Silsoe Materials

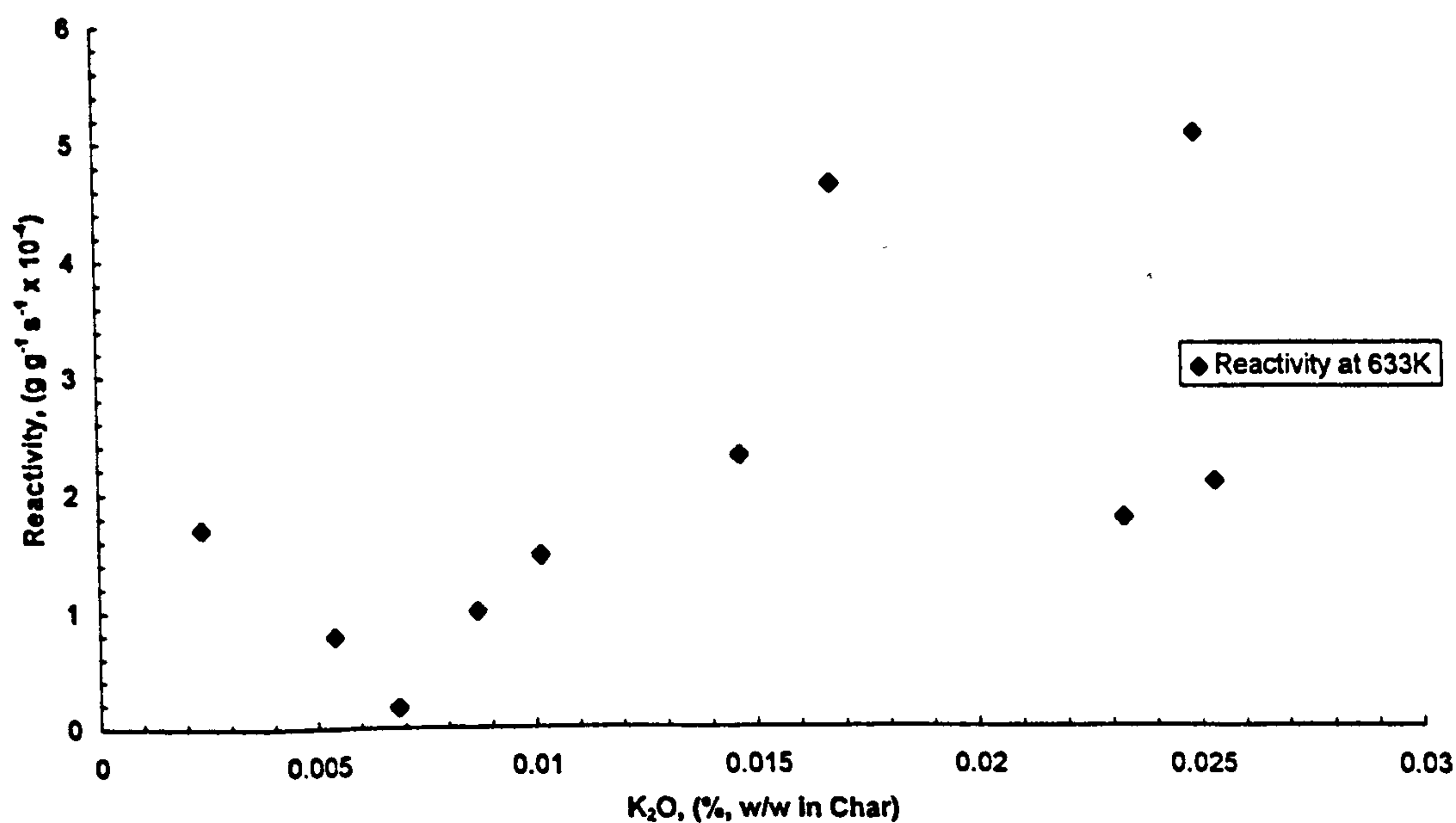


Figure 7.6 Plot of the 900 °C (1173 K) Char Isothermal Reactivity in Oxygen Determined at 360 °C (633 K) Versus Char K₂O Concentrations for the Long Ashton and Silsoe Materials

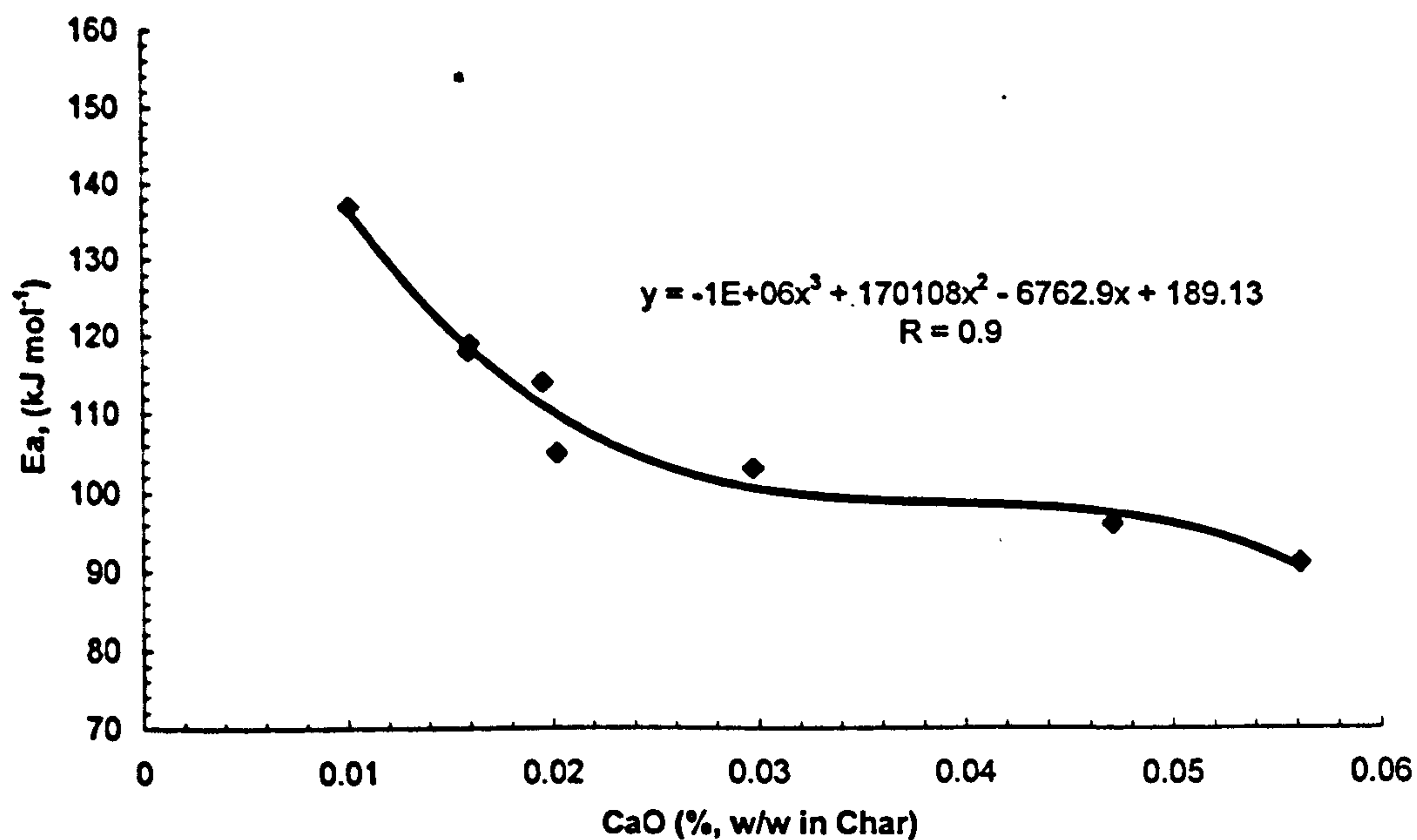


Figure 7.7 Plot of the Activation Energies for Char Isothermal Reaction in Oxygen in the Temperature Range 340–440 °C (613–713 K) Versus Char CaO Concentration for Long Ashton and Silsoe Materials

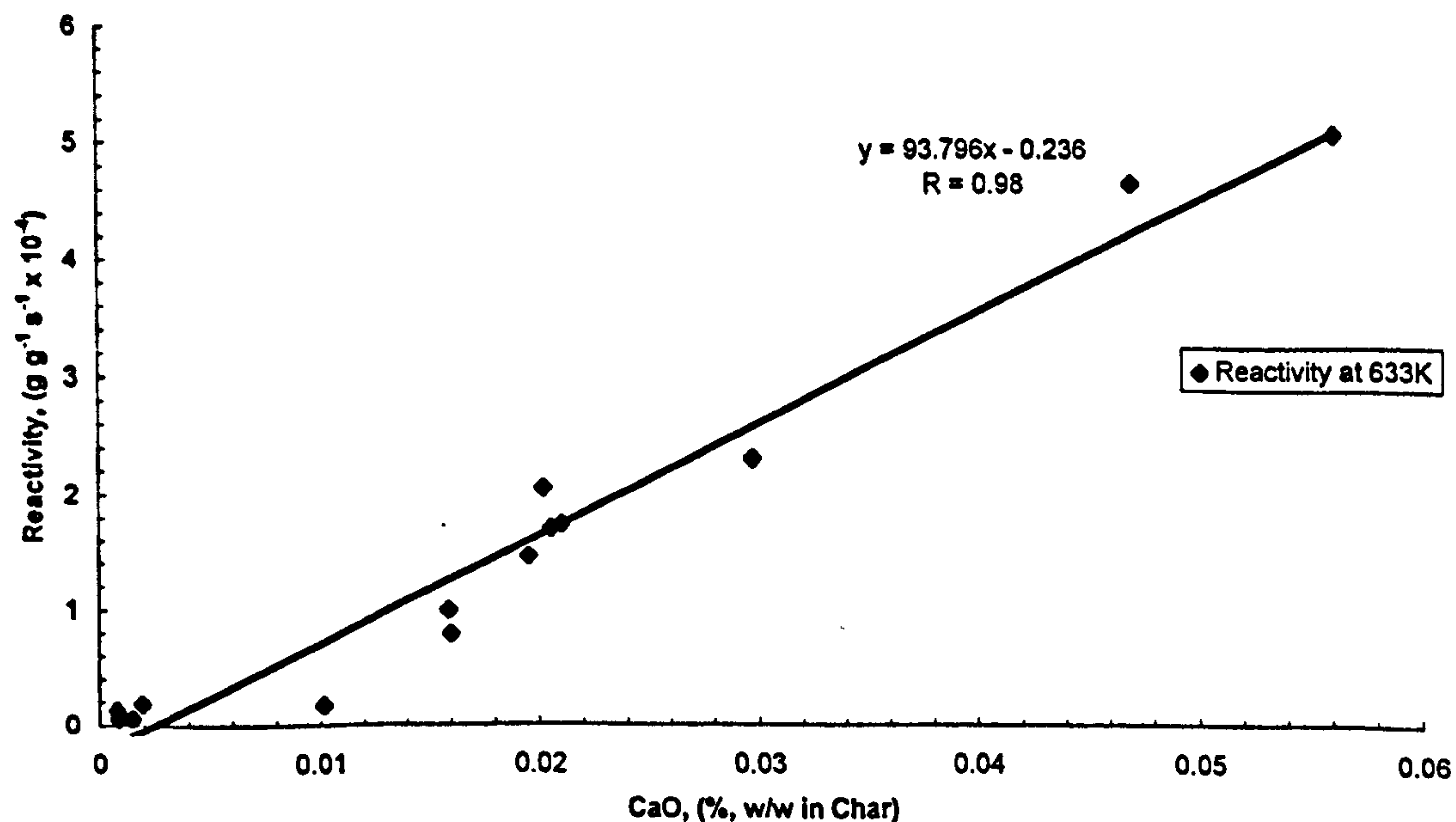


Figure 7.8 Plot of the 900 °C (1173 K) Char Isothermal Reactivity in Oxygen at 360 °C (633 K) Versus Char CaO Concentrations for Untreated and Acid Washed Biomass Materials

PAGE

NUMBERING

AS ORIGINAL

Chapter Eight

Conclusions

8.1 Biomass Materials

8.1.1 Basic Analyses of the Biomass Materials

The basic analysis data for the biomass materials, which had been selected for this study, indicated that they were all similar chemically, despite wide variability in crop type, age and source, viz;

- Proximate analysis data indicated that the volatile matter contents were high, in the range 77-91% (dry basis) while ash contents were low, ranging from 0.8-4.5% (dry basis)
- Ultimate analysis data were fairly similar with carbon contents 40-45% and hydrogen contents 5.0-5.5%. The nitrogen and chlorine contents of all the samples were relatively low, except for the nitrogen content of Danish pine which was significantly higher for reasons which are not understood.
- The biomass ash materials were found to be rich in SiO_2 , CaO , K_2O and MgO with the SiO_2 and CaO contents varying significantly from sample to sample.

Overall, the basic analyses data were typical of most biomass materials and were comparable to the data for similar materials available in literature.

8.1.2 Biomass Char Materials

The biomass materials gave char yields in the range 22-29% (daf) when heated to 1173K (900°C) in a flowing nitrogen atmosphere at 10 K min⁻¹, and then being held at that temperature for 1 hour. When the relationships between the parent material characteristics and char characteristics were investigated, no overall trends were found. There were, however, trends for individual groups of materials, and in particular, the fractionated Silsoe samples. The char yields from these materials range from 23-27% with the sap producing the lowest yield and the bark producing the highest yield. The bulk and twig materials which contain quantities of both sap and bark had intermediate char yield values. The relationships between the separated Silsoe material char yield data and the parent material characteristics and resultant char characteristics, on a dry ash free basis, are as follows:

- The char yield increased with increasing parent material fixed carbon content (daf) as expected.
- The char carbon contents (daf) increased linearly with decreasing char yields (daf).
- The char nitrogen contents increased linearly with increasing char yield.

The Long Ashton material data indicated that similar materials grown at the same location produced chars of a similar nature. These materials gave char yields in the range 25-29% (daf) with the resultant chars containing 80-85% carbon (daf), around 0.5% hydrogen (daf), 14-18% oxygen (daf) and 0.5-1.9% nitrogen (daf). Despite these similarities, there was no evidence that the char yields were related to either the parent material characteristics or the characteristics of the resultant chars.

The relationship between the parent material ash content and the char characteristics were investigated for all of the samples and again correlations were found only for the separated Silsoe materials. These were:

- The fixed carbon contents increased linearly with increasing ash content.
- The char yields increased linearly with increasing ash content.

The char carbon concentrations increased linearly with increasing ash content.

8.1.3 Biomass Char Surface Area

The measured surface areas of the biomass chars (N₂, BET) were found to range from 4-29 m² g⁻¹. The cereal straw char sample value was notably higher than those of the other materials. When the relationships of the char surface area data with parent material characteristics and char characteristics were investigated, no overall trends were found. However, once again, there were correlations for the separated Silsoe material data. The Silsoe sap char had the highest surface area of 18m² g⁻¹ and the bark char had the lowest at 4 m² g⁻¹. The bulk and twig material chars had intermediate values of around 7 m² g⁻¹. The relationship between the Silsoe char surface area data and the parent material characteristics and the resultant char characteristics are as follows:

- The char surface areas increased with decreasing fixed carbon content (daf).
- The char surface areas decreased with increasing char yield (daf).
- The char surface areas increased with increasing char carbon content (daf).

The Long Ashton materials char surface area values were very similar at 5-11 m² g⁻¹.

8.1.4 Biomass Char Isothermal Reactivity in Oxygen

The Silsoe bark char and Long Ashton char were by far the most reactive materials while the least reactive material was the Silsoe sap char. No evidence was found

of any general correlations relating the parent or char material properties with reactivity behaviour of the chars. There were however trends for the Silsoe materials and these are listed below:

- The char reactivity increased with increasing fixed carbon content (daf) of the parent materials.
- The char reactivity increased with increasing yield of char (daf).
- The char reactivity decreased with increasing char carbon content (daf).

The effects of the ash content and the ash components on the reactivity of the chars were also studied. In the first instance, the char reactivity was found to increase linearly with increasing char ash content. The sole exception to this was the cereal straw data. The influence of the major ash components of all the char samples namely, SiO_2 , CaO and K_2O were investigated and an excellent linear relationship was found which indicated that the reactivity increased with increasing CaO concentration.

In order to investigate the kinetics of the char reaction in oxygen under the experimental conditions, and in particular the order of reaction with respect to the carbon concentration, the Differential Method of J H Van't Hoff was applied to the rate data. It was evident that the oxidation reaction of all the chars were approximately first order. These results agreed well with previously published data.

The activation energy of the char reaction in oxygen over the temperature range studied was also calculated, using the Arrhenius equation and the char reaction rate data, and these were found to be in the range 91-137 kJ mol^{-1} . When these data were compared to the activation energy values of a wide range of graphitic materials, carbons, cokes and peat cokes, they were found to be typical of those for highly disordered and impure carbonaceous materials.

The activation energy values were plotted the char reactivity values measured at 613 and 633K, and a reasonable linear relationship was found.

The influence of CaO on the reactivity of the biomass chars was further studied by investigating the relationship between its concentration in the chars with the calculated activation energy values. An excellent non-linear relationship was found and two distinct regions can be defined. From 0.01 to 0.02% w/w CaO, the activation energy was found to decrease sharply from 138 to 105 kJ mol⁻¹, while from 0.02 to 0.06% w/w CaO, it decreased from 105 to 92 kJ mol⁻¹.

8.1.5 The Effects of Acid Washing on the Biomass Samples and Resultant Char Behaviour

In an attempt to investigate further the mineral matter effects, the straw and Danish pine samples were treated by ingestion in 1M HNO₃ and HCl solutions at 35-40°C for two hours followed by washing in distilled water until the washings were neutral. The effects of the treatment can be summarised as follows:

- The hydrogen, nitrogen and chlorine concentrations in the treated samples were reduced. The materials which were washed in HNO₃ also had higher oxygen concentrations.
- The volatile matter contents were significantly increased and the ash contents were reduced. The principle effects on the ash were reductions in the CaO, MgO, K₂O and Na₂O and more specifically for the HCl washed samples, the Fe₂O₃ concentrations were greatly reduced.
- The char yields for the acid treated samples were significantly lower than those of the untreated materials.
- The chars of the acid treated samples were found to have lower surface area than those of the untreated materials. For both materials, the chars prepared from the HNO₃ washed samples had the lowest surface area.

- When the char reactivities were measured in oxygen, the chars prepared from acid-treated biomass were found to be significantly less reactive than those prepared from the parent materials.

The influence of CaO on the reactivity of the acid-washed material chars was investigated and correlations were found for the straw and Danish pine groups of samples individually. These trends indicated that for each group of chars the reactivity decreased with decreasing CaO concentration. When the acid-washed data were combined with the that of the other biomass reactivity and CaO data, the acid-washed values fitted the trend which had previously been established for the biomass char data. This provides further compelling evidence that, for this collection of biomass chars, the reactivity to oxygen at relatively low temperatures was greatly influenced by the Ca content of the char.

8.2 Refuse Derived Fuel and Refuse Derived Fuel Individual Components

8.2.1 Basic Analyses Data of Untreated and Acid-Washed Refuse Derived Fuel Materials

The major components of RDF are paper/board and sheet plastic, and this was reflected in the basic analysis data.

The proximate analyses of the untreated materials were generally similar with high volatile matter components in the range 73-76% (dry basis), and low fixed carbon contents in the range 10-14% (dry basis). The Byker material had a higher ash content at 15.6% (dry basis) compared to 10.8% for the Isle of Wight material.

Washing samples of Byker and Isle of Wight RDF materials separately in HNO₃ and HCl had the effect of increasing the volatile matter contents and reducing the ash contents and mainly the CaO contents. Both acids were effective in reducing the nitrogen contents while HNO₃ washing was particularly effective in extracting Cl.

8.2.2 Untreated and Acid Washed Refuse Derived Fuel Material Char Analysis and Reactivity Results

The untreated RDF samples produced similar char yields of 20-21% (daf) during pyrolysis at 10 K min^{-1} to 1173K in a N_2 atmosphere. The measured char yields for the acid washed materials were slightly lower, 18-19% (daf), with the lower yields being obtained for the HNO_3 washed samples.

When the isothermal reactivity of the chars were measured in oxygen, the untreated Isle of Wight sample char was the most reactive, however both untreated material chars were far more reactive than those prepared from the acid washed samples. For each set of RDF material chars, those prepared from the HCl washed materials were the least reactive.

The BET surface area values for the chars produced from the untreated RDF material were similar at $25\text{-}30\text{ m}^2\text{ g}^{-1}$ and these were significantly higher than those for the chars prepared from the acid washed RDF materials. These chars had surface area values of $8\text{-}14\text{ m}^2\text{ g}^{-1}$, with the chars prepared from the HNO_3 washed samples having the lowest values for both types of RDF.

When the relationship between the char surface area values of both the untreated and acid washed RDF materials were investigated, it was found that in all cases, the char surface area increased both with increasing fixed carbon content and with char yield.

8.2.3 Refuse Derived Fuel and Model Composites of RDF Components

The study of the carbonisation behaviour of the mixed materials contained in municipal solid waste and RDF, involved the preparation of a number of artificial bi-component blends of a cellulosic material (cellulose or cereal straw) and a synthetic polymer (either poly(ethene), poly(vinylchloride) or saran). The pure compounds and the blends were analysed using the approach adopted for the biomass and RDF materials.

Cereal straw was the only material to have a significant ash content while the poly(ethene) material completely devolatilised.

The proximate analysis data for the poly(ethene)/cellulose blends were additive while fixed carbon data for the blends containing chlorinated polymers were greater than expected. This indicated that some interaction between the components occurred during the devolatilisation procedure.

The yield of chars obtained from the pure material were found to vary from 0-32%, and in a similar fashion to the fixed carbon data, PVC had a significantly lower value than saran. The chars prepared from the non chlorinated-polymer containing mixtures were directly additive while the chars prepared from the mixtures containing chlorinated polymer produced chars with a greater than expected char yield. Again, this indicated that there was interaction between components. These chars also contained higher than expected amounts of hydrogen and oxygen which suggested that the carbonisation of these mixtures had not reached completion under the test conditions.

The observed increases in fixed carbon and char yield values for the blends containing some chlorinated polymer may be due to the presence of evolved HCl, with the cellulosic material, as suggested by Shafizadeh^(ref 63, Chapter5). Shafizadeh proposed that HCl initiates acid catalysed dehydration reactions and also catalyses condensation reactions of the intermediate products. The condensation reactions give rise to products which can not escape from the heated zone by evaporation, and thus, would remain to be charred.

The measured surface area values for the poly(ethene)/cellulose mixtures were additive, and were very similar to the value for the cellulose char alone. The surface areas of the chlorinated polymer containing blend chars were not simply additive. In the instance of the PVC containing blend chars, the surface area values were lower than expected, while for the saran containing blend chars, higher than expected values were obtained.

Of the pure material chars, the straw char was by the most reactive material while the PVC char was the least reactive.

The reactivity values for the poly(ethene)/cellulose mixture chars were very similar to those for pure cellulose char. This indicated that when these chars were being prepared, the poly(ethene) fraction was completely released as volatile material, leaving a cellulose char residue. This agrees with the observations that the char yield data were additive and that the measured surface area values were very close to that of the pure cellulose char.

The reactivity values for the chars prepared from the blends containing PVC were notably different from those containing saran, with the former being less reactive than expected while the latter were more reactive than expected. This was attributed to the different behaviour of PVC compared and saran during devolatilisation.

8.2.4 Effectiveness of the Synthetic Blends at Modelling Refuse Derived Fuel Behaviour During Thermal Processing and the Resultant Char Characteristics

From the char yield data there was evidence that the behaviour of the RDF materials was influenced by both chlorine and ash contents. The 1/9 Saran/cellulose and 1/9 PVC/cellulose blends produced char yields approaching or equal to those of the Byker and Isle of Wight RDF materials. The 1/9 poly(ethene)/cellulose, which contained no chlorine, had the lowest char yield value. The 1/9 PVC/straw blend, which contained both chlorine and ash, produced a higher char yield than the RDF materials. Further evidence for this was apparent in the char yield data for the acid-washed RDF materials. These had both reduced ash and chlorine contents compared to the untreated RDF materials, and they produced lower char yields.

When the effectiveness of the blends at modelling RDF char reactivity was examined, only the reactivity value for the 1/9 PVC/straw char was comparable to

those of the RDF chars. The reactivity values for other blend chars were much lower. This was attributed to the effect of the ash component present in the 1/9 PVC/straw blend. This suggestion was further supported by the observation that those blend chars which had no ash, had reactivity values close to those of the chars prepared from the acid-washed RDF materials.

Overall, therefore, there was some indication that the behaviour of the RDF materials can be modelled using blends prepared from suitable polymer and cellulose-based constituents, provided that the blends contained the appropriate chlorine and ash contents.

Future Work

The combustion and gasification processes and the energy recovery systems which are currently employed for biomass and waste fuels are based on technologies originally designed for coal. One of the key prerequisites of the successful application of existing technologies to these non-conventional fuels is an improved understanding of the behaviour of these materials. However, obtaining an improved understanding will be difficult since, as the results of this study suggest, the behaviour of biomass and waste materials is subject to wide variation depending on their type and origin. In the case of biomass materials the first stage of a characterisation technique should be based on a fractionation method, similar to that adopted for the Silsoe SRC in this study, in which the materials would be separated into their main components for subsequent analysis and testing. This would allow the behaviour of these components during various thermal processing procedures to be related to inherent characteristics such as volatile content, ash content and ash composition. The second stage of characterisation would involve a study of the interactions of these fractions during thermal processing. This would be achieved by the preparation and analyses of a range of bi-component blends of known composition with all the individual components being paired with each of the others. The results would assist in predicting the behaviour of a bulk material based on a knowledge of main components.

A similar approach to that described above for the biomass materials should also be adopted for future studies of RDF materials. It was clear from the results in this document, that the behaviour of some RDF components were altered dramatically by the presence of others such as chlorinated polymers. As RDF is heterogeneous nature, there are many possible combinations of interactions of these materials, and these need to be addressed. Since the composition of RDF is known to vary considerably with the time of year and the production process, an increased knowledge of component interactions would be an invaluable tool to combustion

engineers. As is the case with biomass materials, this information would allow the behaviour of a particular RDF source to be predicted from its component assay using computer combustion modelling programs which take into account these interactions.

One of the accepted limitations of laboratory work is that it does not always reflect the behaviour of systems or procedures employed in full-scale operations. The limitations of laboratory work in this study was illustrated by the biomass char reactivity measurement in oxygen. In commercial gasification systems, the char material is exposed to high heating rates and low oxidising gas partial pressure, however, a low heating rate and relatively high oxidising gas partial pressure had to be used during the experimentation to allow reactivity measurements to be made. The results did not directly reflect the behaviour of the materials under conditions of interest. There is therefore, a major requirement to address this problem. One possible solution could be the construction of a small-scale gasifier which has its design based on a proven commercial facility. This would allow the behaviour of a particular candidate fuel to be easily studied under a wide range of relevant temperatures and conditions.

Another invaluable tool for predicting the behaviour of biomass and waste fuels would be the development of a suite of simple standardised laboratory test procedures for fuel characterisation for use with small quantities of fuel, the results of which would be indicative of the behaviour in actual commercial gasification systems. These procedures could be developed using simple laboratory tube furnaces or the small-scale gasifier as described above. If this facility was proven to represent the behaviour of a large-scale gasifier during operation, then the results generated could be used for comparison with laboratory test results. The development of such laboratory-scale experimental procedures would provide a relatively efficient, inexpensive and rapid method of predicting the behaviour of a fuel in full scale plant.